

NASA-CR-169846

JPL PUBLICATION 82-26

NASA-CR-169846
19830009502

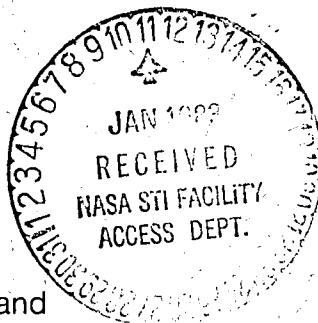
26-Meter Antenna S-X Conversion Project

March 15, 1982



National Aeronautics and
Space Administration

Jet Propulsion Laboratory
California Institute of Technology
Pasadena, California



LIBRARY COPY

JAN 26 1982

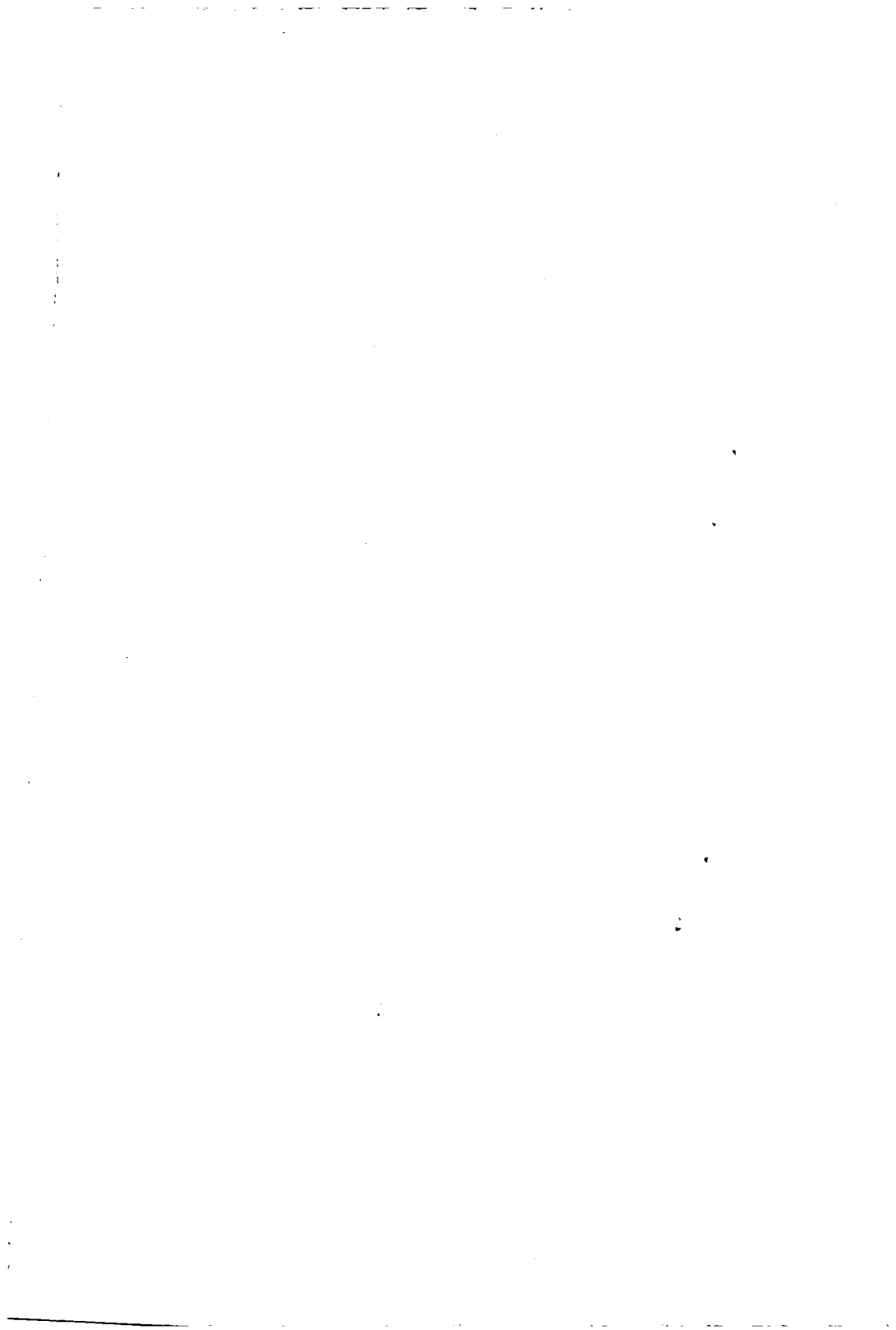
LANGLEY RESEARCH CENTER
LIBRARY, NASA
HAMPTON, VIRGINIA

3 1 1 RM/JPL-PUB-82-26

DISPLAY 03/2/1
83M17773** ISSUE 8~ PAGE 1171 CATEGORY 32 RPT#: NASA-CR-169846
JPL-PUB-82-26 NAS 1.26:169846 82/03/15 223 PAGES UNCLASSIFIED
DOCUMENT

UTTL: The 26-meter antenna s-x conversion project --- Deep Space Network
CORP: Jet Propulsion Lab., California Inst. of Tech., Pasadena. AVAIL. NTIS
SAP: HC A10/MF A01
MAJS: /*ANTENNA DESIGN/*ANTENNA RADIATION PATTERNS/*DEEP SPACE NETWORK/*
SUPERHIGH FREQUENCIES/*ULTRAHIGH FREQUENCIES/*UPGRADING
MINS: / DOWNLINKING/ GROUND SUPPORT EQUIPMENT/ INSTALLING/ MICROWAVE
TRANSMISSION/ RECEIVERS/ SYSTEMS ENGINEERING/ UPLINKING
ABA: A.R.H.
ABS: Programmatic and management aspects of converting an existing 26-meter
S-band subnet to a 34-meter S- and X-band subnet of the Deep Space Network
are described. The stations involved were DSS 12 near Barstow, DSS 44 in
Australia, and DSS 62 in Spain. The main subsystems affected by the
conversion were the antenna mechanical, antenna microwave, and
receiver-exciter. Antenna mechanical modifications and electronic additions
and changes are described. The design and analysis of critical areas are
considered and antenna performance is discussed.

ENTER:



JPL PUBLICATION 82-26

26-Meter Antenna S-X Conversion Project

March 15, 1982



National Aeronautics and
Space Administration

Jet Propulsion Laboratory
California Institute of Technology
Pasadena, California

N83-17713#

The research described in this publication was carried out by the Jet Propulsion Laboratory, California Institute of Technology, under contract with the National Aeronautics and Space Administration.

Reference to any specific commercial product, process or service by trade name or manufacturer does not necessarily constitute an endorsement by the United States Government or the Jet Propulsion Laboratory, California Institute of Technology.

ACKNOWLEDGEMENT

The authors listed below wish to acknowledge the support of Paul S. Goodwin, Richard Z. Toukdarian, and Floyd W. Stoller of JPL and Maurice E. Binkley of NASA.

Edward Burnell

Joseph Carpenter

Paul Lipsius

Verl Lobb

Houston McGinness

Eugene Thom

Ron Van Hek


Robert White

PREFACE

This engineering report describes the conversion of three 26m (85-ft) diameter antennas of the Deep Space Network (DSN) to 34m (112 ft) for downlink operations at both X-band (8.4 GHz) and S-band (2.2 GHz).

The first phase of this activity followed the standard DSN methodology for engineering of new capabilities which requires the preparation of a set of functional requirements to which the technical design must respond and support. These requirements were prepared under the leadership of Paul S. Goodwin of JPL and were approved by M. E. Binkley of NASA's Office of Space Tracking and Data Systems. The requirements and budget based on estimated costs prepared during the requirements phase were then provided to an implementation team headed by Verl B. Lobb. The detailed engineering, manufacturing, and installation were supported by industrial contractors as is the standard practice for most of the implementation in the network.

The project was completed on schedule and within budget. The facilities were transferred to operations in a timely manner so that support for flight projects at X-band was initiated with the Voyager Project.



N. A. Renzetti
Manager, TDA Engineering

ABSTRACT

The 26-meter S-X Conversion Project provided for the conversion of an existing 26-meter S-band subnet to a 34-meter S- and X-band subnet. The subnet chosen for conversion consisted of the following stations: DSS 12 near Barstow, DSS 44 in Australia, and DSS 62 in Spain. The Conversion Project evolved from its formative stages, where many options were considered and alternates chosen, through project implementation, problem identification and solution, to a now completed successful project. The main subsystems affected by this project were the Antenna Mechanical, Antenna Microwave, and Receiver-Exciter. In addition to these, there are many project-related electronic equipments that had been added to the existing station equipment. The completed 34-meter S-X Conversion Network has been used for Pioneer-Venus and Voyager tracking and has now become a functional integral part of the Deep Space Network.

CONTENTS

I.	INTRODUCTION	1
II.	THE 26M S-X CONVERSION PROJECT	5
A.	SUMMARY OF KEY FACTORS	5
B.	JUSTIFICATION	6
C.	FINAL PROJECT ORGANIZATION	8
D.	IDENTIFICATION OF SPECIFIC REQUIREMENTS AND CONSTRAINTS . . .	11
	1. DSN Tracking System	14
	2. DSN Telemetry System	16
	3. DSN Test and Training System	17
	4. Antenna Mechanical Subsystem	18
	5. Antenna Microwave Subsystem	18
	6. Receiver-Exciter Subsystem	18
	7. Transmitter Subsystem	19
	8. Frequency and Timing Subsystem	20
E.	SCHEDULE RISK	21
F.	PROJECT PHASES	29
	1. Concept and Design Studies Phase	29
	2. Design Phase	30
	3. Fabrication Phase	32
	4. Installation Phase	32
	5. Initial Antenna Operations	35
G.	PROJECT MANAGEMENT AND CONTROL	36
	1. Major Contractors	36
	2. JPL In-House Support	37
	3. Reporting and Review	38

CONTENTS (Contd)

H.	SCHEDULE EXPERIENCE	39
I.	RESOURCES	42
1.	Funds	42
2.	Manpower	45
III.	DESCRIPTION OF ANTENNA MECHANICAL MODIFICATIONS AND NEW ELECTRONIC ADDITIONS AND CHANGES	47
A.	GENERAL DESCRIPTION	47
B.	DECLINATION AND HOUR ANGLE WHEEL MODIFICATIONS AND ADDITIONS TO COUNTERWEIGHT AND PEDESTAL STIFFENING	50
1.	Declination Wheel	50
2.	Hour Angle Wheel	50
3.	Pedestal	50
C.	DECLINATION AND HOUR ANGLE SERVO AND ELECTRIC DRIVES	51
1.	Introduction	51
2.	Electronic Control (Servo) Assembly Theory of Operation	51
D.	TIPPING STRUCTURE - EXTENSION TO 34M	57
1.	Extension Panels and Existing Panel Modifications	57
2.	Quadripod	59
3.	Subreflector and Controller	62
4.	Structure for the Extension	64
5.	Reflex Reflectors and Feedcone	66
6.	Reinforcement and Welding of Joints in the Existing Reflector Structure	75
E.	DECLINATION AND HOUR ANGLE ENCODERS	75

CONTENTS (Contd)

F.	ANTENNA RAISING OR TRENCHING FOR SKY COVERAGE	80
1.	Lifting the Antenna 10 Feet and Placing the Foundation	84
2.	Trenching	99
G.	ELECTRONIC CHANGES AND ADDITIONS	99
1.	Cable Trays and Cables	99
2.	Utility Power Modifications	107
3.	Antenna Microwave	107
4.	Receiver-Exciter	109
5.	Planetary Ranging Assembly	109
6.	Wideband Data Interface	110
IV.	DESIGN AND ANALYSIS OF CRITICAL AREAS	111
A.	REFLECTOR AND SUBREFLECTOR DESIGN STUDY	111
B.	SELECTION OF THE RATIO OF FOCAL LENGTH TO DIAMETER OF THE PRIMARY REFLECTOR	115
C.	STUDY ON POLAR SHAFT BEARING LIFE	116
D.	STUDY OF THE USE OF ELECTRIC DRIVES	121
1.	Rationale	121
2.	Costs	122
E.	SAFETY OF THE ANTENNA LIFT, LIFT FRAME, AND FOUNDATION DESIGN	131
1.	Safety of Raising the Antenna	131
2.	Lift Frame Design	136
3.	Foundation Design	136
F.	DECLINATION AND HOUR ANGLE WHEEL MODIFICATION DESIGN	138
G.	RECEIVER-EXCITER DESIGN	145
H.	ANTENNA MICROWAVE DESIGN	154

CONTENTS (Contd)

V.	ANTENNA PERFORMANCE	161
A.	GENERAL DISCUSSION	161
B.	OVERALL PERFORMANCE SPECIFICATIONS	162
	1. Radio Frequency Performance	162
	2. Pointing Accuracy Requirements	162
	3. Environmental Requirements	163
C.	OVERALL PERFORMANCE MEASUREMENTS	164
	1. Radio Frequency Performance	164
	2. Pointing Accuracy Performance	165
	3. Environmental Performance	165
	4. Summary	165
D.	X-BAND PERFORMANCE	165
	1. Background	165
	2. Measured Performance Results and Investigation	167
	3. Recommended Modifications	179
	4. Conclusions	179
	5. Recommendations	182
	6. DSS 12 Antenna Modifications	183
E.	ANTENNA ACCIDENT AT DSS 61	186
	1. General	186
	2. Description of the Accident	188
	3. Personnel Involved	189
	4. Damage Caused by Accident	189
	5. Investigations and Engineering Analysis	192

FIGURES

1.	Typical 34M Antenna After Completion of S-X Conversion Project	xvi
2.	Deep Space Stations of the DSN at the Inception of the Project	2
3.	Goldstone Deep Space Communications Complex	3
4.	26M Conversion Project	9
5.	Implementation Project	10
6.	Functional Work Assignments	12
7.	DSS 12 Modified Overall S-X Conversion Schedule	22
8.	DSS 13 Alternate Plan, Proposed 1978 Modification Block Diagram	26
9.	DSS 13 Alternate Plan Schedule	27
10.	DSS 12 Overall Schedule	40
11.	Milestone Schedule	41
12.	S-X Conversion Project Resource Profile	44
13.	S-X Conversion Project Functional Block Diagram	48
14.	Structural Changes to Antenna Mechanical Subsystem for Extension to 34 Meters	49
15.	Antenna Drive Block Diagram	52
16.	Measurement of Surface Tolerance	58
17.	Placement of Targets on Panels	60
18.	Quadriopod Preassembly	61
19.	Raising the Quadriopod for Installation on the Antenna	63
20.	Installation of New Rib and Hoop Assembly	65
21.	Rib and Hoop Subassembly on Fixture	67
22.	Closeup View of Rib and Hoop Subassembly on Fixture	68
23.	Removal of Rib and Hoop Subassembly on Fixture	69

FIGURES (Contd)

24.	Installation of Rib and Hoop Subassembly	70
25.	Installation of the Last Hoop Trusses	71
26.	Feedcone	72
27.	Installation of Feedcone on Reflector	73
28.	Installation of Reflex Reflectors	74
29.	Tracking Type R/D Converter Functional Block Diagram	76
30.	Angle Encoder Mounting Arrangement	78
31.	Angle Encoder Mounting Arrangement	79
32.	Unmounted Transducer	81
33.	Transducer Electronics	82
34.	Data Converter Assembly	83
35.	Antenna Lifting Frame	85
36.	Initial Cribbing Base and 200-Ton Jacks for Raising Antenna	86
37.	Cribbing Base in Place Under Antenna	87
38.	200-Ton Jacks	88
39.	Safety Lines	89
40.	Antenna Raised to Inspection Position	90
41.	Antenna Resting on Support Column Because of High Winds	91
42.	Antenna Resting on Support Column Because of High Winds	92
43.	Closeup View of Support Column	93
44.	Closeup View of Support Column	94
45.	Closeup View of Support Column	95
46.	Antenna During 2-Day Period of High Winds	96
47.	Support Column During 2-Day Period of High Winds.	97
48.	Antenna in Position with Jack Pads Installed	98

FIGURES (Contd)

49.	Typical Form for Concrete Foundation	100
50.	Concrete Foundations	101
51.	Finishing Concrete Foundation	102
52.	Resumption of Work on Antenna	103
53.	Check of Trench Profile at DSS 42	104
54.	Closeup View of Reflector and Trench	105
55.	Completed Trenches	106
56.	Antenna Microwave S-X Conversion	108
57.	Reflector Rib Extension Profile Extension	112
58.	34M Model A and B Structural Weight vs RMS Designed for Gravity	113
59.	34M Model B Final Design	114
60.	Servo Block Upgrade, 26M Net Life Cycle Cost Analysis, Cumulative Inflated Dollars Versus Years	132
61.	34M Extension, Concrete Base Raising and Reinforcing	135
62.	34M Antenna Lift Frame	137
63.	Added Counterweight	139
64.	Isometric View of Hour Angle Wheel	140
65.	Added Counterweight Boxes	141
66.	Hour Angle Wheel Modification on Front Face	142
67.	Hour Angle Wheel Modification on Back Face	143
68.	Hour Angle Wheel Modification, Reinforcement on Back Face	144
69.	26M Declination Wheel Modification	146
70.	Detail of Declination Wheel Modification	147
71.	26M S-X Conversion Receiver-Exciter Block Diagram	150
72.	26M S-X Conversion Receiver-Exciter S-X Converter Block Diagram	151

FIGURES (Contd)

73.	26M S-X Conversion Receiver-Exciter Doppler Extractor Block Diagram	152
74.	26M S-X Conversion Receiver-Exciter Test Translator Block Diagram	153
75.	S-X Microwave Subsystem Interfaces	156
76.	S-X Band Block Diagram	157
77.	Switch Control Block Diagram	159
78.	DSS 12 X-Band Antenna Gain vs Hour Angle	168
79.	DSS 12 X-Band System Temp vs Antenna Elevation	169
80.	DSS 61 X-Band Antenna Gain vs Hour Angle	170
81.	DSS 61 X-Band System Temp vs Antenna Elevation	171
82.	DSS 42 X-Band Antenna Gain vs Hour Angle	172
83.	DSS 42 X-Band System Temp vs Antenna Elevation	173
84.	DSS 12 X-Band Beam Map	175
85.	DSS 12 X-Band Aperture Efficiency from Radio Source Measurements	176
86.	DSS 12 34M Computed Efficiency vs Hour Angle	177
87.	DSS 12 Antenna Performance, X-Y Offset Errors at 8420 MHz Before vs After SRC Card Modification	178
88.	DSS 12 X-Band Aperture Efficiency from Radio Source Measurements	180
89.	Subreflector Mounted to Test Fixture	184
90.	Subreflector Bracing and Push-Pull Adjusters	185
91.	Final RMS of 34M HA-DEC Field Readings	187
92.	HA Structure Damage	190
93.	Pedestal Structure Damage	191
94.	Impact Force Configuration	196
95.	Two-Inertia Model	197

FIGURES (Contd)

96.	Impact Forces from Model	199
97.	Model for Emergency Braking	200

TABLES

I.	Dual Feed S-Band Relative Performance vs Antenna Diameter	13
II.	Resource Impact of Accelerated S-X Conversion Schedule Relative to WAD 76-1	24
III.	DSS 13 Alternate Plan, Expected X-Band RF Performance Comparison	28
IV.	Cost Summary of Baseline Items	42
V.	Equipment Funding Summary	43
VI.	26M and 34M Bearing Loads	118
VII.	Predicted Number of Turns Remaining in Bearing Life	119
VIII.	M & O Spares Requirements for Option 2	128
IX.	Power Costs for Options 0, 1, and 2	129
X.	Power Costs for Option 3	130
XI.	Servo Block Upgrade, 26M Net 10-Year Life Cycle Cost Analysis . .	131
XII.	Weight Summary of HA-DEC Antenna Showing 26M and 34M Reflector Diameter	138
XIII.	Maximum Load at Bearings	148
XIV.	Bearing Life Calculation	148
XV.	X-Band TWM Performance	158
XVI.	Performance Calculations	181
XVII.	Maximum Member Stresses, KSI	207

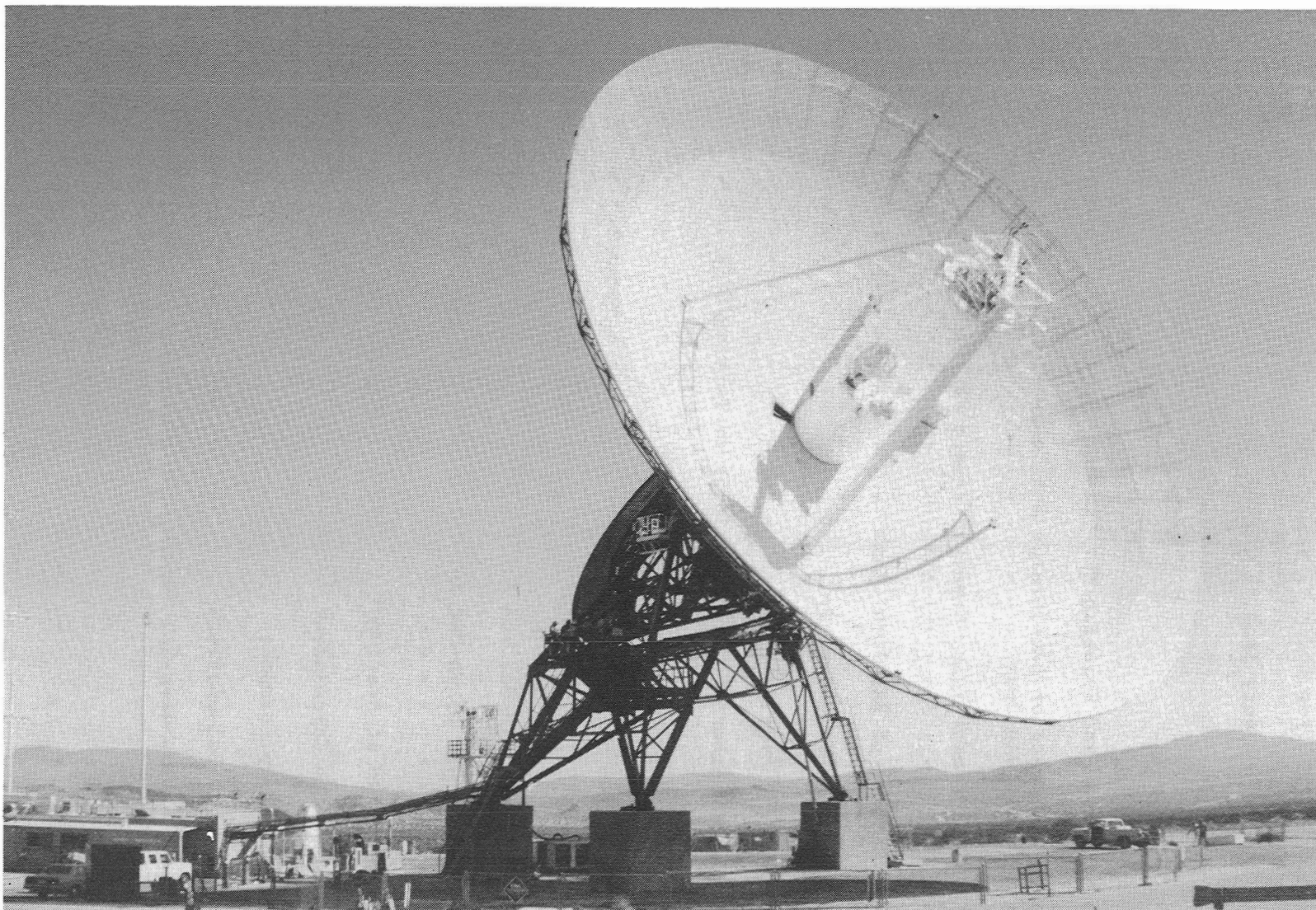


Figure 1. Typical 34M Antenna After Completion of S-X Conversion Project

I. INTRODUCTION

The Deep Space Network (DSN) is a worldwide network of space communication stations which provide one and two-way communications with spacecraft involved in planetary and interplanetary exploration. The network is designed, implemented, and operated by the Jet Propulsion Laboratory for the National Aeronautics and Space Administration's (NASA) Office of Space Tracking and Data Systems (OSTDS).

The Deep Space Stations (DSS) in this network are located at three complexes. Each complex consists of a 26m (85-ft), a 34m (112-ft), and a 64m (210-ft) diameter antenna. Figure 1 is a typical 34m diameter antenna. The three complexes are located approximately 120 degrees apart in longitude in order to provide continuous communications with the spacecraft in or near the plane of the ecliptic on its trajectory through the solar system (Figure 2).

The 64m diameter stations are located at Goldstone, California (DSS 14); Tidbinbilla, Australia (DSS 43); and Cebreros, Spain (DSS 63). The 26m diameter stations are located at Goldstone, California (DSS 11); Orroral Valley, Australia (DSS 44); and Robledo, Spain (DSS 62). The 34m diameter stations are located at Goldstone, California (DSS 12); Tidbinbilla, Australia (DSS 44); and Cebreros, Spain (DSS 61). The 64m and 34m antennas provide both X- and S-band communications capability. Additional support is provided by a Spacecraft-DSN Compatibility Test Area at the Jet Propulsion Laboratory in Pasadena, California; a launch support station at Merritt Island, Florida; and a research and development station (DSS 13) at Goldstone, California. An example of the Goldstone Complex is shown in Figure 3. The 34m subnetwork is the result of the 26m S-X Conversion Project. This project converted an existing 26m S-band antenna to a 34m S- and X-band antenna.

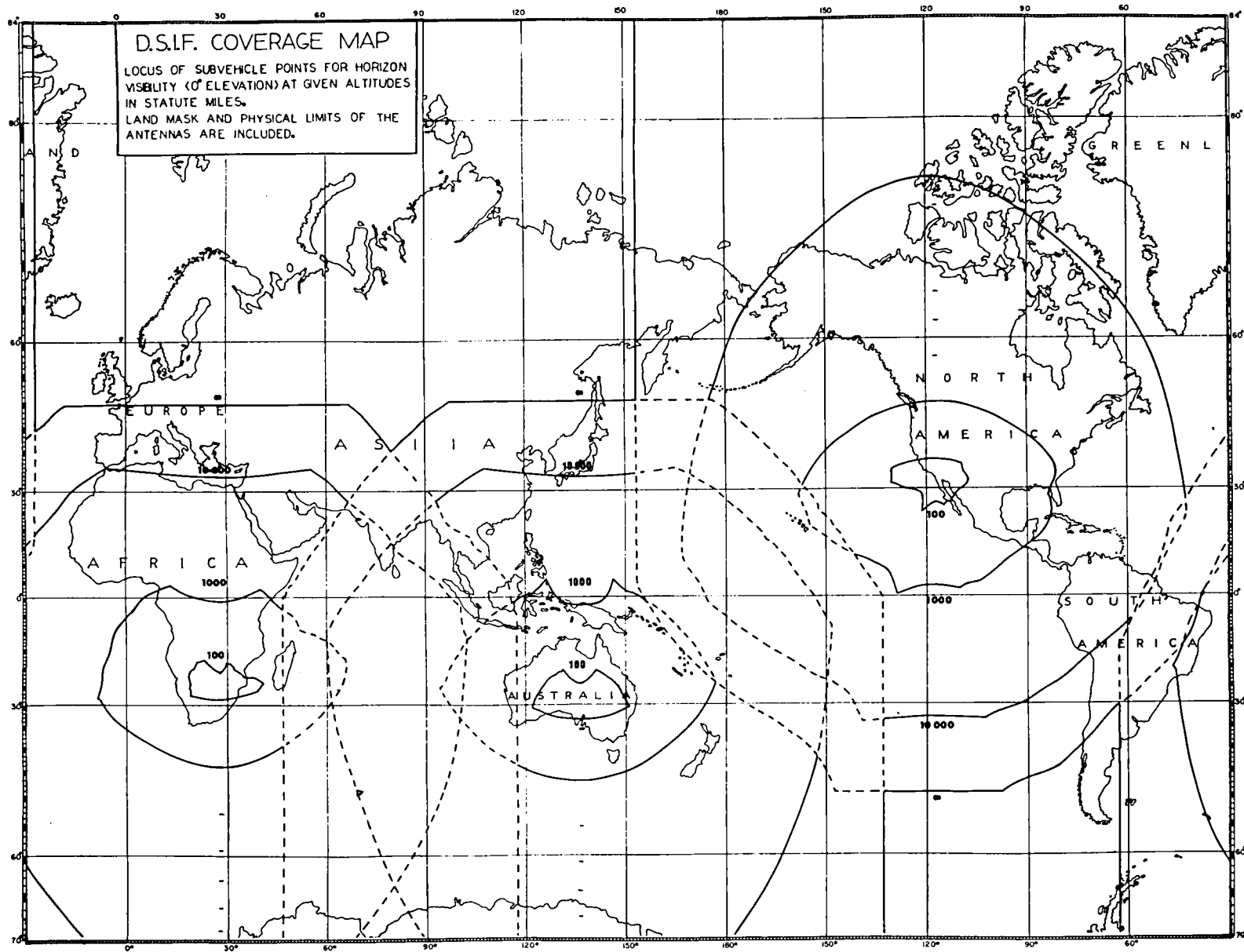


Figure 2. Deep Space Stations of the DSN at the Inception of the Project
(Overlapping Station Coverage Ensures Continuous Monitoring of
Spacecraft)

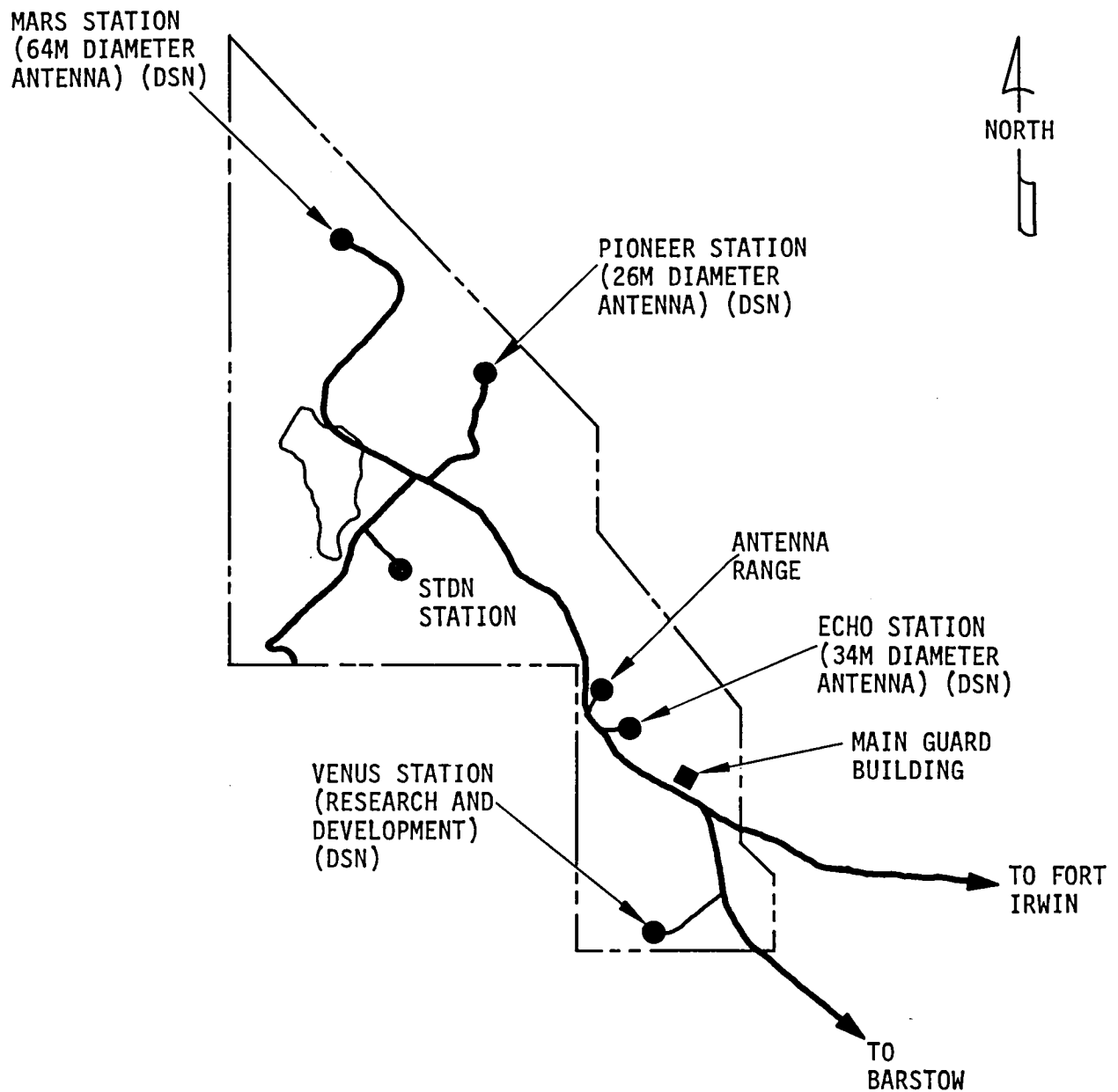


Figure 3. Goldstone Deep Space Communications Complex (STDN Station is part of Goddard Spaceflight Tracking and Data Network)

The basic justification for the addition of an X-band capability to existing DSN 26m stations lies in the support requirements approved and near-term projected NASA flight project missions. An analysis of the mission objectives for that set showed the following characteristics:

- (1) A significant number of the NASA missions were directed toward the outer planets; namely, Jupiter, Saturn, and Uranus. Due to the vastly increased distances from Earth, higher frequencies must be employed by the spacecraft and the DSN to determine the trajectory and to achieve a greater science return.
- (2) The combination of very long flight times to the outer planets, plus the relative positions of the planets that enable the use of intervening planet gravity assist trajectories, produces a bunching effect of enroute spacecraft as seen from Earth. This places several spacecraft, which require 64m station support, in the same area of the sky for months, even years, at a time. The solution to alleviating the 64m station overload created by these two characteristics is to increase the X-band capability of the DSN, either by adding stations or by converting existing S-band-only stations to an S- and X-band capability. The latter, more economical, approach was selected.

The extension of the antenna diameter to 34m provided a sufficient level of X-band performance to partially alleviate the 64m subnet overload by supporting S-X-band navigation data acquisition out to the planet Saturn while simultaneously providing a usable real-time video capability out to the planet Jupiter. This antenna diameter also proved to be the least diameter suitable for arraying with the 64m antenna.

II. THE 26M S-X CONVERSION PROJECT

This section describes the programmatic and management aspects of the 26m S-X Conversion Project to design and implement the modifications and electronics and the initial use of the antennas at the various locations. Observations on technical aspects of the modifications are incidental and are included only to illustrate the structure or workings of the Project Organization.

A. SUMMARY OF KEY FACTORS

The S-X Conversion Project was completed on schedule, within its original performance specifications and budget allocation. The success of the Project is traceable to an early definition of the Project completed by a study team effort over a period of 3 months which resulted in the publication of a Data System Development Plan. This was followed by excellent support from NASA in making firm commitments and funding available to the Project as needed. The Project had a requirement that all hardware and transfer-to-operations documentation and agreements be completed prior to shipment to the site. The two factors of contingency and preshipment transfer, which started at the same point in time, resulted in a clear definition of status and furnished time to resolve the missing items or problems. In summary, the three main factors for success were (1) a clear definition of the Project at inception, (2) a scheduled contingency period, and (3) a preshipment transfer agreement requiring all hardware and documentation to be completed at the beginning of the contingency period.

The project proved to be cost effective by taking the following approach:

- (1) Maximum use of the existing antenna structure and components.
- (2) Maximum use of existing station equipment, such as down-converters and Block III receivers.
- (3) Maximum use of existing facilities, such as support buildings, control room, etc.

- (4) Use of X-band equipment already in service at the 64m antenna stations.
- (5) Reduction of energy usage by converting from hydraulic to electric antenna drives.

B. JUSTIFICATION

Development of the justification for the S-X Conversion Project started in 1974 and entered the study stage in January 1975 with an exploratory discussion between representatives of the Telecommunications Science and Engineering Division and Tracking and Data Acquisition (TDA) Engineering Office personnel. In April 1975, the S-X Conversion Study Team was established with V. B. Lobb and P. S. Goodwin as co-chairmen, and D. W. Brown, H. R. Buchanan, W. D. Chaney, C. Chatburn, H. Donnelly, E. C. Gatz, N. C. Ham, C. W. Johnson, R. Leu, G. S. Levy, G. A. Madrid, F. Mastrogiovanni, R. P. Mathison, D. L. Nixon, O. A. Rotach, F. W. Stoller, and C. P. Wiggins as members.

This team was responsible to support the on-going investigations, establish and define the overall requirements, and prepare budget guidelines and a detailed Implementation Plan, including the cost and schedule to be presented at an OSTDS/TDA budget review in August 1975.

At the initial meeting in January 1975, the following assumptions were established:

- (1) Use of a Block IV receiver
- (2) Use of a coherent reference generator assembly
- (3) Enlargement of the primary reflector with shaping
- (4) Provision of simultaneous operation (2-way S-band; coherent X-band downlink)
- (5) Microwave hydrogen frequency reference from DSS 14 to DSS 12
- (6) The 34m subnetwork to be comprised of DSS 12, 42, and 61
- (7) No X-band uplink
- (8) Planetary ranging to be included

The study resulted in an Implementation Plan for \$7400k for hardware for three major subsystems; Antenna Mechanical, Antenna Microwave, and Receiver-Exciter. It did not include station electronic equipment. In addition to this basic plan, there were three main options proposed. These options were an aperture increase, shaping, and a 65-kW S-band transmitter, for a total cost of \$3500k. After the plan was presented to OSTDS, the configuration and costs for a baseline system were reviewed. At this stage the required station electronic equipments were added.

After this study effort was completed and presented to OSTDS, the following decisions were made in December 1975:

- (1) Recommended stations were DSS 12, DSS 44, and DSS 62.
- (2) Authorized immediate initiation of design for DSS 12.
- (3) The antenna diameter is to be 34 meters. The 34m design will be reviewed prior to proceeding with the hardware.
- (4) Schedule to be per Figure 10 shown in subsection H.
- (5) Defer all performance enhancement options.

The main options deferred were the 65-kW S-band transmitter and antenna shaping. The baseline concept included the use of existing S-band microwave components such as switches, duplexers, filters, and a maser. The use of the existing Block III Receiver-Exciter Subsystem modified to receive X-band was selected. The deferred performance enhancement options were as follows:

- (1) Electric drives for the antenna
- (2) Antenna thermally painted
- (3) Facility modifications at DSS 13 for cone assembly testing
- (4) Increased S-band doppler frequency range
- (5) 3-Hz loop for the Receiver-Exciter Subsystem
- (6) Remote control for S-X and S-S translators
- (7) Remote control for S-band polarization

Thus the 26m S-X Conversion Project was initiated with the start of the hardware design for DSS 12, and the Project was funded in FY 76. Using

the previous work of the study team, the assigned personnel from the Telecommunications Science and Engineering Division and the TDA Engineering Office embarked on the development of a Data Systems Development Plan (DSDP) for the project, which was completed and published on 1 July 1976.

The resulting efforts of the team were the above DSDP and budget plan for the task.

C. FINAL PROJECT ORGANIZATION

The Project was organized with a Programmatic Manager, R. Z. Toukdarian, and Project Manager, V. B. Lobb. This was effective on 1 October 1976. The Project Manager and Programmatic Manager reported to the TDA Engineering Office managed by Dr. Nicholas A. Renzetti, assisted by Malvin L. Yeater. They in turn reported to William H. Bayley. The Project, representing the TDA Engineering Office, interfaced with the Telecommunications Science and Engineering and the Applied Mechanics Divisions in the implementation of the S-X Conversion Project through the TDA Division representatives. This is shown in Figure 4. The interface with OSTDS and TDA was through the Programmatic Manager.

Cognizant development engineers and technical group supervisors were assigned to each major component of the electronics and antenna modifications and were responsible through their line management to the Project Manager for the design, engineering, procurement, testing, delivery, and installation of their assembly. In the execution of this task, the Project Manager used a close working relationship with H. R. Buchanan, E. L. Yinger, and C. B. Bricker to ensure that technical progress, reviews, budgets, and problem solving were accomplished.

Initially, C. Koscielski, JPL Goldstone Complex Manager, was responsible for the DSS 12 site implementation. Later in the Project he selected J. Curtright to manage this task. J. Curtright worked closely and diligently with the Project Manager in overcoming many difficult problems that occurred in the implementation of the DSS 12 station. This Project organization is shown on Figure 5.

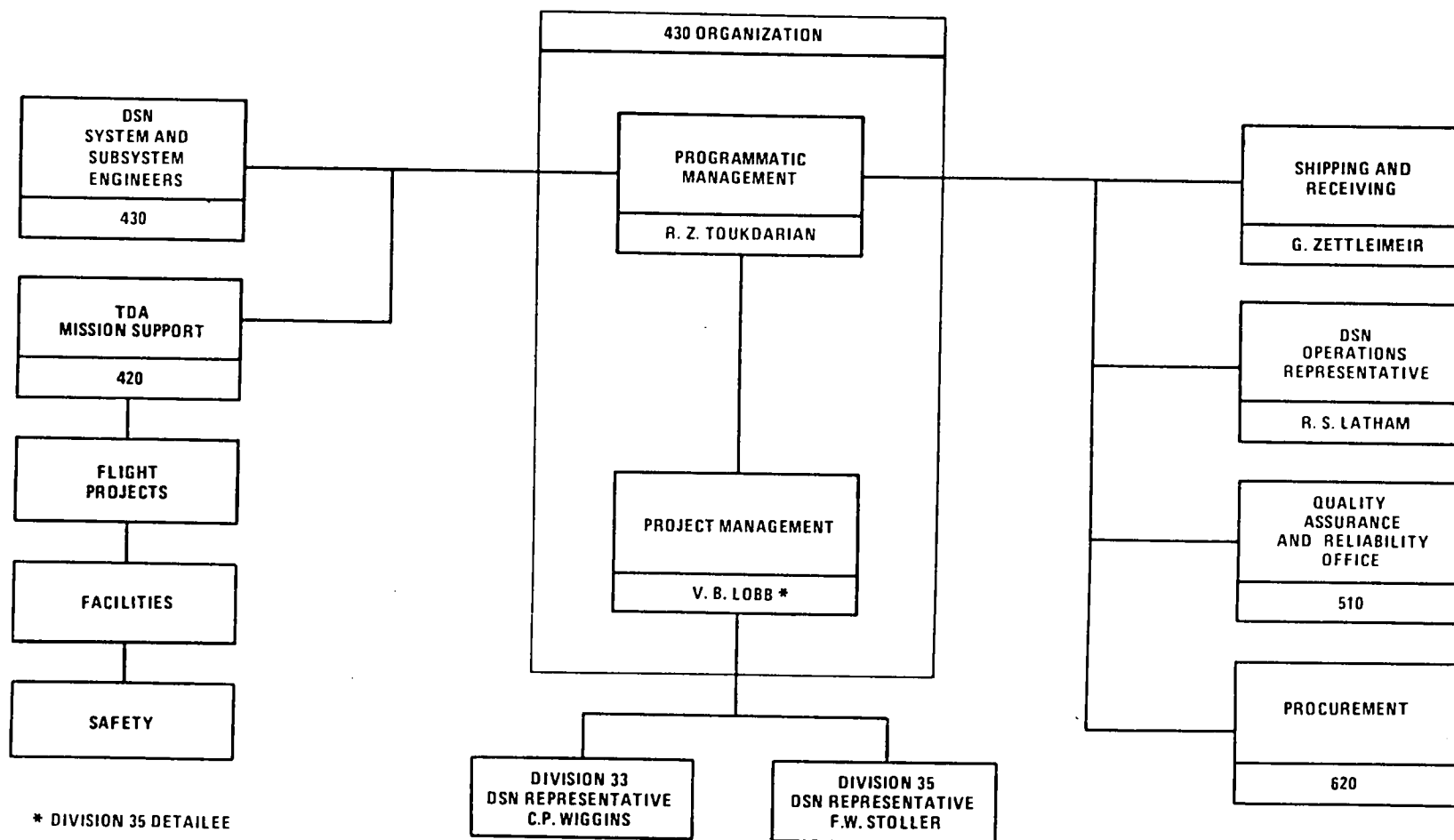


Figure 4. 26M Conversion Project

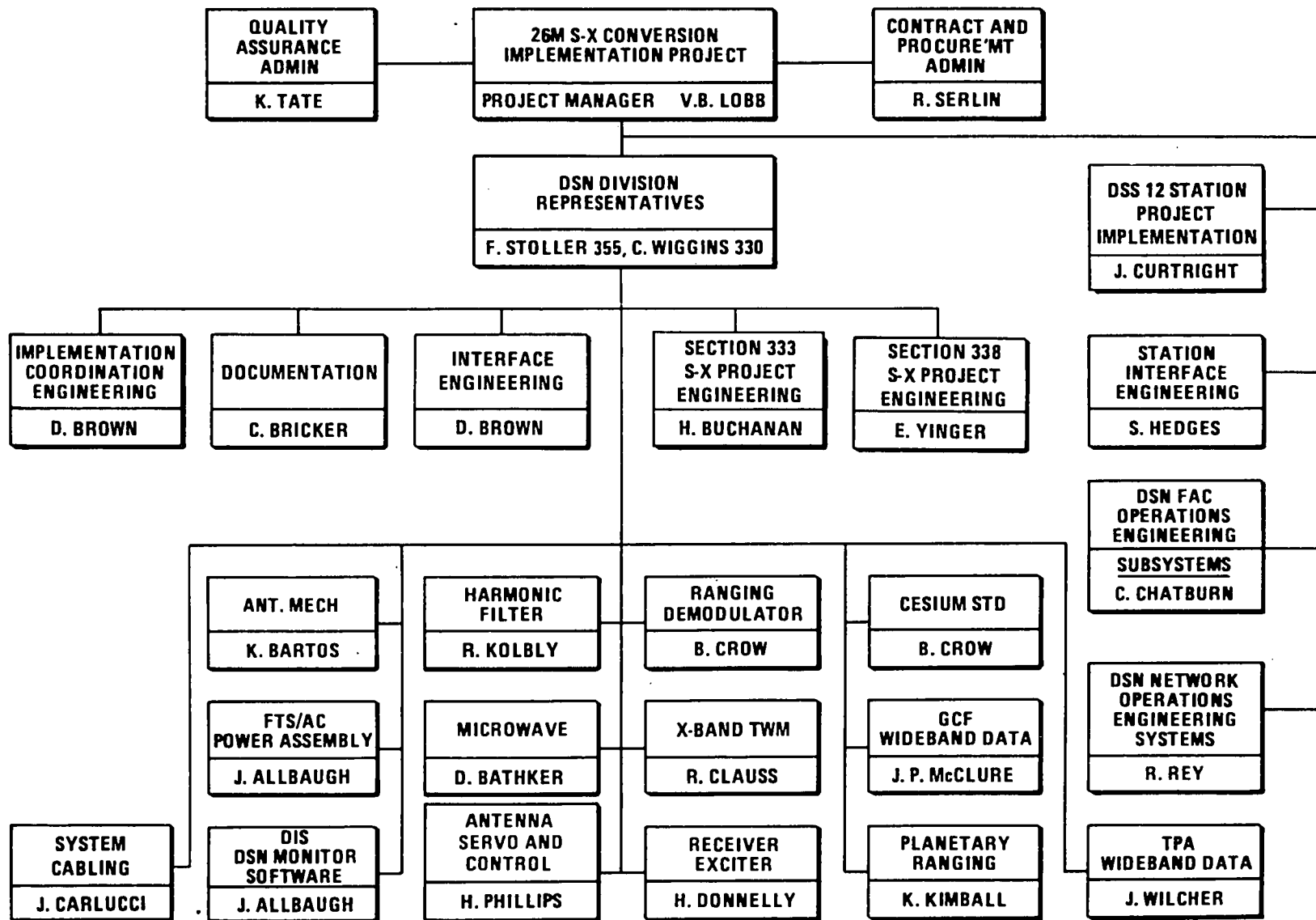


Figure 5. Implementation Project

The Project Team represented many years of practical experience in the areas of responsibility. Figure 6 shows the functional work assignments down to the working engineer level.

D. IDENTIFICATION OF SPECIFIC REQUIREMENTS AND CONSTRAINTS

The S-X Conversion Project was designed to suit the spacecraft designs and mission profiles for the Pioneer Venus and Voyager projects, which were selected for a detailed telecommunications link analysis. The former had S-band requirements, while the latter had both S- and X-band requirements, with telemetry on X-band. These two spacecraft designs are highly representative of the classes of spacecraft needed for the proposed missions shown in the NASA-OSTDS Mission Set.

Having made this selection, the key parameter of the DSN portion of the link was the ratio of the gain (G) of the ground station antenna to its total system noise temperature (T); i.e., G/T. This parameter was key because the spacecraft transmitter power and antenna gains were already selected on the basis of link performance using a 64m station. For these representative projects to accept alternate support from the 34m S-X converted stations, the station performance must meet, to a reasonable degree, the Project's mission objectives. Future projects may have somewhat more flexibility, but the problem at hand was to achieve a practical level of 64m station off-loading during the early 1980's. That could only be done by maximizing the antenna gain and minimizing the system noise temperature, each within practical limits, for the 26m station S-X upgrade.

The starting point for performance evaluation was to determine whether or not the present 26m diameter antenna could fulfill Pioneer Venus and Voyager navigation and telemetry requirements. The first approximation was to employ a straight frequency-scaling factor to extrapolate present S-band performance up to X-band. Next, it was necessary to adjust downward the scale factor to include the effects of increased aperture blockage caused by a reflex S- and X-band antenna feed system compared to an S-band-only feed. Thirdly, and much more difficult, some evaluation

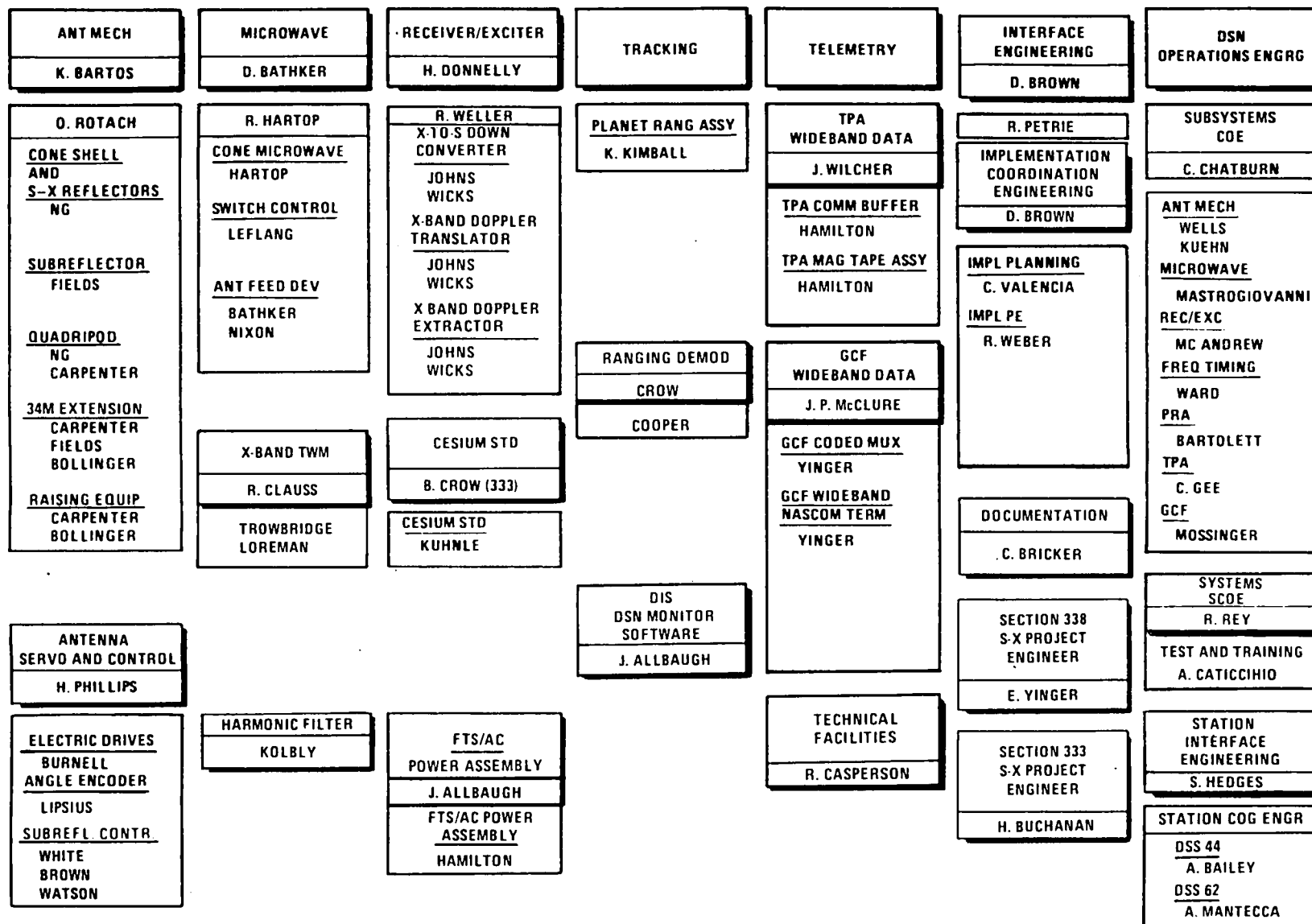


Figure 6. Functional Work Assignments

had to be made regarding the influence of the reflex feed design (i.e., aperture blockage) on the total system noise temperature, independent of the waveguide portion of the feed design.

The aperture blockage (reduced efficiency) gain loss correction can be evaluated using graphic scale drawing techniques, wherein the size of the hyperbolic subreflector and Cassegrainian cone structure can be determined for various antenna diameters. The S-band gain of a given size dual S-X antenna aperture then can be calculated relative to the present 26m antenna design. The graphic results appear in Table I.

Table I. Dual Feed S-band Relative Performance vs Antenna Diameter

Antenna Diameter (Meters)	Area Gain (dB)	Blockage Loss (dB)	Relative Aperture Gain (dB)
26	Ref	-0.31	-0.31
28	+0.64	-0.24	+0.40
30	+1.24	-0.19	+1.05
32	+1.80	-0.15	+1.65
34	+2.33	-0.11	+2.22

While the data in Table I ignores the impact upon G/T of the antenna pattern side-lobe (including back-lobe) structure as it relates to system noise temperature, two aspects become immediately apparent. First, there is a reduction of at least 0.31 dB in 26m S-band gain performance; and second, this reduction can be rapidly offset by an increase in antenna diameter (columns 2 and 3 change in opposite directions).

It was clear that at S-band if the performance was not to be degraded by the addition of X-band, some diameter increase would be required.

The X-band telemetry performance was the key factor in the selection of the 34m antenna diameter based on the following:

- (1) To achieve the Voyager far-Jupiter encounter video playback rate of 67.2 kb/s with a small allowance for weather degradation, the

antenna diameter had to be extended to 34m. The Voyager maximum video playback rate could, therefore, be achieved with a 34m diameter antenna.

- (2) For the Voyager Saturn encounter, a 34m S-X antenna diameter could provide a limited backup to the 64m subnetwork; under ideal conditions it could support the 21.6 kb/s (playback) or 19.2 kb/s (real-time) video in the event of a 64m station failure. However, if available, the 64m station would normally be used to support either the 44.8 kb/s or 29.87 kb/s video modes. These rates are beyond the expected capability of the 34m S-X-band station.
- (3) The next smaller antenna size considered (using practical construction steps) was the 30m diameter. In terms of Voyager projected performance, the far-encounter data return from Jupiter would possibly drop to the 44.8 kb/s mode. This would cause an interruption to the navigation tracking pattern, requiring interspersed 64m station passes. At Saturn, the science and engineering data return would drop to the 7.2 kb/s (nonvideo) mode, thereby greatly reducing the potential 64m station backup capability.

From the foregoing, it became quite evident that there was a marked increase in the usefulness to Voyager of a 34m antenna enlargement compared to that provided by a 30m diameter. It was, therefore, concluded that the S-X Conversion Project should be implemented using a 34m diameter aperture. The functional requirements for the various systems for the addition of X-band receive capability and an increase in antenna diameter to 34m follow:

1. DSN Tracking System.

- a. Single Station S-band Doppler Requirements:

Doppler accuracies had to be less than 0.045m (0.1476 ft) and 1.0m (3.3 ft) when integrated over 60 seconds or 12 hours,

respectively, for round-trip light times of 1.5×10^4 seconds.

b. Single Station Differenced S-X-band Doppler Requirements:

Differenced S-X-band doppler accuracy had to be less than 0.045m (0.1476 ft) and 1.0m (3.3 ft) when integrated over 60 seconds or 12 hours, respectively. S-X-band doppler is used for charged particle calibration.

c. Two-Station S-band Doppler Requirements:

Each station must meet its single-station doppler requirements. In addition, interstation frequency synchronization knowledge had to be less than 3.3 parts in 10^{13} .

d. Single-Station S-band Range Requirement:

S-band range data accuracy had to be less than 30m (99 ft) for navigation; however, it is anticipated that a future radio science accuracy requirement will be less than 3m (9.8 ft).

e. Two-Station Range (Near-Simultaneous) Requirement:

Two-station S-band range accuracy had to be less than 3m (9.8 ft) for each station. Differenced S-X-band range accuracy of 1.0m (3.3 ft) was required at each station for charged particle calibration.

f. Differenced Range Versus Integrated Doppler (DRVID) Requirement:

DRVID stability of less than 1.0m (3.3 ft) was required over periods of 60 seconds to 12 hours for charged particle calibration.

In addition to the above, the Network Tracking System places the following requirements on the Frequency and Timing Subsystem:

- a. Interstation time synchronization of <20 ms.
- b. Interstation frequency synchronization of better than 3.3 parts in 10^{13} .
- c. Frequency stability of better than 5 parts in 10^{13} from 100 seconds to 12 hours.

2. DSN Telemetry System

a. RF Carrier Reception:

Simultaneous S- and X-band carrier: One each

Frequency Range: S-band 2290-2300 MHz
X-band 8400-8440 MHz

Gain S-band 56.1 \pm 0.6 dBi
X-band 66.9 \pm 0.6 dBi

System Noise
Temperature: S-band 27.5 \pm 2.5 K (diplexed mode)
X-band 25.0 \pm 2.0 K

Polarization: S-band Selectable RCP, LCP, Manually
Rotatable Linear
X-band Selectable RCP, LCP

b. Symbol Synchronization and Channel Decoding:

One stream 8 to 250,000 symbols per second (s/s) (coded or uncoded) and one stream at 40 s/s (uncoded)

Decode long constraint convolutional (sequential decode) up to 2048 b/s maximum.

Decode short constraint convolutional (Viterbi decode) up to 115 kb/s maximum.

c. Ground Communications:

Both high-speed and wideband output to Mission Control and Computing Center.

3. DSN Test and Training System

- a. Implementation of an X-band test carrier capability in the Receiver-Exciter Subsystem, and an interface to permit input of a simulated telemetry subcarrier from the Simulation Conversion Assembly. Comparable capabilities are also required at the Compatibility Test Area.
- b. Implementation of the Wideband Data (WBD) Subsystem interface to the existing WBD input port of the Simulation Conversion Assembly for mission simulation support.
- c. Implementation of Wideband Data Subsystem interfaces to the Communications Monitor and Formatter (CMF) Assemblies so that the backup CMF can be used for system performance testing of the Network Telemetry System.

The following paragraphs keynote the required changes to the DSN subsystem functional requirements resulting from the introduction of an X-band receive capability into the new 34m class subnetwork. These subsystem changes derive either directly or indirectly from the foregoing changes to the DSN systems requirements.

4. Antenna Mechanical Subsystem

Antenna diameter: 34m

Feedcone: Adequate to house both S- and X-band components in a single cone

Pointing Accuracy: 0.039 degrees root-sum-square (RSS) in a 48 km/h (30 mi/h) wind with no external compensation

Surface Tolerance: 0.039 inch rms maximum in a 48 km/h (30 mi/h) wind

Slew Rate: Not less than 0.4 deg/s, both axes

Tracking Rate: 0.001 deg/s minimum, both axes

5. Antenna Microwave Subsystem

The 34m S-X functional requirements are included in the Telemetry System requirements (paragraph 2).

6. Receiver-Exciter Subsystem

- a. An X-band (1 GHz) to S-band (2 GHz) down-converter compatible with the input of the Block III DSN receiver. The down-converter is driven by the output signals of the standard 8 GHz traveling-wave maser amplifier. The 8-GHz band signal-to-noise ratio is as specified in the Telemetry System requirements (paragraph 2). The S-X down-converter will not degrade this signal-to-noise ratio by more than 0.2 dB.
- b. Doppler frequency shift extractor for 8-GHz band operations. This extractor handles two-way (2-GHz uplink and 8-GHz downlink) doppler frequency excursions originated by relative DSS versus spacecraft velocities from 0 to +80 km/s (50 mi/s). Performance should be comparable with the 64m doppler extractor.

- c. Ranging demodulator capability compatible with the 2-GHz uplink and 8-GHz downlink band configuration. The demodulator should operate with the continuous and discrete spectrum codes and meet the 64m ranging demodulator performance requirements.
- d. Modification of the existing S-band test and calibration capabilities is required to support the X-band configuration.

7. Transmitter Subsystem

- a. Fourth Harmonic Filter. The S-band Transmitter Subsystem for the 34m S-X stations is equipped with a harmonic suppression filter in its output to reduce the uplink spurious radiation in the 8400 to 8440 MHz band to a level below that which the X-band receiver channel can obtain phase lock, and to levels outside this band which would raise the X-band system noise temperature by a maximum of 1 degree Kelvin.
- b. Transmitter Shielding. The S-band Transmitter Subsystem, as repackaged for the 34m S-X stations, is sufficiently well-shielded to:
 - (1) Prevent any station-internal performance degradation
 - (2) Comply with all pertinent governmental radio frequency interference regulations
 - (3) Meet all pertinent governmental, JPL, and DSN regulations and/or specifications pertaining to personnel radiation hazard.

All enclosure covers or doors, etc., are interlocked so that transmitter operation is prevented if removal and/or opening of the closure material violates any of the foregoing three criteria. Further, the packaging design provides for both transmitter adjustment and all but major maintenance without the necessity of removing any of the above enclosure material.

8. Frequency and Timing Subsystem

The Frequency and Timing Subsystem was to provide any new required reference frequencies to the X-to-S-band down-converter or to the Test and Training Subsystem for X-band test signal generation.

In order to provide sufficient long-term frequency stability for outer planet navigation (and potential VLBI applications to increase the utility of the S-X-band conversion), an upgrade of the existing 26m frequency standards was required. Two new standards (one portable) per converted station were required. Each has the following stability performance characteristics:

One part in 10^{11} for 1-second averaging

5 parts in 10^{12} for 1000-second averaging

One part in 10^{13} for 12-hour averaging

One part in 10^{13} for 10-day averaging

In addition, a capability was required to synchronize these station standards (both in frequency and time) against the hydrogen maser master standard located at the 64m stations. Portability of one of the two standards at each converted station met this requirement.

The constraints placed on the project were primarily the least expenditure of NASA resources, which meant the following limits were followed:

- a. The maximum use of existing equipments and facilities.
- b. That any equipment replaced for nonfunctional performance reasons would pay for itself via reduced maintenance and operations costs within a 5-year period.

- c. Any desirable enhancement for performance or operations which did not meet the criteria of b above would be held for future options.

A second general constraint was that a design review be held of the raising methods and procedures for the antenna as a whole and its safety prior to proceeding with the S-X Conversion Project. The review was held and authorization to proceed was given to the project.

E. SCHEDULE RISK

An independent study was performed to ascertain the risk associated with the 26m S-X Conversion Project. The study concluded that the technical approach presented was sound, but that there was concern regarding the schedule. Of particular concern was the 1 December 1978 operational date for Goldstone. The flight projects had no flexibility to delay their respective planetary encounters should unforeseen circumstances cause the implementation at DSS 12 to slip. On the other hand, the budget guidelines were not amenable to an earlier start at Goldstone. The study therefore undertook to evaluate two alternatives: (1) the selective acceleration of certain critical or pacing items to ensure on-site delivery of the equipment well before the DSS 12 scheduled downtime; or (2) the possible use of Goldstone developmental station DSS 13 to relieve the need for DSS 12 to be converted to S-X operation by 1 December 1978. The relative merits and/or demerits of these two alternatives are discussed in the following paragraphs.

An item-by-item study of the subelements and their schedules revealed that there were, indeed, several items whose fiscal year funding paced the overall readiness of the equipment due to installation at Goldstone. A schedule, Figure 7, was then developed that provided for an earlier delivery to Goldstone of the pacing items. To minimize the risk of unforeseen delays, a 3-month contingency factor was employed.

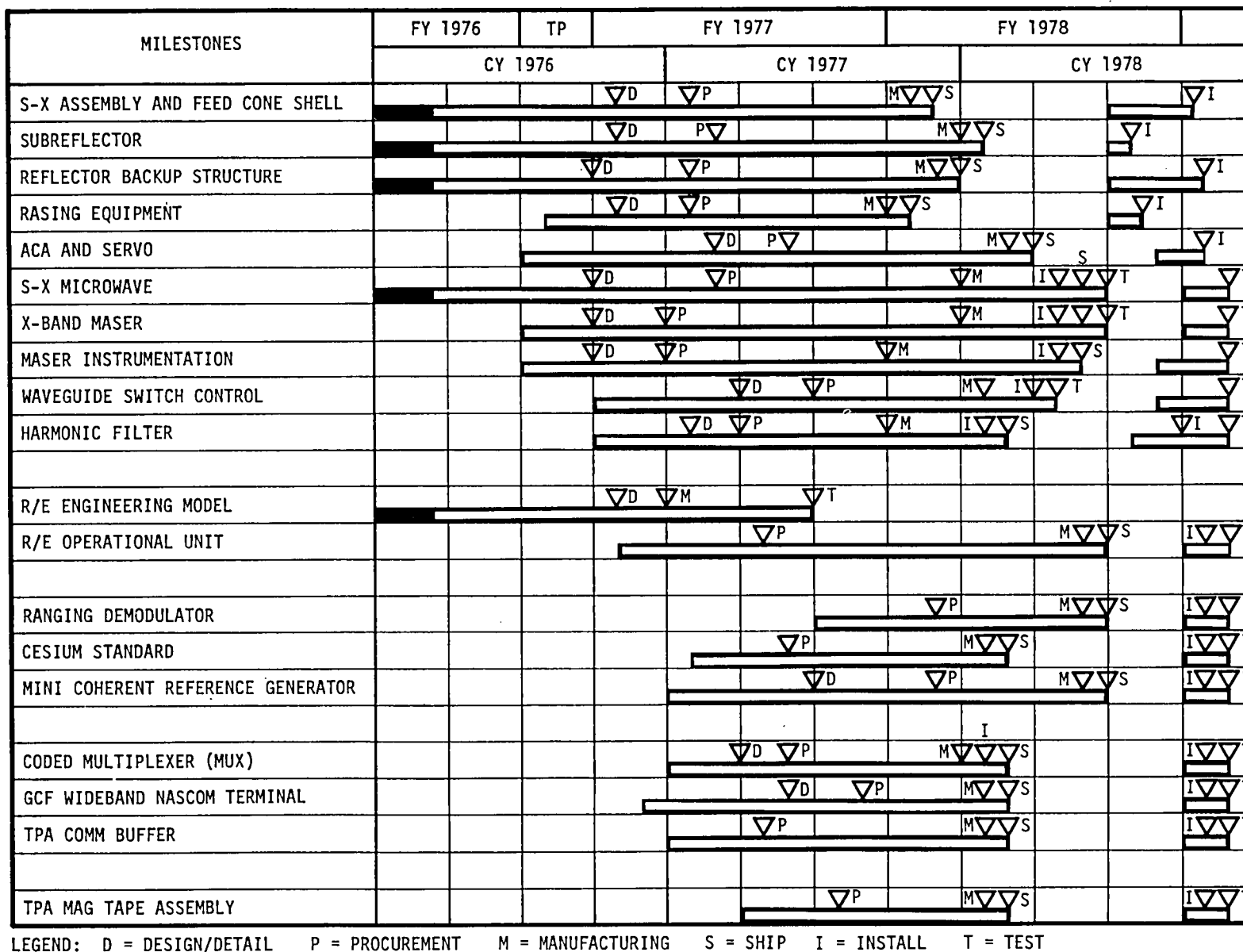


Figure 7. DSS 12 Modified Overall S-X Conversion Schedule

The schedule impacted the FY 76 funding, as shown in Table II, with the most significant element being the shift forward of \$490k from FY 78 into prior fiscal years, particularly into FY 77. There was no net change in the run-out cost of the equipment budget and only a relatively minor change in the engineering budget, which was accommodated by adjustments within other tasks.

The other alternative to reducing the risk was to consider methods by which the Goldstone developmental station (DSS 13) could be used to support the high density support requirements from December 1978 through September 1979. After reviewing the types and amount of equipment available at DSS 13, the most practical approach appeared to be the use of DSS 13 to support the Voyager X-band requirements, while the present 26m S-band capability of DSS 12 was concurrently employed to support the Voyager uplink and downlink S-band requirements. It was thought that such a two-station combination would provide the needed off-loading of Voyager support from the Goldstone 64m station and at the same time allow the S-X conversion of DSS 12 to be delayed until at least the Fall of 1979.

The salient capabilities of the modification to DSS 13 were as follows:

- (1) X-band listen-only configuration
- (2) Carrier detection -- microwave baseband telemetry to DSS 12 for detection and processing
- (3) Three-way coherent ranging
- (4) Three-way coherent doppler
- (5) Partial metric data transmitted by high-speed data lines

The design and implementation approach included minimizing engineering and new equipment requirements, minimizing a total equipment implementation at DSS 13, utilizing the DSS 12 capability as much as possible, and using existing SRT equipment where applicable.

Table II. Resource Impact of Accelerated S-X Conversion Schedule
Relative to WAD 76-1

Item	OBLIGATIONS									
	FY 76		TP		FY 77		FY 78		Net Chance	
	MY	\$K	MY	\$K	MY	\$K	MY	\$K	MY	\$K
Engineering (311-)										
Microwave	--	--	--	--	--	+15	--	+15	--	+30
Receiver-Exciter	--	+8	--	+8	--	+30	--	+30	--	+76
Ranging Demodulator	--	--	--	--	+0.2	+20	--	--	+0.2	+20
Cesium Standard	--	--	--	--	+0.2	+30	--	--	+0.2	+30
Minicoherent Reference Generator	--	--	--	--	+0.5	+28	-0.5	-28	--	--
Wideband Data	--	--	--	--	+0.2	+11	--	--	+0.2	+11
Subtotal \$K	--	+8	--	+8	+1.1	+134	-0.5	+17	+0.6	+167
Equipment (312-)										
Antenna Mechanical	--	--	--	+26	--	-26	--	--	--	--
Microwave	--	--	--	--	--	+45	--	-45	--	--
Receiver-Exciter	--	+45	--	+8	--	+255	--	-308	--	--
Recording Equipment	--	--	--	--	--	+41	--	-41	--	--
Minicoherent Reference Generator	--	--	--	--	--	+33	--	-33	--	--
Wideband Data	--	--	--	--	--	+63	--	-63	--	--
Subtotal \$K	--	+45	--	+34	--	+411	--	-490	--	--
Change Total \$K	--	+53	--	+42	+1.1	+545	+0.5	-473	+0.6	+167

A block diagram of the modified DSS 13 station is shown in Figure 8. The Block III receiver shown within the broken lines was a NASA spare.

The proposed schedule for the DSS 13 alternate plan is shown in Figure 9. It should be noted that the Receiver S-X Converter schedule in Figure 9 was the same as the Receiver-Exciter Operational Unit schedule in Figure 7. In other words, there was no additional schedule relief for this critical item as a result of using the DSS 13 alternate plan.

The following list of constraints regarding the maintenance and operation of DSS 13 as an element of the operational DSN was developed, along with an estimate of the DSS 13 X-band performance (Table III) compared to expected performance of DSS 12 as a 34m S/X station:

- (1) Augment DSS 13 staff rather than use normal maintenance and operations personnel.

- (2) Spares philosophy:

- (a) Support operational equipment from network
 - (b) Some R&D equipment requiring spares procurement

- (3) Sustaining engineering:

- (a) Additional engineering required for nonstandard equipment
 - (b) Operational equipment to be sustained by normal sustaining and change order activity (COE and CSE)

In addition, assuming the DSS 13 antenna subreflector was replaced, the loss of 1.6 dB in X-band performance due to the 26m diameter of DSS 13 would have a significant impact on the amount of Voyager X-band telemetry that could be supported.

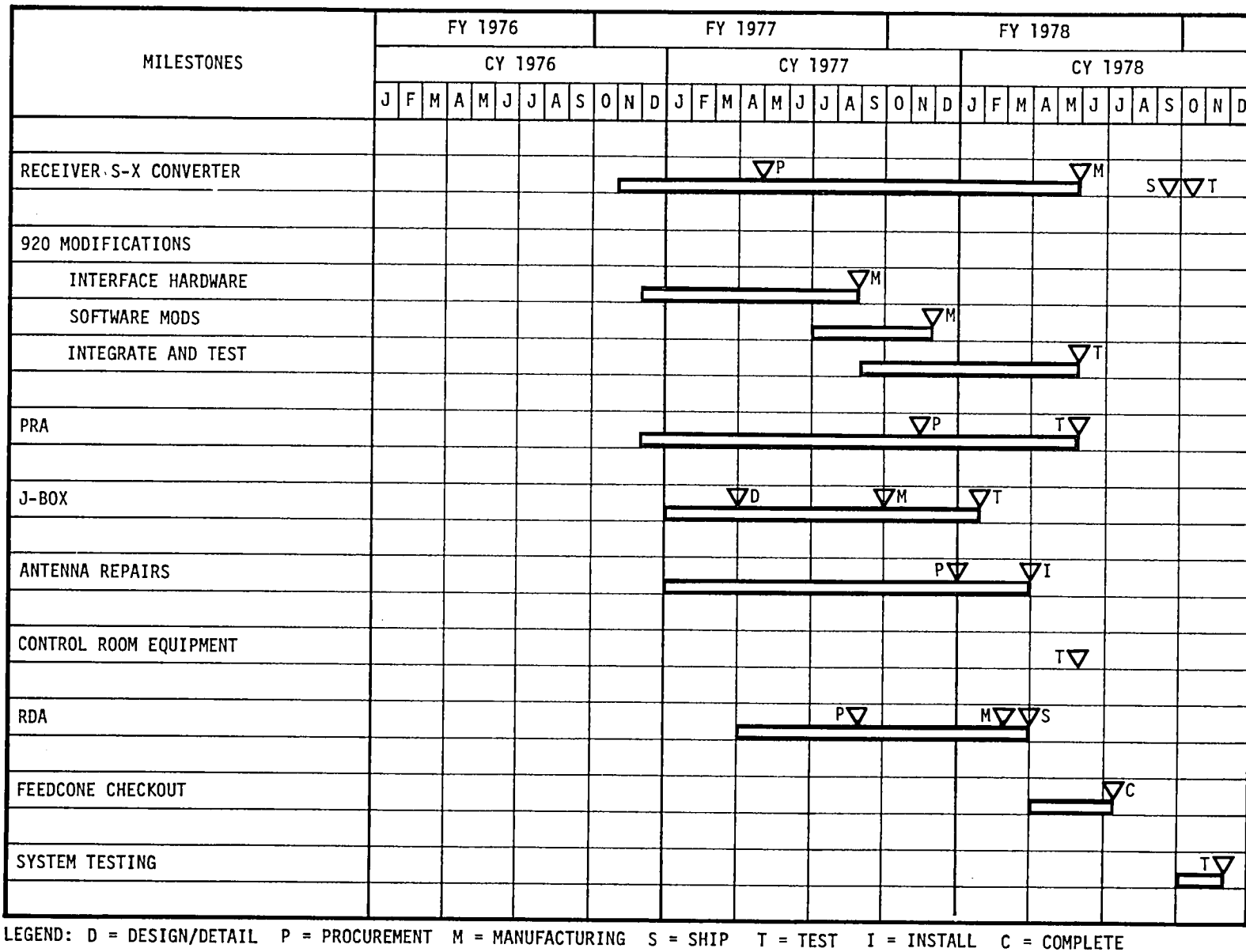


Figure 9. DSS 13 Alternate Plan Schedule

Table III. DSS 13 Alternate Plan, Expected X-Band RF Performance Comparison

Item	26M DSS 13	34M DSS 12	DSS 13 Difference
Antenna Gain ($\eta = 55\%$)	+64.5 dB	+66.9 dB	-2.4 dB
Subreflector Loss	-1.0 dB	---	-1.0 dB
System Noise (30-degree elevation)	26 K	31 K	+0.8 dB
Net System Noise	---	---	-2.6 dB
Net System Noise (Replace Subreflector)	---	---	-1.6 dB

Other degradations or risks within the overall DSS 13/DSS 12 system involved the following:

(1) Telemetry:

(a) Expected degradation for baseband microwave to DSS 12 was less than 0.3 dB.

(b) Required microwave phase stability test for assurance.

(2) Doppler:

(a) Required frequency reference cleanup loop and timing reference

(b) Required detailed navigation analysis to determine expected performance.

(3) Ranging:

(a) Three-way capability existed in Planetary Ranging Assembly but was untried.

(b) Required detailed accuracy study and navigation analysis

There was, therefore, some concern that the overall performance for both navigation and telemetry might not be sufficient to achieve a significant level of off-loading from the Goldstone 64m station.

In addition to the points already mentioned, the DSS 13 alternate plan raised several issues for which answers were not immediately available. These issues were as follows:

- (1) Use of DSS 12 conversion equipment for DSS 13.
- (2) DSS 13 support of Voyager navigation requirements.
- (3) Accuracy of coherent three-way ranging and doppler for navigation.
- (4) Impact of SRT automation and radio science support.
- (5) Antenna elevation drive repair at DSS 13.

F. PROJECT PHASES

1. Concept and Design Studies Phase

The concept of the 26m S-X conversion was formulated over a period of several months and covered three main areas of definition. The largest antenna diameter extension that could be implemented was the basic issue to be determined before the RF configuration and system gain and noise temperature could be defined. The next choice was whether to use a new Block IV Receiver-Exciter Subsystem or to provide an X- to S-band down-converter for the Block III Receiver-Exciter Subsystem existing in the 26m S-band stations.

The third area considered was to use electric drives versus retention of the existing hydraulic drives. The decision was made to replace them based on energy savings and maintenance and operations costs that had a payback period of less than 5 years.

The study indicated that an extension of the antenna diameter to 34m was the largest that could be implemented. Since it was necessary to either raise the antenna or to dig a trench for antenna diameters in excess of 30m, a comparison was made of the two diameters to determine cost and performance factors of each.

The results of the concept and design studies were as follows:

- a. Use a 34m diameter antenna on raised pedestals rather than digging trenches.
- b. Use an X-to-S band down-converter for the existing S-band Block III receiver-exciter.
- c. Use a parabolic (not shaped) offset reflex feed microwave system with gain at 66.9 dB (at X-band) and 27.5 K noise temperature (at X-band).
- d. Use electric drives in place of the existing hydraulic drives on the antennas.

It was, however, evident that a more definitive and specific design effort was required to enable a sufficiently comprehensive definition of the total antenna and electronics modifications. This effort was funded by NASA and JPL, and proceeded into the design phase.

2. Design Phase

The design phase was done from 1 July 1976 to 1 July 1977, with various subsystems completing the design at different points in time and with some site-specific designs lasting beyond July 1977. The DSS 44 antenna design was halted after significant effort was expended, and a decision was made by NASA and the TDA Office to convert DSS 42 instead of DSS 44. This decision necessitated an additional 3 months of design to adapt the DSS 12 design to the DSS 42 antenna. The DSS 42 antenna was an hour angle-declination (HA-dec) mount type similar

to DSS 12 instead of the X-Y antenna mount type of DSS 44, which is totally different and not adaptable.

The decision to change from the original selected stations of DSS 44 and DSS 62 to DSS 42 and DSS 61 was made principally on the dollars which could be saved by NASA if it became necessary to close a subnetwork of the 26m stations. Both DSS 44 and DSS 62 were stand-alone stations, while DSS 42 and DSS 61 were conjoint or co-located, and shared equipment with the 64m antennas.

Some savings were realized by deleting the requirement for cesium frequency standards at these two stations since they already were in place.

Another change that occurred during the design phase was the advance of the DSS 61 antenna schedule by one calendar year to provide more operating time with the new converted antennas prior to the Voyager Jupiter encounter. The principal effect of this change was to move \$1900k dollars of hardware funds ahead to FY 78; \$1500k from FY 79 and \$400k from FY 80. The drawback to this plan was a loss of time to debug any problems that might occur on the first antenna hardware before being well into the procurement of follow-on hardware. Both the DSS 61 move-ahead of one year and the change of antenna stations were implemented.

The DSS 12 design when applied in the field proved difficult in the area of electric drive design. The problem areas included difficulty in setting and maintaining the counter torque settings, thermal overheating of relays in the power amplifier cabinet, and poor air circulation in the cabinet. In addition, there was a violent cyclic action on declination that occurred when one of the two declination motors dropped out because of the above-mentioned problems. Engineering changes were made to the hardware at DSS 12, which was the

initial station. These hardware changes corrected the problems at DSS 12 and hardware modification kits were subsequently sent overseas to be installed at DSS 42 and DSS 61.

3. Fabrication Phase

The fabrication phase basically started in FY 77 for DSS 12 and FY 78 for DSS 61 and DSS 42. The approach taken was to contract with vendors on the hardware assembly level. Typical examples of hardware procured in this way are the S-X reflex reflector and feedcone shell, subreflector and quadripod, servo electronics, harmonic filter, cesium standard and reflector panels for the extension. Examples of hardware fabricated at JPL are the receiver-exciter, waveguide switch control, and subreflector control.

The original plan for the receiver-exciter was to contract the fabrication of the overseas units to drawings that were to be made and corrected upon completion of the first unit for DSS 12 at Goldstone. The move-ahead of DSS 61 by a year made this option infeasible, and the overseas units were also fabricated at JPL. This change resulted in a significant reduction in the cost of the receiver-exciter units for the overseas stations.

The reflector backup structure extension, reflector structure reinforcement, and the declination and hour-angle wheel modification hardware for the overseas antennas were fabricated in Spain by Talleres de Coslada, who also did the installation work for the DSS 42 antenna. The work was well done and fit well in the field when erected.

4. Installation Phase

The installation phase started on 1 June 1978 at DSS 12 and was completed 1 May 1980 at DSS 42. The installation effort involved up to 140 separately scheduled tasks that were to be done by an

erection contractor and station personnel who were available from the operations crew and maintenance and integration personnel.

The period of installation varied from 5 months at DSS 12 to 6 months at DSS 42 and DSS 61. This period was followed by subsystem, system, and operational verification tests for 1 month at Goldstone and 6 weeks at Canberra and Madrid.

The plan, as mentioned earlier, was to have all hardware and documentation ready at preshipment transfer, 3 months before the downtime. The DSS 12 downtime was planned to start on 1 July 1978, with the preshipment transfer date being 1 April 1978. The downtime schedule was moved ahead 1 month to 1 June 1978, but it was not possible to move the preshipment transfer date back. In fact, for the first station (DSS 12), many hardware and documentation package deliveries were running into the contingency period. It was agreed with operations to use preliminary documentation in lieu of the complete documentation for their planning purposes.

During the contingency period, work by the antenna erection contractor was underway as the DSS 12 station continued to meet tracking commitments. This effort included installation of declination (dec) and hour angle (HA) wheel modifications, building and installation of the antenna lift frame, coring into the existing antenna foundation and installing reinforcing bars. In addition, quadripod and subreflector ground erection foundations were laid and preparation for site erection was made. Similiar work was done overseas prior to the station downtime, except for the installation of the declination and hour angle wheel modifications.

On 25 May 1978, all pertinent facts concerning the DSS 12 downtime start were reviewed at a project meeting. It was agreed to proceed with the downtime on 1 June 1978.

The station personnel stripped the antenna of all cables, power and utility conduits, servo lines and equipment, coolant lines, etc., in preparation for the erection contractor to begin his work. Work continued with the contractor essentially working days and the station personnel working nights to complete the scheduled 140 tasks.

Each of the three stations used a different erection contractor, and work was accomplished in a different manner. For example, installation of electric drives was done by a local contractor at DSS 12, by the main erection contractor at DSS 61, and by station personnel at DSS 42. Measurements and rework of existing panels at DSS 12 were done by the JPL fabrication shop. In Spain this work was done by the main erection contractor and in Australia by the station personnel.

The agreements as to what work would be planned and who would accomplish the effort were negotiated with the Program Office, the Station Directors, and the Project. These agreements were followed during the installation period without any significant exceptions.

The erection effort at DSS 12 went well except for some difficulties with the Ironworkers Union on who would handle the reflector panels for the extension. The Union stopped work for 2 days until a compromise was worked out. Also, because of a disagreement between the Contractor and the Union over travel time pay, work slowdowns and numerous calls to Cal/OSHA about safety were made by the Union steward. JPL Contracts negotiated a modification to cover some of the cost of the travel time to help resolve this issue.

The erection effort in Spain would have been completed on schedule except for an antenna accident that took 3 weeks to verify the damage and repair. This accident and repair is covered in greater detail in section V, subsection E.

The erection effort in Australia was completed 2 weeks ahead of schedule. This time was used to verify subreflector focus calibration and antenna gain as part of the 34m X-band Gain Loss Study. This is described in further detail in section V, subsection D.

5. Initial Antenna Operations

The DSS 12 antenna was operational on 2 December 1978 and was used to support the Voyager spacecraft in its cruise mode and far encounter phase. It was also used to support the Pioneer Venus mission, but more importantly, it off-loaded the 64m antenna during this peak tracking period.

During the month of November, several star tracks were run and an X-band gain loss of 1.5 dB from an anticipated gain of 66.9 ± 0.3 , -0.9 dB, or 0.5 dB below the lower minimum gain was discovered. Since this was below the minimum requirement and 1.2 dB below the calculated gain, some effort at correction was tried but proved unsuccessful.

A request to extend the downtime by 6 weeks was submitted to the Flight Projects to solve this missing antenna gain by dish realignment. Since the antenna performance was able to supply the needed project support, this request was denied. A limited downtime of a few days was supplied in January 1979 to replace an X-band maser. A limited amount of dish alignment from the top of the in-place feedcone was done. The net results were to improve the peak antenna X-band gain to 66.0 dB, or up by 0.5 dB.

All further work was deferred until the DSS 61 antenna conversion was completed to see if there was a systematic problem in the design or a station-peculiar problem. A complete description of the 34m X-Band Study Team results and DSS 12 modifications is covered in section V, subsection D.

G. PROJECT MANAGEMENT AND CONTROL

1. Major Contractors

Under the system management of JPL, many industrial firms from the United States, Canada, Spain, and Australia were involved in the Project.

The major contractors involved and the assembly or service provided were:

Capital Westward Corp. Paramount, CA	Feedcones, quadripods, subreflectors and replacement reflector panels for DSS 12
Toronto Iron Works Toronto, Canada	Reflector panels for all three stations. Rib extension structure and HA and dec modifications for DSS 12
Almas International Paramount, CA	Lift of the DSS 12 and DSS 61 antennas
Micro-T Pittsburgh, PA	Erection of the DSS 12 antenna modifications
Talleres de Coslada Madrid, Spain	Fabrication of the DSS 61 and DSS 42 rib extension structure and HA and dec modifications. Erection of the DSS 61 antenna modifications
Electric Power Transmission Sydney, Australia	Erection of the DSS 42 antenna modifications
Prodelin Inc. Santa Clara, CA	Installation of hardline cables at all three sites and installation of the power for the electric drives and the aircraft warning lights.

2. JPL In-House Support

The procurement of the hardware and contracts for the installation contractor at all three sites were handled by the JPL Procurement Division. Jack Shea and Hal McIntosh were very helpful in the procurement of the hardware.

A Quality Assurance Management Plan was published in January 1977. Quality Assurance engineers were assigned to the project during the fabrication stages, and each site had a full-time Quality Assurance engineer in residence during the installation. Supplemental assistance was furnished as needed. The conduct of their work was such that, although they worked directly with the project technical team, their line of supervision was under the JPL Quality Assurance Division, thus enabling independent objective evaluation of overall quality assurance aspects. Joe Kundrat, Carlos Flores, and Tom Such furnished the above service and were important to the successful completion of the Project. R. Sirpilla and K. Anhalt provided the interface in the formation and assignment of the Quality Assurance Program for the Project.

The overseas antennas were implemented under the direction of T. Reid in Australia and J. Fernandez in Spain. Their selected representatives were Allen Bailey in Australia and A. Manteca in Spain, who were the Station Cognizant Engineers for the DSS 42 and DSS 61 station implementations. The JPL site resident engineers and alignment engineers for those stations and for the DSS 12 effort were as follows:

- a. DSS 12 J. Carpenter and E. Fields
- b. DSS 42 R. Van Hek and E. Fields
- c. DSS 61 O. Rotach and J. Carpenter

The assembly and inventory of the electronic modification kits for DSS 12 and supporting efforts for the implementation of the DSS 12, DSS 42, and DSS 61 antenna modifications were provided to the Project by W. Bollinger, who was assisted by J. May, J. Horner, and D. White. Their efforts, particularly in the solution of the DSS 12 problems, were critical to the accomplishment of the Project.

3. Reporting and Review

Reporting was continuous throughout the Project and provided information in the depth required for the NASA Office of Space and Data Systems (OSTDS) and JPL management control and evaluation. Internal JPL weekly reports were prepared based on material from each activity location and daily observation of each technical area. These reports covered the progress and schedule status in narrative and tabular form. Monthly narrative letters were provided by JPL to the OSTDS, based on the weekly reports and on the evaluation of monthly reports submitted by the cognizant engineers.

Report formats were kept as simple as possible, using photographs to show the progress and status. Expensive printing and excessive detail in reporting were avoided to minimize costs.

Schedule monitoring was based on simple forms: bar and activity block charts. In addition, a standard progress status report form was used twice a month that could be quickly filled in and forwarded to the project manager.

Formal reviews were held as follows:

- a. Review "B" DSN System Requirements and Design
- b. Review "C" DSN Subsystem Requirements
- c. Review "D" DSN Subsystem Functional Design
- d. Review "E" DSN Subsystem Detail Design

In addition to the above reviews, progress and status reviews were held every 2 months until the implementation in Australia for DSS 42 had started.

H. SCHEDULE EXPERIENCE

A steady pace was maintained in schedule activities from the official beginning of the Project in October 1976 through June 1980 (a total of 45 months) to completion and full operational status.

Figure 10 shows an overall schedule dated 1 December 1977 for DSS 12, the first station to be implemented. Figure 11 shows the major milestone schedule for all three converted stations. The downtime dates for the three stations were planned as follows:

	<u>DSS 12</u>	<u>DSS 61</u>	<u>DSS 42</u>
Off-Track before	Jun 3, 1978	Aug 9, 1979	Oct 1, 1979
Implementation completed before	Oct 1, 1978	Jan 9, 1980	Mar 1, 1980
Subsystem Testing completed before	Oct 17, 1978	Jan 24, 1980	Mar 16, 1980
System Testing completed before	Nov 1, 1978	Feb 9, 1980	Apr 2, 1980
Test and Training completed before	Dec 1, 1978	Mar 9, 1980	May 1, 1980

The implementing Divisions were required to have the DSS 61 hardware available on site by 1 April 1979 to allow for a contingency period or a possible earlier downtime start, and the DSS 42 hardware available on site by 1 July 1979 to allow for a contingency period.

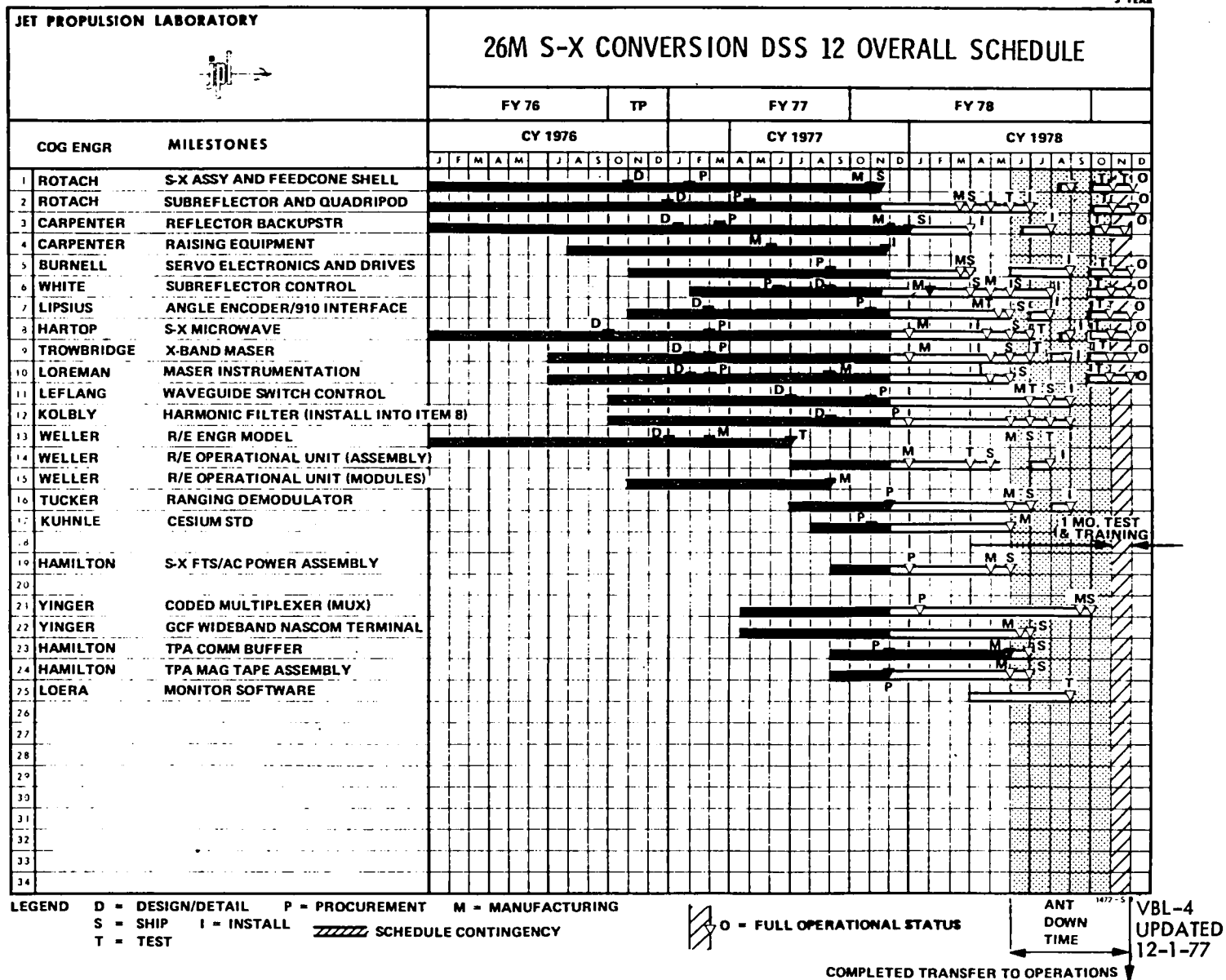


Figure 10. DSS 12 Overall Schedule

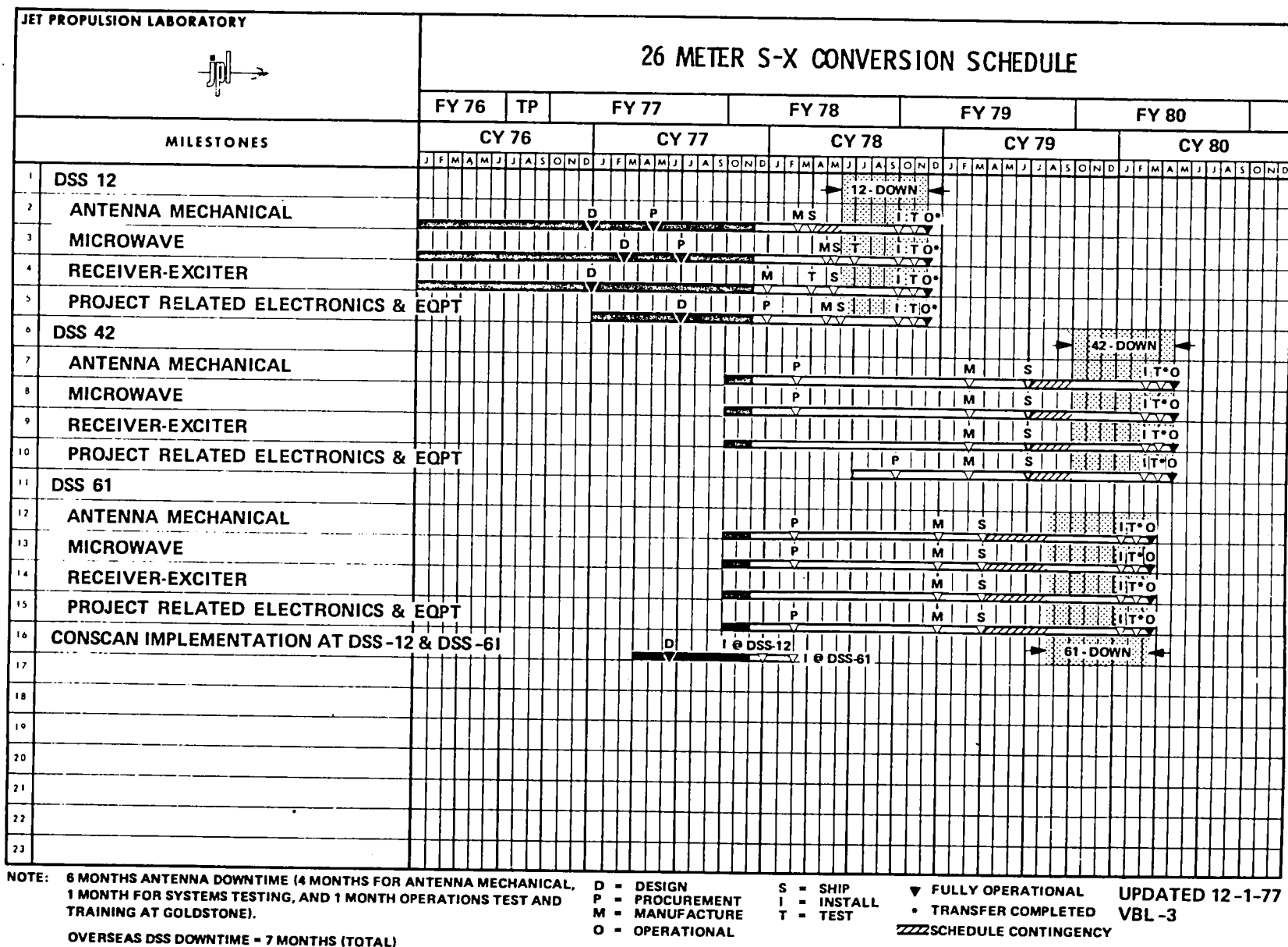


Figure 11. Milestone Schedule

I. RESOURCES

1. Funds

The costs shown in Table IV were defined and established after the baseline study was completed. Table V is a refinement of the costs shown in the baseline study.

Table IV. Cost* Summary of Baseline Items

Item	DSS		
	12	44 and 62	Total base
Antenna mechanical	867	1624	2491
Microwave	606	1146	1752
Antenna feed	93	--	93
Transmitter/harmonic filter	75	70	145
Receiver-exciter assembly	635	650	1285
Ranging demodulator	44	177	221
Planetary ranging	--	105	105
Intrasite frequency distribution	277	--	277
Wideband data	98	174	272
Welding	91	179	270
Angle encoders	41	--	41
Extension to 34m	507	752	1259
Cesium standard	--	50	50
Equipment total	3334	4927	8261
*Costs are in \$k			

Table V. Equipment Funding* Summary (Three Stations)

Task 59 Equipment	DSS		
	12	44 and 62	Total
Antenna mechanical (C of F)	--	993	993
Antenna mechanical (R&D)	1531	1842	3373
Microwave	652	1165	1817
Antenna feed	71	--	71
FTS-UPS Equipment	50	94	144
Transmitter/harmonic filter	59	70	129
Receiver-exciter	749	675	1424
Ranging demodulator	44	177	221
Planetary ranging	--	105	105
Minicoherence reference generator	104	180	284
Recording (TPA/GCF)	41	82	123
Wideband data	67	85	152
Cesium standard	<u>73</u>	<u>152</u>	<u>225</u>
Total	3441	5620	9061
*WAD A, \$k obligation.			1 Oct 76

The cost of the added options, such as electric drives and microwave switch control, along with cost updates, operational manpower support by JPL and station personnel, brought the planned total cost of the Project to \$14,000k. The spending profile is shown in Figure 12. The difference between the original estimate and the actual plan was caused by the move ahead of the implementation at DSS 61. The higher cost overrun of \$250k was caused by the replacement of defective panels at DSS 12. The overrun was a fraction of a percent and, essentially, the Project was completed as budgeted.

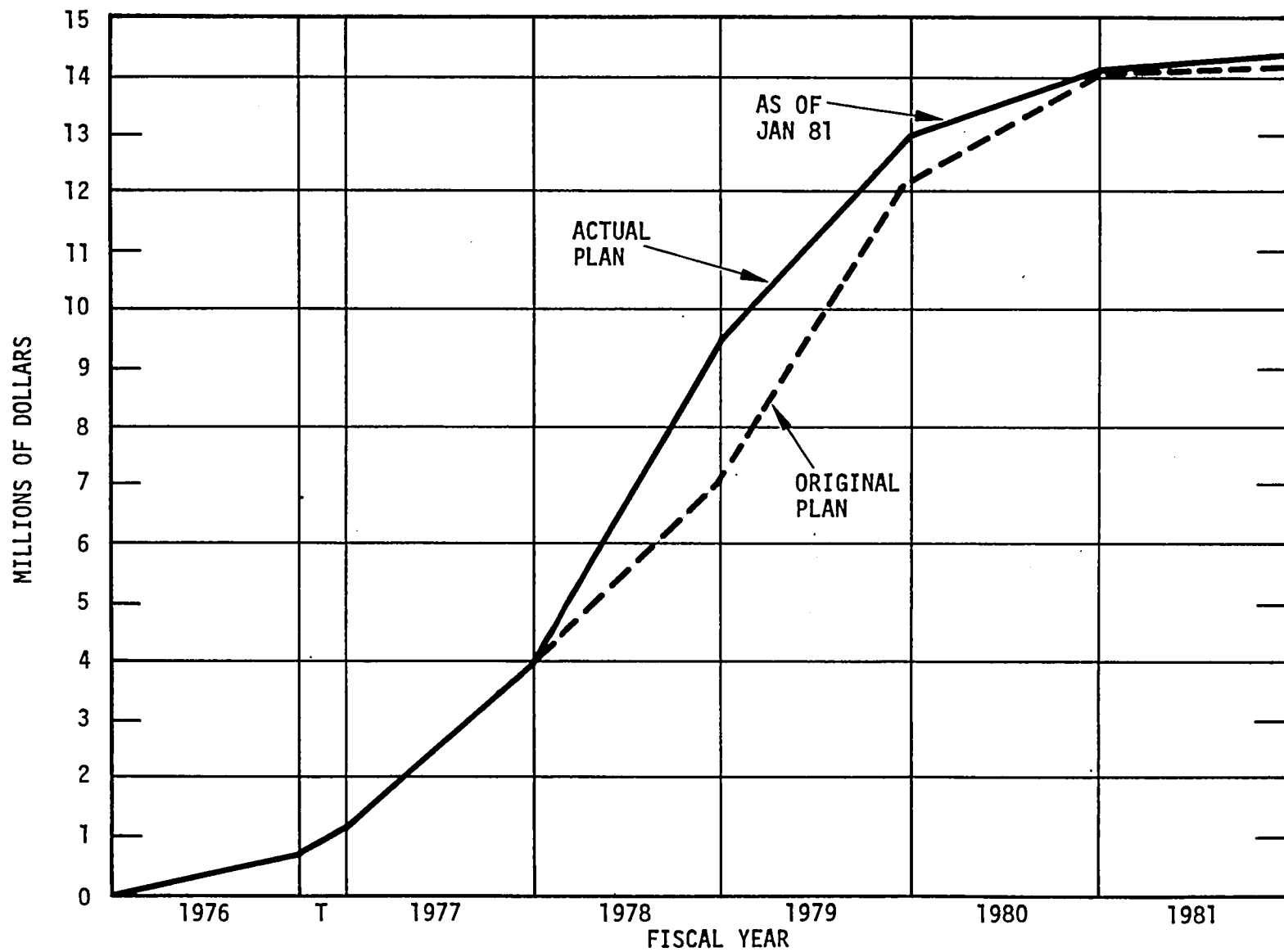


Figure 12. S-X Conversion Project Resource Profile

2. Manpower

It is estimated that 70 JPL man-years were required for the planning, design, and implementation of the Project. Considering the many contractors and station personnel involved in the project, it is not possible to provide an accurate count of total man-years used in all the effort provided. It is estimated, however, that the number was in the neighborhood of 150 man-years to complete the implementation.

III. DESCRIPTION OF ANTENNA MECHANICAL MODIFICATIONS AND NEW ELECTRONIC ADDITIONS AND CHANGES

A. GENERAL DESCRIPTION

In order to provide an X-band receiver capability to the stations, the following equipment was added: a dual S- and X-band reflex microwave feed, an X-band maser, an X- to S-band down-converter and X-band test translator for use with the existing Block III Receiver-Exciter Subsystem, and an X-band harmonic filter for use with the existing S-band transmitter to prevent internal station interference. The microwave components are housed in a new dual cone shell, which supports the reflex feed reflectors.

Within the station control room, the new X-band receive capability required the addition of a string of doppler extractors for X-band and two ranging channels, one for S-band and one for X-band. Having this dual S- and X-band doppler and range (radio metric data) capability required the introduction of cesium frequency standards and a minicoherent reference generator to provide the long-term frequency stability to navigate spacecraft to outer planets. The X-band radio metric data must be processed in real-time and recorded. This was accomplished by the addition of a planetary ranging assembly, communication buffer, coded multiplexer, and dual high-rate, high-density tape recorders. The above functions are shown on Figure 13.

The aperture increase from 26m to 34m required extensive changes to the shaft angle encoders and servo electronics (see Figure 14). These modifications also applied at DSS 42, except for those associated with raising the antenna. Instead of raising the antenna structure, the topography was such that trenching adjacent to the antenna foundation allowed for the necessary sky coverage.

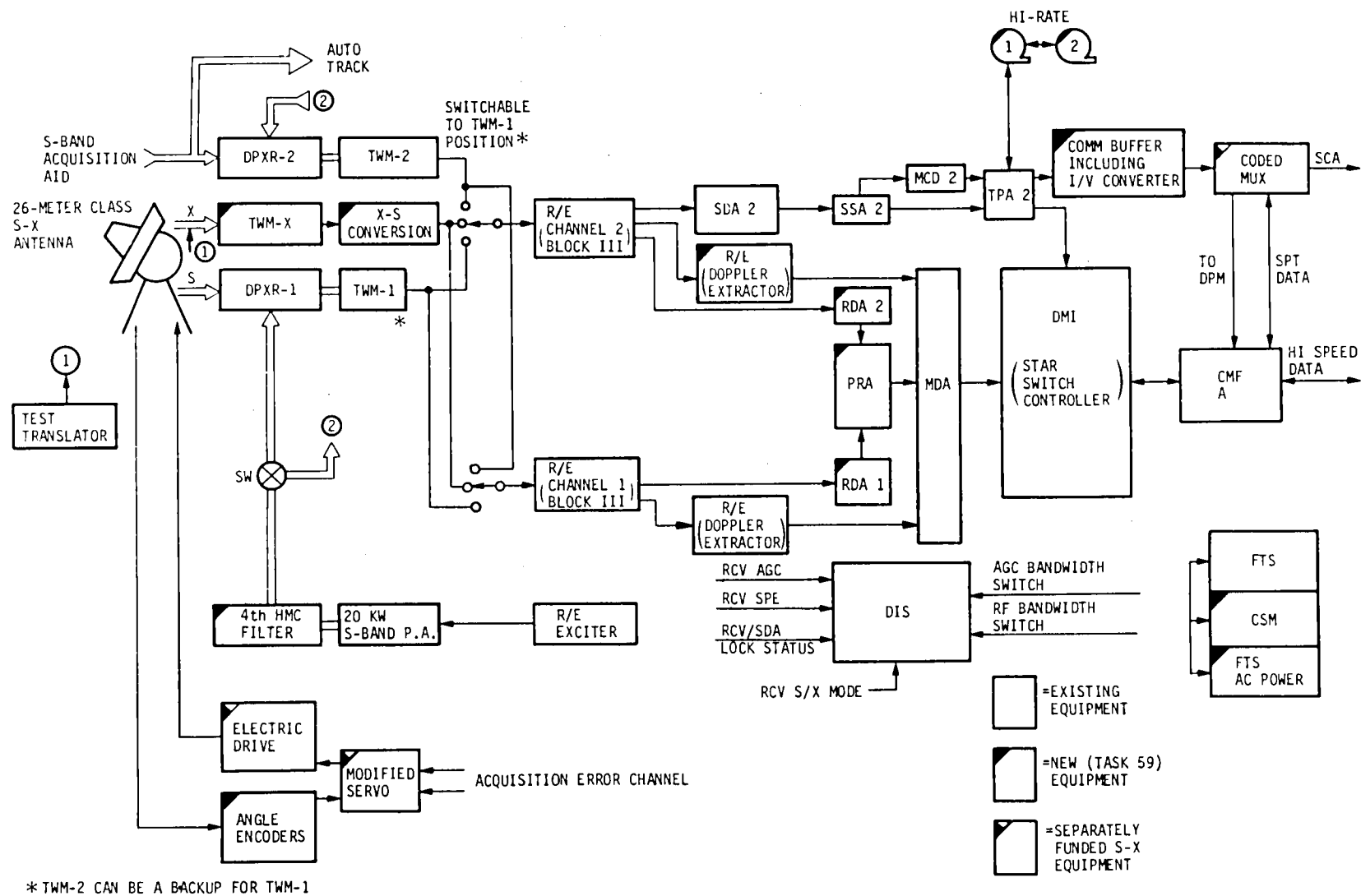


Figure 13. S-X Conversion Project Functional Block Diagram

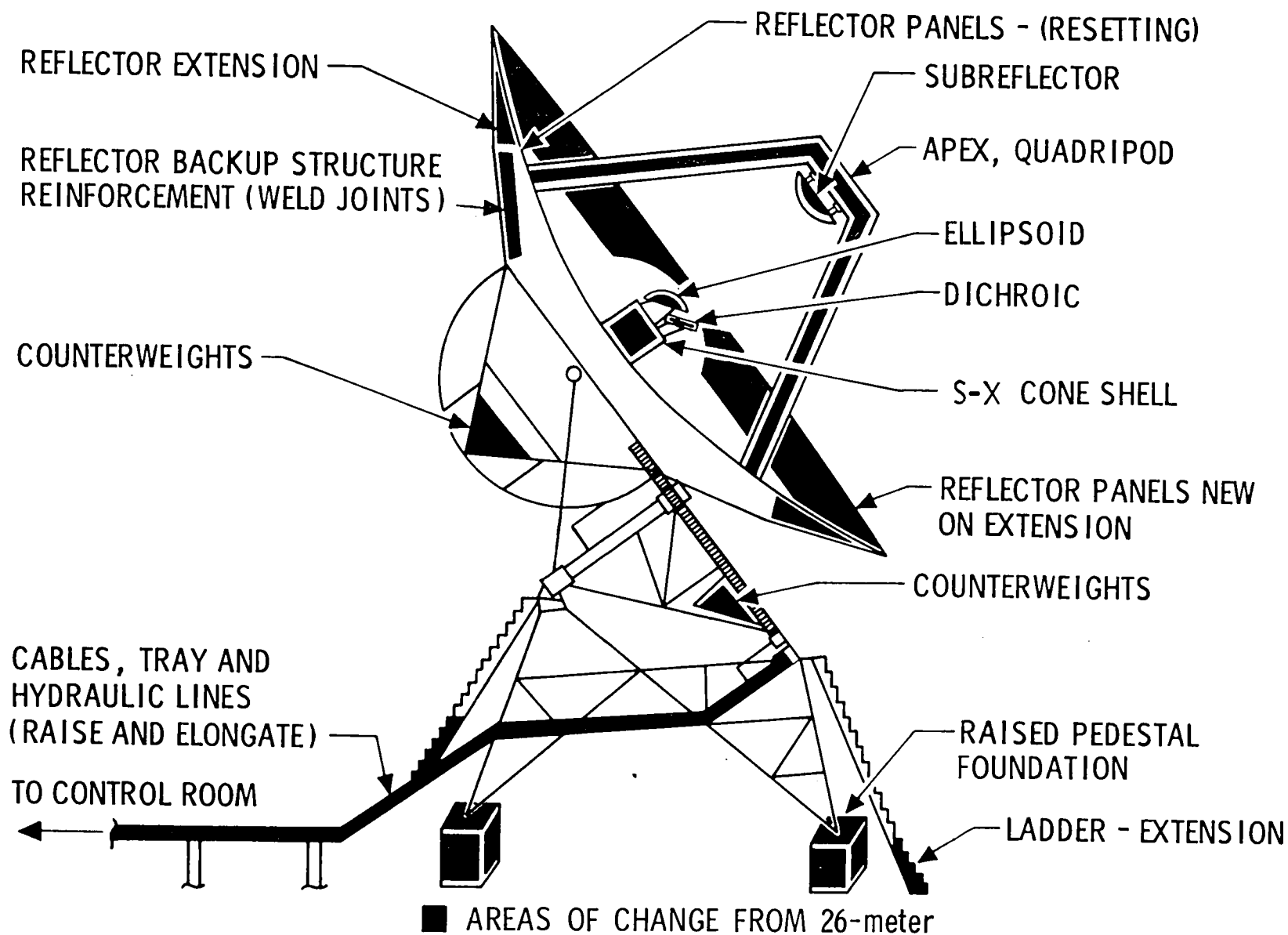


Figure 14. Structural Changes to Antenna Mechanical Subsystem for Extension to 34 Meters

B. DECLINATION AND HOUR ANGLE WHEEL MODIFICATIONS AND ADDITIONS TO COUNTERWEIGHT AND PEDESTAL STIFFENING

1. Declination Wheel

Stiffening of the declination wheel was required because of the additional reflector weight and the counterweight additions to balance the tipping structure.

Four members of the wheel structure and their end connections were increased in size, and end connections on four other members were reinforced. The wheel was then stiff enough for the 34m reflector. The counterweight area did not have enough space to add approximately 27,180 kg (60,000 lb) of lead billets so additional mounting plates were installed to accommodate the remainder of the lead billets. Part of the lead was installed in the lower area of the electronics room, as well as on the outside walls of the room.

2. Hour Angle Wheel

The stiffening requirement for the hour-angle wheel was more extensive than for the declination wheel. Many spoke members were stiffened by adding plates between the existing angles and/or doubling the double angles to four. Also, additions were made to the end gussets and the joints were welded to increase the wheel stiffness. In addition to the two counterweight boxes on either side of the center member of the wheel, two new boxes were installed to accommodate approximately 67,950 kg (150,000 lb) of lead billets. Most of these were enclosed in egg-crate weldments.

3. Pedestal

In the pedestal, only eight members and two joints required strengthening. Additional bars, as well as back-to-back angles,

were installed and welded or bolted in place. Larger bolts and additions to the gusset plates strengthened the joints.

C. DECLINATION AND HOUR ANGLE SERVO AND ELECTRIC DRIVES

1. Introduction

The antenna drive modifications consisted of removing the hydraulic drives and associated power supplies and controls, and substituting the electric equivalents.

The constituent electric drive utilities include the following:

DC drive motors	four total, two per axis
DC motor controllers	four total, two per axis
DC tachometers	four total, one per dc motor
AC blower motors	four total, one per dc motor
Axis junction boxes	two total, one per axis
Servo monitor assembly	one total
28-volt power supply	two total, redundant
5-volt power supply	two total, redundant
+15 volt power supply	two total, redundant
Antenna controller	one total

The following paragraphs provide the theory of operation of the Electronic Control (Servo) Assembly (SVO) and describe the interfaces between the SVO and other equipments required to control the movement of the 34m antenna.

2. Electronic Control (Servo) Assembly Theory of Operation

The major items of equipment in the SVO are the servo control panel assembly and the motor controller, which is part of the antenna drive assembly (see Figure 15). The combined circuits of these equipments

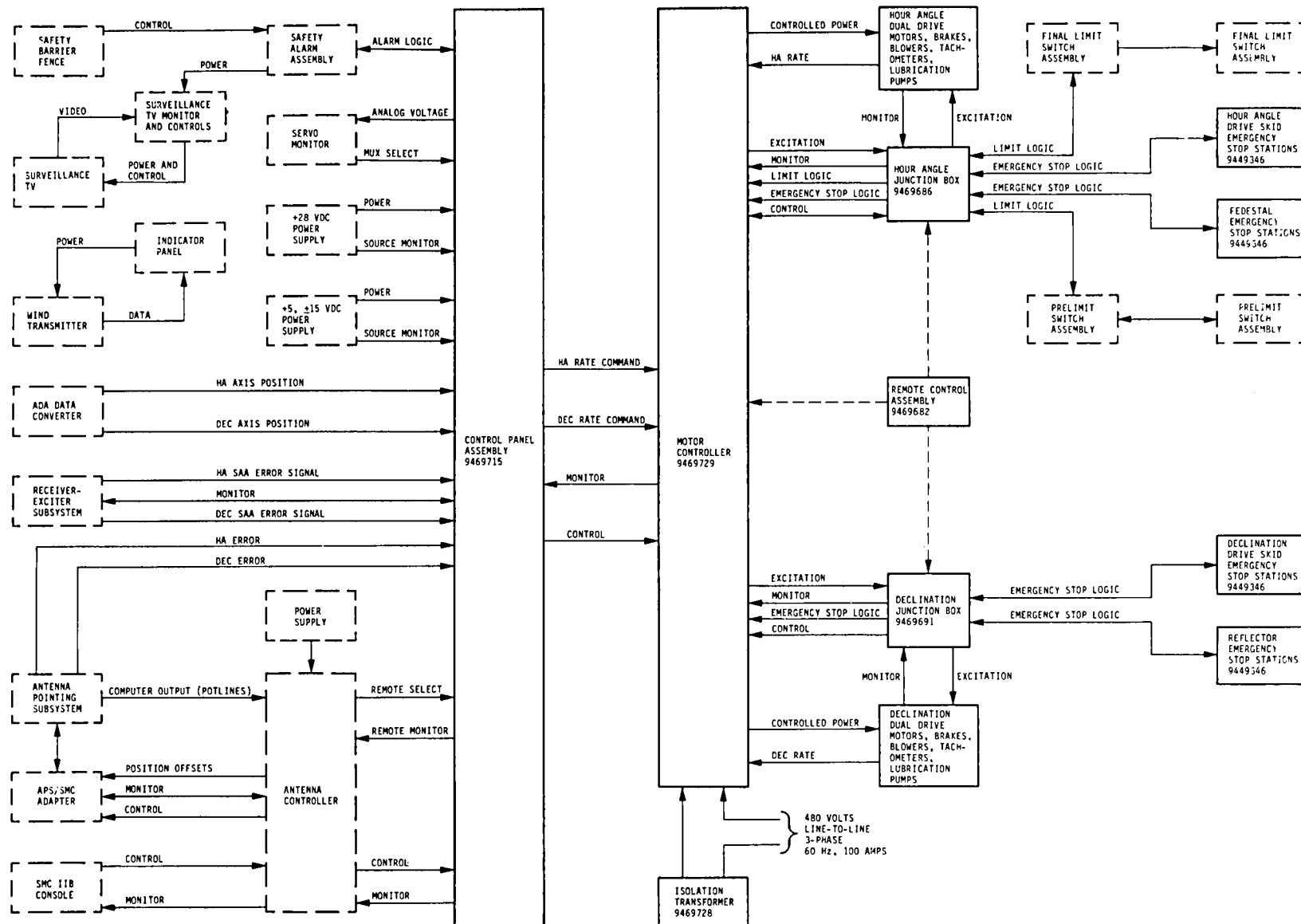


Figure 15. Antenna Drive Block Diagram

provide for controlling the antenna movement either in a rate mode, under computer control, or under RF autotracking (SAA) control.

The ancillary items of equipment in the SVO that are described herein are the drive motors, tachometers, blower motors, axis junction boxes, emergency stop stations, servo monitor assembly, +28 Vdc servo power supply assembly, +5 and +15 Vdc servo power supply assembly, 5-Vdc antenna controller power supply, hour angle and declination limit switch boxes, and the antenna controller. The motor controller is detailed only to the extent necessary to describe the theory of operation of the total SVO. For detailed theory of operation information for the motor controller, refer to TM 20648.

a. Servo Control Panel Assembly

Subsystem servo control and motor signals are generated in the servo control panel assembly. A system of electronic interlocks within the servo control panel assembly provides a logic that limits operation within a range of normal operating parameters (position, motor temperature, etc.). The primary control signals generated by the servo control panel assembly are two rate commands, one for each axis. The rate commands are analog voltages that represent direction and speed commands to the axis drive motors (via the motor controller). In manual slew mode, the rate commands are simply voltages generated by front panel manual slew control settings. In computer command or SAA track mode, the rate commands are generated by processing of the position error signals from the Antenna Pointing Subsystem or Receiver-Exciter Subsystem to drive the antenna to a zero-error position. Monitor functions are provided by both the servo control panel assembly and the servo monitor assembly. The servo control panel assembly

provides display of general status data, including the HA and dec axis position displays which receive inputs from the angle data assembly converter.

b. Motor Controller

The primary function of the motor controller is to accept the rate command signals from the servo control panel assembly and supply the appropriate motor armature currents to the axis drive motors. Tachometer signals are used as feedback control to maintain the speed by the rate command signals. In addition, the armature currents for each set of motors are compared and a feedback signal is developed to balance the motor drive signals. The motor controller also provides an interface for control signals (e.g., EMERGENCY STOP, WARNING HORN, etc.) from the servo control panel assembly to the drive/sensor equipment and for monitor signals from the drive/sensor equipment to the servo control panel assembly. A remote control assembly can be connected to the motor controller, the hour angle junction box, or to the declination junction box. When remote operation is selected at the motor controller, the remote control assembly may be used to manually slew the antenna. In either mode, interlock protection prohibits drive operation if an improper condition exists (e.g., motor overtemperature, lube pressure loss, etc.)

c. Drive Motors

The drive motors are shunt field, totally enclosed dc motors rated for 15 horsepower at 1750 r/min. Mounting of the motors is by means of a D flange. Integral to the drive motors are a tachometer and a blower.

d. Tachometers and Blower Motors

The tachometers attached to the drive motors are totally enclosed, C face-mounted, size 56 frame devices. The output scale factor is 50 volts per 1000 r/min. The blower motors attached to the drive motors are totally enclosed, 1/3 horsepower, 3450 r/min devices designed to blow air over the outside of the motor frame.

e. Antenna Controller

The antenna controller provides an interface between the SVO and the Station Monitor and Control Assembly IIB (SMC IIB). In addition, the antenna controller provides an interface for control and monitor functions between the SMC IIB and the Antenna Pointing Subsystem (APS). During normal station operation, the control of the antenna movement and monitoring of antenna status is performed by the SMC IIB operator. These control and monitor signals are routed between the SMC IIB and the antenna controller via a 14-line bidirectional interface. Both the control and monitor functions are multiplexed into the 14-line cable. When the SMC IIB operator selects the local mode, the control of antenna movement resides at the servo control panel assembly. In either SMC IIB remote or local mode of operation, monitor data is routed via the 14-line interface and displayed at the SMC IIB console. The SMC IIB remote and local modes of operation define only which operator has control. In either case, the designated operator can control the antenna manually, or select computer control (computer command) or tracking control (SSA track).

f. Servo Monitor Assembly

The servo monitor assembly has three independent monitoring functions. One monitoring function drives a digital panel meter and the other two are applied to front panel output jacks.

Each of the monitoring functions selects one of 48 channels that are multiplexed at the servo control panel assembly. The 48 channels represent a sampling of important inputs to, outputs from, and internal signals of the servo control panel assembly.

g. +28 Vdc Servo Power Supply Assembly

The +28 Vdc servo power supply assembly contains two 28-volt power supply modules that are connected to a common output bus through isolating diodes. Each power supply module is overvoltage and overcurrent protected, and failure of either one will permit continued operation of the servo control panel assembly.

h. +5 and +15 Vdc Servo Power Supply Assembly

The +5 and +15 Vdc servo power supply assembly contains two 5-volt power supply modules and two +15 volt tracking power supply modules. Each voltage is connected to a common output bus through isolating diodes. Each power supply module is overvoltage and overcurrent protected, and failure of either module on a bus will not deter continued operation of the servo control panel assembly.

i. Hour Angle and Declination Limit Switch Boxes

The hour angle and declination switch boxes (final and prelimit switch assemblies) consist of eight (at DSS 12 and 61) or nine (at DSS 42) sets of normally closed switch contacts in each assembly. The switches are interconnected and the actuating cams are adjusted such that the motion limits of each axis interact to produce a contour required because of the axis configuration (HA-dec) of the antenna.

j. Axis Junction Boxes

The axis junction boxes provide termination and routing of sensor signals and control circuits for remote operation of the antenna. Incorporated into the junction boxes are an emergency stop switch and a final limit bypass switch.

k. Emergency Stop Stations

The emergency stop stations provide a closed circuit to the emergency stop logic. The circuit becomes open when a switch is actuated. The stop stations are configured for series and branched type arrangements as required by the specific installation.

l. 5-Vdc Antenna Controller Power Supply

The 5-Vdc power supply converts 120 Vac input voltage to a 5-Vdc output voltage for use by the antenna controller.

D. TIPPING STRUCTURE - EXTENSION TO 34M

1. Extension Panels and Existing Panel Modifications

The reflector diameter increase to 34m from the existing 26m required two rows of additional panels, each row consisting of 48 panels. The panels, which have a perforated surface, were manufactured at T.I.W. Systems Inc. in Toronto, Canada, in accordance with JPL specifications.

The existing panels were checked at the site for deviations from the required curvature using special jigs and templates. Cold working of the panels to meet a set tolerance of 0.010-inch rms was then accomplished using a fixed frame and hydraulic jacks. Measurements of the rms surface tolerance of the reworked panels were done using a JPL machine shop fabricated fixture. This fixture had a sweep blade with dial indicators mounted to measure surface deviations from the curve (see Figure 16).

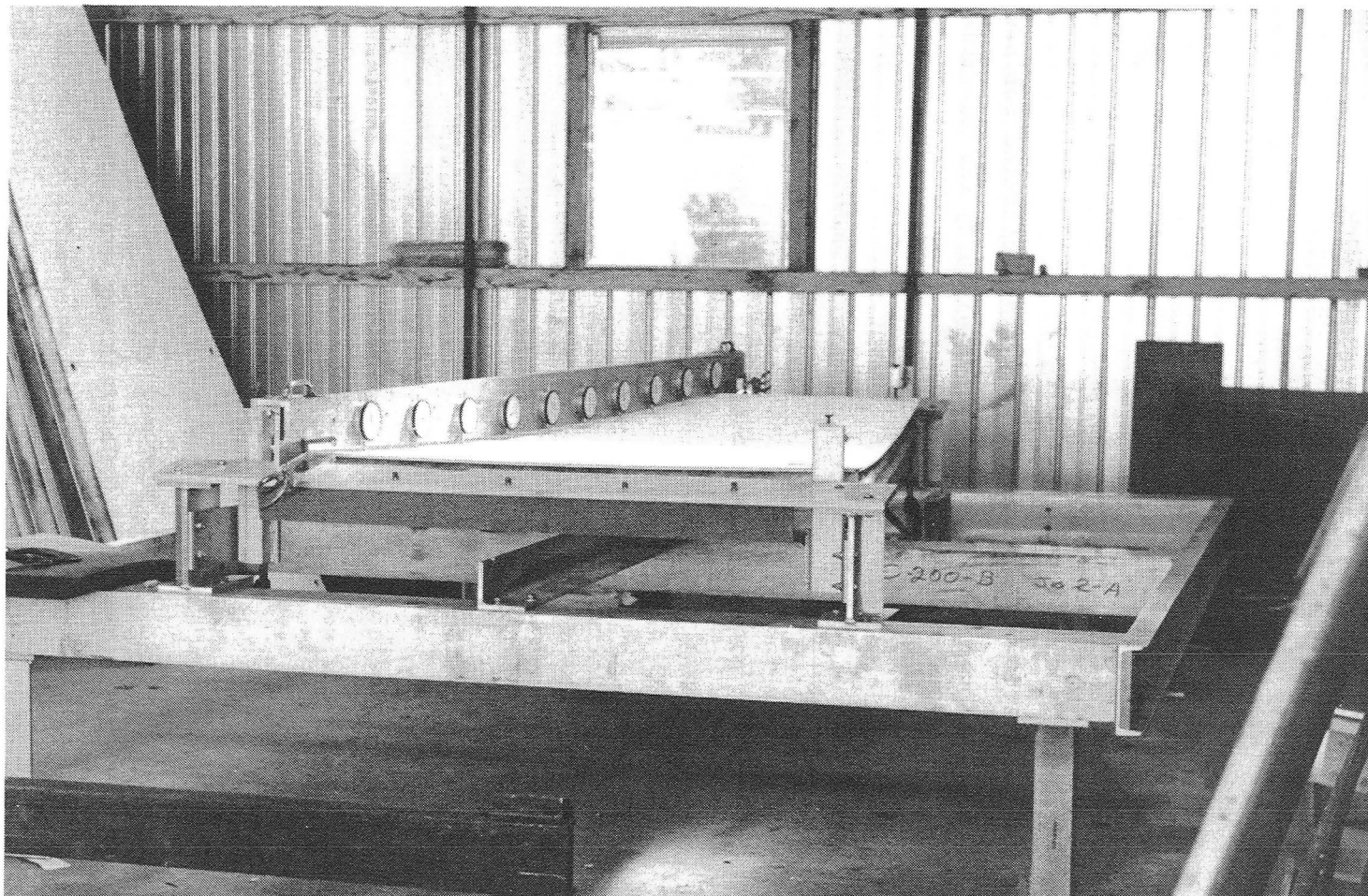


Figure 16. Measurement of Surface Tolerance

Also, nut plates were added to the panel corners to adapt to the "ball stud" adjustment design supporting the panels. Prior to installation of the panels, the ball studs were installed on the panels, which were then fastened to the panel clips on the backup structure. Targets were installed on the panels for alignment. These targets were located and mounting holes drilled by use of a JPL-fabricated strap gage (see Figure 17).

Panel alignment was accomplished at the end of all installations but prior to the feedcone installation. A theodolite was placed at the reflector vertex and adjusted for plane through the four primary targets on the backup structure in the "rigging" position of approximately 40 degrees elevation angle. A night reading of the panel targets was taken, and after reduction of the data, each panel corner was then adjusted up or down through the ball stud. The reading was then repeated the following nights and readjustments made until the desired accuracy of not more than 0.010 inch rms was achieved.

2. Quadripod

The quadripod structure was fabricated and preassembled by Capitol Westward, Inc. of Paramount, CA. The quadripod is a four-legged structure terminating into the apex frame on the top side. Each leg is a trapezoidal truss frame comprised of welded tubular steel members. Two legs house a 12.7-cm (5-in.) diameter tube for the full length, which in turn houses all cables required at the apex structure. At each site, four concrete pads were provided for the quadripod preassembly. As part of the preassembly, four tie members were installed, connecting the legs at the base, as well as four braces, making the tie frame a rigid frame (see Figure 18). All field-welded joints were made and dimensions of the structure were checked. The quadripod supports the subreflector and the subreflector controller, consisting of jackscrews and motors to provide movement of the subreflector in the X, Y, and Z direction. The second phase of the preassembly was the installation of the subreflector with all mechanical supports and adjustment mechanisms, electrical services and control boxes. A checkout was then performed to assure that ± 7.6 -cm

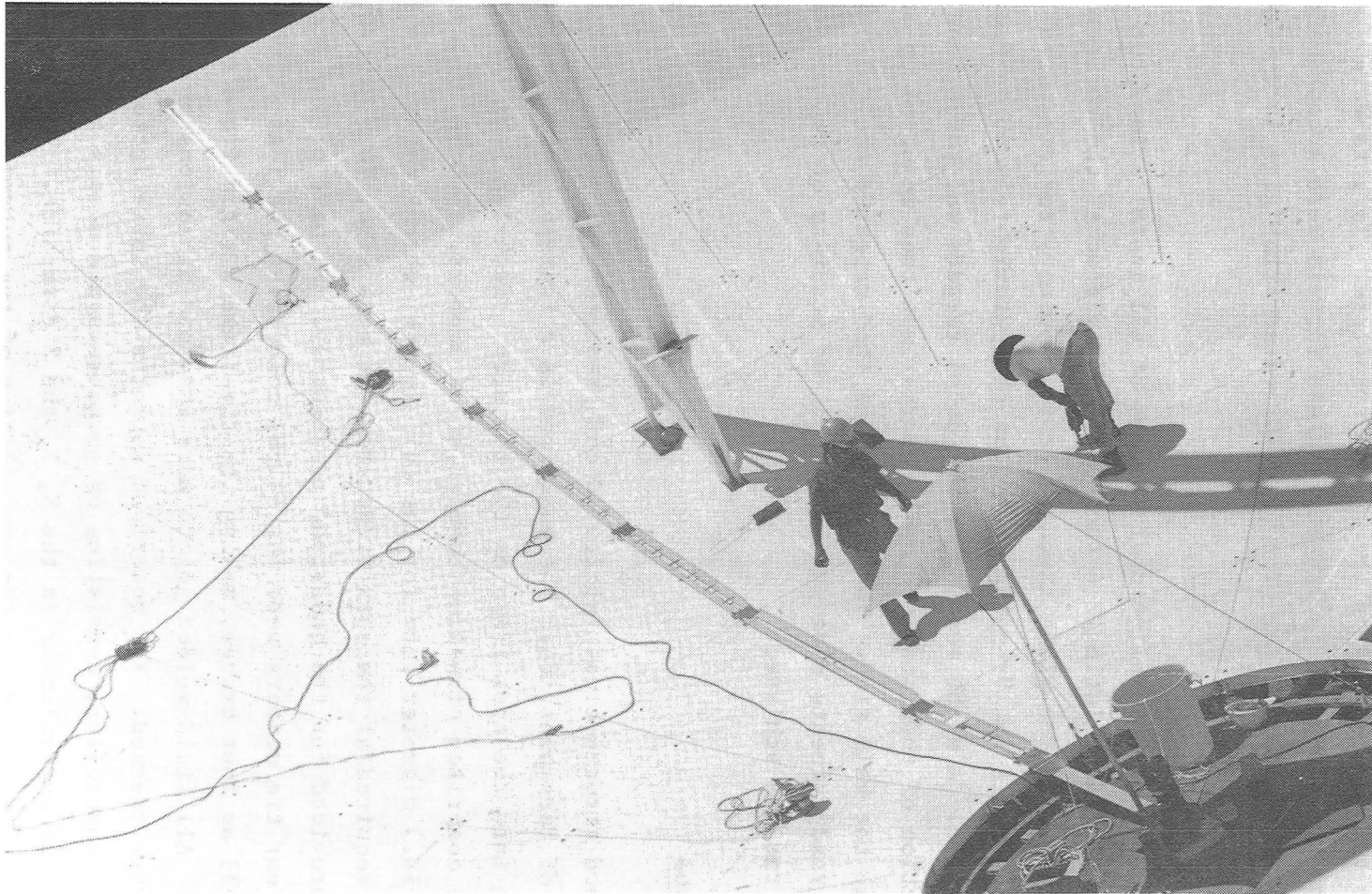


Figure 17. Placement of Targets on Panels



Figure 18. Quadripod Preassembly

(+3-in.) adjustment in X, Y, and Z coordinates could be made from the nominal position. The entire quadripod subreflector assembly was raised with a crane (see Figure 19) and welded in place on the reflector structure after removal of the outer ribs and prior to installation of the new rib assemblies.

3. Subreflector and Controller

The S-X subreflector consists of an all-welded aluminum surface, the shape of which is an offset hyperbola of revolution backed up by aluminum stringers. The panels are mechanically fastened to a steel frame made from tubular sections. Fabrication was done by Capital Westward, Inc., of Paramount, CA, to an acceptable manufacturing tolerance of 0.015-inch rms using special welding techniques. Six pads are provided for the interface to the support and adjustment mechanism connected to the quadripod and apex structure. The interface consists of a total of six jackscrews with associated motors, gearboxes, and shafts to provide movement in three directions, +7.6 cm (+3 in.) in X, Y and Z coordinates.

The subreflector position controller is remotely controlled from the control console to position the subreflector in X, Y, and Z coordinates as a function of hour angle and declination position of the reflector. This is to minimize gain loss due to the defocussing which arises from the gravity displacement of the reflector/ subreflector assembly. It is assumed that the antenna will operate in a CONSCAN mode during normal operation. The subreflector position controller operates in a manner not to disturb the CONSCAN operation, and the CONSCAN operation corrects pointing errors resulting from repositioning the subreflector. For target acquisition and for missions requiring blind pointing, it is necessary to provide a pointing correction to the APS to compensate for the pointing offset due to the displacement of the subreflector. The subreflector controller provides a gain improvement of up to 1 dB over a fixed position of the subreflector, not corrected for pointing positions.



Figure 19. Raising the Quadripod for Installation on the Antenna

The subreflector drives consist of synchronous motors with spring-set electric release brakes, and couplings for connection to the positioning jacks furnished as a part of the subreflector. A position transducer was mounted on each positioning jack to transmit subreflector position to the computer and the operator control console. The interface control box is mounted on the antenna and contains interface electronics between the apex-mounted elements and the control room elements.

It was decided that the subreflector control assembly was to provide antenna pointing offset correction data, with this data based on subreflector position, and that this data be used to provide pointing offset correction to the Antenna Control Assembly (ACA) when the ACA becomes available. This mode of operation was to provide minimum gain loss from defocus and antenna pointing offset from refocusing at all times and requires no human interface.

It was also decided that until the ACA is available, this same automatic mode of operation should be used by interfacing the APS. Even with the APS interface, a human interface can be used to enter pointing offset correction at acquisition. Then after acquisition, the subreflector controller will limit subreflector movement so that the resulting pointing offset gain loss will not exceed 0.1 dB. The controller will also allow enough time between subreflector movements to allow CONSCAN to remove the pointing offset gain loss.

4. Structure for the Extension

The reflector structure consists of radial trusses called ribs tied together with hoop trusses called hoops. Integral with the structure is a very stiff frame consisting of four straight trusses called square girders. The part of the structure outside the square girder was removed and replaced with a stiffer rib and hoop assembly to make a 34m dish (see Figure 20). The new ribs, hoops, and torsional bracing were prefabricated by Tallares de Coslada in Madrid, Spain, and Toronto Iron Works in Canada and shipped to the various sites. The ribs and hoops were then assembled

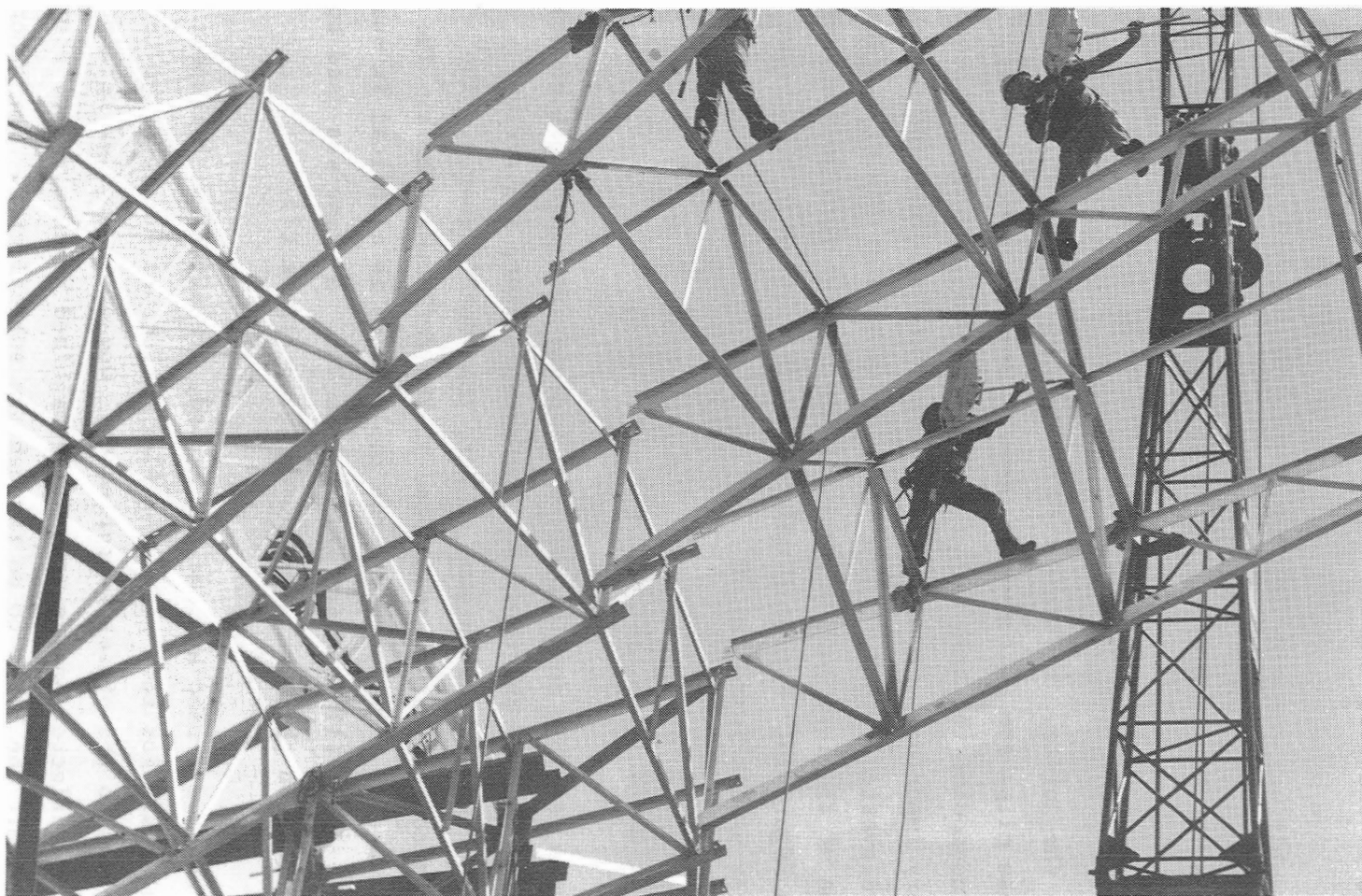


Figure 20. Installation of New Rib and Hoop Assembly

to subassemblies consisting of three ribs and the hoops to interconnect them. All joints were welded. A special assembly jig was fabricated to assure proper geometry. A total of eight subassemblies was produced. (See Figures 21 and 22.)

Each subassembly was removed from the fixture (Figure 23) and was later lifted in place with a crane (Figure 24), set to the proper elevation, and temporarily held in place with bolts. The space between two subassemblies was then filled with the hoops and braces until the entire reflector was closed. After proper alignment of the ribs, the structure was welded together at the joints. The next step was the installation of the panel clips. These clips are four shaped sections, with either two or four slots to accommodate the ball stud assemblies. The location of these clips is very important; therefore, they were set for proper distance, angle, and elevation before welding to the top chord of the ribs. The installation of the last hoop trusses to complete the reflector structure is shown in Figure 25. Figure 25 shows the structure with 40 percent of the reflector panels installed.

5. Reflex Reflectors and Feedcone

The Cassegrain assembly consists of one feedcone structure that houses the electronics, including the feedhorn, one subreflector, and reflex reflectors, to operate the antenna in more than one frequency. The feedcone is a conical structure mounted at the reflector Z-axis. The base of the structure is a cylinder and the top section is elliptical in shape, approximately 3.35m (11 ft) high (see Figure 26). A crane was used to install the cone on the antenna structure (see Figure 27).

The feeds, one for S-band and one for X-band, are offset with respect to the antenna axis. For this reason, reflex reflectors are required to divert one beam to the offset subreflector. One of the reflex reflectors is a dichroic reflector having accurately machined holes over the entire surface to permit the beams to go through the subreflector. The other one is a passive type reflector to direct the beam to the dichroic, where it is directed to the subreflector (see Figure 28). Both reflex reflectors

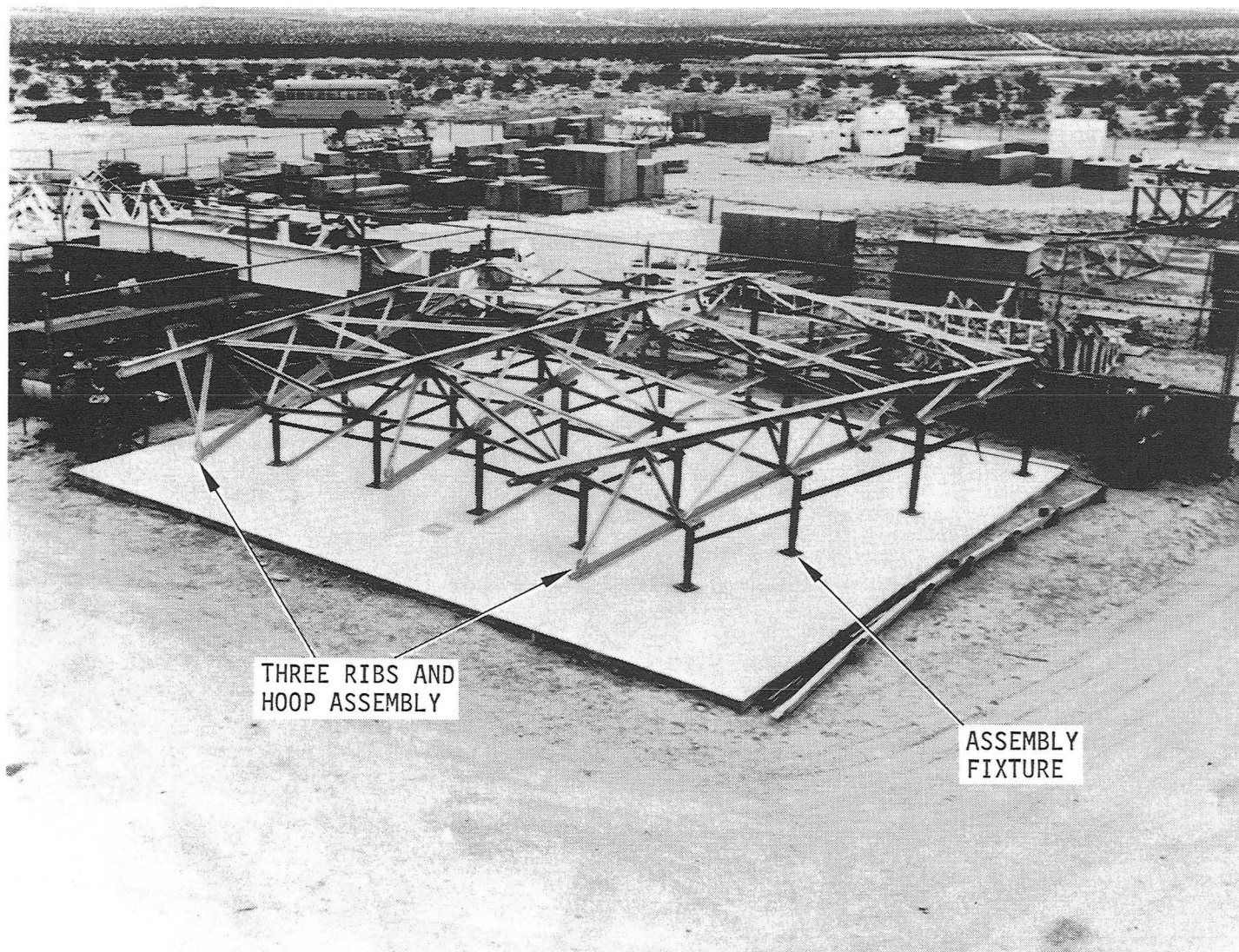


Figure 21. Rib and Hoop Subassembly on Fixture

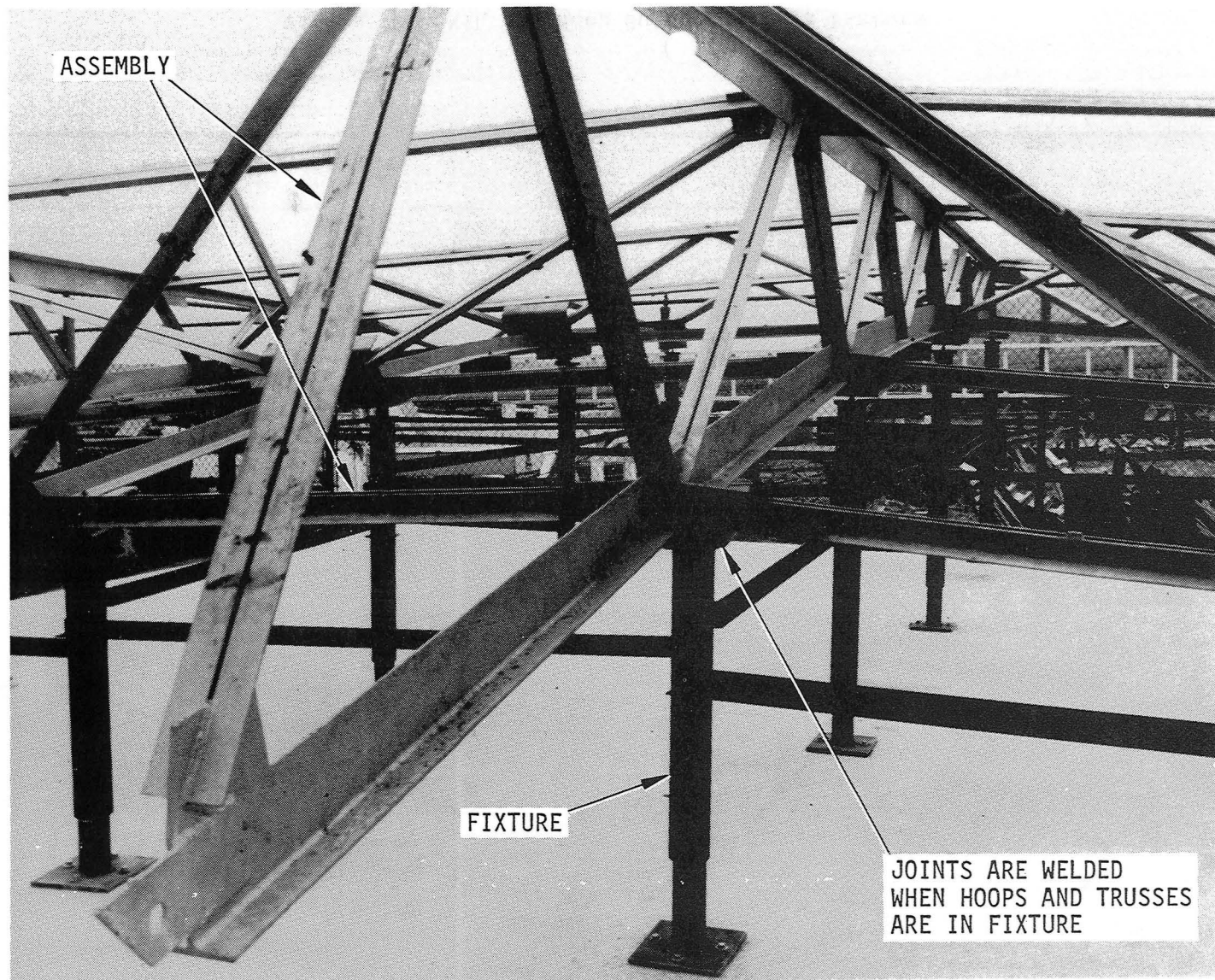


Figure 22. Closeup View of Rib and Hoop Subassembly on Fixture



Figure 23. Removal of Rib and Hoop Subassembly on Fixture

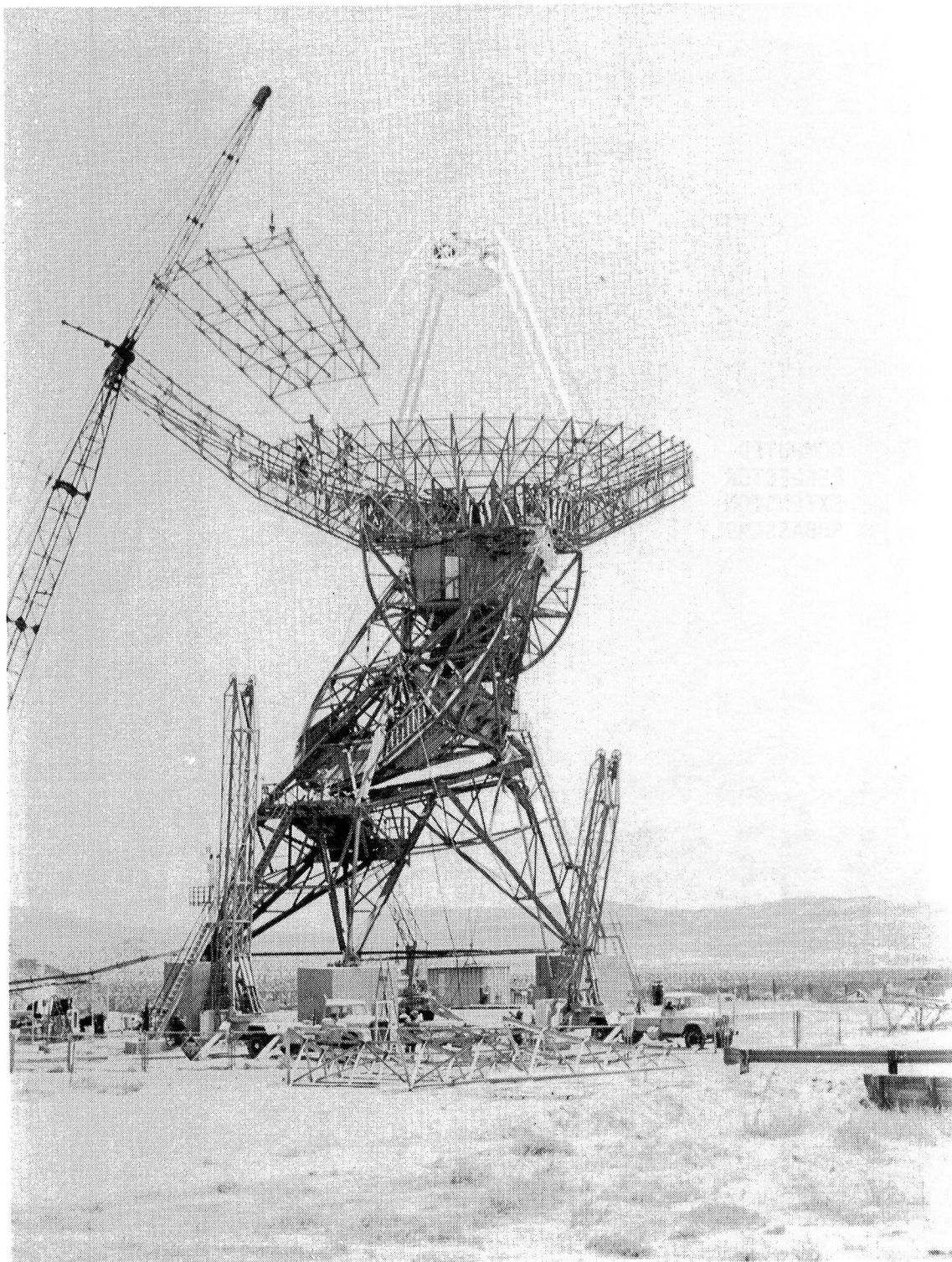


Figure 24. Installation of Rib and Hoop Subassembly



Figure 25. Installation of the Last Hoop Trusses

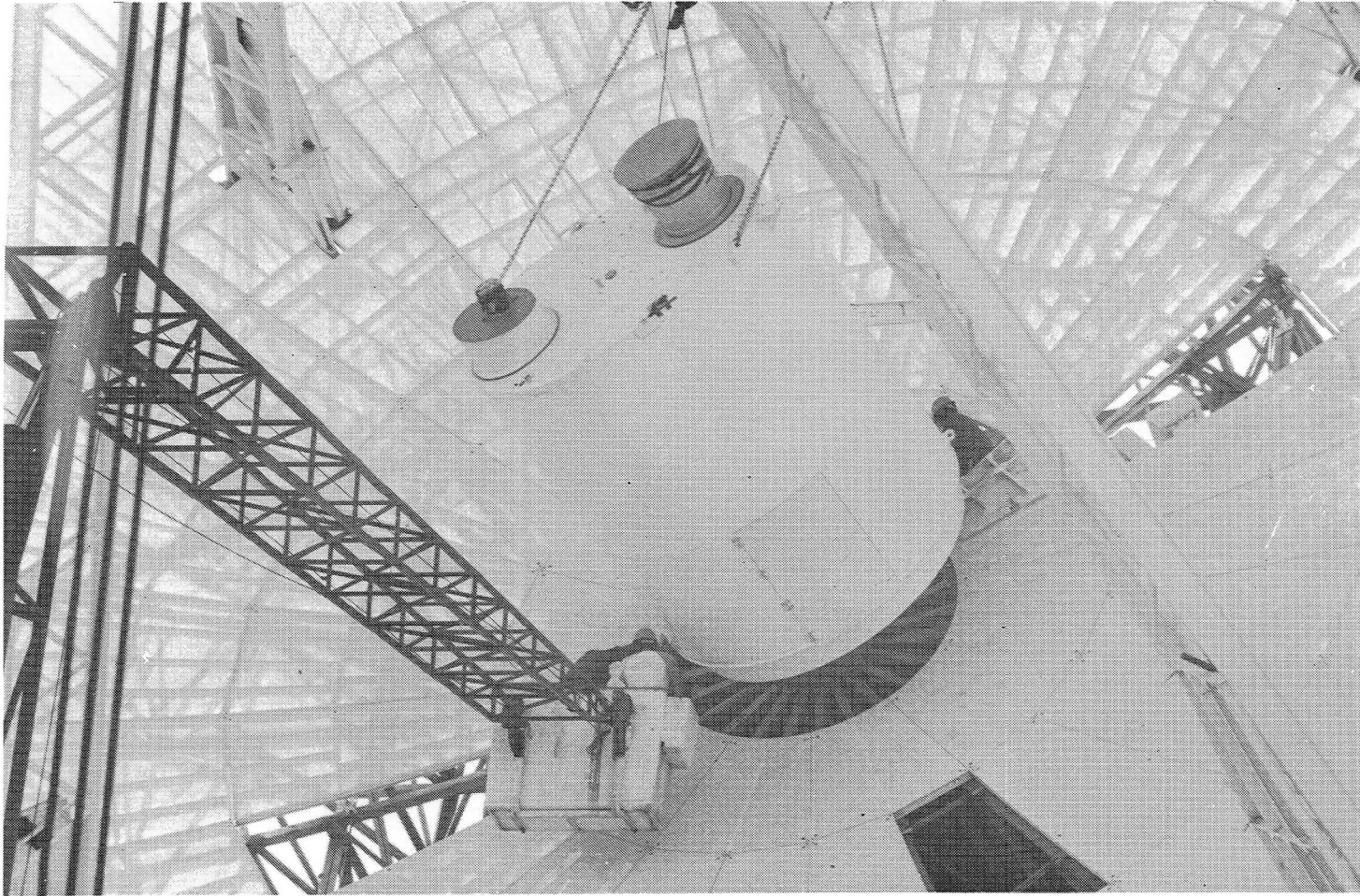


Figure 26. Feedcone



Figure 27. Installation of Feedcone on Reflector

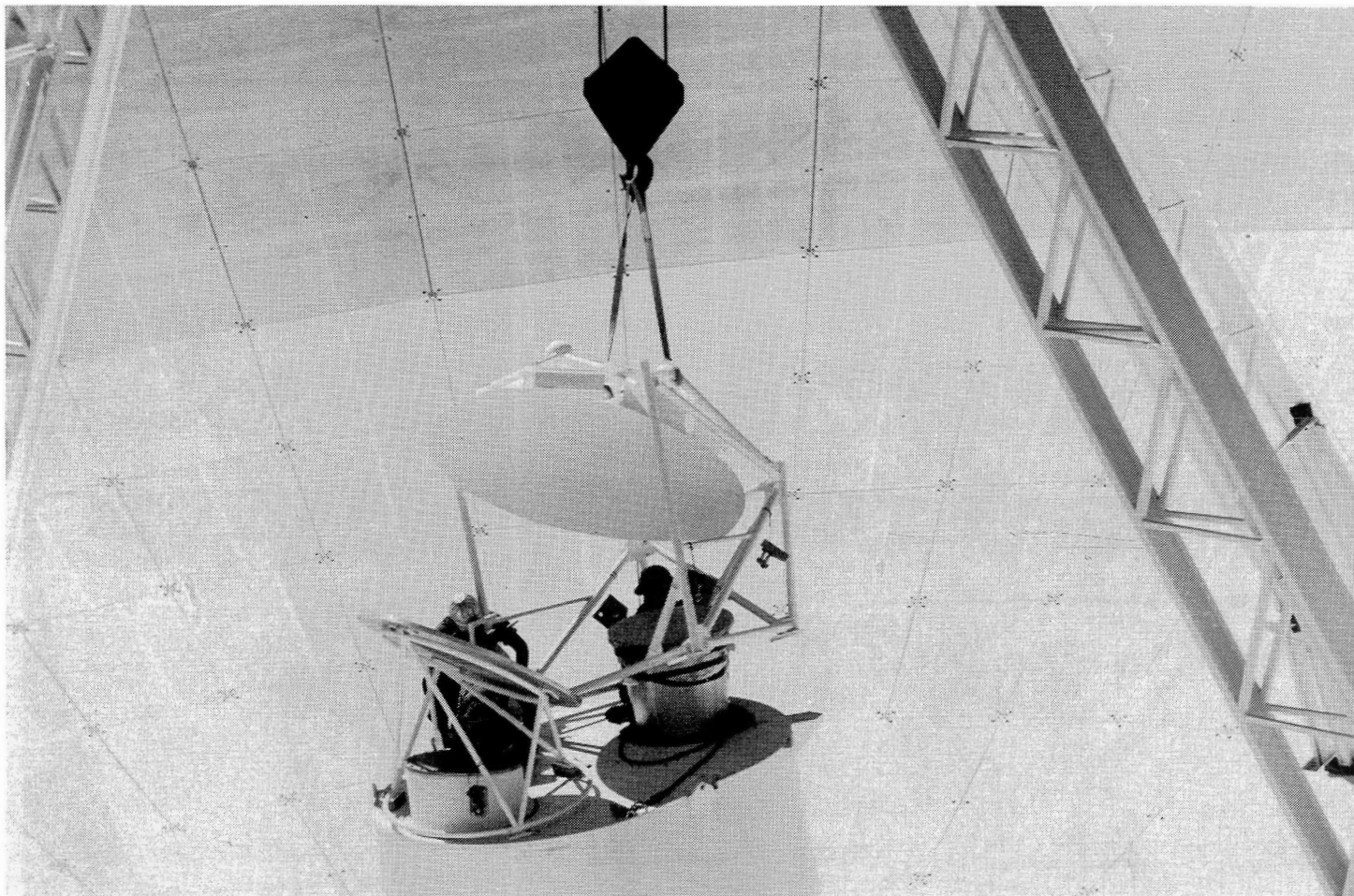


Figure 28. Installation of Reflex Reflectors

were accurately aligned with respect to the machined feedcone base and the feedcone is attached to a very accurately aligned ring on the reflector structure.

6. Reinforcement and Welding of Joints in the Existing Reflector Structure

After removal of the outer ribs and hoops (as described in paragraph 4), the center section remained with the square girder, which is connected and supported by the declination wheel. Stresses and deflections required a stiffening of the center section. Plates and angles were welded to many of the members, especially the square girder, to increase the stiffness. In addition, all joints were welded solid to prevent future slippage which could cause degradation of the rms and loss of performance at X-band.

E. DECLINATION AND HOUR ANGLE ENCODERS

By the time the 34m S-X upgrade project started, it was apparent that the angle encoders in use at the 26m stations needed to be replaced. The system was designed in the late 1950's and the last purchase of a similar system was in 1971 for DSS 43 and 63. The vendor had ceased production and was phasing out his support of the system and its components. This led to increasingly more expensive repairs and longer repair turnaround times.

A conceptual system design was formalized as interface drawings and a performance specification by July 1977. A Request for Proposal (RFP) was issued and a purchase order awarded for the DSS 12 system on 29 September 1977. The total cost for the deliverable detail design drawings, operation and maintenance manual, two-axis system, and one set of unique spare parts was \$72,886.53. Delivery was completed by 3 July 1978.

Figure 29 shows a functional block diagram of the encoders selected. The system is basically a solid-state, resolver-to-digital converter (RDC) using a closed error loop to form a tracking converter. To develop the required angle resolution ($360/2^{-20} = 0.000343$ degree), a two-speed resolver system was used. Each resolver has an RDC, and the resultant

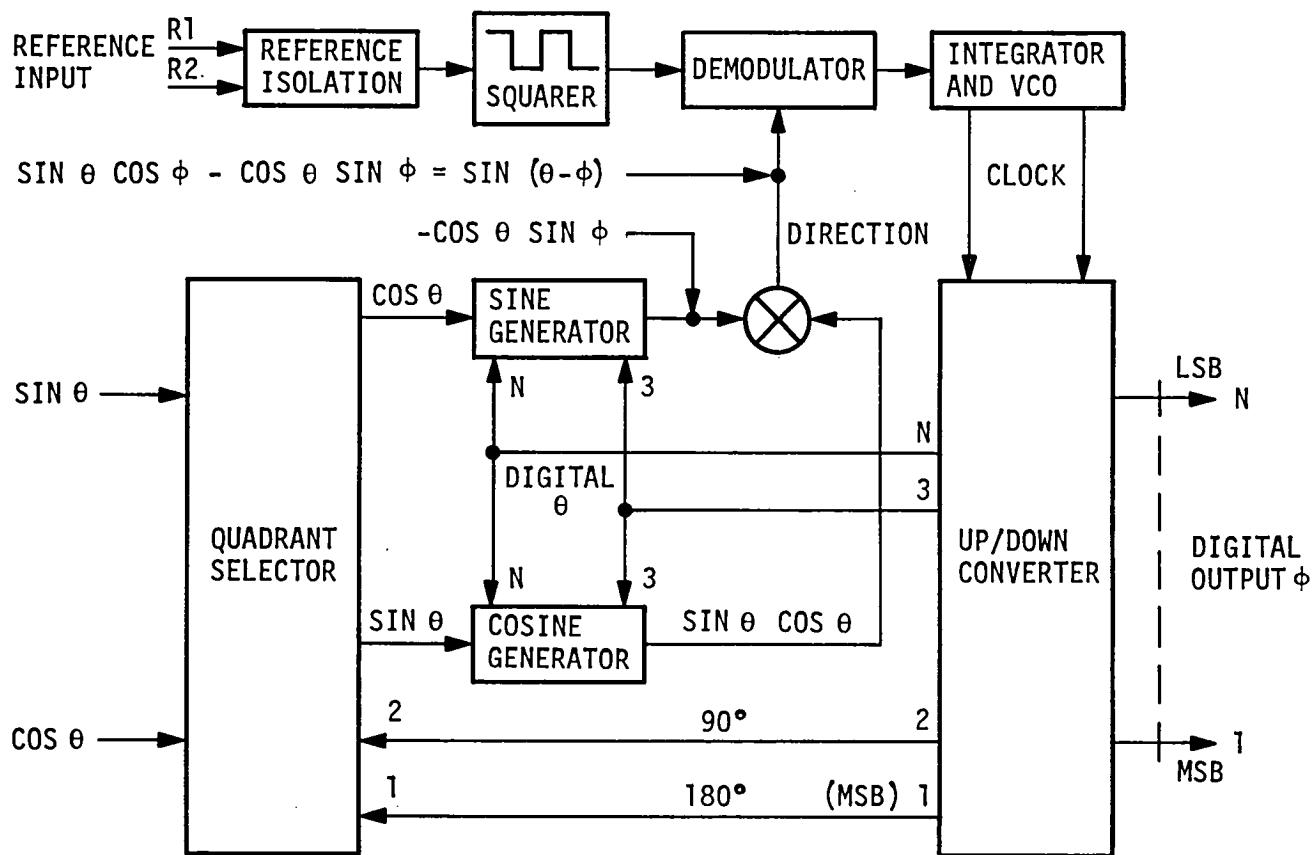


Figure 29. Tracking Type R/D Converter Functional Block Diagram

combined 20-bit digital angle word is sent to a data converter. The data converter contains multiple, independently strobed latches that update and hold the latest angle word for use by other subassemblies in the antenna. The features that simplified installation of the transducer on the antenna structure were (1) zero set switches that allowed the transducer to be coupled to the antenna without having to adjust the transducer shaft to a specific reading by adding, bit-by-bit, a correction to the transducer angle so that the correct mechanical angle could be displayed, and (2) direction of rotation switches that eliminated transducer selection as field rewiring to get correct count up/down sequence.

The system is designed such that all functionally equivalent circuit boards are interchangeable without need of adjustment, as are the transducers. Resetting the zero set switches places the system in an operational condition.

Extensive use is made of TTL low-power Schottky (LS) and CMOS circuits for minimum power consumption. To the maximum extent feasible, all integrated circuits are purchased with MIL-STD-883, level B processing for reliability.

To simplify the mechanical installation and alignment requirements, a mechanical plug-in approach was used for the transducer and drive shaft mounting. Two precision anticorrosive plates were used as the mounting surfaces for the transducer support and the driving shaft support. Each plate was provided with adjustment devices so that each plate could be adjusted and then locked in place to have minimum angular and parallel misalignments. The transducer and driving shaft were then bolted into these plates in precisely machined surfaces and so retain the mechanical alignments. The drive shaft is mounted on the rotating arm (or knee) and the transducer housing is mounted on the fixed axis shaft. Figures 30 and 31 are representative views of the mounting arrangements (both figures are of the DSS 12 dec axis).

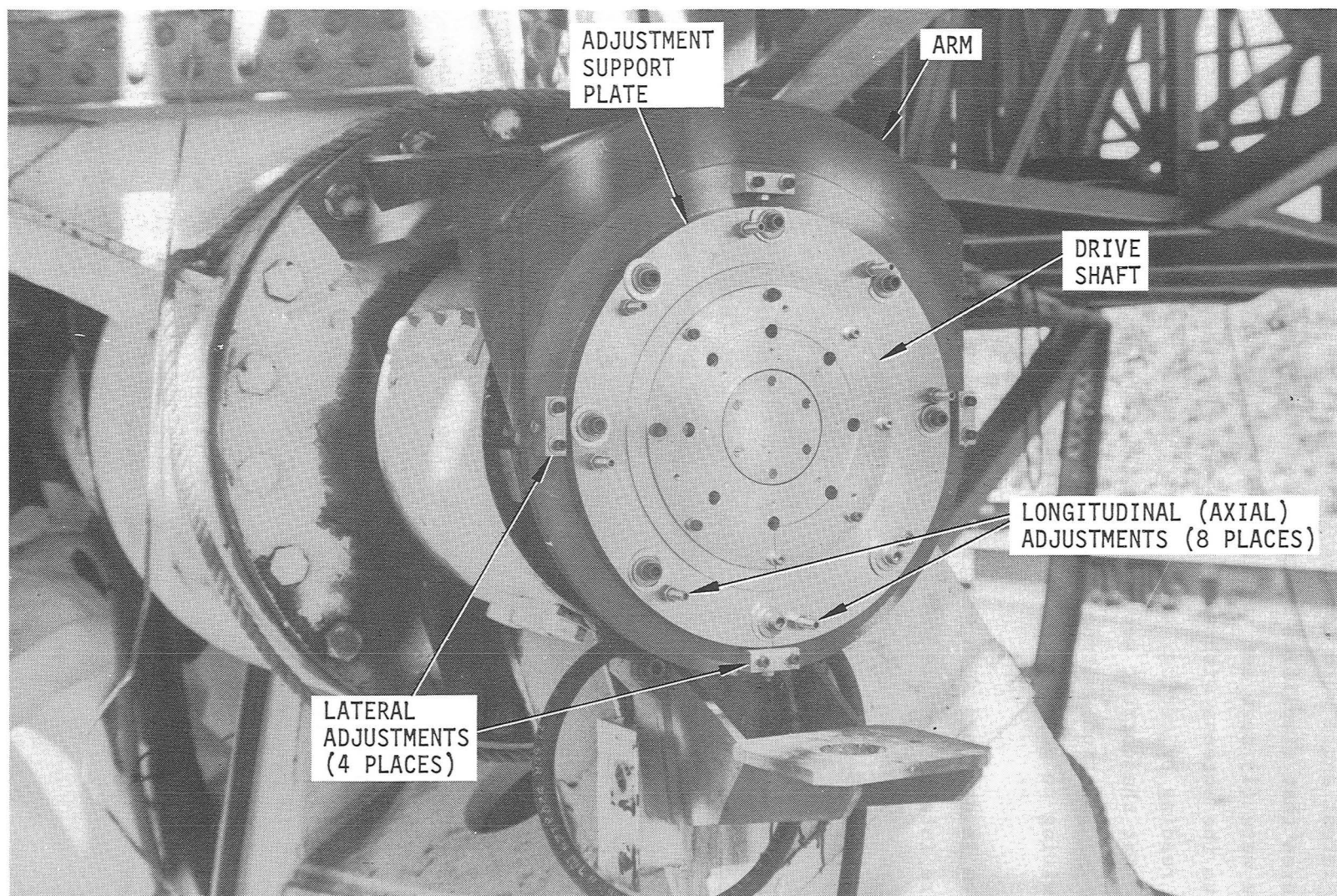


Figure 30. Angle Encoder Mounting Arrangement (DSS 12 Dec Axis)

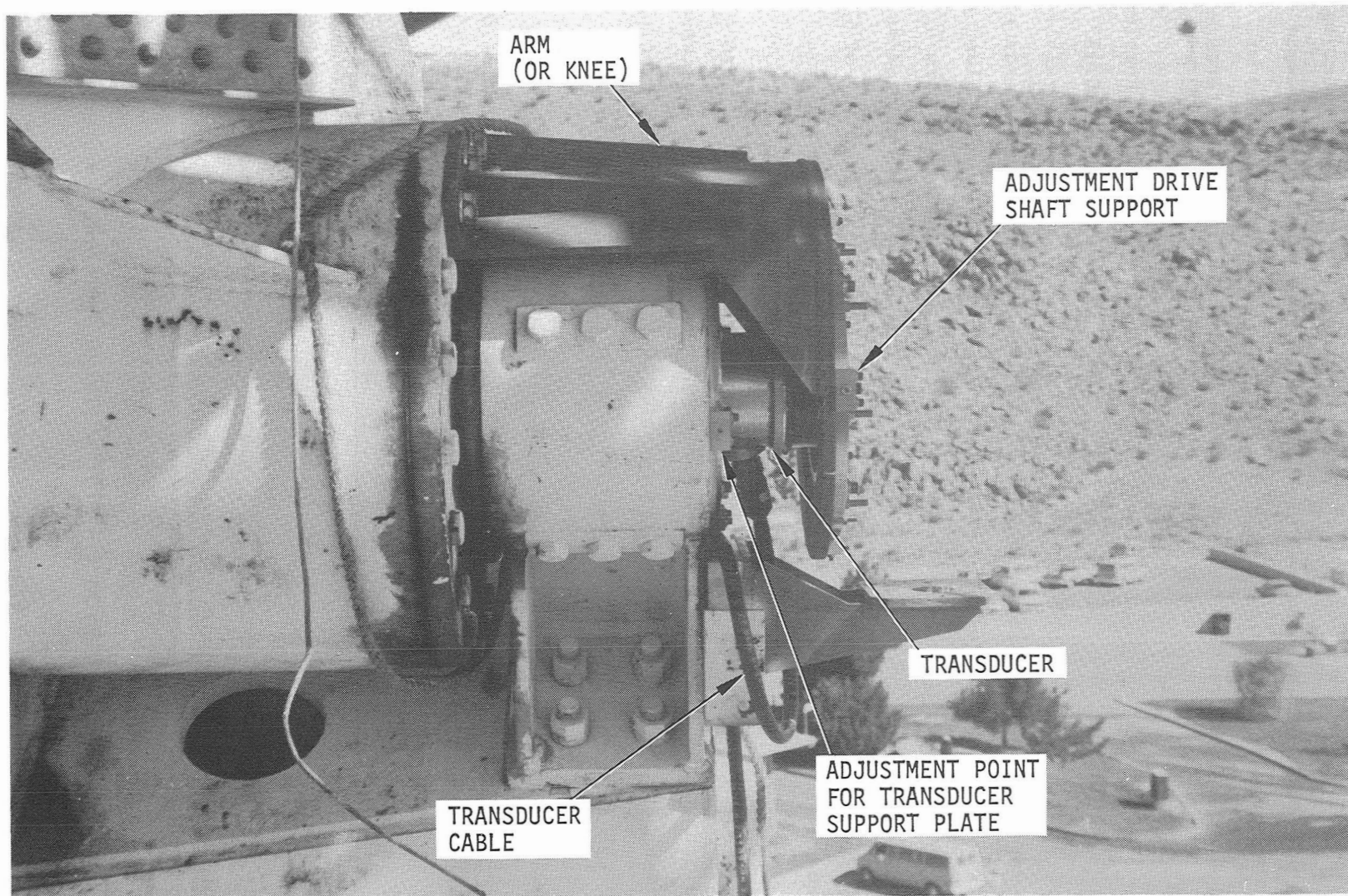


Figure 31. Angle Encoder Mounting Arrangement (DSS 12 Dec Axis), Side View

A significant problem affecting the accuracy was the relative motion between the transducer mounting surface (the end of the fixed axis shaft) and the drive shaft mounting surface (the arm attached to the rotating bearing housing). Measurements made at DSS 12 showed that there were parallel offsets (offsets between the shaft and arm center lines) of approximately 0.10 cm (0.040 in.), angular offsets (angular difference between axis shaft end plane and corresponding plane of arm) of approximately 5.5 arc min, as well as axial offsets (changes in spacing between axis shaft end plane and plane of arm) of approximately 0.137 cm (0.054 in.). These offsets created difficulties in obtaining flexible couplings that would accurately transmit arm rotation to the transducer shaft. The type of couplings used were manufactured by welding along the inner and outer circumferences of a stamped and shaped ring to form a bellows-shaped device. Laboratory testing of the encoder system under combined offset conditions showed that the system had an accuracy of 0.005 degree.

Subsequent to the DSS 12 encoder installation, two more systems were installed on the DSS 42 and DSS 61 antennas. At present, more systems utilizing different transducer configurations but identical electronics are under contract for the 64m antennas.

Figure 32 is a photo of an unmounted transducer, Figure 33 is of the transducer electronics, and Figure 34 is of the control room located Data Converter Assembly.

F. ANTENNA RAISING OR TRENCHING FOR SKY COVERAGE

Because of the increase in the reflector diameter, provisions had to be made to prevent the reflector from hitting the ground in order to meet the sky coverage in east and west directions.

Two methods were used to accomplish this task. At Goldstone and Robledo, Spain, the antenna was raised 3m (10 ft), while at Tidbinbilla, the decision was made to trench the site.

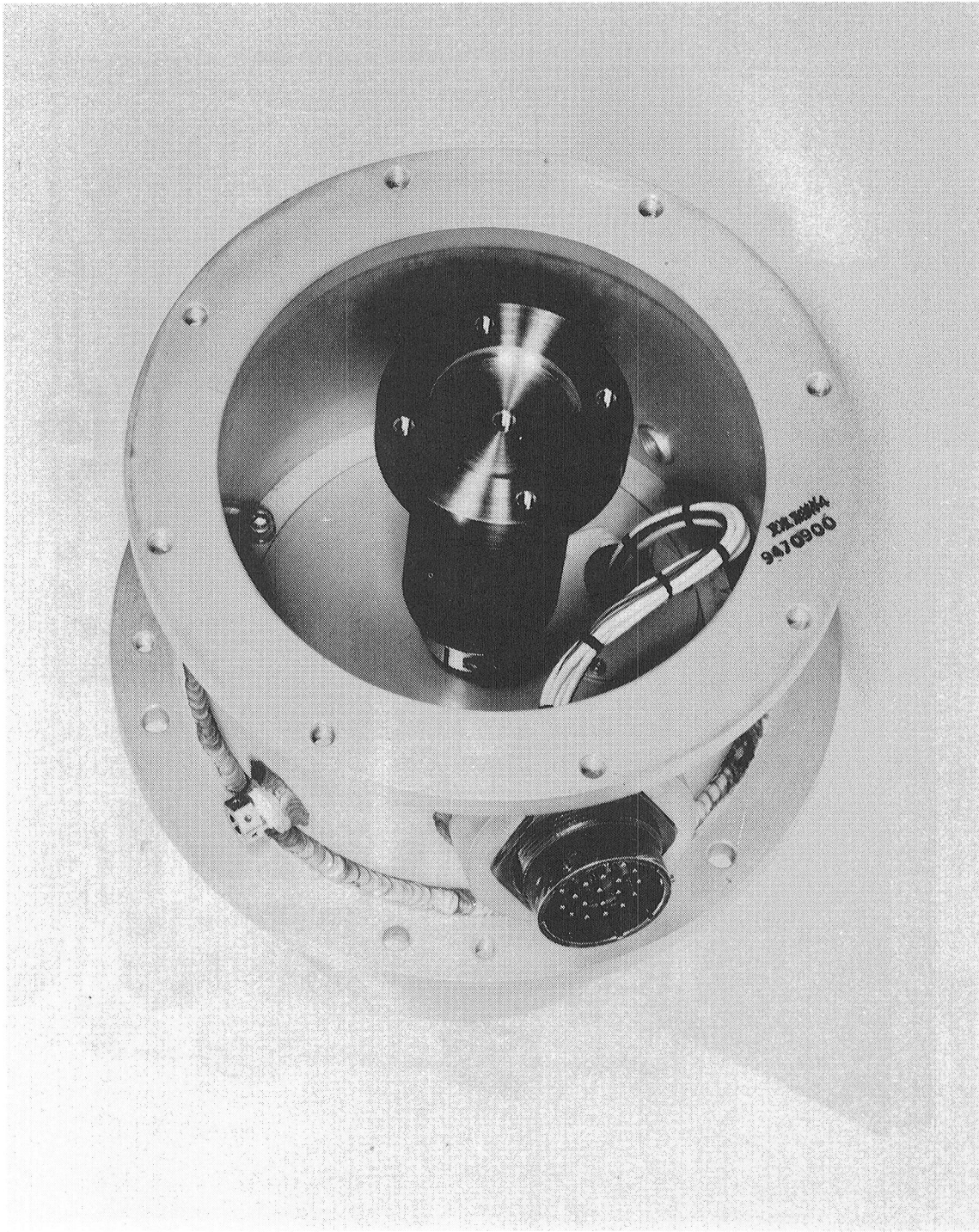


Figure 32. Unmounted Transducer

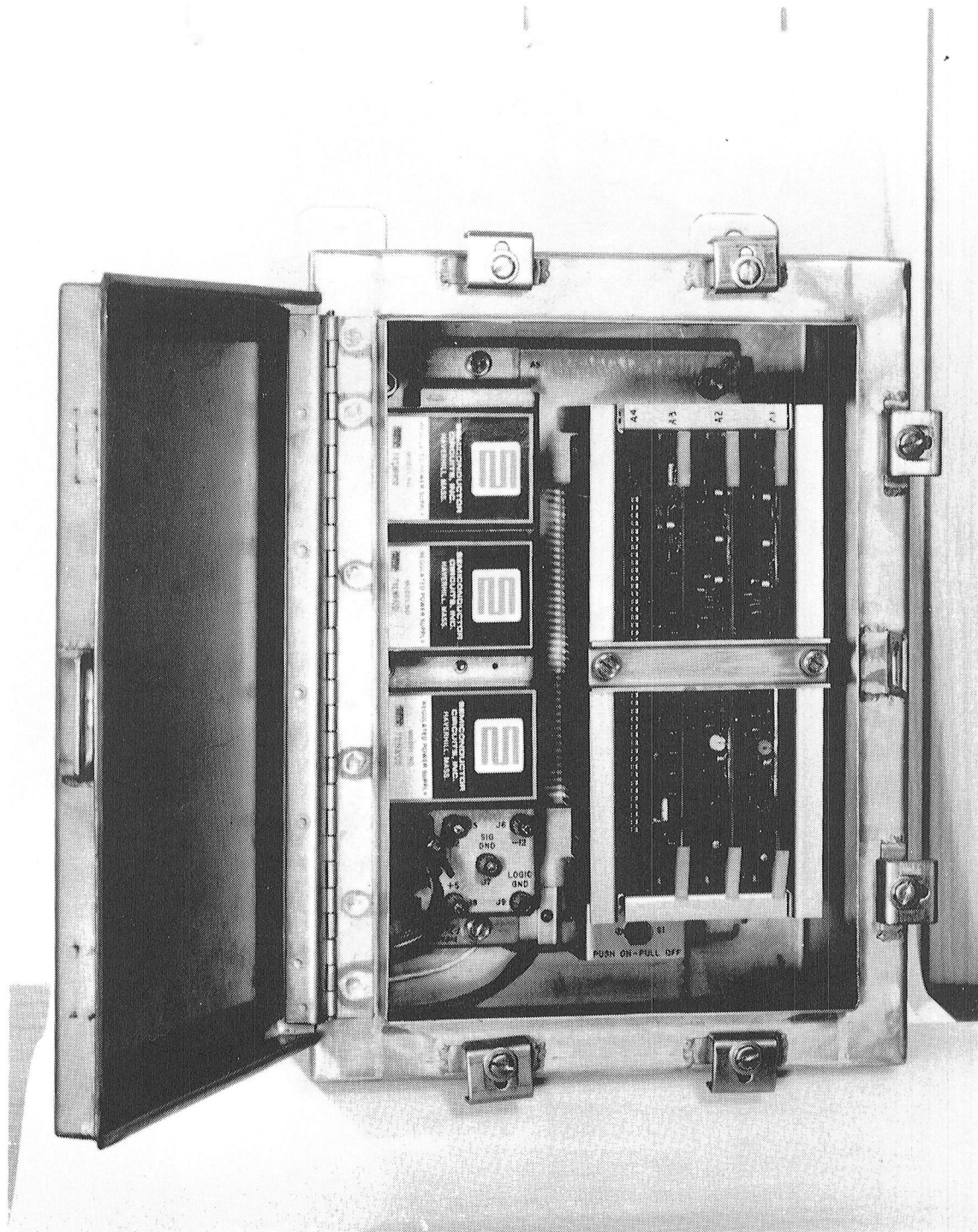


Figure 33. Transducer Electronics

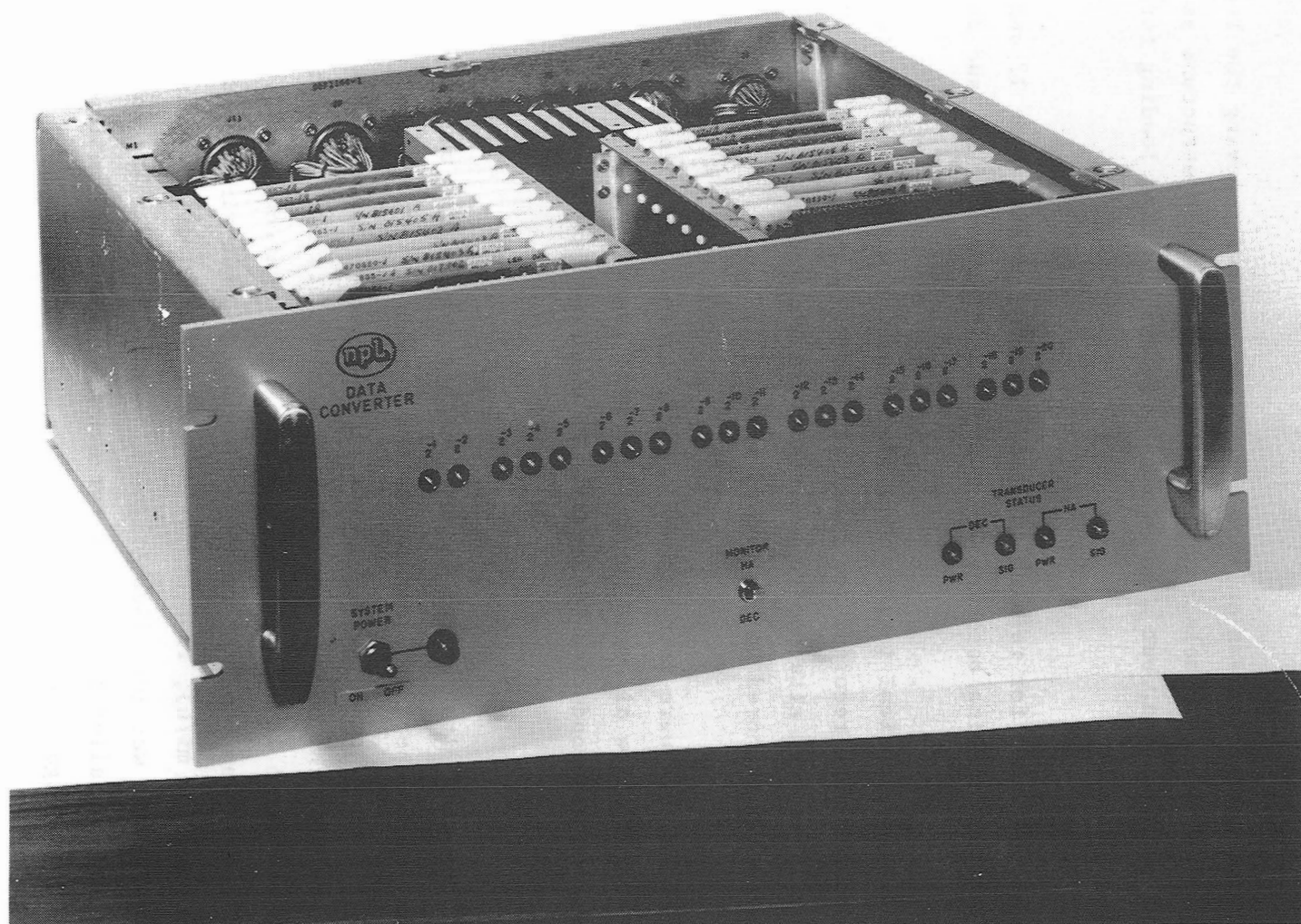


Figure 34. Data Converter Assembly

1. Lifting the Antenna 10 Feet and Placing the Foundation

Prior to awarding the contract for raising the antenna, JPL designed, fabricated, and installed a lifting frame on the antenna (Figure 35).

The prime contractor was on site June 1 and started removing the feedcone, quadripod, surface panels, and a portion of the backup structure as part of the modification, but also to reduce weight and wind loading for the raising project.

The subcontractor for raising the antenna moved on site June 12 and set the initial cribbing base and 200-ton jacks (Figures 36, 37, and 38).

At this time, optical targets were placed on the antenna structure and the coordinates were recorded for final alignment. Also, three 30m (100-ft) safety lines were attached to the structure above the center of gravity and securely anchored to the ground (Figure 39).

The anchor nuts were then removed and the antenna was raised 5 cm (2 in.) and stopped while all weld connections were inspected for cracks. This inspection was conducted by several JPL engineers and field personnel (Figure 40).

After checking with several airport weather services on the high desert and in the Southern California area and obtaining forecasts of wind no greater than 32 km/h (20 mi/h), the field engineer made the decision to start raising the antenna early the next morning. At 6:00 am the wind speed was 32 to 48 km/h (20 to 30 mi/h) and the antenna was 1.4m (4.5 ft) off the base and too late to stop. At 3:00 pm, the wind speed was gusting to 80 km/h (50 mi/h), the antenna was 3.4m (11 ft) off the base, and the support column was installed (Figures 41 through 45). The anchor bolts were then installed and torqued for safety. The wind continued to blow for 2 days (Figures 46 and 47).

On June 20 the antenna was positioned, the anchor bolts reset and torqued, and the jack pads installed (Figure 48).

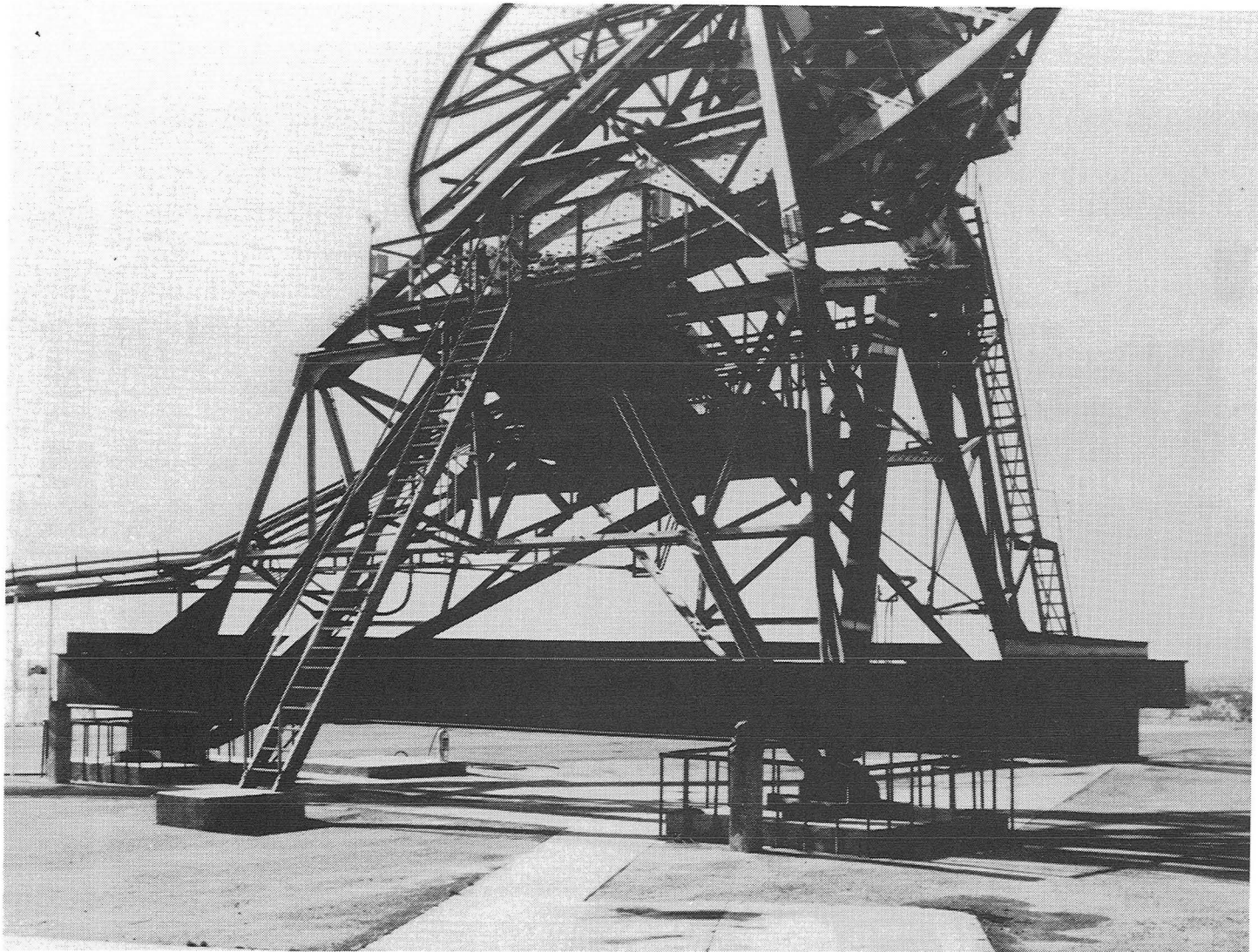


Figure 35. Antenna Lifting Frame

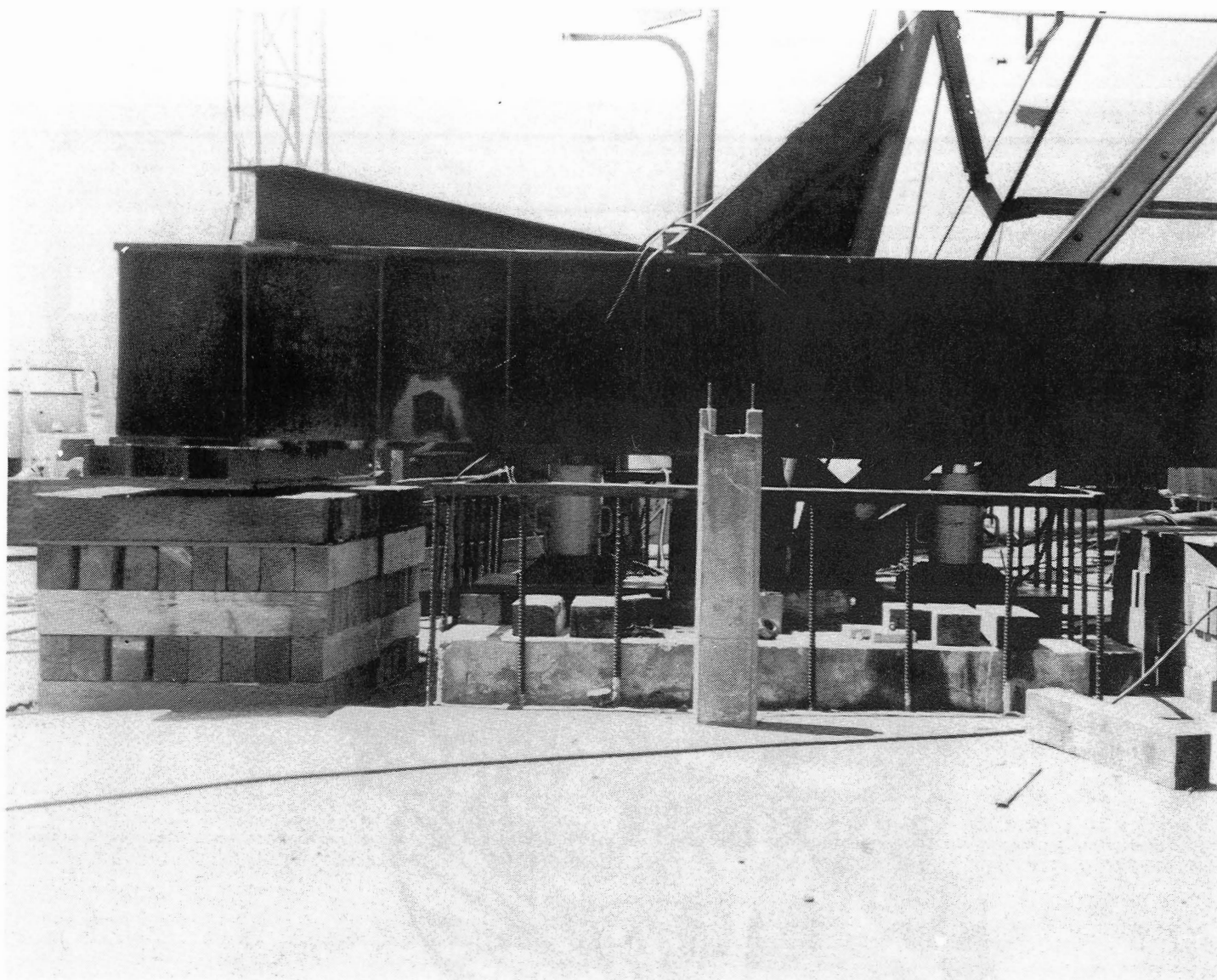


Figure 36. Initial Cribbing Base and 200-Ton Jacks for Raising Antenna

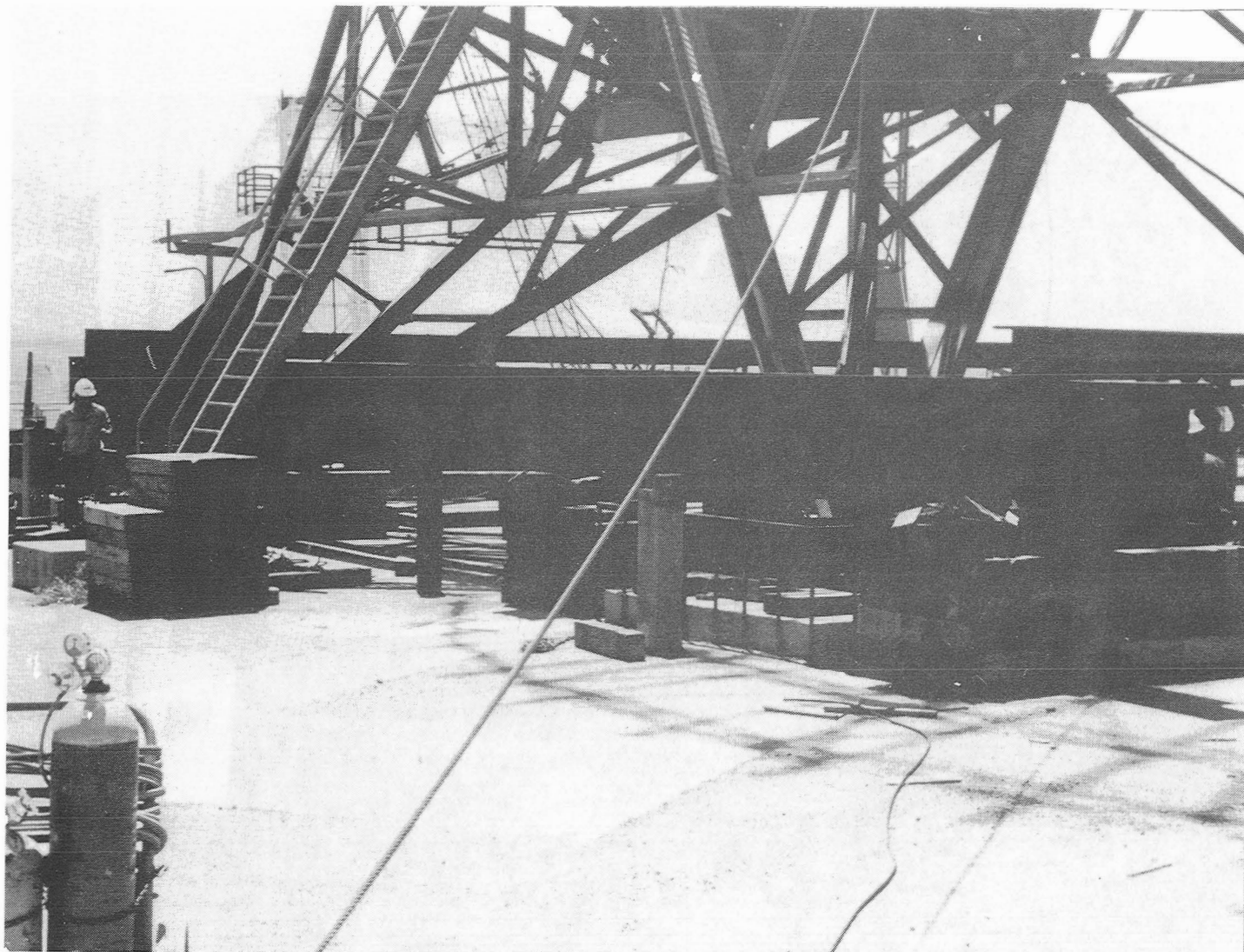


Figure 37. Cribbing Base in Place Under Antenna

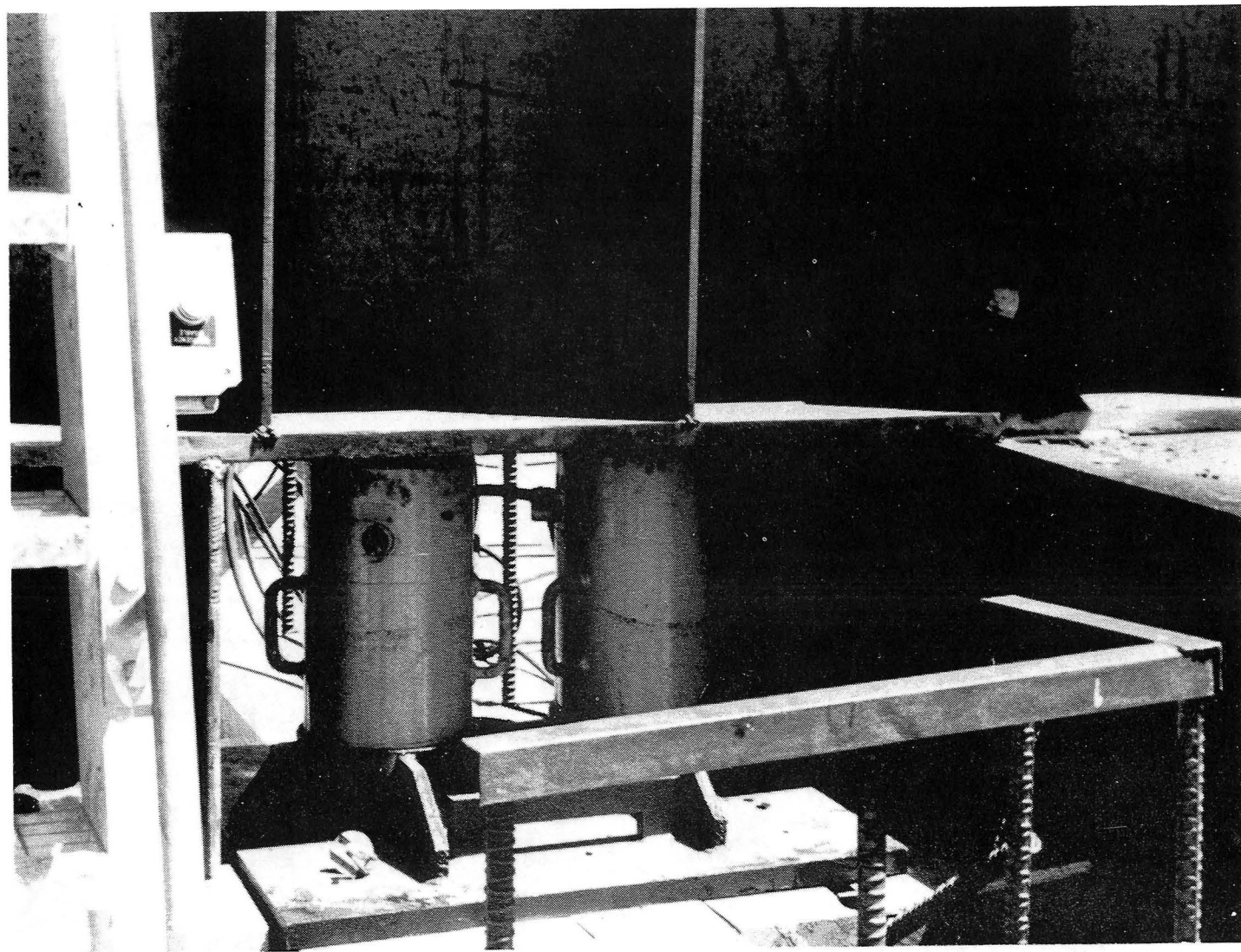


Figure 38. 200-Ton Jacks

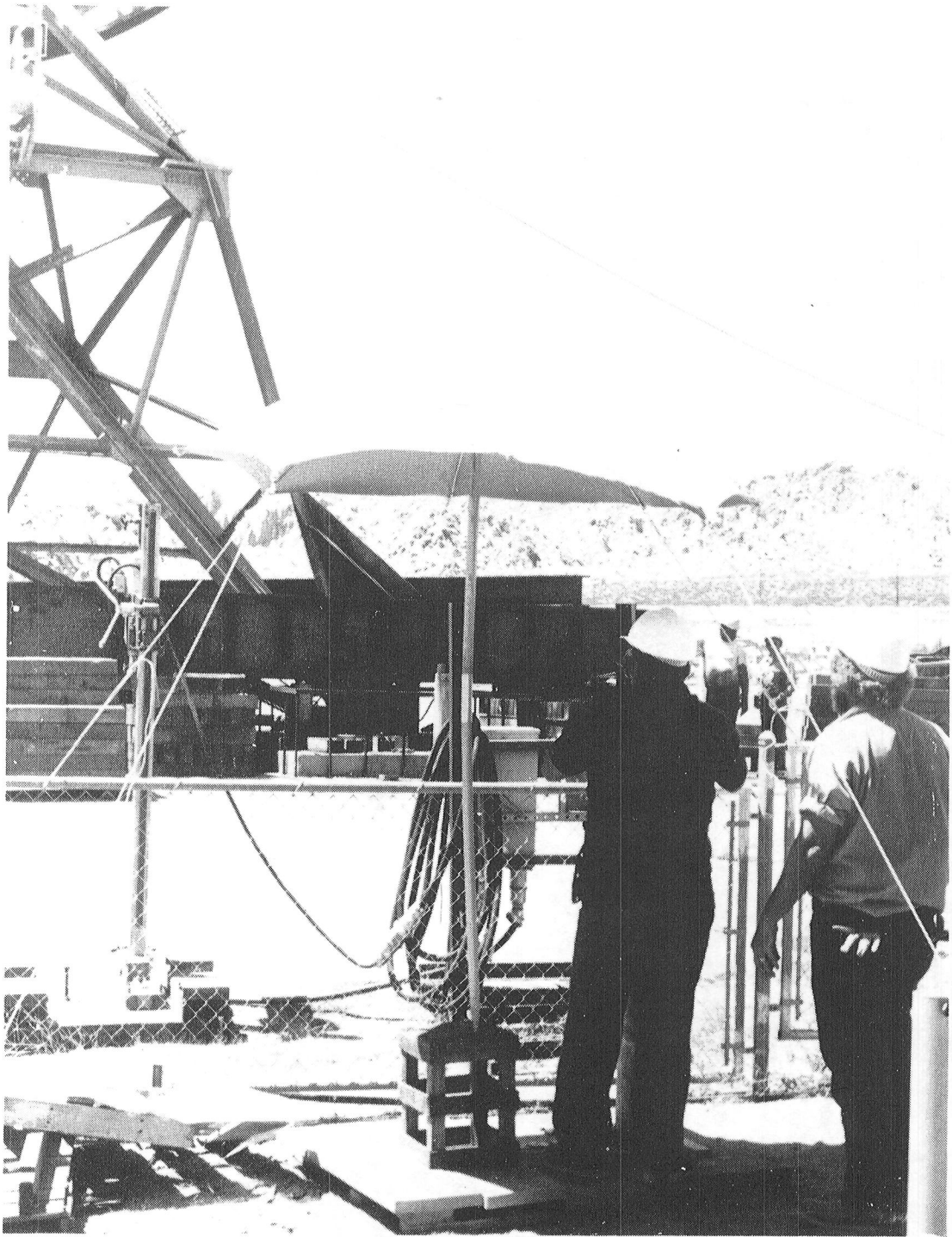


Figure 39. Safety Lines

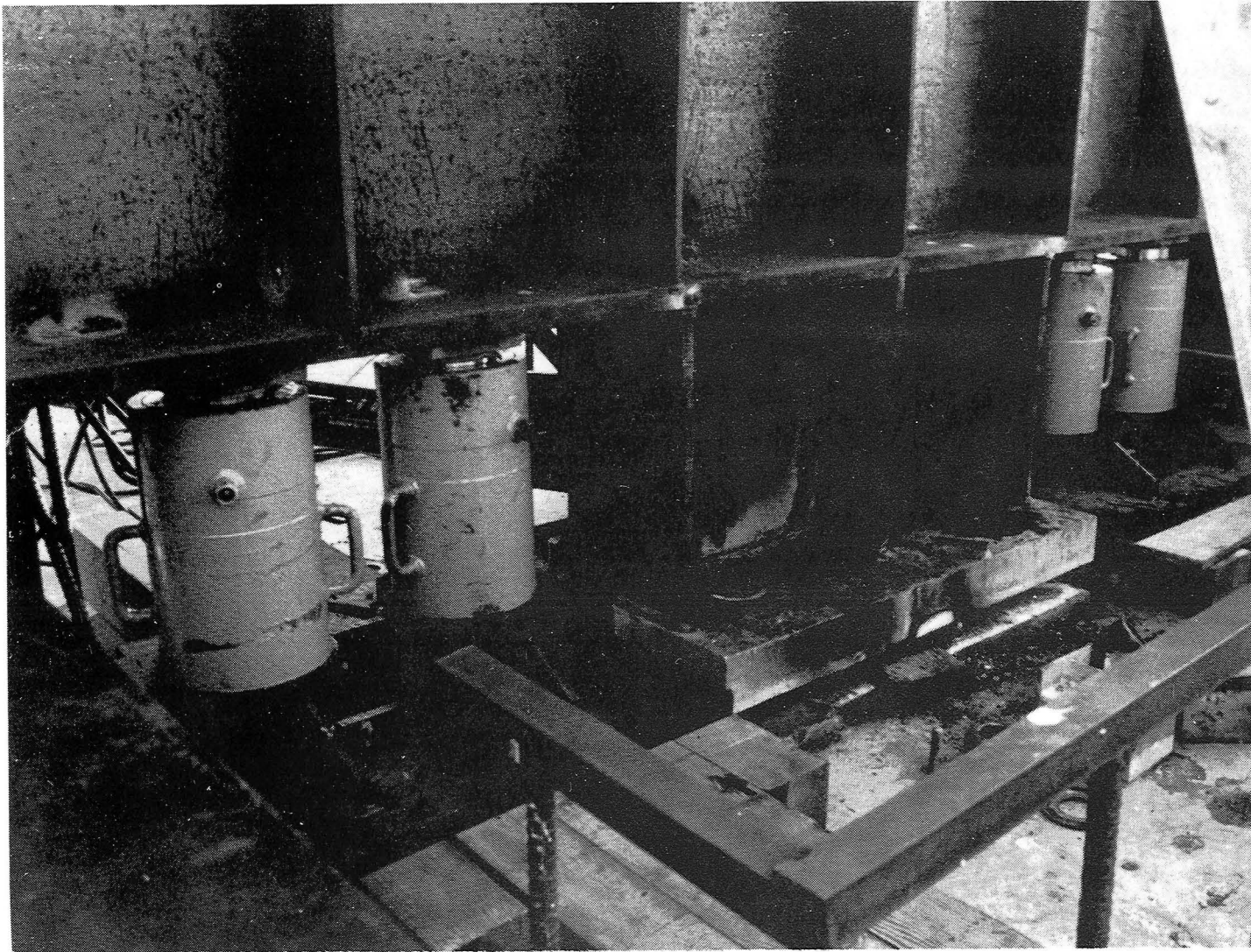


Figure 40. Antenna Raised to Inspection Position



Figure 41. Antenna Resting on Support Column Because of High Winds

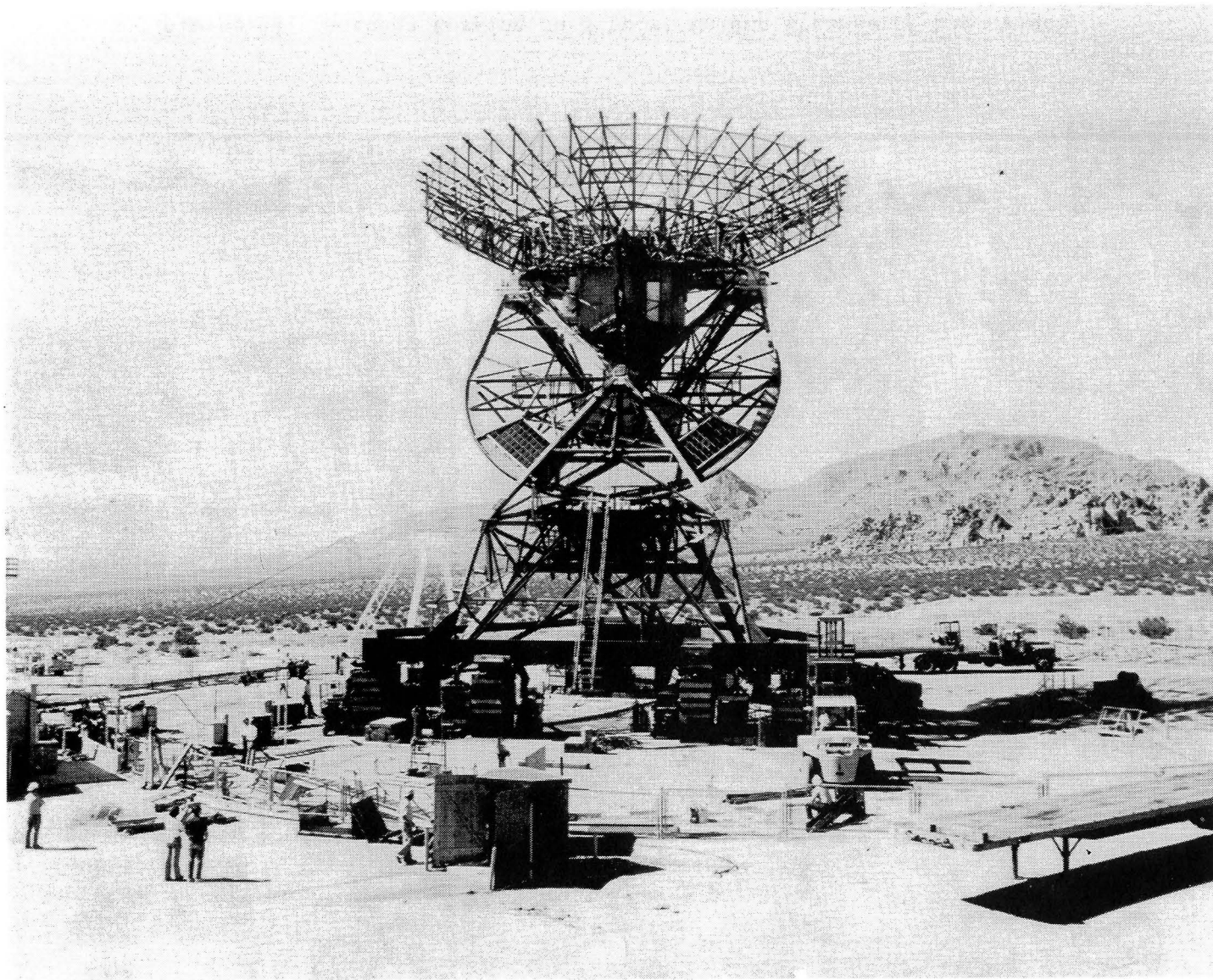


Figure 42. Antenna Resting on Support Column Because of High Winds, Second View

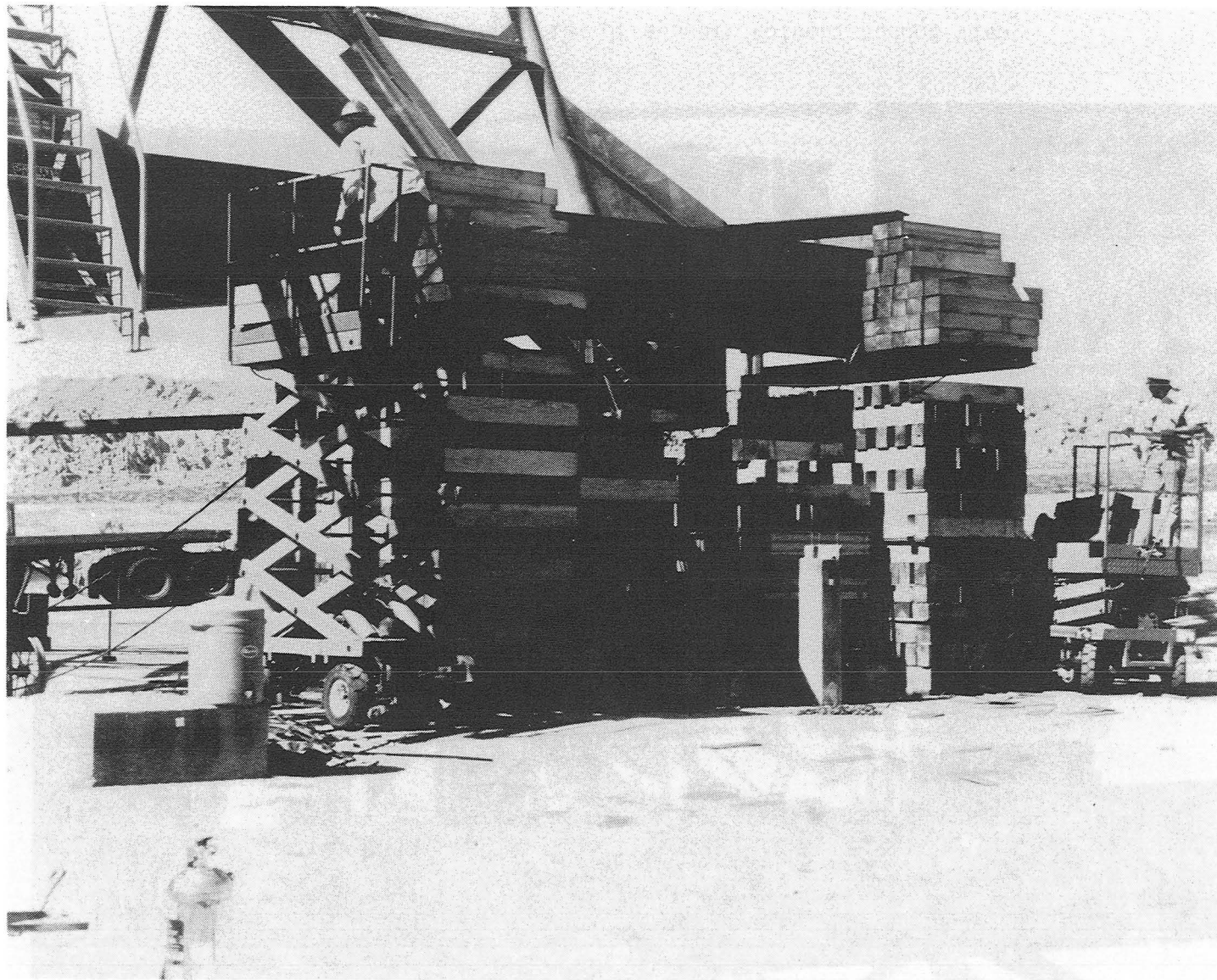


Figure 43. Closeup View of Support Column



Figure 44. Closeup View of Support Column, Second View

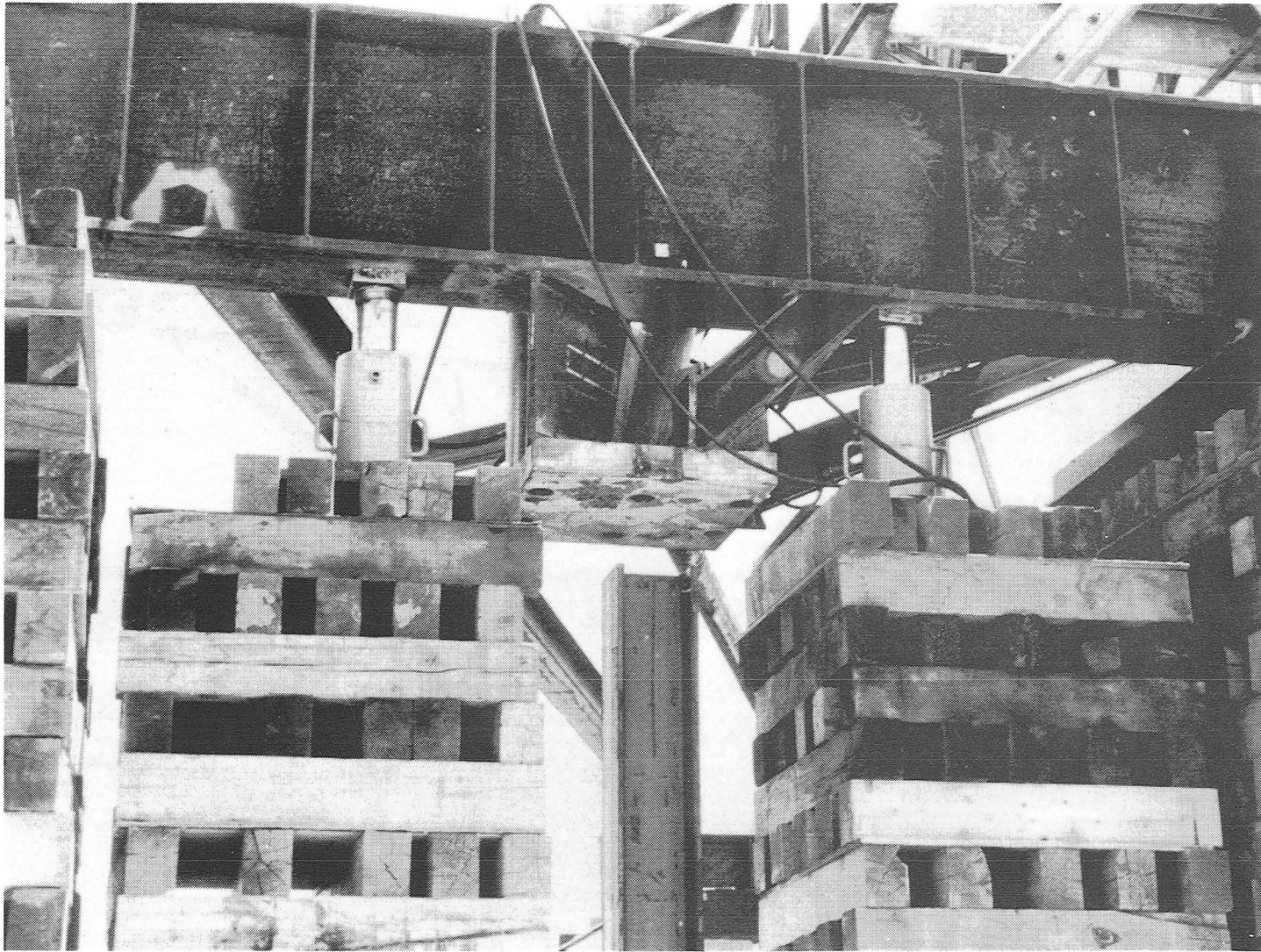


Figure 45. Closeup View of Support Column, Third View

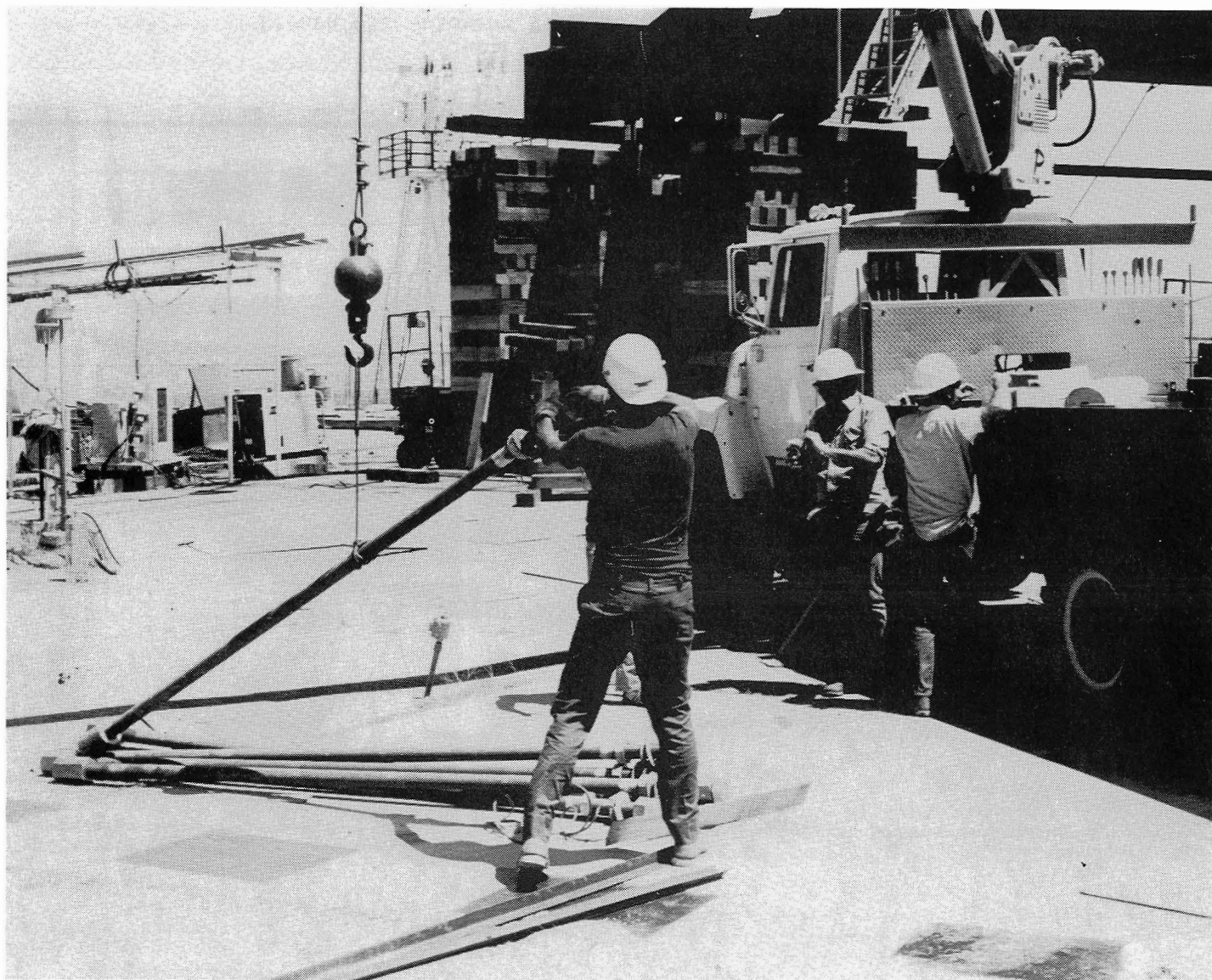


Figure 46. Antenna During 2-Day Period of High Winds

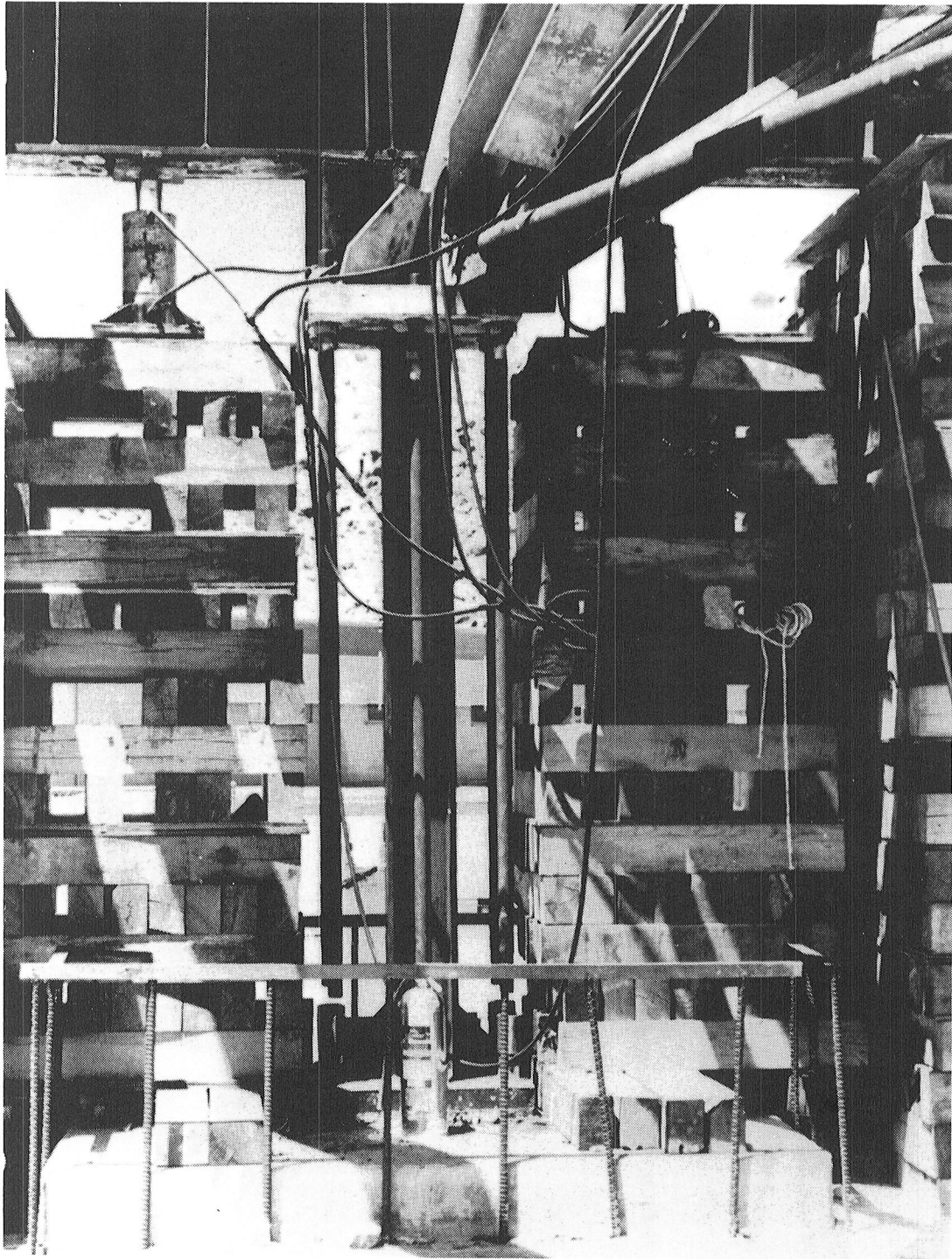


Figure 47. Support Column During 2-Day Period of High Winds

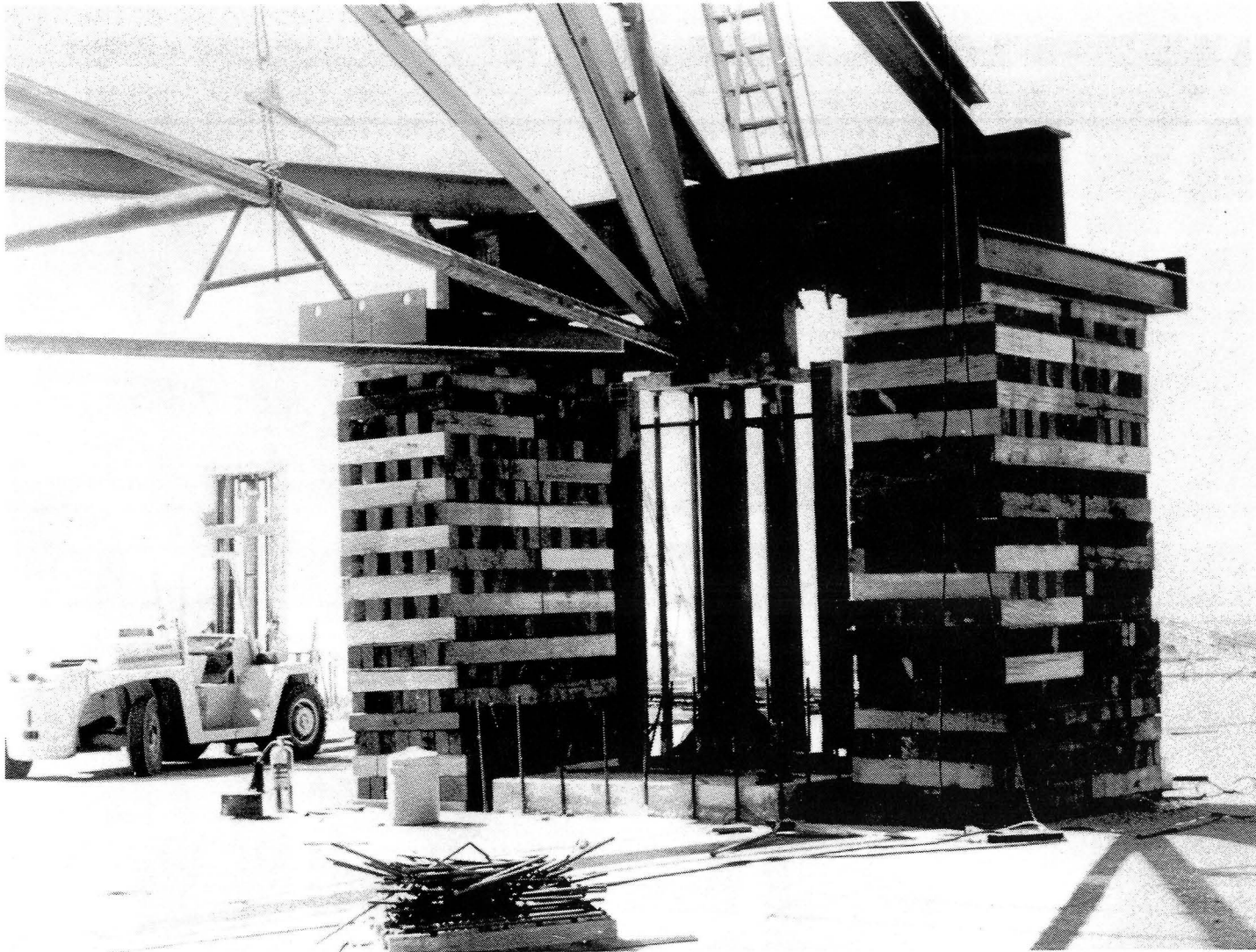


Figure 48. Antenna in Position with Jack Pads Installed

On June 29 the rebar and forms were complete and the concrete foundations were poured on June 30 (Figure 49).

The lifting frame, cribbing, and forms were removed on July 12 and structural work resumed full time on the antenna (Figures 50 through 52).

2. Trenching

Due to the sloping terrain at the Tidbinbilla site, the depth of the trenches was not equal. The work was performed by the Australian Department of Works, located in Canberra, Australia. To verify the trench profile, a check of the excavation was made using the complete antenna (see Figure 53 and 54). The east trench is 2m (7 ft) deep and the west trench is 2.5m (8.25 ft) deep, each having a grating covered sump of 0.6m (2 ft) wide and 0.9m (3 ft) deep. The trenches, as well as the sumps, were finished with reinforced concrete (see Figure 55). To relieve pressure on the walls, weep holes were provided. The sumps are equipped with pumps to remove storm water. A minor part of the south pier foundation was removed for reflector clearance purposes. Although drawings were prepared for the trench section, a special clearance check was made by rotating both the hour angle and declination wheels in the trenches, maintaining the tracking limit at 6 degrees of elevation because of the 9-degree horizon mask to the east and the ground terrain around the antenna. It was cost effective at Australia to trench, which resulted in both time and costs savings by not raising and realigning the antenna axes.

G. ELECTRONIC CHANGES AND ADDITIONS

1. Cable Trays and Cables

Cable tray modifications were needed only where the antennas were raised. The modifications included extensions of the trays and splicing of the existing cables.



Figure 49. Typical Form for Concrete Foundation



Figure 50. Concrete Foundations

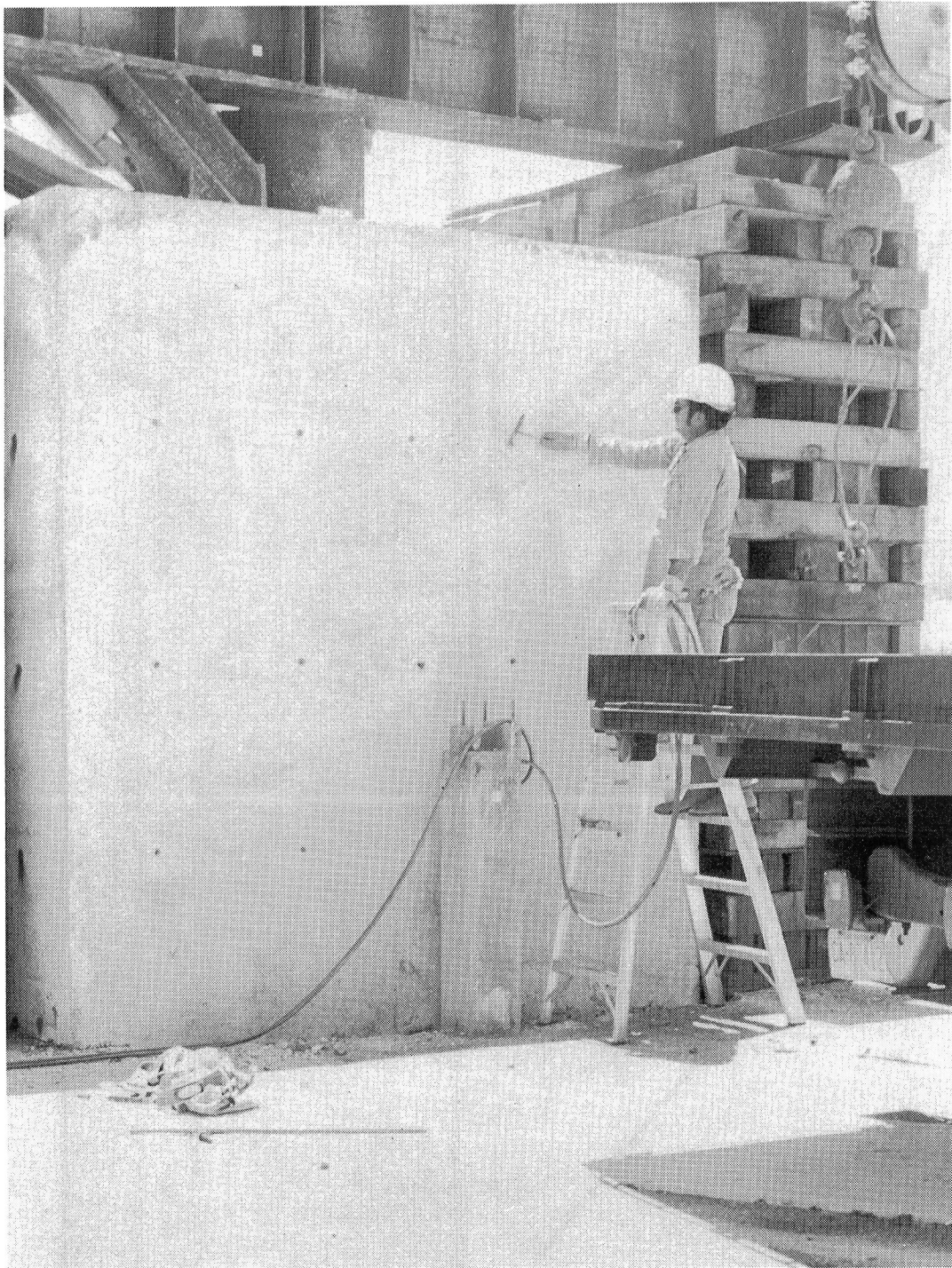


Figure 51. Finishing Concrete Foundation

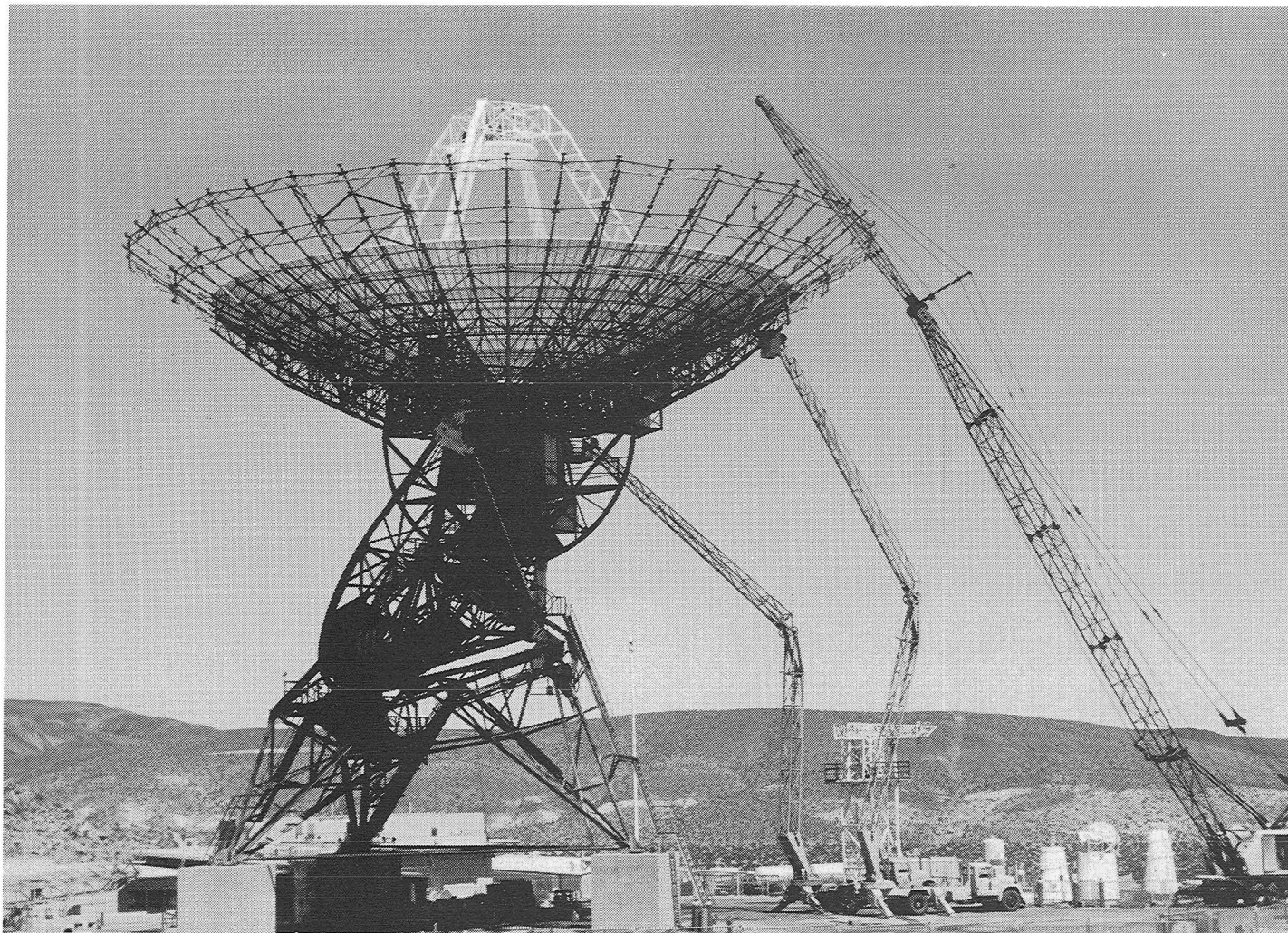


Figure 52. Resumption of Work on Antenna

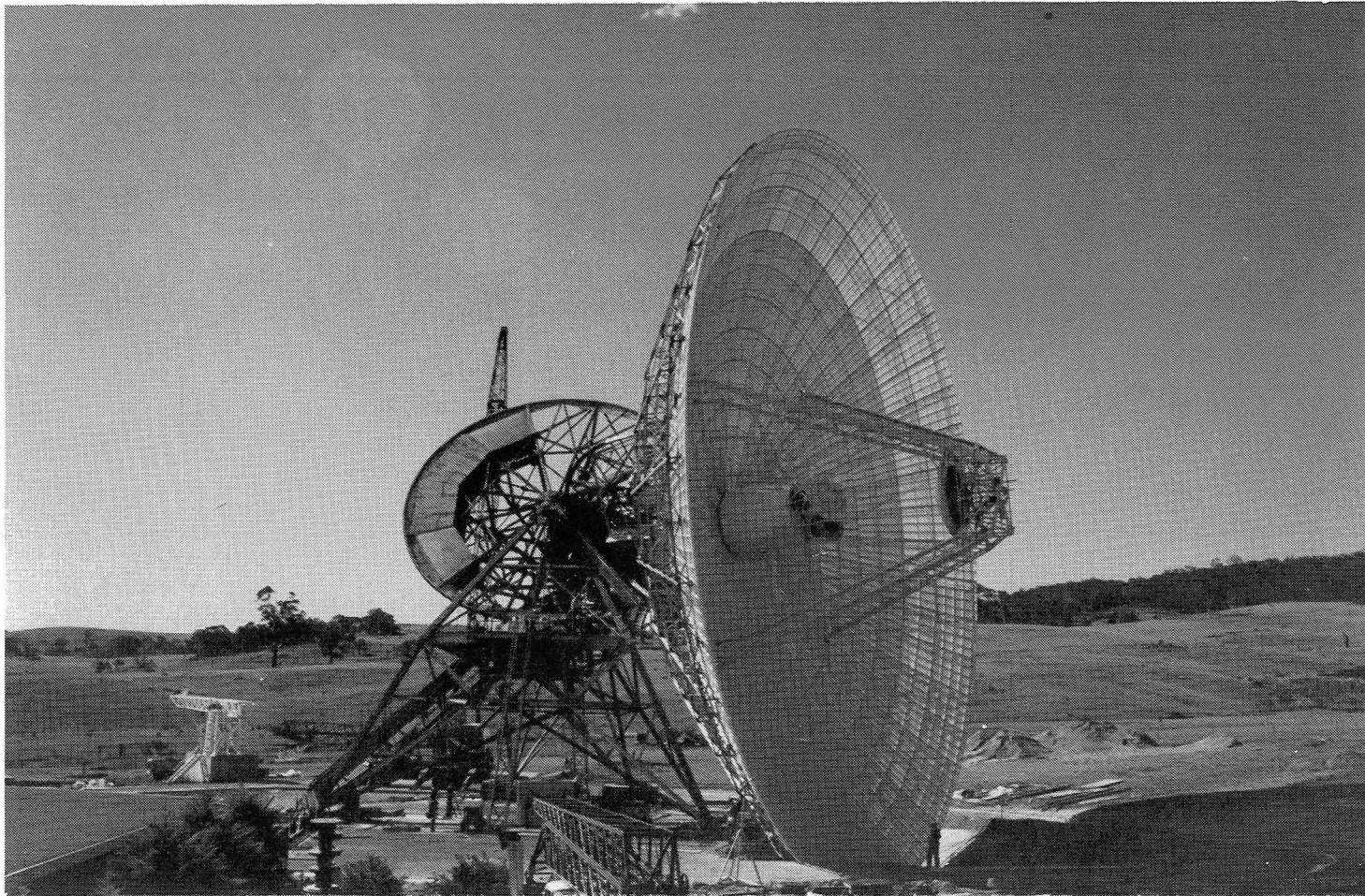


Figure 53. Check of Trench Profile at DSS 42

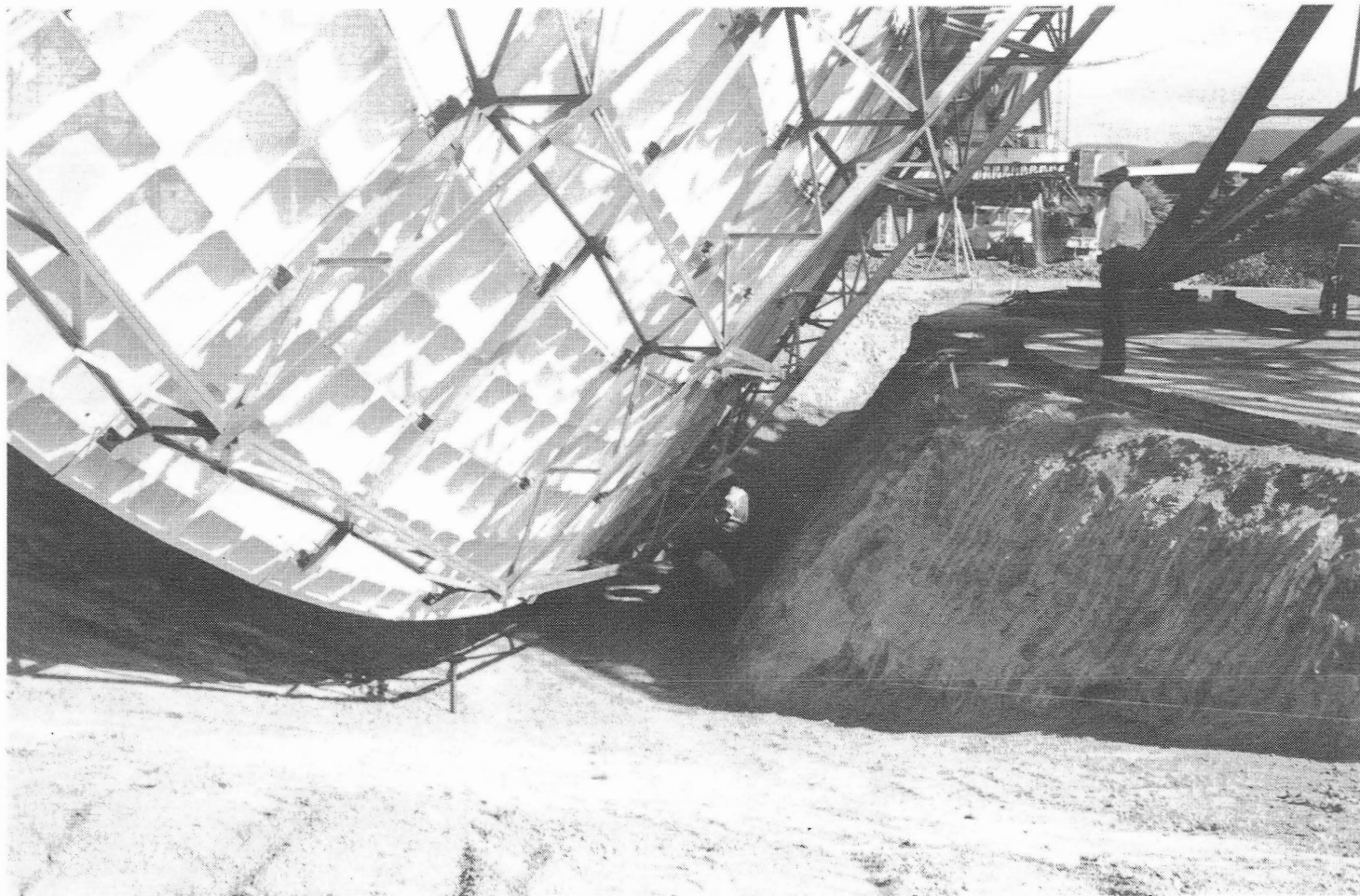


Figure 54. Closeup View of Reflector and Trench (DSS 42)

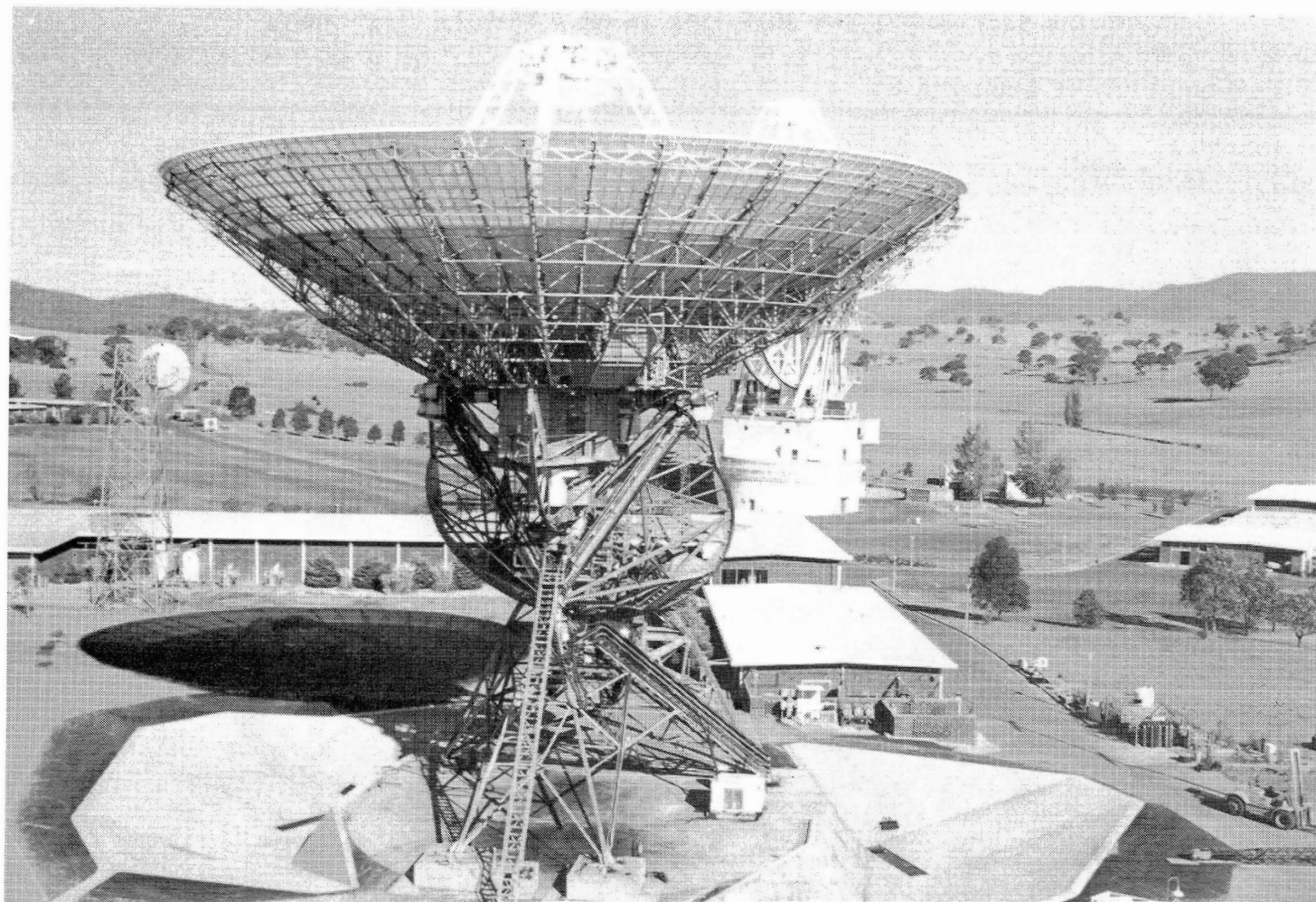


Figure 55. Completed Trenches (DSS 42)

2. Utility Power Modifications

These modifications included power to one aircraft warning light on the quadripod and four aircraft warning lights at the edge of the reflector. The installation of power wires and aircraft warning lights on the quadripod and apex were accomplished on the preassembly location on the ground, with the final interconnect made after the installation of the quadripod and subreflector on the antenna structure. The installation on the reflector edge and power wiring was accomplished prior to the final completion of the antenna modification. Junction boxes were installed near the angle encoders, which require 120V power.

Temporary power was supplied at the antenna base for welding equipment, including a safety cutoff switch.

3. Antenna Microwave

The antenna microwave hardware for the conversion consists of a new X-band maser, microwave switch control system, S-band feedhorn and associated waveguide, X-band feedhorn and associated waveguide, waveguide equipment to accommodate the existing S-band Block III maser and diplexing components, S-band feed polarizations for manually selectable RCP or LCP, and X-band feed polarizations remotely selectable.

The installation of the microwave conversion package consisted of installing the control room X-band maser rack and interfacing it to the antenna. The new automated switch control rack, which provides improved generation and verification of subsystem microwave switch positions, replaced the manual switch control rack. A dual S-X feedcone assembly was installed on the antenna. The microwave equipment in the dual S-X feedcone assembly is shown in Figure 56, along with the Cassegrain elements of the Antenna Mechanical Subsystem. A third closed-cycle refrigerator (CCR) compressor and ancillary equipment were installed in the hydromechanical room. New cryogenics from the control room to the antenna feedcone were also installed. A new waveguide between the existing 20-kW transmitter output and the dual S-X feedcone was installed

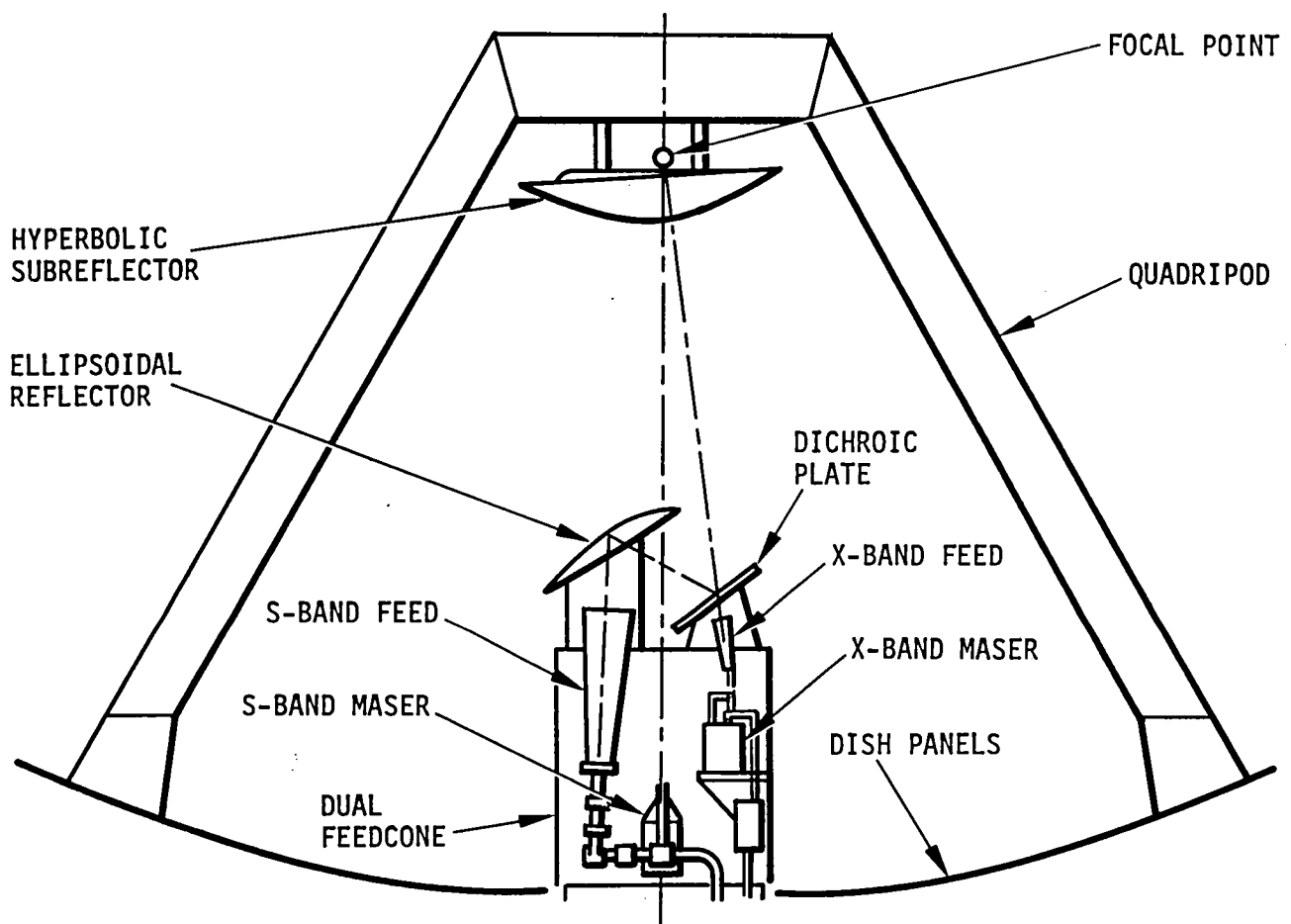


Figure 56. Antenna Microwave S-X Conversion

in this waveguide run to remove the fourth harmonic. Maser subsystem tests of both S- and X-band, transmitter high power tests, and microwave switch control and related automation tests were then run.

Firmware was included in the switch control assembly to provide the logic for generation of microwave configuration displays as well as to provide for the control of the switches. This software provides for 10 programmed modes that can be called by typing in a single code to change the microwave system to the desired configuration. The switch control rack has a keyboard and a computer graphics TV for display of the selected configuration.

4. Receiver-Exciter

The receiver-exciter conversion consists of the following assemblies:

- (a) Stable frequency converter used to convert the S-band input signal to X-band.
- (b) X-band doppler extractor to provide X-band data.
- (c) Translator to provide a coherent X-band test signal generated from the S-band exciter frequency. This signal will then be used to evaluate the subsystem performance.

These assemblies were fabricated and assembled in the JPL fabrication shop. This fabrication included the new module types, such as the frequency shifter, doppler fixer, doppler reference, frequency distribution, and frequency multiplier.

The station personnel installed the receiver-exciter modifications which included the installation of receiver hardlines and multiconductor cables from the control room to the electronics room on the antenna.

5. Planetary Ranging Assembly

This hardware provides simultaneous S-X ranging capability. This assembly consists of two ranging demodulation assemblies at each station. The

planetary ranging assembly was procured for DSS 42 and existing assemblies were used for DSS 12 and DSS 61.

6. Wideband Data Interface

This hardware provides the processing of X-band video rates at the conversion stations for both on-site recording capability and wideband communications interface equipment for real-time transmission of video data to the mission control center. The equipment to provide this function includes the following:

- (a) Wideband communication buffers
- (b) Dual magnetic high rate tape recorder assemblies and current-to-voltage (I/V) converters
- (c) GCF-coded multiplexers and wideband NASCOM terminal for DSS 12

System performance tests were run which included all inflight missions at threshold conditions in both coded and uncoded modes at min/max data rates for each modulation index. Emphasis was placed on the S-X capabilities for Voyager and Viking. These tests proved successful for implementation of the wideband interface.

IV. DESIGN AND ANALYSIS OF CRITICAL AREAS

The design of the 34m hour angle-declination (HA-dec) antenna mechanical modifications presented a number of new and difficult engineering problems. The conversion of an existing antenna limits new loads that can be carried by the existing foundation and bearings. Also, there is limited available space to add counterweight material needed to balance the added new structure. Similarly, cost-effective approaches to the design of the new microwave additions required constraints of using some existing equipment and available electronic room areas. The lifting of a 400-ton antenna structure to provide for ground clearance of the extended structure was also a very difficult engineering task.

A. REFLECTOR AND SUBREFLECTOR DESIGN STUDY

A design study was made on the reflector rib extension profile. The primary difference was a profile of a rib that comes to a point or a rib that has some end depth. Figure 57 shows the two models, labeled A and B.

Figure 58 shows both models when run as an integral part of the reflector structure to determine the rms versus the weight used. Figure 58 clearly shows that Model B had a significant rms improvement for gravity loads over model A. The same figure also shows model A slightly better for wind. Because gravity loads are a constant effect on the antenna during its use and 48-km/h (30-mi/h) wind loads only occur about 10 percent of the time, the model B structure was selected.

The model B antenna reflector structure was then run on a computer using five iteration cycles of the JPL "IDEAS" structural analysis program. The resultant best design for structure weight is shown on Figure 59.

The subreflector control assembly positions the subreflector in X, Y, and Z coordinates as a function of the HA and dec position of the antennas. This positioning minimizes the gain loss due to defocusing of the RF beam which arises from the gravity displacement to the reflector and subreflector assemblies. The subreflector control assembly also provides antenna pointing offset correction in HA and dec as a function of X and Y positions of the subreflector. Because the antenna will operate in a CONSCAN

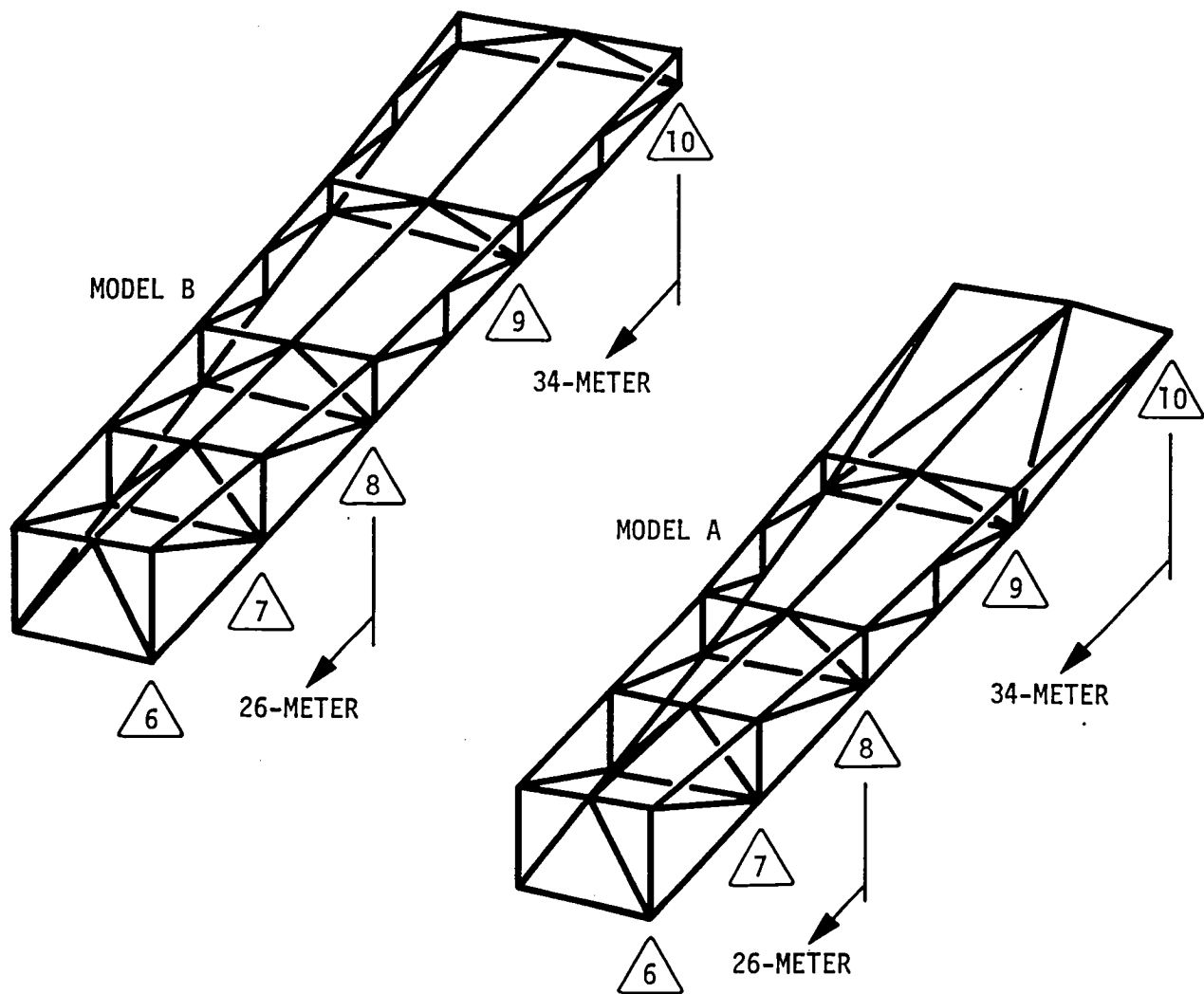


Figure 57. Reflector Rib Extension Profile Extension

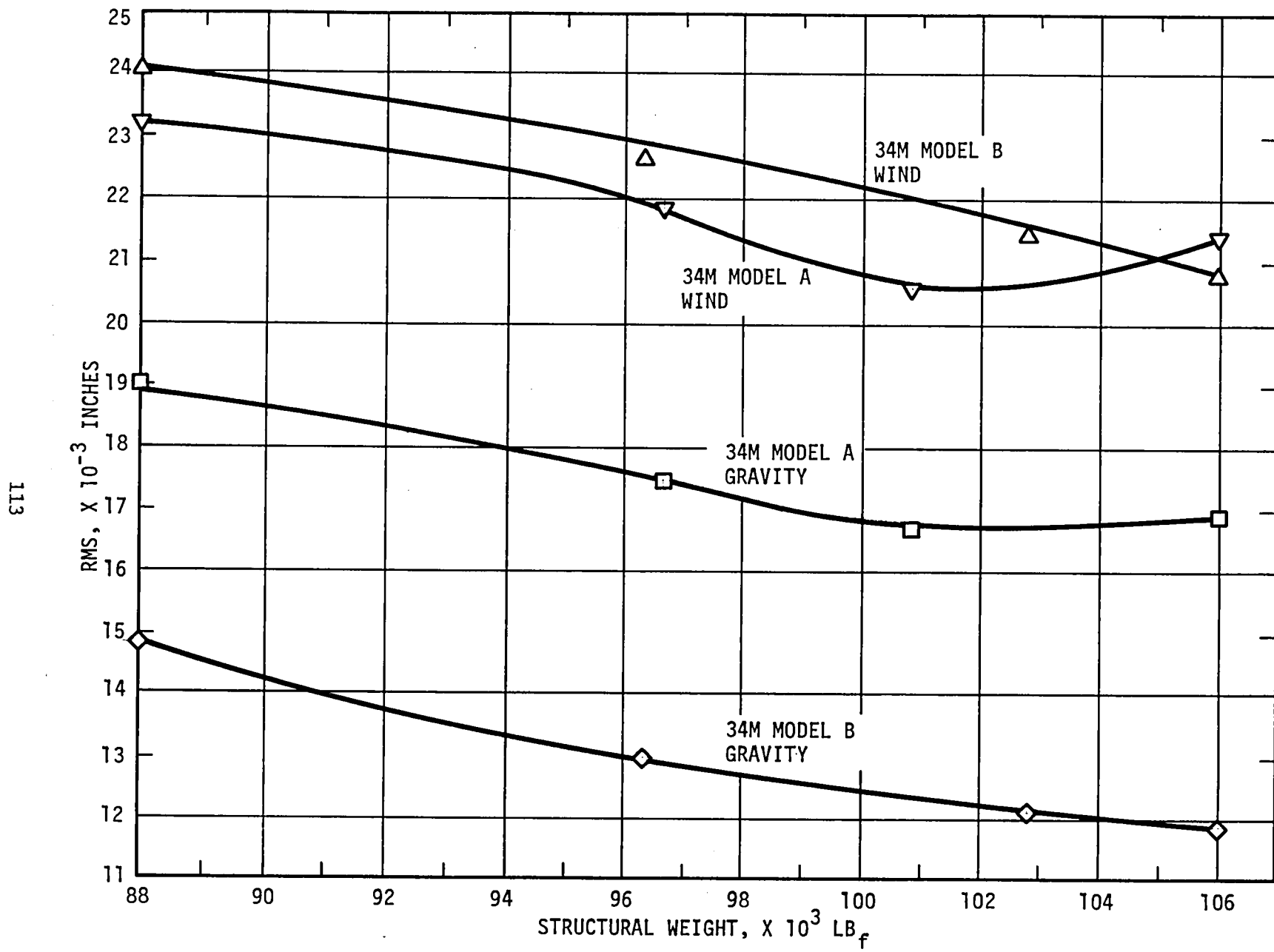


Figure 58. 34M Model A and B Structural Weight vs RMS Designed for Gravity

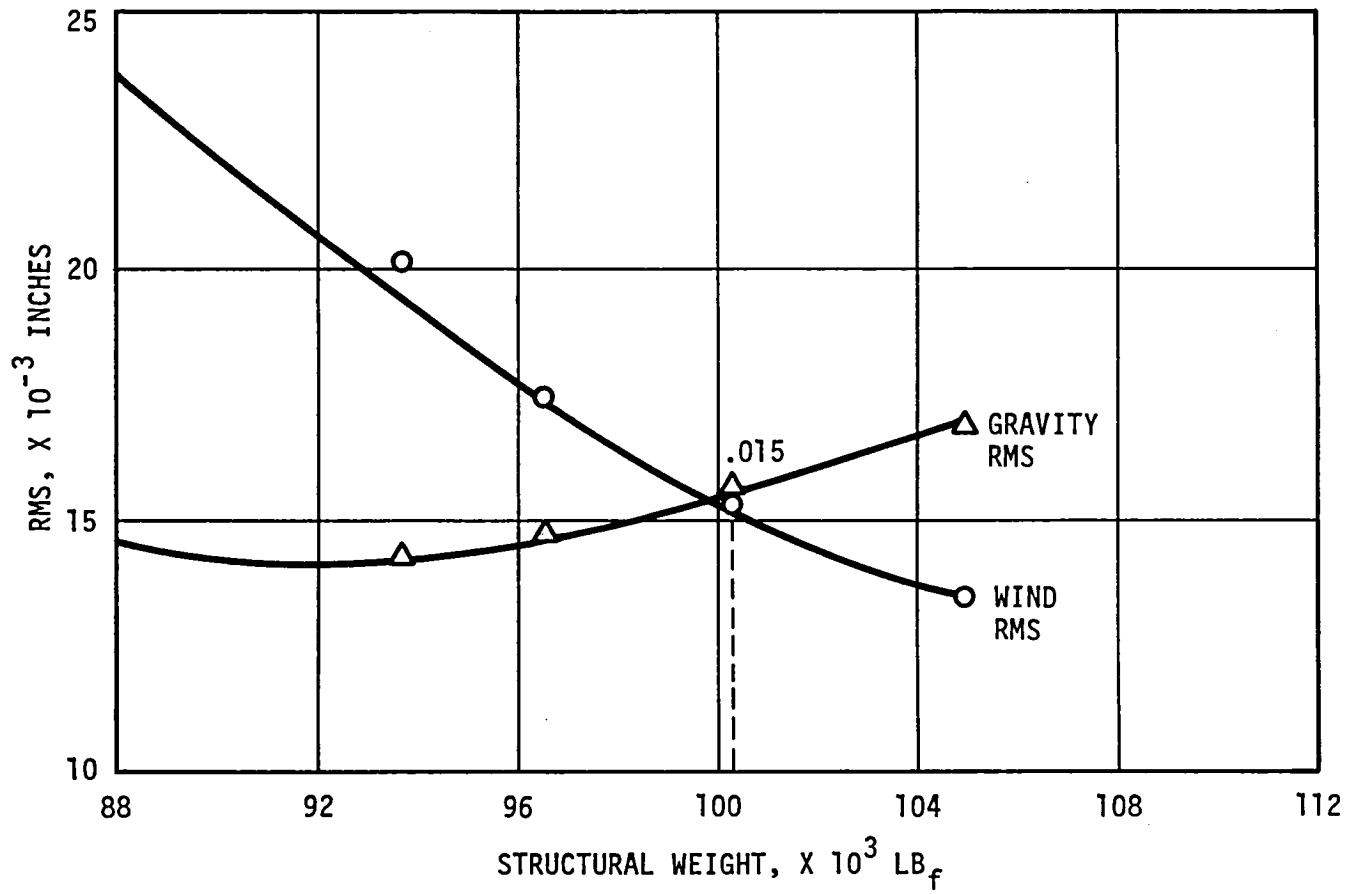


Figure 59. 34M Model B Final Design

pointing mode in normal operation, the subreflector control assembly was designed to operate in conjunction with CONSCAN, with CONSCAN correcting any residual antenna pointing offset errors.

It was then calculated that if no subreflector position change was provided, losses of 0.7 dB would be incurred. One of the complexities of the position offsets in X and Y is that they would induce pointing errors that could, if not compensated, also cause gain loss. The CONSCAN mode maintains gain by moving the antenna in a circle described by the points where gain is 0.1 dB less than the peak gain. This mode compensates for the induced errors caused by subreflector position changes. A correction program for the position pointing error was included in the microcomputer designed for the subreflector controller.

The travel limits were calculated from computer runs made on the primary reflector structure that showed where the subreflector should be positioned for different positions of the antenna structure. A look-up table was developed from several antenna computer runs with different gravity orientations.

The travel limits were determined and the design was essentially a set of jackscrew assemblies, link systems, and constant speed motors that could be driven a set time to position the subreflector in the X, Y, and Z axes.

B. SELECTION OF THE RATIO OF FOCAL LENGTH TO DIAMETER OF THE PRIMARY REFLECTOR

The need to use a different f/D ratio was a primary concern since from a cost standpoint, when it was decided to enlarge the existing 26m antenna to 34m, it required the use of the existing structure and panels. The existing f/D ratio was 0.417, which is a fairly flat parabolic reflector. The new configuration using the existing panels would result in an f/D ratio of 0.324, which is a deeper reflector than the existing DSN antennas.

The antennas used by the DSN (64m, 26m, and 9m) have all had an f/D ratio of 0.417 and there was some concern as to the effect on the RF performance of the antenna with a deeper dish.

Both f/D ratios were run structurally and by microwave by using computer software for a 34m reflector diameter and different focal lengths.

The deeper reflector ratio of 0.324 results in the position of the subreflector being more critical than in the shallower reflector with an f/D ratio of 0.417. Since a subreflector position controller was provided in this project, this problem was overcome.

The structural comparisons showed that with the 0.417 ratio, the structure was nearer the axis of rotation, but the subreflector, quadripod, and feedcone were farther from the axis of rotation. The results showed no appreciable weight or cost difference to favor either ratio. Since both were acceptable and a great savings would be realized by using the existing structure and panels, this option was selected.

C. STUDY ON POLAR SHAFT BEARING LIFE

A study was made to verify that the polar bearing on the 26m antenna was sufficient for the increased loading, and also to resolve concern over metal particles found in the oil. The results of the study were:

- (1) There is adequate calculated life remaining in the bearings for the anticipated additional 20,000 cycles under the increased loads.
- (2) The metal particles detected in oil samples taken from the bearings were probably from adjacent material and not from the bearings themselves.
- (3) The bearing lubricant would be changed to one of a higher viscosity because of the low rotational speed of the bearing.

The following paragraphs provide a more detailed description of the bearing arrangement, the applied loads, the predicted turns remaining, and the lubricant.

The polar axis is supported by two spherical radial roller bearings spaced approximately 6.25m (20.5 ft) apart and a spherical roller thrust bearing located below the lower radial bearing. The thrust bearing and lower radial bearing are oil lubricated, whereas the upper radial bearing is grease lubricated.

Table VI shows the loads applied to these bearings for both the original 26m dish configuration and for the dish expanded to 34m. Also listed are the cubic mean loads and the bearing rated dynamic capacity of the roller bearings. The ability of the bearings to withstand increased loading must be considered conservatively. The low speed makes an elastohydrodynamic lubrication film impossible to achieve; nevertheless, it was desirable to use maximum viscosity oils that are chemically compatible with oils previously used, since it was not feasible to remove all of the oils.

From a safety standpoint, there need be no concern about the strength of the bearings under the increased loading. Table VI shows that none of the new loads is more than 75 percent of the rated static capacity. When it is realized that the actual breaking strength of a roller bearing is at least eight times the static capacity rating, it becomes clear that very large safety factors exist.

The critical bearing from the standpoint of fatigue failure is the upper radial bearing. This bearing has new loadings slightly above the rated dynamic capacity, which is the loading that 90 percent of a large group of bearings will endure for one million turns of the bearing race. It is estimated that the antenna has so far made the equivalent of 20,000 turns and is expected to make an additional 20,000 turns without a bearing fatigue failure. Table VII lists the predicted number of turns remaining in the life of the bearings based upon good lubrication and a 10 percent failure rate. The lowest entry of 777,739 turns is 39 times as many as the required additional 20,000 turns. It is believed that this large ratio between the expected life of a normally lubricated bearing and the required life of the antenna bearing is enough to compensate for the lack of normal lubrication.

Table VI. 26M and 34M Bearing Loads

Bearing	Existing Antenna, 20,000 Cycles to Date		Modified Antenna		Cubic Mean of (2) and (4) After Additional 20,000 Cycles
	(1) Gravity Loading	(2) Cubic Mean Load (Wind)	(3) Gravity Loading	(4) Cubic Mean Load (Wind)	
Upper Radial SKF 230-500/C1 C = 272,727 kg (600,000 lb) Co = 393,182 kg (865,000 lb)	169,091 kg (372,000 lb)	171,363 kg (377,000 lb)	291,818 kg (642,000 lb)	294,091 kg (647,000 lb)	247,727 kg (545,000 lb)
Lower Radial SKF 23072/C1 C = 204,545 kg (450,000 lb) Co = 254,545 kg (560,000 lb)	13,181 kg (29,000 lb)	13,636 kg (30,000 lb)	22,727 kg (50,000 lb)	23,182 kg (51,000 lb)	19,545 kg (43,000 lb)
Lower Thrust SKF 29372 C = 249,150 kg (550,000 lb) Co = 568,182 kg (1,250,000 lb)	128,636 kg (283,000 lb)	128,636 kg (283,000 lb)	218,182 kg (480,000 lb)	218,182 kg (480,000 lb)	184,091 kg (405,000 lb)
C is dynamic capacity in kilograms (pounds) Co is static capacity in kilograms (pounds)					

Table VII. Predicted Number of Turns Remaining in Bearing Life

Compare Loading with Capacity, C:

Assuming Cubic Mean Loads given are = P

230-500MC/C1 C = 600,000

Existing $\frac{C}{P} = \frac{600}{377} = 1.59$

$L_n = (1.59)^{10/3} \times 10^6 = 4.71 \times 10^6$ turns

Modified $\frac{C}{P} = \frac{600}{647} = 0.927$ $L_n = 777,739$ turns

Cubic Mean of Existing and Modified:

$\frac{C}{P} = \frac{600}{545} = 1.10$ $L_n = 1.38 \times 10^6$ turns

23072CAMC/C1 C = 450,000

Existing $\frac{C}{P} = \frac{450}{30} = 15.0$ $L_n = 8315 \times 10^6$ turns

Modified $\frac{C}{P} = \frac{450}{51} = 8.82$ $L_n = 1418 \times 10^6$ turns

Combined $\frac{C}{P} = \frac{450}{43} = 10.47$ $L_n = 2505 \times 10^6$ turns

29372MC C = 550,000

Existing $\frac{C}{P} = \frac{550}{283} = 1.94$ $L_n = 9.16 \times 10^6$ turns

Modified $\frac{C}{P} = \frac{550}{480} = 1.15$ $L_n = 1.57 \times 10^6$ turns

Combined $\frac{C}{P} = \frac{550}{405} = 1.36$ $L_n = 2.77 \times 10^6$ turns

C and P are 0.001 of values.

L_n is the 90 percent reliability level.

Analyses were made of oil samples taken from three different 26m polar antennas. Although certain metal particles were found in all the samples, it is most significant that the amount of chromium was nil in each sample, which indicates negligible wear on the bearing races and rolling elements. The other metal particles were most likely from seals and other parts. Since the bearings have not been damaged under the loadings and lubrication used with the 26m antenna, there is very good reason to believe that no significant damage will occur under the increased loadings provided lubricants of maximum viscosities are used. It should be remembered that bearing life is defined as the number of turns that 90 percent of a large number of bearings will endure without any evidence of fatigue failure. A considerable amount of certain kinds of fatigue failure could exist without impairing the operation of an antenna.

Because of the foregoing reasons, it was believed that the probability was very high that 20,000 additional ± 90 degrees oscillations of the 34m antennas can be made.

To improve the viscosities of lubricants in the 26m polar axis, two lubricants were suggested. Because it was physically impossible to thoroughly clean the existing lubricants out of the chambers, the improved viscosity lubricant had to be miscible with Darina 2 at the north polar position and Dentax 140 at the south polar position. A synthetic hydrocarbon (SHC) oil that showed quite high viscosity was available, was more temperature and age stable than ordinary mineral oils, and was miscible with ordinary mineral oils such as Dentax 140. By using an SHC oil in the lower location, the available viscosity can be somewhat more than doubled. The grease at the north polar position showed a viscosity of only 530 seconds at 100°F , and was a microgel or clay base grease. There are clay base greases available with a viscosity of 2400 seconds at 100°F that are miscible with the grease at the north polar position, and it might be valuable to consider these. Also, test work done showed that at extremely slow speeds the wear potential in rolling bearings is improved by incorporating about 3 percent M_0S_2 in the grease. These greases are available commercially.

Therefore, because of the life expectancy calculations and the chance to improve the lubricant viscosities, there is excellent confidence to be placed in expecting 20,000 additional cycles from the present bearings under the new greater loads.

D. STUDY OF THE USE OF ELECTRIC DRIVES

One of the options omitted in the initial study on the S-X Conversion Project was use of new electric drives to replace the existing hydraulic drives used on the 26m antennas. The initial proposal to use electric drives indicated that the proposed change would pay for itself in energy and maintenance savings in less than 10-year period.

To further check this preliminary study, four different options were developed, with a complete servo upgrade, life-cycle cost analysis developed for each option. The analysis showed a break-even point for the three-station subnetwork of 5.6 years. The date the payback was to start was 1977.

The rationale and costs considered in the study, along with the assumptions made, are discussed in the following paragraphs.

1. Rationale

The purpose of the cost study was to examine the cost impact of four servo drive alternatives considered for the 26m servo upgrade project. The alternatives considered were:

- a. No change. This meant proceeding with the existing servo and hydraulic drives as they were, with the exception that the antenna servo group cables would be replaced and the servo documentation upgraded.
- b. Provide new control room electronics. Also provide new antenna servo group cables and upgrade the servo documentation.

- c. Provide new control room electronics, cables, and hydraulic drive equipment for single-speed operation of the servo drives.
- d. Provide new control room electronics, cables, and replace the hydraulic drives with dc electric drives.

2. Costs

The life cycle costs considered were:

a. Implementation Costs

- (1) Nonrecurring
- (2) Hardware
- (3) Initial spares
- (4) Installation
- (5) Shipping

b. Maintenance and Operation (M&O) Costs

- (1) Maintenance (manpower)
- (2) Expendable supplies
- (3) M&O spares
- (4) Power

This cost study assumed implementation simultaneously with the 26m network S-X upgrade:

<u>Station</u>	<u>Completion</u>
DSS 12	December 1978
DSS 44	April 1980
DSS 62	October 1980

For purposes of this analysis, DSS 12 implementation funds were in 1977 dollars. DSS 44 and DSS 62 implementation funds were in 1977 dollars escalated at 6 percent for 2 years (1.1236 factor), assuming mid-1979 commitment of funds.

a. Implementation

- (1) The nonrecurring costs consisting of design, documentation, and M&O manuals were:

Option 0	\$150k
Option 1	\$230k
Option 2	\$152k
Option 3	\$110k

- (2) The recurring implementation costs consisting of hardware initial spares, installation, and shipping were:

Option 0: Cables - \$100k

Option 1:

<u>Item</u>	<u>DSS 12</u>	<u>DSS 44</u>	<u>DSS 62</u>
Hardware	\$74k	\$96k	\$83k
Initial spares	8k	9k	9k
Installation	11k	19k	12k
Shipping	<u>1k</u>	<u>4k</u>	<u>4k</u>
Total	\$94k	\$128k	\$108k

Total net recurring implementation cost for

Option 1: \$330k

Option 2:

<u>Item</u>	<u>DSS 12</u>	<u>DSS 44</u>	<u>DSS 62</u>
Hardware	\$109k	\$159k	\$122k
Initial spares	19k	21k	21k
Installation	17k	31k	19k
Shipping	<u>3k</u>	<u>9k</u>	<u>9k</u>
Total	\$148k	\$220k	\$171k

Total net recurring implementation cost for

Option 2: \$539k

Option 3:

<u>Item</u>	<u>DSS 12</u>	<u>DSS 44</u>	<u>DSS 62</u>
Hardware	\$96k	\$145k	\$108k
Initial spares	28k	31k	31k
Installation	18k	32k	20k
Shipping	<u>4k</u>	<u>15k</u>	<u>15k</u>
Total	\$146k	\$223k	\$174k

Total net recurring implementation cost for
Option 3: \$543k

b. M&O Costs

- (1) Maintenance Manpower - The annual rate of \$30k for maintenance manpower at Goldstone was used. An hourly rate of \$10.50 was used for overseas maintenance personnel. The overseas annual rate would then be \$21,840. For purposes of this project, \$22k was used. Both of these rates were fully burdened. For salary escalation, a 6-percent factor was used.

In order to establish which portion of the existing maintenance effort was to be directed toward a 26m antenna servo hydraulic system, several approaches were used:

- (a) At the time of the study, the work force at Goldstone was composed of nine men. It was established by the group that a 64m antenna hydraulics system is eight times more complex than a 26m antenna hydraulics system. Assuming nine men, the degree of complexity, and the

number of antennas, 0.9 man must devote his time to a 26m antenna. This was reduced to 0.6 man as a conservative number.

- (b) As a check on (a) above, Operations was asked to provide the number of hours devoted to the 26m hydraulics by the maintenance personnel. The estimate was 24 hours per week or 0.6 man based on 2080 hours per year. It was assumed that this number would not change for Option 0, 1, or 2.
- (c) Operations was asked to estimate the number of hours required to support a 26m antenna, the estimate was 303 hours per year. For this study, it was estimated that another 303 hours by other personnel would be required to support the Monitor and Control Subsystem (DMC) effort. It was assumed that this estimate would not change for Option 0, 1, or 2.
- (d) The time estimated to maintain the existing electronics equipment associated with the servo was 0.2 man per year. No attempt was made to verify this number with Operations.
- (e) The M&O time associated with the dc drives of Option 3 was originally estimated at 309 hours per year. Following this estimate, many users and manufacturers of this type of equipment were contacted for their actual experience with these drives. In summary, it was felt that a mean time between failure (MTBF) of approximately 4000 hours is possible with both drives on each axis operating to full capability. Based on

continued tracking with some reduced performance and less than 72 km/h (45 mi/h) winds, with one of the dual drives nonfunctional, an effective MTBF of 7000 hours is realizable. From the preventive maintenance standpoint, it was felt that 200 man-hours per year is conservative. Based on these facts, an estimate of 309 hours per year for all maintenance actions is considered realistic.

Annual M&O costs ($C_{M\&O}$) were computed by the following:

$$C_{M\&O} = \text{Goldstone cost} + 2 \left[\frac{22}{30} \text{ Goldstone Cost} \right]$$

The inflated M&O cost for any year (C_i) was computed by:

$$C_i = C_{M\&O} (1+R)^{(i-1)}$$

where C_i = Annual Cost

$C_{M\&O}$ = Annual rate in 1977 dollars

R = Inflation factor = 6 percent

i = Year - 1, 2, 3, etc.

The following paragraph provides the annual inflated M&O dollars for the options considered. The annual M&O costs for Option 1, 2, or 3 are a composite of Option 0 costs on the DSSs which were not implemented, plus the new M&O costs of the implemented station.

M&O Costs for Option 0

Annual Goldstone costs = $0.60 (2080) + 303 +$
 $303 + 0.2 (2080) = 2270$
hours

$$\text{Cost} = \frac{2270}{2080} \times 30k = 32.74k; \text{ 10-year inflated cost} \\ = 1059k$$

M&O Costs for Options 1 & 2

Annual Goldstone Costs = $0.6 (2080) + 393 +$
 $393 = 1754$ hours

$$\text{Cost} = \frac{1854}{2080} \times 30k = 27k; \text{ 10-year inflated cost} \\ = 894k$$

M&O Cost for Option 3

$$\text{Annual Goldstone costs} = \frac{309}{2080} \times 30 = 4.5k; \\ \text{10-year inflated cost} \\ = 232k$$

- (2) Expendable Supplies - Expendable supplies for Options 0, 1, and 2 consisted primarily of hydraulic fluid, filters, and O-rings. An estimate of \$2k per year was made, and further it was assumed to be the same for Option 0, 1, or 2.

Expendable supplies for Option 3 were considered to be fuses, air screens and filters, and lubricants. An estimate of \$300 per year was made for this item.

- (3) M&O Spares - M&O spares requirements for Options 0 and 1 were assumed to be zero on the basis that Operations stated that they would not have to buy any spares for the next 10 years. Present stocks are assumed to be sufficient.

In calculating the M&O spares requirements for Option 2 (Table VIII), it was assumed that the hydraulic motor rotating groups would be replaced every 2 years at a 1977 cost of \$1500 each. There are eight motors on the antenna and two motors in spares inventory. The cost at each period in 1977 dollars was:

$$10 \times 3 \times \$1500 = \$45k$$

Table VIII. M&O Spares Requirements for Option 2

Year i	Annual Spares 1977 Dollars (K)	$(1+R)^{(i-1)}$	Annual Inflated M&O Spares Dollars (K)
2	45	1.06	47.7
4	45	1.19	53.55
6	45	1.34	60.30
8	45	1.50	67.50
10	45	1.69	76.05
12	45	1.90	85.50
14	45	2.13	95.85

*R = 0.06

Total 1977 Inflated Dollars = \$229k (10-year subnetwork total).

The M&O spares calculation for Option 3 was based on one full set of spares, supplied on installation, to be required during year 7. Total 1977 inflated cost would be:

$$75k \times 1.42 = \$107k \text{ (Total for subnetwork)}$$

- (4) Power - Monthly power consumption for Option 0, 1, and 2 was 6677 kwh based on measurements at DSS 12 plus estimates of other auxiliaries. At \$0.035 per kwh, the first annual cost was:

$$6677 \times 0.035 \times 12 = \$2804$$

Table IX lists the annual inflated cost for power required by Option 0, 1, or 2. An annual inflation rate of 10 percent was used; overseas power costs were assumed equal to Goldstone costs.

Table IX. Power Costs for Options 0, 1, and 2

Year i	Annual Power cost 1977 Dollars (K)	$(1+R)^i$	Annual Inflated Power Dollars (K)	
			Goldstone DSS 12	Network Total
1	2.80	1.00	2.80	8.40
2	2.80	1.10	3.08	9.24
3	2.80	1.21	3.39	10.17
4	2.80	1.33	3.72	11.16
5	2.80	1.46	4.09	12.27
6	2.80	1.61	4.51	13.53
7	2.80	1.77	4.96	14.88
8	2.80	1.95	5.46	16.38
9	2.80	2.14	5.99	17.97
10	2.80	2.36	6.61	19.83
11	2.80	2.59	7.25	21.75
12	2.80	2.85	7.98	23.94
13	2.80	3.14	8.79	26.37
14	2.80	3.45	9.66	28.98
15	2.80	3.80	10.64	31.92

*R = 0.10

Monthly power consumption for Option 3 was estimated at 2380 kWh. At \$0.035 per kWh, the first annual cost was:

$$2380 \times 0.035 \times 12 = \$1,000$$

Table X lists the annual inflated cost for power required by Option 3. An annual inflation rate of 10 percent was used; overseas power costs were assumed equal to Goldstone.

Table X. Power Costs for Option 3

Year i	Annual Power Cost 1977 Dollars (K)	$(1+R)^{(i-1)}$	Annual Inflated Power Dollars (K)		
			Goldstone DSS 12	Two Overseas	Network Total
1	1	1.00	1.00	5.60	6.60
2	1	1.10	1.10	6.16	7.16
3	1	1.21	1.21	2.42	3.63
4	1	1.33	1.33	2.66	3.99
5	1	1.46	1.46	2.92	4.38
6	1	1.61	1.61	3.22	4.83
7	1	1.77	1.77	3.54	5.31
8	1	1.95	1.95	3.90	5.85
9	1	2.14	2.14	4.28	6.42
10	1	2.36	2.36	4.72	7.08
11	1	2.59	2.59	5.18	7.77
12	1	2.85	2.85	5.70	8.55
13	1	3.14	3.14	6.28	9.42
14	1	3.45	3.45	6.90	10.35
15	1	3.80	3.80	7.60	11.40

*R = 0.10

A summary of the previous data is listed in Table XI. Figure 60 shows the intersection of Option 0 and Option 3, the 5.6-year break-even point, which led to the decision to provide electric drives conversions.

Table XI. Servo Block Upgrade, 26M Net 10-Year Life Cycle Cost Analysis
(First Subnetwork)

Cost	Option 0 (\$K)	Option 1 (\$K)	Option 2 (\$K)	Option 3 (\$K)
Implementation	250	561	691	650
M&O Costs				
Maintenance	1059	894	894	232
Expendables	79	79	79	19
Spares	0	0	229	107
Power	<u>134</u>	<u>134</u>	<u>134</u>	<u>53</u>
Subtotal	1272	1107	1336	411
Total	1522	1668	2027	1061
<p>Notes: 1. All costs burdened in 1977 dollars, including 6-percent inflation factor for procurements not in FY 77.</p> <p>2. Three antennas per subnetwork.</p>				

E. SAFETY OF THE ANTENNA LIFT, LIFT FRAME, AND FOUNDATION DESIGN

1. Safety of Raising the Antenna

The safety of raising the antenna was a concern of all involved in the Project. The problems involved lifting the antenna structure and frame (weighing 350 tons) a height of 10 feet, locating it in a new position within ± 0.25 mm (± 0.010 in.) above its original position, and then holding it in this position until a concrete foundation could be poured in place and cured.

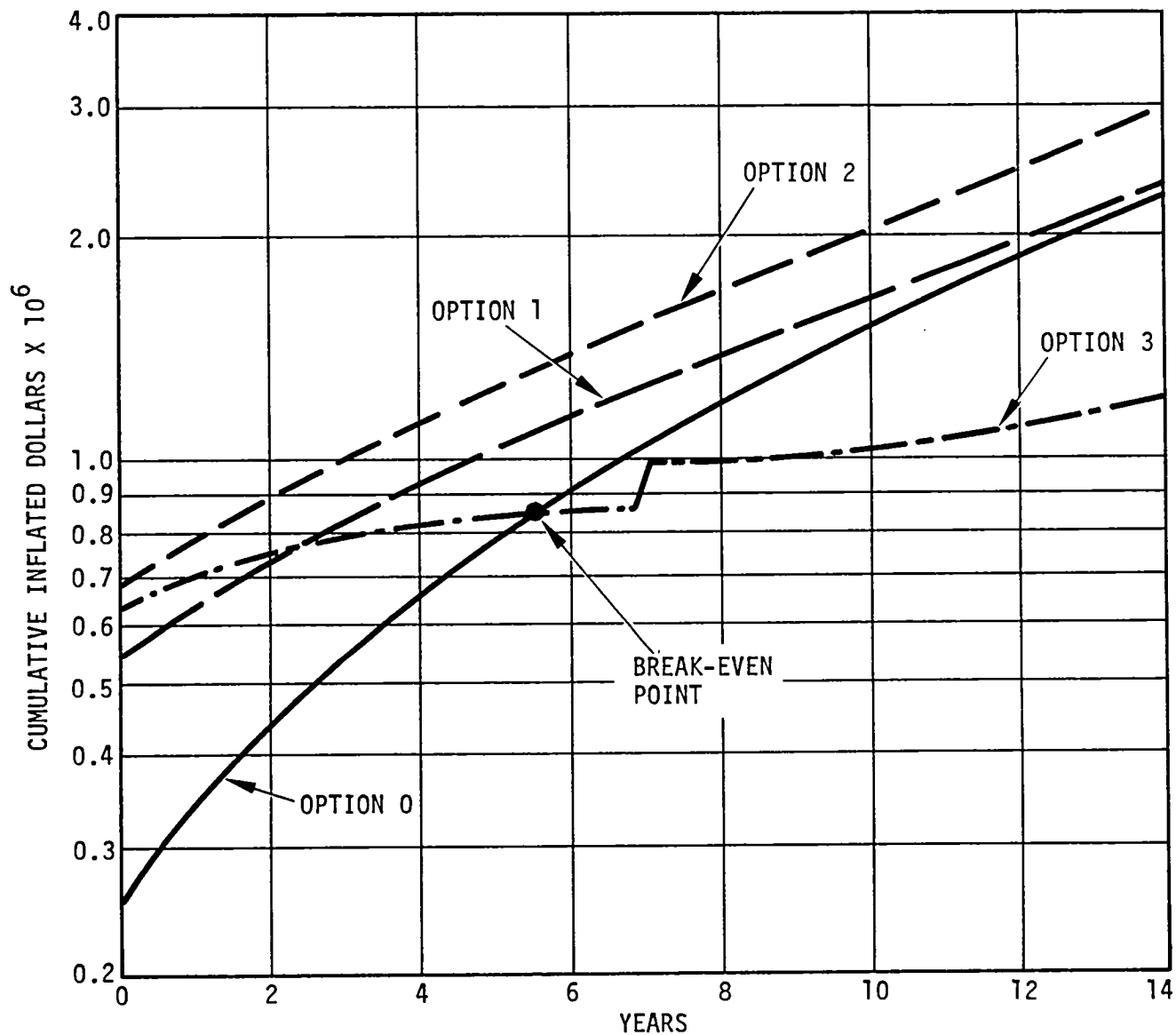


Figure 60. Servo Block Upgrade, 26M Net Life Cycle Cost Analysis, Cumulative Inflated Dollars Versus Years

To solve these problems, the following steps were taken:

- a. A safety factor of 3.4 was used on the lift by using six 200-ton jacks, furnishing a 1200-ton capacity to lift 350 tons. In addition, another six 200-ton jacks, making a total of twelve, were used to guard against a failure of a hydraulic hose. Then a manifold, which compensated and controlled the hydraulic flows and furnished an automatic shutoff if hose failure occurred, was used to control the jacks.
- b. The next consideration was the wind load safety factor against the antenna sliding off the jacks during the lift or uplift off the jacks. The antenna panels were removed and the antenna reflector structure was cut back to the point where the new reflector structure extensions were to be connected to reduce the wind shear and overturning forces to a minimum. Then, to be very conservative, the safety factor was developed using a wind speed of 161 km/h (100 mi/h), which is a wind speed that should not occur more than once in 75 years. The wind load safety factors then calculated were 4.0 against sliding and 2.6 against uplift for wind shear and overturning moments. To further insure safety, safety cables and "dead men" supports were used. The lift was planned to be done in July when the wind speed is normally very low. Since the estimated lift duration was 2 days, a stable wind forecast had to be projected during the lift. This last factor did not prove out, however, as high winds did develop, and since the lift had reached the point of no return, it was completed in winds up to 97 km/h (60 mi/h). As a result of the high winds, the antenna drifted several inches and had to be brought back to the correct position using check-head angle blocks. (After waiting 2 days for the wind to stop blowing.) This experience left all feeling very pleased that a very complete safety analysis and design was done for this task.

- c. Another design concern involved controlling the lift height to a very precise position, and then securing the antenna at that position until concrete pedestals could be placed underneath the raised antenna. The solution was to make precision stand-offs which had baseplates identical to the antenna baseplates and had the capacity to support the raised antenna. The precision standoffs were fabricated and then machined to the exact same height to within ± 0.25 mm (0.010 in.). To quickly anchor the antenna after it was raised, anchor extensions were fabricated with sleeve nuts to tie into the existing anchor bolts (see Figure 61).
- d. The next concern was a way in which to quickly form, reinforce, and pour a 3m (10-ft) cubical concrete pedestal in the shortest possible time around the cribbing and standoffs for the antenna. The solution was to use prefabricated metal forms that quickly bolted together and had tie rods to withstand the fluid concrete loads. A plan to tie the reinforcing of the new concrete pedestal into the existing footing was developed and consisted of coring 7.6 cm (3-in.) by 91.4 cm (36-in.) deep holes into the existing concrete and grouting in rebars to lap with the new prefabricated reinforcing cages. After all of this was assembled (see Figure 61) 27 m^3 (35 yd^3) of concrete were poured into the forms.
- e. The final factor involved the use of a contractor with past experience in raising and lifting heavy equipment. The lifts made by the contractor selected were as heavy as 1800 tons. He had routinely moved Alaska pipeline tanks and other tanks weighing 350 tons, 6m (20 ft) in diameter and 49m (160 ft) in length, with clearances of less than an inch. The contractor had been in this business for 25 years.

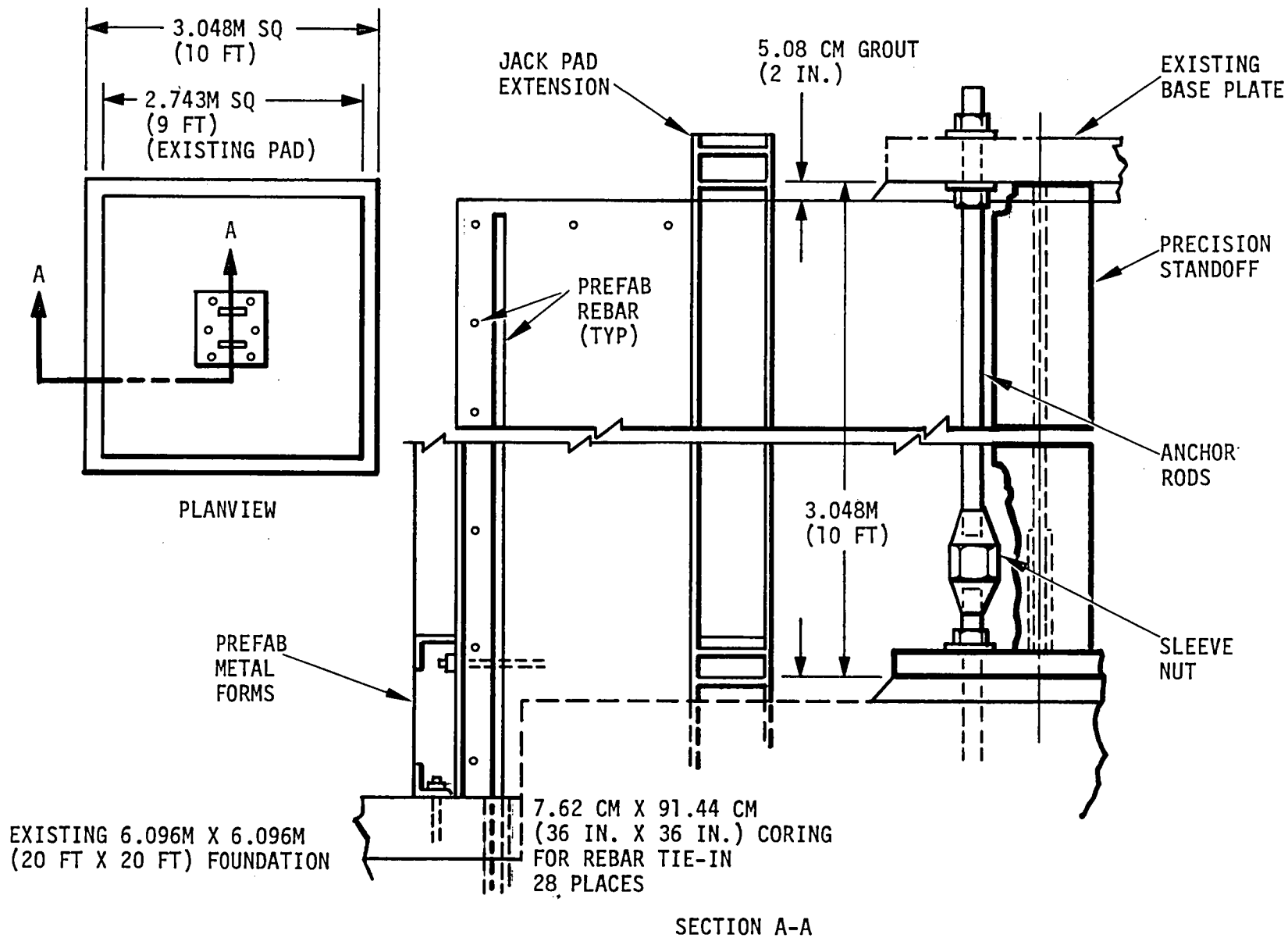


Figure 61. 34M Extension, Concrete Base Raising and Reinforcing

2. Lift Frame Design

Raising the antenna safely was the primary concern in the design of the antenna lift frame. The frame basically consists of two wide flange, 91-cm (36-in.) wide by 762-cm (300-in.) deep beams welded to the front and rear of the antenna pedestal and stabilized by two 36-cm (14 in.) wide by 290-cm (114-in.) deep beams (see Figure 62). This was tied together by angle braces and plates. The lift frame was designed with a factor of safety of 3.4. That meant the frame could lift 3.4 times the weight of the antenna and not fail. In addition to a very conservative design for the frame, it was decided to test the frame by lifting the antenna baseplates until light could be seen under all the baseplates. The antenna was then left at that position for 30 minutes.

3. Foundation Design

The foundation design began with checking the existing footings. Initial checks indicated that the footings could take the added dead load of the antenna modifications plus the added wind loads of the larger reflector diameter. This was possible because the antennas, which were about 15 years old, were designed for solid surfaces where 50-percent porosity panels were actually used. In addition, the antennas were designed for survival at 140 km/h (87 mi/h) winds with the reflector in any position or 193 km/h (120-mi/h) winds with the antenna at zenith. Since that time these wind loads have been reduced to 113 km/h (70 mi/h) and 161 km/h (100 mi/h), respectively. These two overdesign factors allowed the existing footings to carry the increased loads.

The calculated total dead load plus live load caused a soil pressure of 2,727 kg (6,000 lb) per square foot, which is about 75 percent of the Uniform Building Code (UBC) allowance. The stability of the individual footings against overturning was 2.0 versus 1.5 required by the UBC. The stability of the whole antenna against overturning is eight.

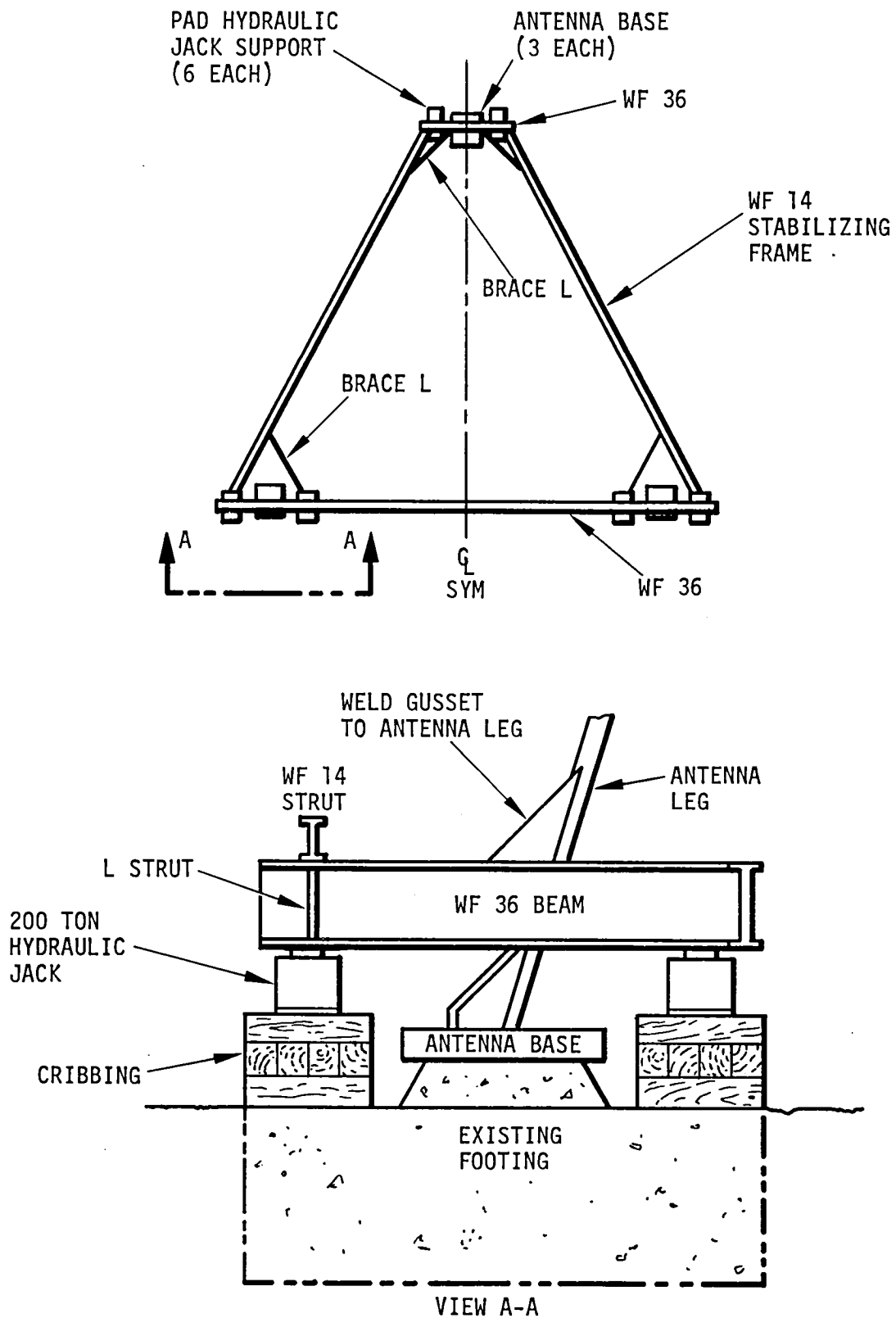


Figure 62. 34M Antenna Lift Frame

F. DECLINATION AND HOUR ANGLE WHEEL MODIFICATION DESIGN

One of the most difficult design tasks was finding sufficient room to put all the counterweight needed to balance the larger structure required for the increased diameter. The added counterweight on the declination axis was 27,272 kg (60,000 lb), or an increase of 90 percent (see Figure 63).

In order to hold the volume of lead needed to support the 90,909-kg (200,000-lb) weight, it was decided to add two new counterweight boxes alongside of the existing counterweight boxes (see Figures 64 and 65).

The total weight summary showing the weight change for the declination and hour angle wheel, and the increase in the structure and counterweight elements is provided in Table XII. The additional members added to the hour angle wheel to carry the 90,909-kg (200,000-lb) counterweight load are shown in Figures 66 and 67. The reinforcement of the existing member is shown in Figure 68.

Table XII. Weight Summary of HA-DEC Antenna Showing 26M and 34M Reflector Diameter

Item	Weight in K-in.-lbs.	
Quadripod, main reflector, and dec wheel	74.2	107.0
Subreflector	0.8	1.5
Cone	5.0	7.0
Panel	12.2	22.0
Counterweight at dec wheel	40.0	100.0
Estimated nonstructural material	52.5	52.5
Subtotal (upper structure)	184.7	290.0
HA wheel structure	83.3	118.0
Counterweight of HA wheel	<u>220.0</u>	<u>420.0</u>
Total (pedestal not included)	488.0	828.0

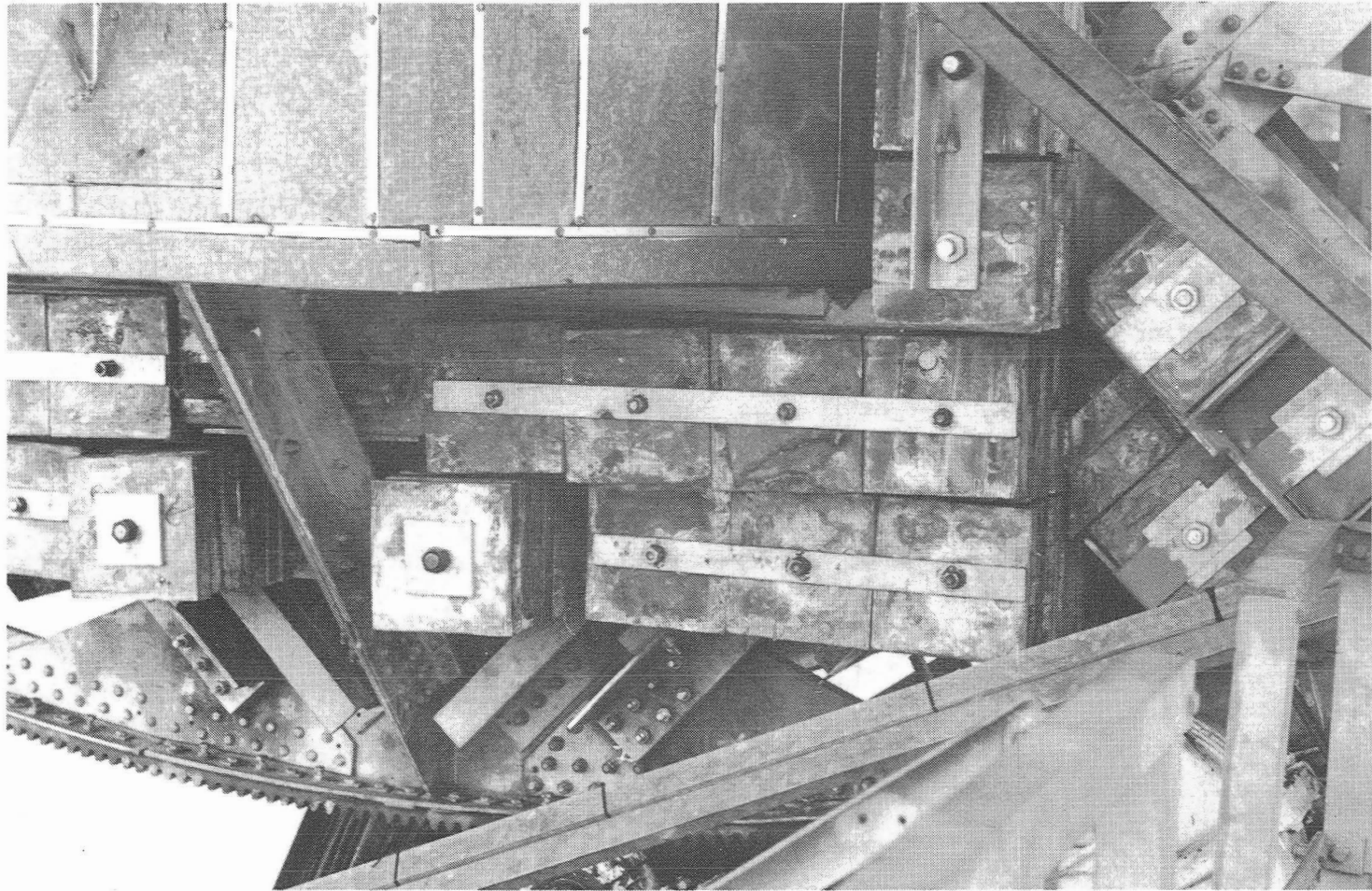


Figure 63. Added Counterweight

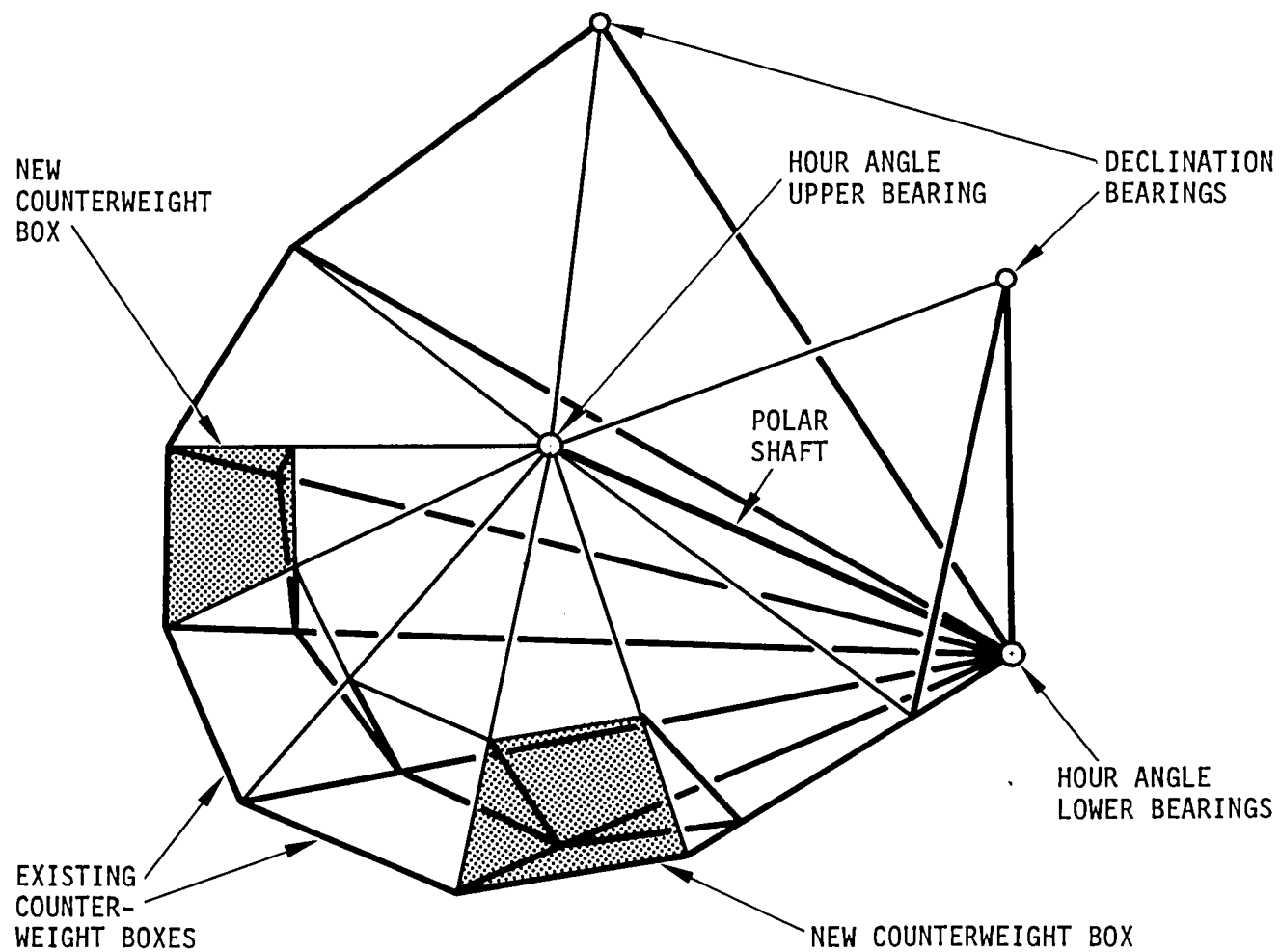


Figure 64. Isometric View of Hour Angle Wheel

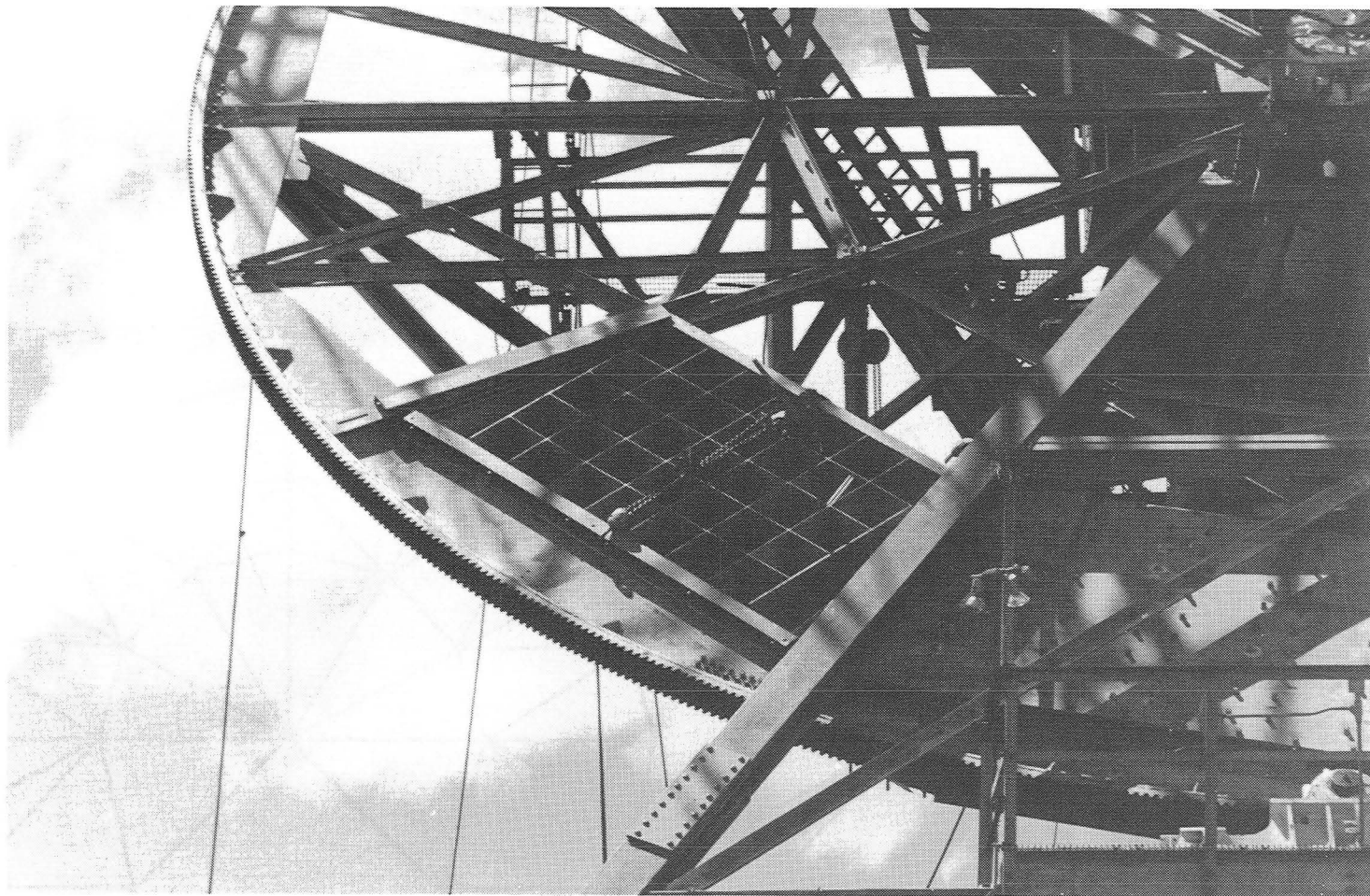
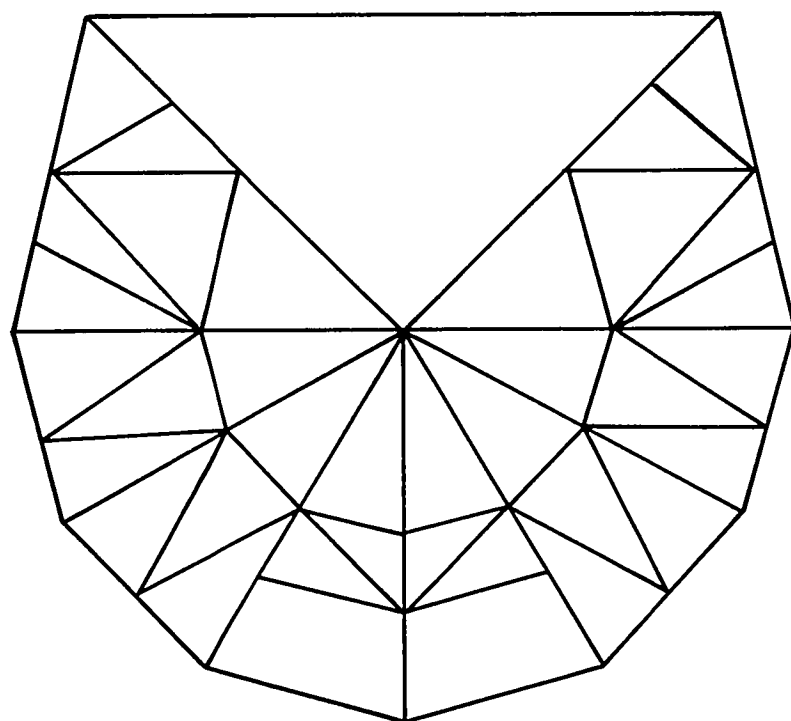
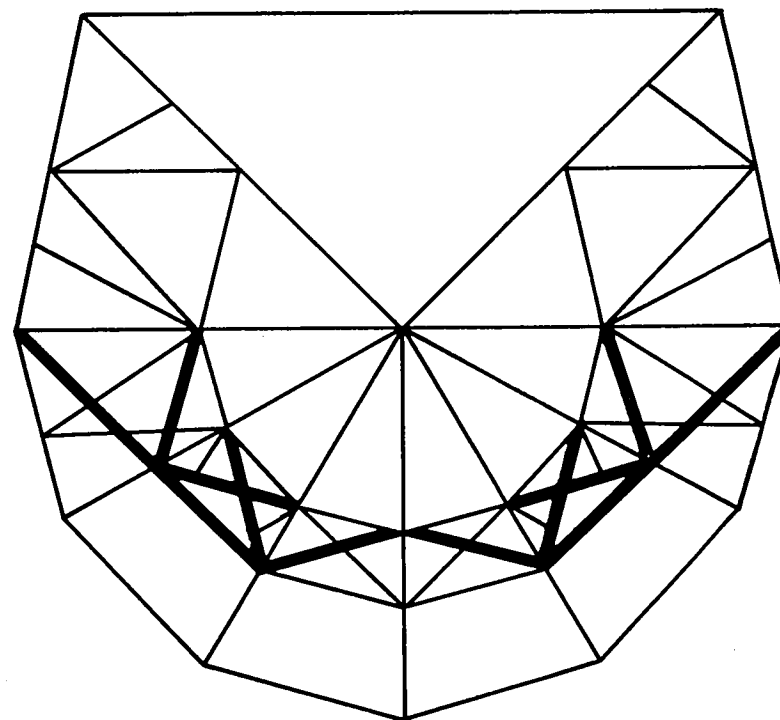


Figure 65. Added Counterweight Boxes



26-METER



34-METER

— EXISTING

— NEW

Figure 66. Hour Angle Wheel Modification on Front Face

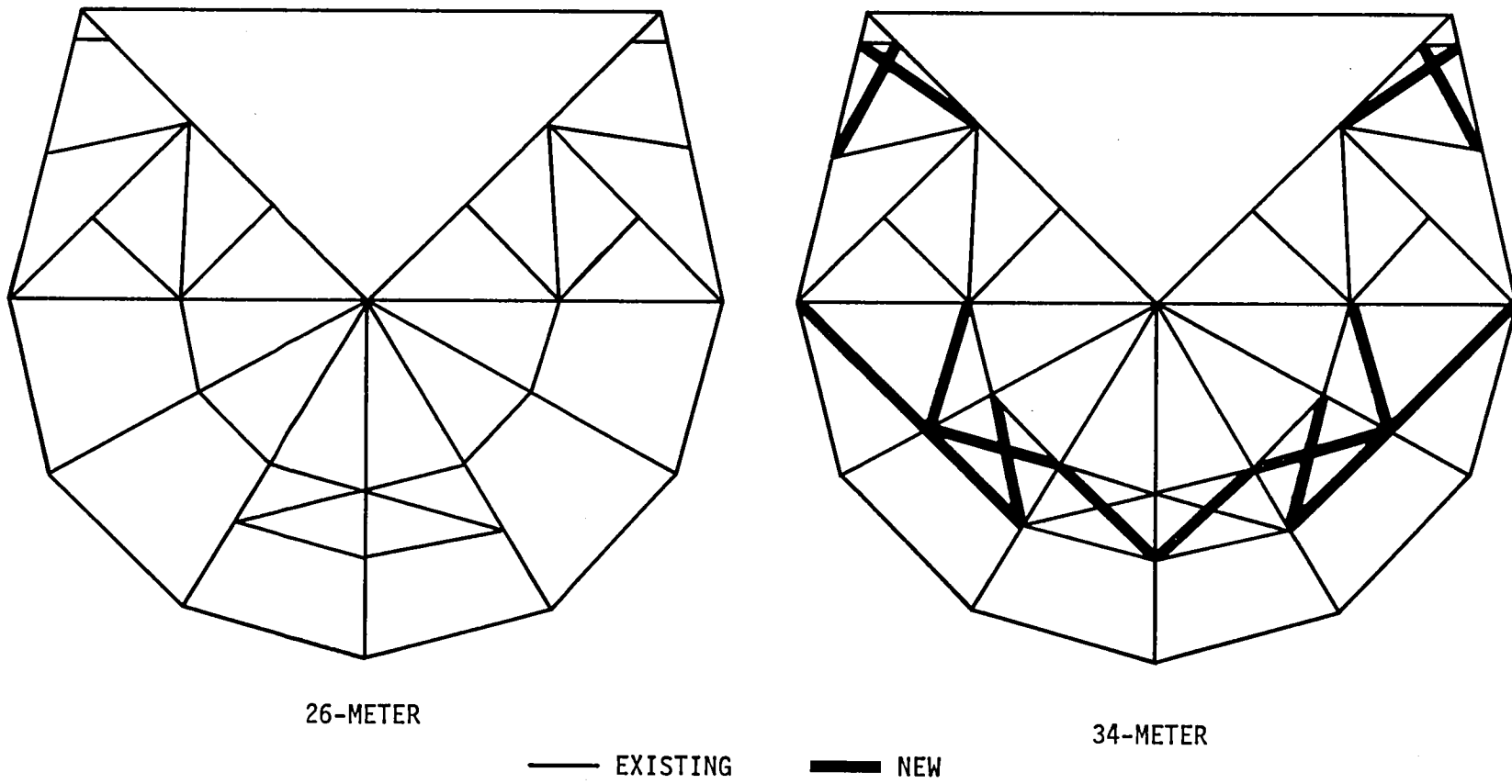


Figure 67. Hour Angle Wheel Modification on Back Face

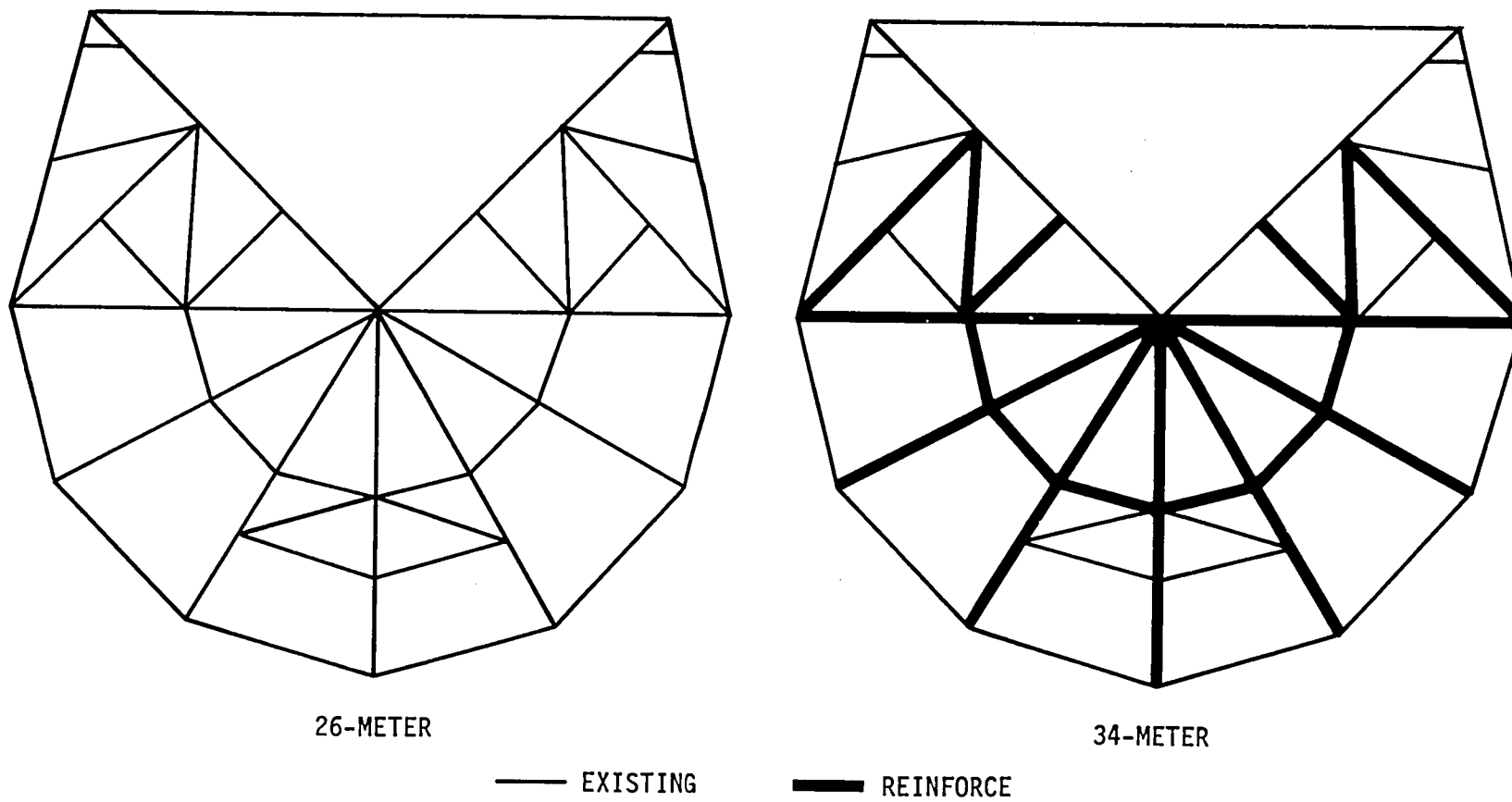


Figure 68. Hour Angle Wheel Modification, Reinforcement of Back Face

The declination wheel modifications are shown on Figures 69 and 70. The moment and weight counterbalance is 1,000,000 foot-pounds with a total counterweight of 66,500 pounds (for the added loads).

The member capacities of all the wheel members, along with the joint capacities, were checked and redesigned for added strength. Stiffeners were required throughout the hour angle wheel and in the areas of counterweight on the declination wheel.

The design of the hour angle wheel also included a check of the bearing loads and the remaining factor of safety. Because of the extremely slow revolution speed of the antenna, the bearing factor of safety was determined on a static basis. The static rating capacity is defined as that bearing load which will cause a permanent deformation at the maximum loaded rolling element and at the weaker of the inner or outer raceway contacts of 0.0001 diameter. The required factor of safety should be greater than 1.0 for bearings in ordinary service.

A summary (Table XIII) of maximum loads at the bearings shows that all safety factors are above 1.0, with the most heavily loaded bearing being the upper radial bearing of the hour angle wheel with a factor of safety of 1.12.

Table XIV shows the calculated total life of the various bearings with the lowest number being 515,000 cycles; the estimated number of cycles for 20 years of usage on the antenna is 54,000. The life of all the existing bearings should last well beyond the design life required.

G. RECEIVER-EXCITER DESIGN

The initial design proposal developed in the study was to use a Block IV receiver-exciter essentially the same as was being used in the 64m antenna subnetwork for S- and X-band frequencies. It was decided not to use the Block IV receiver-exciter because the cost was too high, and instead, a down converter approach was used with the existing Block III S-band receiver.

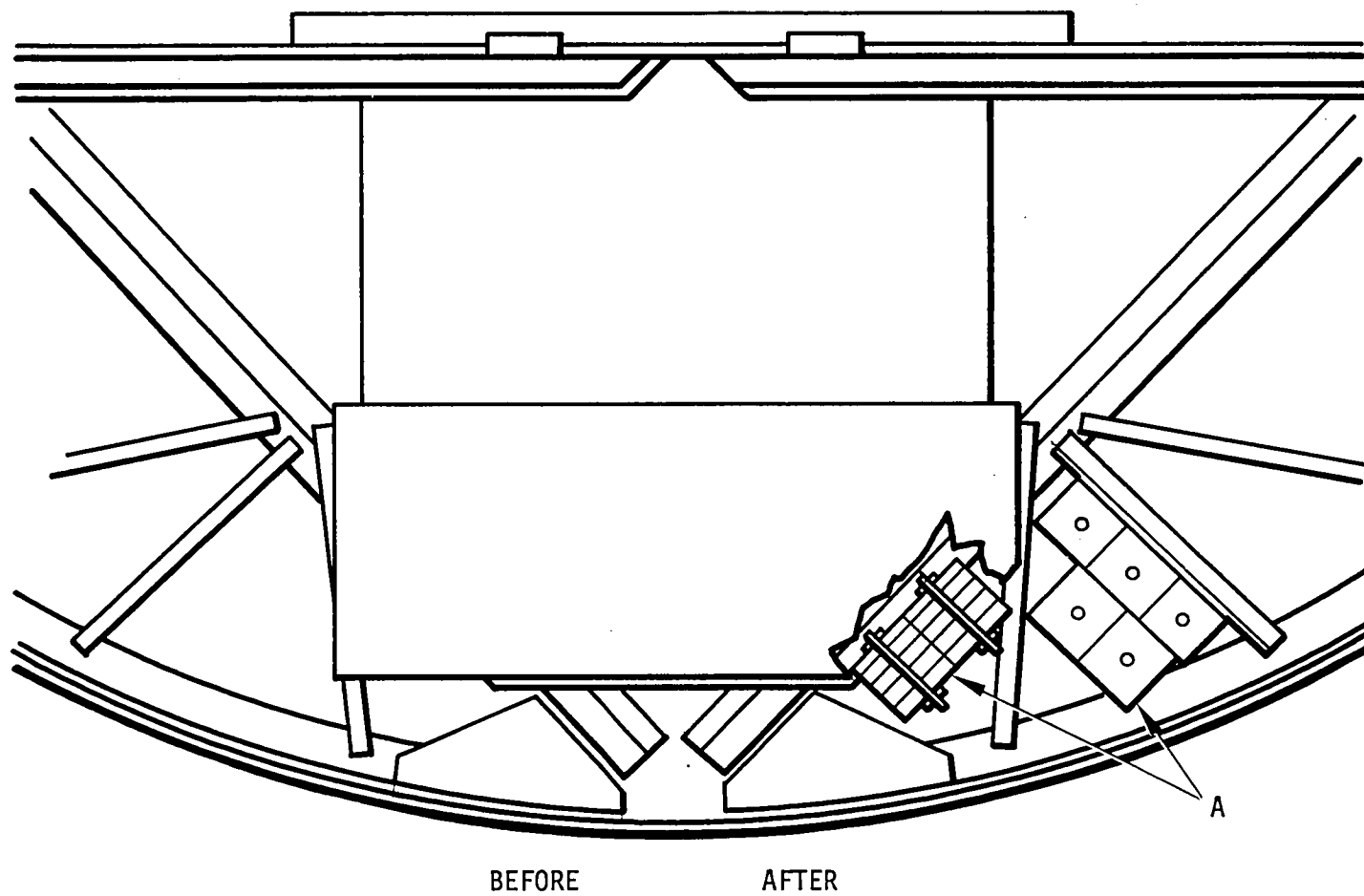


Figure 69. 26M Declination Wheel Modification

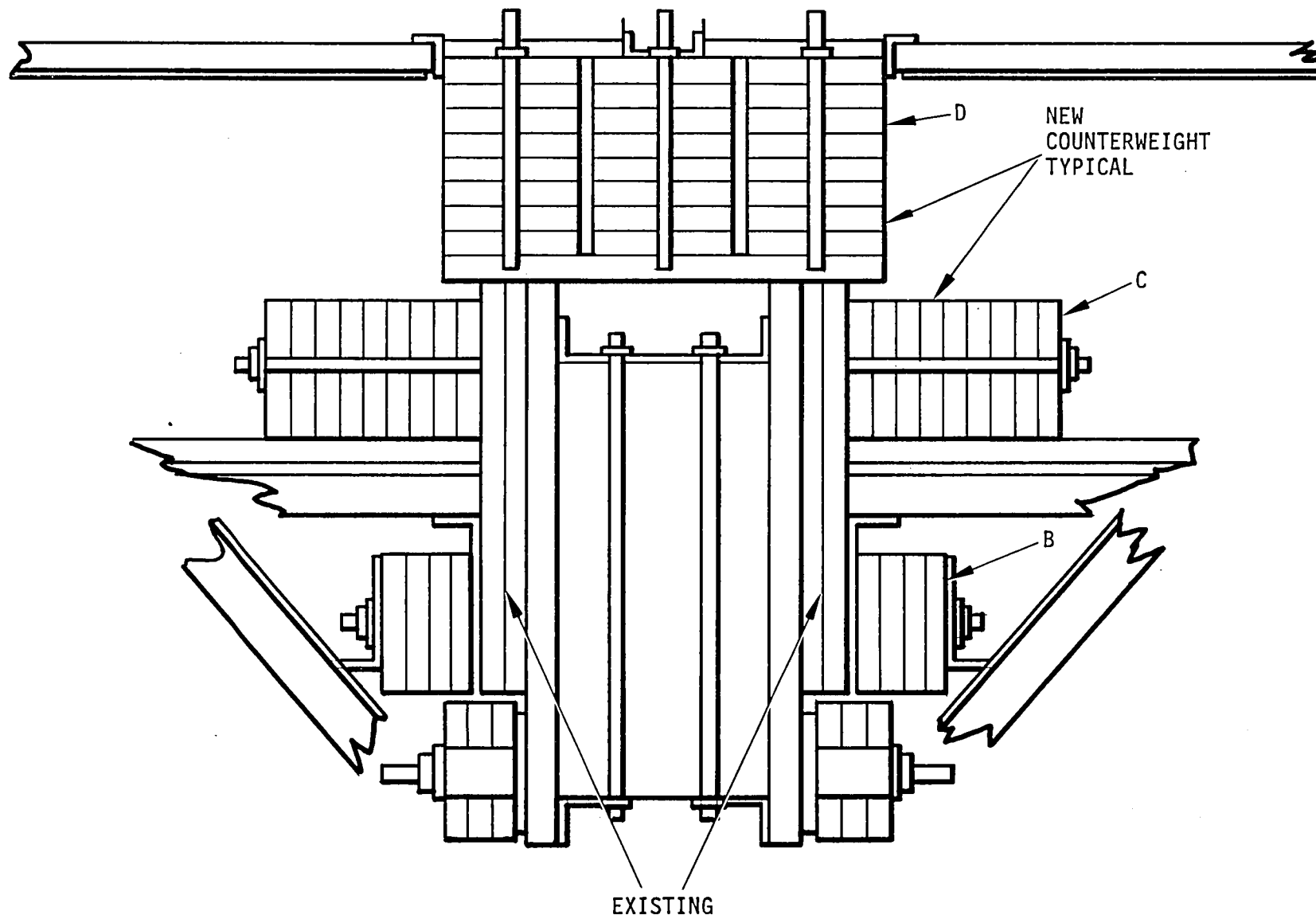


Figure 70. Detail of Declination Wheel Modification

Table XIII. Maximum Load at Bearings

Bearing	Capacity (K-in.-lbs)			Max Load (K-in.-lbs) Gravity (0 Wind)			Factor of Safety		
	Static	Dynamic	V	26M	34M*	34M**	26M	34M*	34M**
DEC wheel	853	700	1.2	93	145	145	7.6	4.9	4.9
HA wheel upper radial	863	532	1.2	372	570	642	1.9	1.26	1.12
HA wheel lower radial	581	436	1.2	29	55	50	16.7	8.8	9.7
HA wheel lower thrust	1250	511	1.0	283	433	480	4.4	2.9	2.6
*Based on counterweight of 340 K-in.-lbs on HA wheel. **Based on counterweight of 420 K-in.-lbs on HA wheel.									

Table XIV. Bearing Life Calculation

HA Wheel Bearing	F (Gravity Alone) (K-in.-lbs)				F _M Life X 10 ⁶ Cycles (K-in.-lbs)			
	Dynamic Capacity	26M	34M*	34M**	(1)*	(2)*	(1)*	(2)**
Upper Radial	532.0	372.0	570.0	642.0	524.0	541.0	0.573	0.515
Lower Radial	436.0	29.0	55.0	50.0	46.0	42.0	981.0	1329.0
Lower Thrust	511.0	283.0	433.0	480.0	373.0	405.0	2.9	2.2
$F_M = \sqrt{\frac{F_{26M}^3 + F_{34M}^3}{2}}$ <p> *Based on counterweight of 340 K-in.-lbs **Based on counterweight of 420 K-in.-lbs Estimated cycles required by past 15 years = 0.027 X 10⁶ cycles Accumulated cycles expected by next 15 years = 0.054 X 10⁶ cycles </p>								

In addition to the requirement for a low-cost receiver-exciter, the delivery schedule did not allow for the design of a new receiver-exciter. The equipment necessary to adopt the selected option of the Block III receiver-exciter for X-band operation included an S-X down converter, a doppler extractor, and a test translator. A block diagram of the receiver-exciter is shown in Figure 71. Block diagrams for these three main hardware elements are shown in Figures 72, 73, and 74. The design of the various modules used standard Block IV modular construction and test procedures. The receiver-exciter can be operated locally at the rack in the control room or remotely using the Station Monitor and Control Assembly (SMC). The Block III design provides the same reliability as the Block IV has done. The receiver-exciter converts the X-band input signal to S-band, provides X-band doppler, and provides a coherent X-band test signal with level control. The design was such that either receiver 1 or 2 can be switched from the S-band maser or the X-S converter. The above functions can be monitored and controlled by the Monitor and Control Subsystem.

The design approach was to build an engineering model for the frequency shifter, doppler mixer, doppler reference, frequency distribution S-X converter, and test translator, and then test these modules with a modified laboratory Block III receiver-exciter.

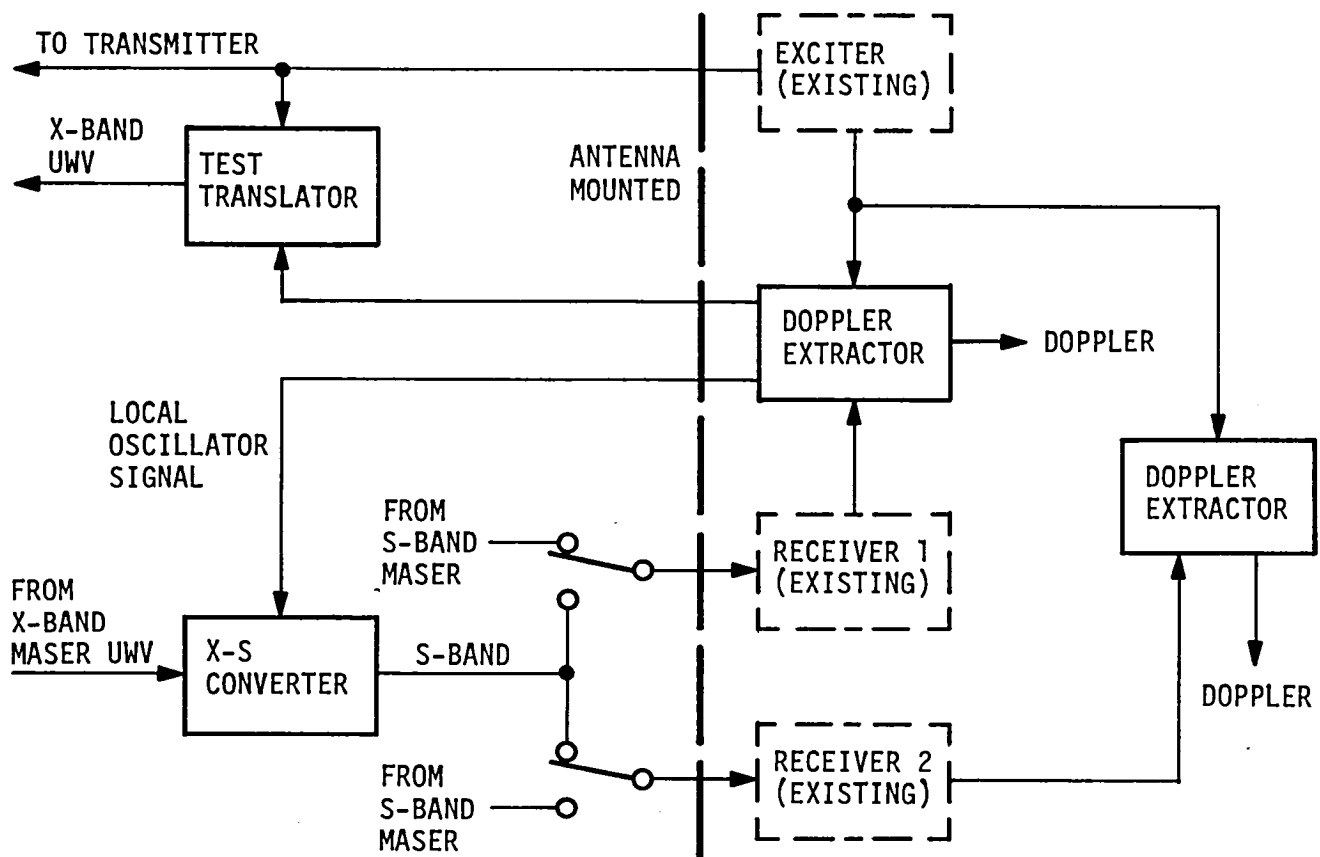


Figure 71. 26M S-X Conversion Receiver-Exciter Block Diagram

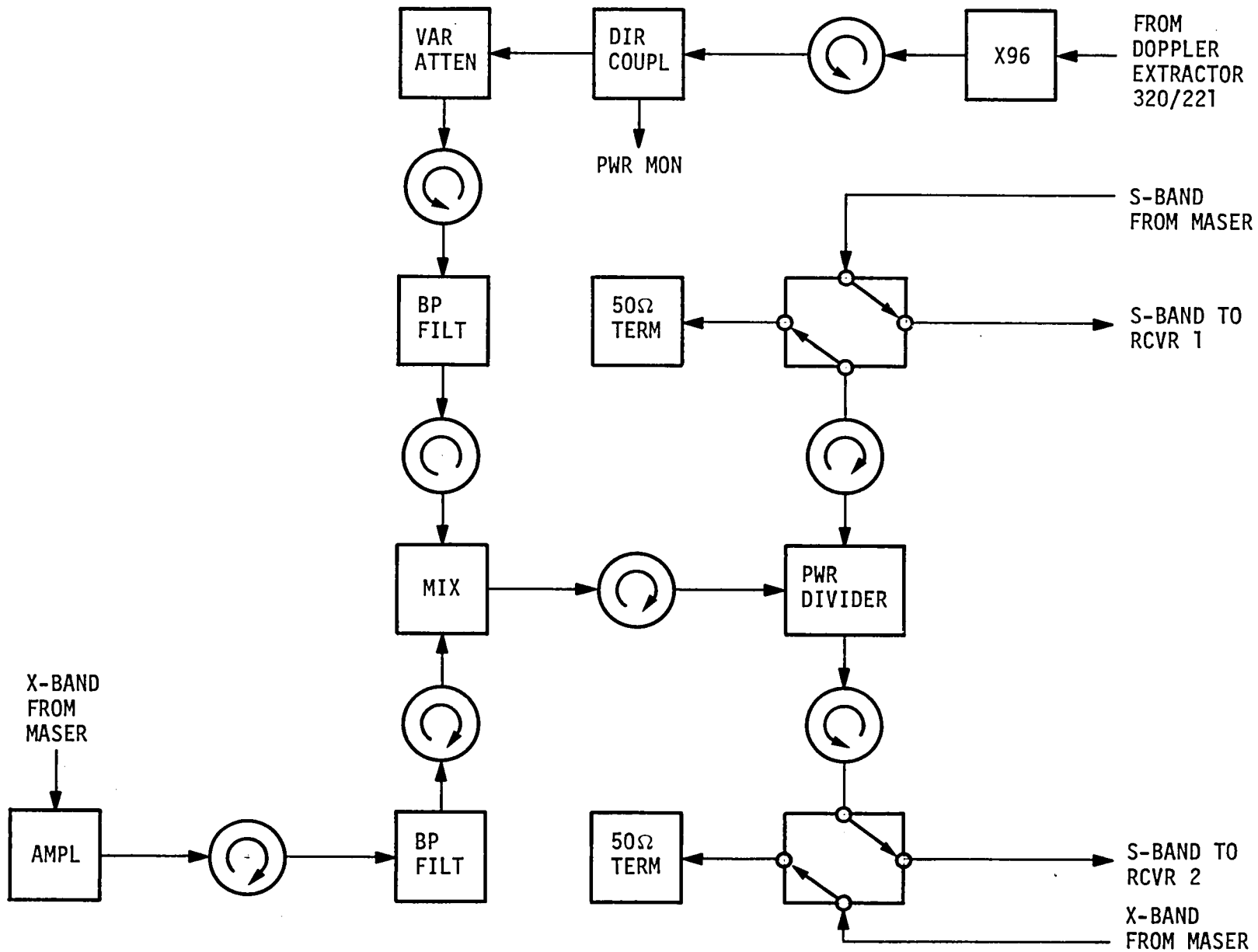


Figure 72. 26M S-X Conversion Receiver-Exciter S-X Converter Block Diagram

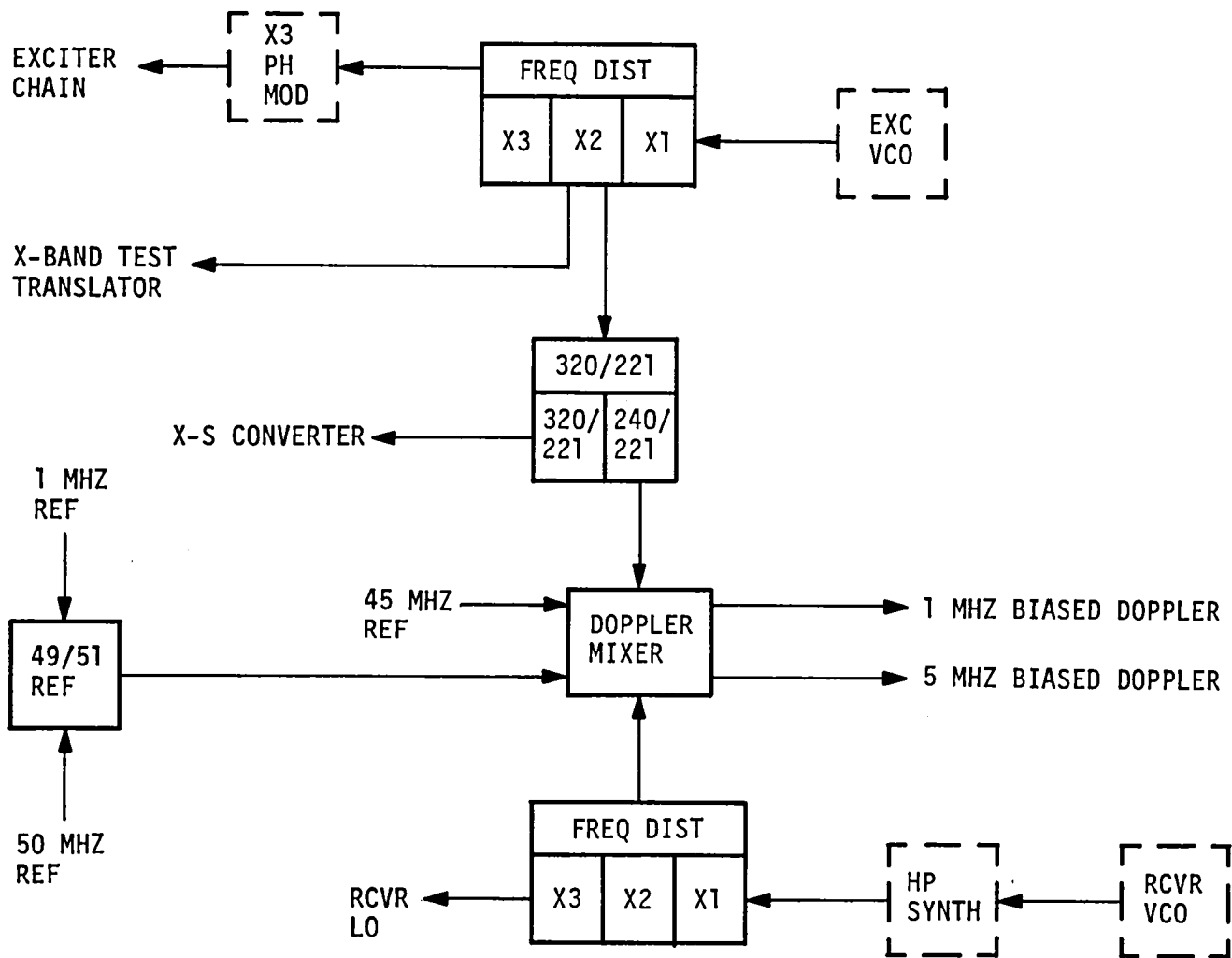


Figure 73. 26M S-X Conversion Receiver-Exciter Doppler Extractor Block Diagram

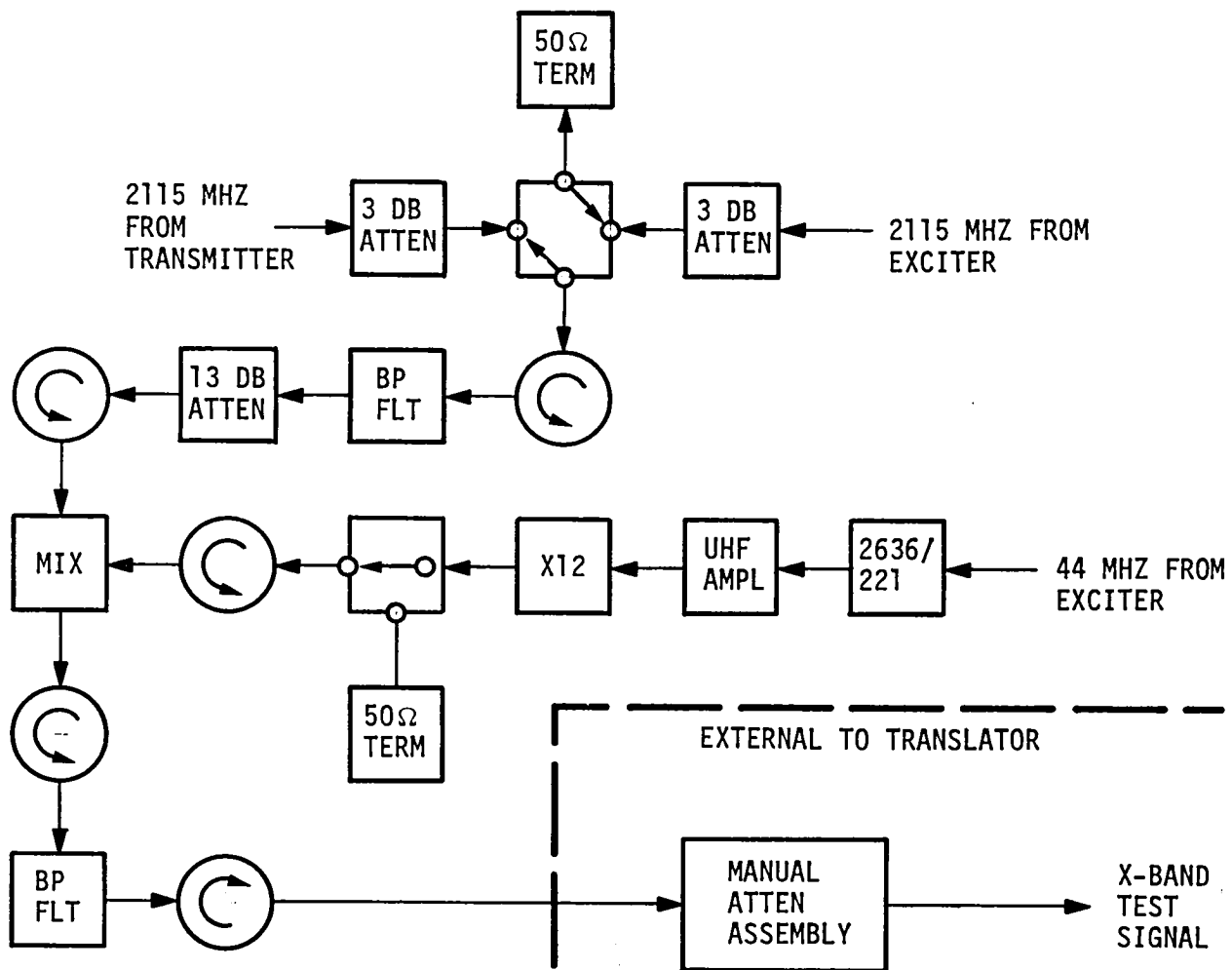


Figure 74. 26M S-X Conversion Receiver-Exciter Test Translator Block Diagram

H. ANTENNA MICROWAVE DESIGN

The design of the antenna had to meet the following requirements:

S-Band

Transmit	2100 to 2120 MHz 20-kW continuous wave power capacity RCP or LCP, manually selectable 55.3 ± 0.7 dBi gain
Receive, Traveling Wave Maser (TWM) No. 1	2270 to 2300 MHz 27.5 ± 2.5 K duplexed system temperature* 21.5 ± 2.5 K low-noise system temperature* RCP or LCP, manually selectable 56.1 ± 0.3 -0.9 dBi gain

X-Band

Receive	8400 to 8440 MHz 25.0 ± 3 K system temperature RCP or LCP, remotely selectable 66.9 ± 0.3 -0.9 dBi gain
---------	---

The approach used in the feed design was to use DSN standard microwave components where feasible; use a reduced, existing, S-band, polarization diversity design for the S-band feed system; use an existing 64m antenna X-band feed assembly; and use the filters from the existing S-Band Cassegrain Monopulse (SCM) cones.

One of the studies made during the design was the blockage effect of using the 64m antenna reflex feed system on a small antenna. For a 26m antenna the S-band gain loss was 0.3 dB and for the 34m antennas it was 0.1 dB. The 34m antenna size over the 26m antenna provides 2.22 dB of absolute gain improvement. Also studied was the best arrangement of the reflector cone and subreflectors to minimize the blockage effect.

*For TWM No. 2, add 8k

Changes to the Antenna Microwave Subsystem (UWV) design included the addition of an X-band maser, X-band test signal, and an automatic microwave configuration control and verification system. The microwave switch control provides microwave configurations to and from the Monitor and Control Subsystem (DMC). The S-X microwave subsystem interfaces are shown on Figure 75. The S-X block diagram is shown on Figure 76.

The design of the X-band maser instrumentation used a simplified monitor receiver made from commercial components that provide cost-effective performance and reduced power requirements. The design used serial data communications, thus reducing cable and power requirements and providing remote instrumentation power turnoff. The design was also compatible for future dual masers. The actual X-band maser performance is shown in Table XV.

The microwave configuration control group design was done to provide the following:

- a. Local control and indication of UWV switch position
- b. Local indication of transmitter interlock status
- c. Interface for remote control and monitor via DMC star switches
- d. Improved generation and verification of configuration by using named modes
 - (1) Resident standard modes in read-only memory (ROM)
 - (2) Accommodate user-generated modes in read and write memory (RAM)

Design studies were made to determine whether to simply update the existing manual switch control equipment at the 26m station, to duplicate the DSS 14 64m switch control system, which provided individual switch control only and no remote capability, or to provide a new integrated subsystem controller for switch control.

INTERFACING LINK AND SUBSYSTEMS

SPACECRAFT TELECOMMUNICATIONS

RF SIGNALS →

HIGH-POWER RF SIGNALS ←

TRANSMITTER

BEAM VOLTAGE INHIBIT ←

ANTENNA-DUMMY LOAD
SWITCH POSITION ←HIGH-POWER RF TO
DUMMY LOAD ←

HIGH-POWER RF SIGNALS →

WAVEGUIDE SWITCH INHIBIT →

ACQUISITION AID, S-BAND

RF SIGNALS →

HIGH-POWER RF SIGNALS ←

MONITOR AND CONTROL

SUBSYSTEM MONITOR DATA* ←

CONFIGURATION CONTROL* →

FUNCTIONS:

- RECEIVES FOCUSED RF SIGNALS
- DIPLEXES RIGHT OR LEFT CIRCULAR POLARIZATION (20 KW SIGNALS)
- PROVIDES LOW NOISE MICROWAVE AMPLIFICATION
- TRANSMITS COLLIMATED RF SIGNALS
- MEASURES SYSTEM NOISE TEMPERATURE
- PROVIDES TEST SIGNAL ATTENUATION
- PROVIDES AUTOMATIC MICROWAVE CONFIGURATION CONTROL AND VERIFICATION

ASSEMBLIES:

- CASSEGRAIN FEED CONE
- MASER AMPLIFIERS*
- MICROWAVE SWITCH CONTROL*
- TEST SIGNAL CONTROL
- COLLIMATION MICROWAVE
- Y-FACTOR EQUIPMENT

INTERFACING SUBSYSTEMS

RECEIVER/EXCITER

- AMPLIFIED RF SIGNALS*
- MICROWAVE TEST SIGNALS
- CONFIGURATION INDICATION
- EXCITER DRIVE CONTROL
- ← NOISE TEMPERATURE MEASUREMENT
- ← MICROWAVE TEST SIGNALS*
- ← NAR-PSPM SWITCHING*

ANTENNA MECHANICAL

- ← FEED MECHANICAL SUPPORT
- ← SUBREFLECTOR POSITION
- ← FOCUS AND COLLIMATE

DSIF TECHNICAL FACILITIES

- ← SPACE
- ← PRIMARY POWER
- ← INTERSUBSYSTEM CABLES
- ← AIR CONDITIONING

*DENOTES CHANGES

Figure 75. S-X Microwave Subsystem Interfaces

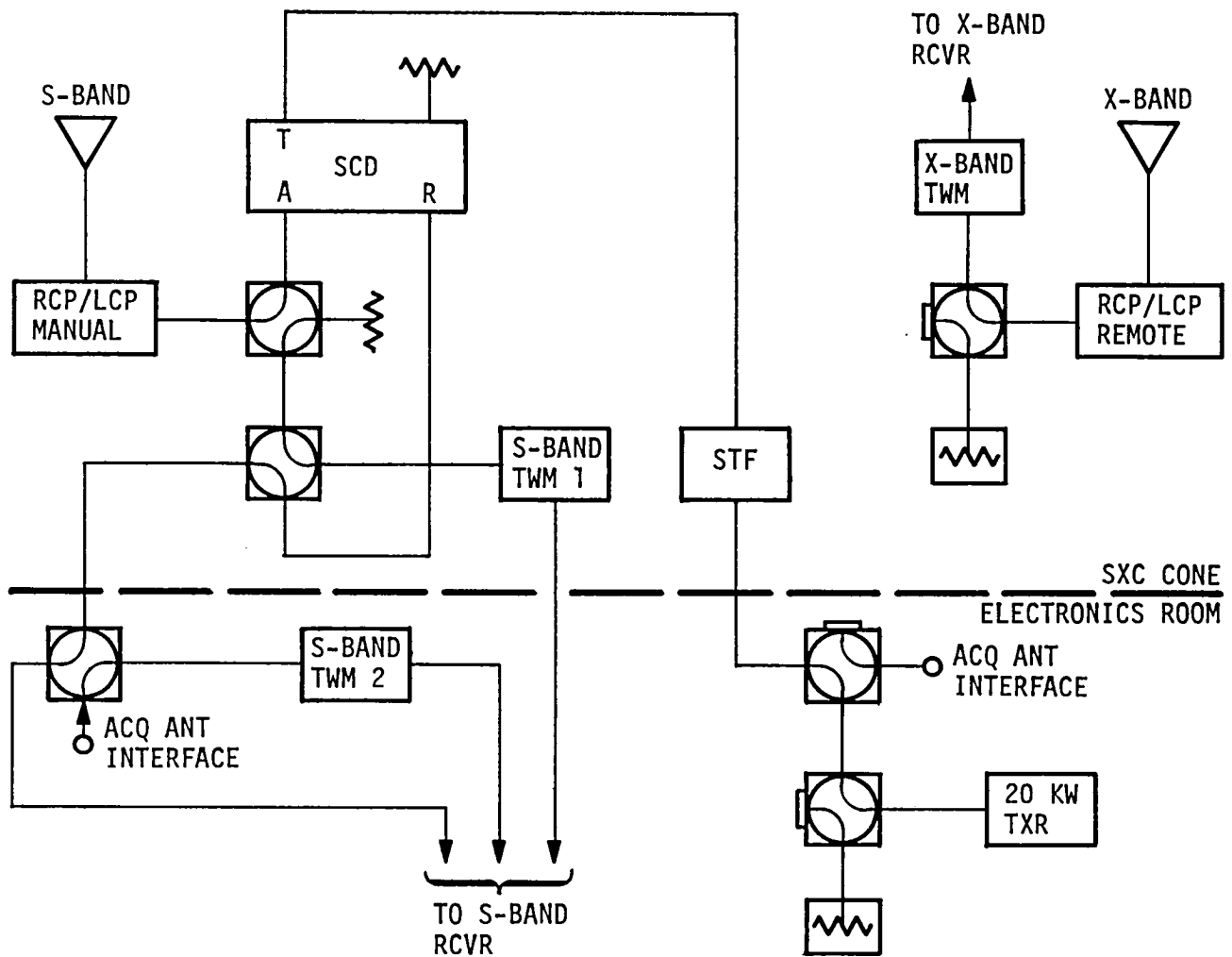


Figure 76. S-X Band Block Diagram

Table XV. X-Band TWM Performance

Parameter	Specification	Test Results
Gain	45 \pm 1 dB	45 $\begin{smallmatrix} +0 \\ -0.5 \end{smallmatrix}$ dB
Bandwidth	40 MHz, -1 dB, 8400-8440 MHz	54 MHz, -1 dB
Stability	\pm 0.03 dB per 10 sec \pm 0.5 dB per 12 hr \pm 0.5 dB, 0.2 deg/sec tilt rate	\pm 0.025 dB per 10 sec (Not measured) (Not measured)
VSWR	1.4, input 1.7, output	<1.3, input 1.45, output
Noise Temp	8 \pm 2K over entire band	7.5 to 8.2K
Signal Level	-90 dBm max, 1-dB gain compression 0 dBm max for recovery	-84 dBm, 1 dB compression

The selected option was the integrated subsystem controller. This design reduced rack space requirements and is very flexible. It also provides operator interface at high levels. In addition, the controller provides for remote control and monitor in the attended or unattended mode and is interfaceable with the Station Monitor and Control Assembly (SMC). The design provides for 10 microwave configurations that can be automatically called by a simple code instruction. The following is the SXD cone mode chart:

S-Band Feed*

RCP

LCP

S-Band Waveguide

Diplex TWM 1

Diplex TWM 2

Listen TWM 1

Listen TWM 2

Calibrate TWM 1

Calibrate TWM 2

X-Band Feed

RCP

LCP

X-Band Waveguide

Receive

Calibrate

*Manual operation only.

The switch control block diagram is shown in Figure 77.

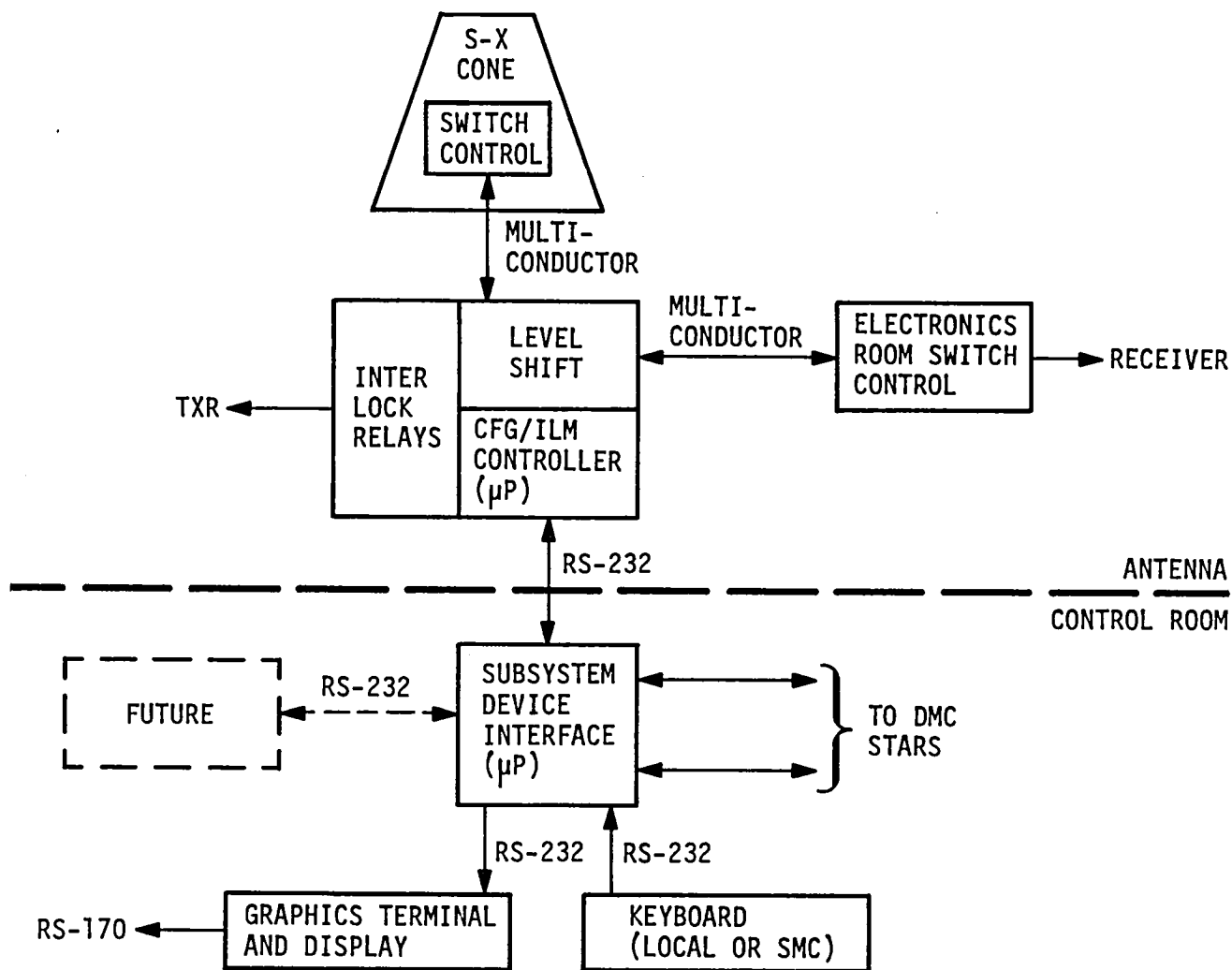


Figure 77. Switch Control Block Diagram

V. ANTENNA PERFORMANCE

A. GENERAL DISCUSSION

The significant measure of the antenna performance is its operation as a complete system under environmental conditions.

Of prime importance are the RF antenna gain, noise temperature, and beam pointing performance of the antenna. This section provides the results of the antenna performance evaluated from data on RF signal strength and pointing accuracy at known locations of RF-emitting radio stars. These tests furnished data and results for both S-band and X-band frequencies.

The X-band pointing requires the use of the CONSCAN automated program, which rotates the antenna on the beam 0.1 dB off the maximum gain and allows pointing accuracies of 0.006 to 0.009 degree.

The particular value of the performance data at the X-band frequency of 8.4 GHz, as compared to the S-band data at 2.2 GHz, is that at the higher frequencies the system performance is much more sensitive to reflector surface errors, as was shown by the missing X-band gain that developed at DSS 12. A study team was formed to determine the X-band performance and the reason for the loss of gain at DSS 12. This is covered in subsection D of this section, which contains a great deal of antenna gain and subreflector focus measurements.

During the final stages of the DSS 61 conversion, and after some performance tests were run, an accident occurred that caused some damage and delay to the completion schedule. This is covered in subsection E of this section.

B. OVERALL PERFORMANCE SPECIFICATIONS

1. Radio Frequency Performance

The system specifications as established in the Data System Development Plan (DSDP) and later in the functional requirements were as follows:

Frequency Range: S-band 2290-2300 MHz

X-band 8400-8440 MHz

Gain: S-band 56.1 $\begin{matrix} +0.3 \\ -0.9 \end{matrix}$ dBi

X-band 66.9 $\begin{matrix} +0.3 \\ -0.9 \end{matrix}$ dBi

System Noise Temperatures: S-band 27.5 \pm 2.5 K in the X-band 25.0 \pm 2.0 K
diplexed mode

Polarization: S-band selectable RCP, LCP, manually rotatable linear
X-band selectable RCP and LCP.

2. Pointing Accuracy Requirements

One of the key factors in the ability to use the existing antenna mechanical system within reasonable costs (and hence modifications) was the existence of the CONSCAN antenna pointing program. This program rotates the antenna within a radius of about 0.006 degree from the peak gain, causing a minor gain loss of about 0.1 dB but eliminating all repeatable and long-term pointing errors and, hence, allowing for acceptable X-band performance to be met by an original antenna structure designed to meet the larger allowed errors for S-band pointing.

The actual specified pointing was 0.039 degree root-sum-square (RSS) in a 48-km/h (30-mi/h) wind with no external compensation. This meant that the antenna could not perform at X-band if CONSCAN were not used because the total beam width was 0.068 degree and the pointing error exceeded the half beam width.

3. Environmental Requirements

The antenna was specified to be capable of operation and survival, as applicable, under the combinations of environmental conditions set forth below. There was no requirement for environmental testing.

- a. Outside ambient temperature: -17.7°C (0°F) to 46°C (115°F).
- b. Indoor ambient temperature: 18.3°C (65°F) to 25.5°C (78°F) (azimuth building); other internal locations 10 to 40°C .
- c. Sunlight exposure: Partial or full sunlight in any attitude within the mount capabilities (this exposure includes 12-hour tracks of targets whose subtended angle from the sun is constant at an angle of 2 degrees or greater)
- d. Outside relative humidity: 0 to 100 percent
- e. Inside relative humidity: 20 to 80 percent
- f. Rainfall:

<u>Duration</u>	<u>Amount</u>
5 min	1.27 cm (0.50 in.)
10 min	2.03 cm (0.80 in.)
15 min	2.54 cm (1.00 in.)
30 min	3.81 cm (1.50 in.)
60 min	5.08 cm (2.00 in.)

- g. Dust: Desert environment
- h. Lightning: Protection to be provided as required
- i. Ice and snow loads:
 - (1) Operational - none
 - (2) Stowed position - survival with simultaneous applications of winds with average velocity up to 97 km/h (60 mi/h) and a 2.54 cm (1-in.) glazed ice load (specific gravity 0.5) or a 76.2 cm (30-in.) snow load (specific gravity 0.1)
- j. Altitude 1219 meters (4000 feet)
- k. Earthquakes: 0.25 gravity applied horizontally for a total base shear. (Wind loads shall not be applied simultaneously with seismic loads.)

1. Wind operating conditions:

0 to 72 km/h (0 to 45 mi/h) - Full operation

80 km/h (50 mi/h) - Drive to stow

80 km/h (50 mi/h) - Stow at zenith

80 to 113 km/h (50 to 70 mi/h) - Survival any position - no structural or mechanical member shall buckle or exceed yield stress.

114 to 160 km/h (71 to 100 mi/h) - Survival at zenith - no structural or mechanical member shall buckle or exceed the yield stress.

Overturning - For the above survival conditions, a safety factor of 1.5 was used against overturning.

C. OVERALL PERFORMANCE MEASUREMENTS

1. Radio Frequency Performance

The radio frequency performance measurements were the results of extensive system performance tests conducted at the 34m stations subsequent to improvements made as a result of the X-band study team recommended changes.

A summary of these results, which met all of the previously defined requirements, follows:

	<u>DSS 12</u>	<u>DSS 42</u>	<u>DSS 61</u>
S-Band Performance			
Gain (56.1 $\begin{smallmatrix} +0.3 \\ -0.9 \end{smallmatrix}$ dB)	56.6 dBi	56.6 dBi	56.3 dBi
Temperature (27.5 K ± 2.5)	27.4 K	27.4 K	27.5 K
X-band Performance			
Gain (66.9 $\begin{smallmatrix} +0.3 \\ -0.9 \end{smallmatrix}$ dB)	66.6 dBi	66.6 dBi	66.3 dBi
Temperature (25 K ± 2.0)	23.7 K	22.3 K	18.5 K

Frequency Range: S-band 2290-2300 MHz; X-Band 8000-8440 MHz

Polarization: S-band selectable RCP, LCP, and manually rotatable linear; X-band selectable RCP and LCP

2. Pointing Accuracy Performance

No special tests were run specifically to check the antenna pointing; however, as expected, there were large repeatable pointing errors that were removed by CONSCAN. The antenna met gain requirements when operating using the CONSCAN program but with additional losses of 0.2 to 0.3 dB above those given in the paragraph above.

3. Environmental Performance

No specific tests were run, but the DSS 12, 42, and 61 antennas all have withstood extremely high winds, heavy rains, and temperature extremes over a collective operating period of 6 years with no damage or residual effects.

4. Summary

After completion of the S-X conversion and resolution of the gain loss problem (which is covered in the following paragraphs), the antennas met or exceeded all of the performance requirements. Much greater detail and performance data are presented in the following paragraphs and figures on the gain loss study and results.

D. X-BAND PERFORMANCE

A study team was formed because of gain loss at DSS 12, which is described in detail in the following paragraph. The team was chaired by E. Thom and consisted of the following members: D. Bathker, E. Fields, A Freiley, S. Katow, J. Kundrat, V. Lobb, J. Maclay, O. Rotach, R. Stevens, and W. Williams. In addition, Dr. M. Klein, D. Girdner, R. Reynolds, and D. Jauncy provided valuable support to the study team.

1. Background

The RF design was covered in detail in TDA Progress Report 42-41, July-August 1977. In that report the gain was computed to be 67.01 dB or

55.87 percent efficiency at the rigging angle.* The antenna panels are set for the best parabolic fit at an equivalent of 40-degree elevation to minimize the gravity distortion for spacecraft traveling close to the ecliptic plane. Since the antenna focal length to diameter decreased with the increase in diameter, the gain was expected to drop off significantly as the antennas are pointing away from the rigging angle. A subreflector controller was designed and installed as a part of the upgrade to compensate for equivalent hyperbola and parabola focal offsets caused by large scale gravity deflections warping the best fit parabolic focus. This controller provides three axes of motion for the subreflector to provide lateral and axial focussing; X to compensate for hour angle motion, Y to compensate for declination motion, and Z to compensate for axial deflections.

A reflex type S- and X-band feed system, similar to the 64m design, was installed which utilized an ellipsoidal reflector and dichroic filter to direct the incoming S- and X-band signals into their respective feedhorns. The entire feed system was offset from the antenna main axis by over 7 degrees to minimize aperture blockage. To compensate for this offset, the subreflector was tilted about the focal point to maintain RF alignment, as in the 64m design.

The upgrade started at DSS 12 in June 1978 and was completed in October 1978; DSS 61 started in August 1979 and finished in February 1980; DSS 42 started in October 1979 and finished in April 1980. After each of the upgrades was completed, approximately 1 month was allowed to make RF performance tests and calibrations.

The requirements document for the 34m stations specified a peak gain of $66.9^{+0.3}_{-0.9}$ dB at the rigging angle, with the gain to drop off no more than 0.1 dB from the peak gain at any sky position.

*Based on an assumed 1.0 mm rms surface tolerance.

2. Measured Performance Results and Investigations

When DSS 12 was completed, a series of star tracks was performed to measure the gain and system temperature. The results of these measurements are shown in Figures 78 and 79. In the figures to follow, the tolerance shown was largely determined by absolute uncertainties associated with radio star flux values and, to a lesser extent, by engineering judgment on the reliability of calculations. Since the peak gain was 0.3 dB below the minimum requirement and 1.2 dB below the anticipated result, considerable effort was expended to ascertain the causes of the missing gain. This was hampered to a large extent by the operational commitments of the station. There were no obvious clues and the decision was made to wait until DSS 61 was completed to see if there was a systematic problem or if the low gain was unique to DSS 12.

When DSS 61 was completed in February 1980, the star tracks were performed and, again, the gain was lower than anticipated, although it was within the requirement. These results are shown in Figures 80 and 81.

At that time, the problem appeared to be at least partially systematic in nature and the 34m X-band Gain Study Team was formed in mid-March 1980. Since the upgrade at DSS 42 was being projected as being completed about 2 weeks ahead of schedule (the end of April instead of mid-May), those 2 weeks were allocated to additional testing to attempt to find the cause of the reduced gain. A test plan was proposed and forwarded to the station. During the next 3 months, many tests, checks, and investigations were performed in parallel, ranging from a recalculation of the RF design and structural shapes to reviewing inspection and alignment procedures and resultant data. (See Figures 82 and 83.)

One item of significance was the removal of one of the panels from the outer ring at DSS 12 for measurement of the surface tolerance. When accepted, the panel had an rms of 0.013 inch. When remeasured, it had an rms of 0.042 inch. Based on this, an additional 14 of the 96 new panels were removed and remeasured. They had individual rms values ranging from

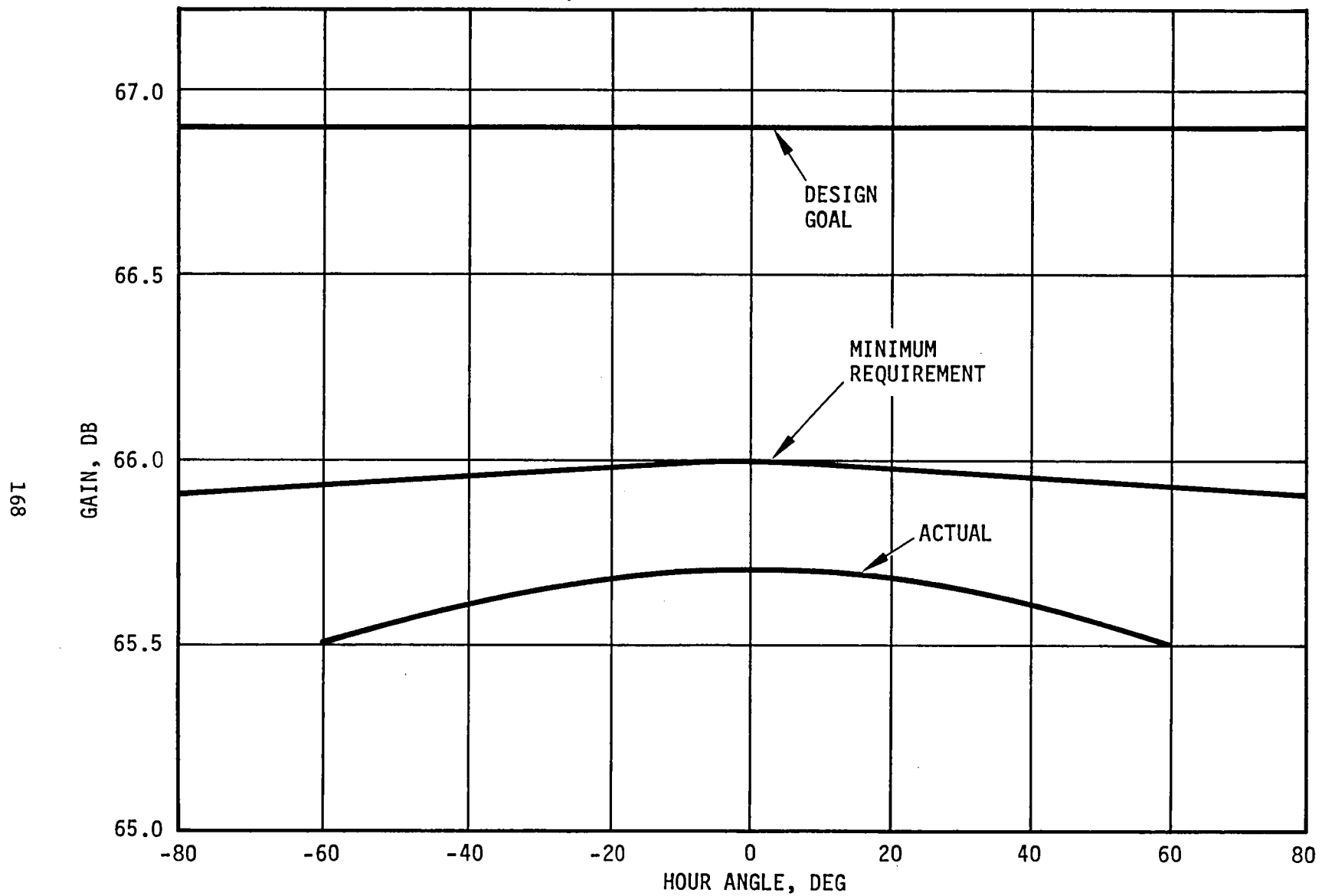


Figure 78. DSS 12 X-Band Antenna Gain vs Hour Angle

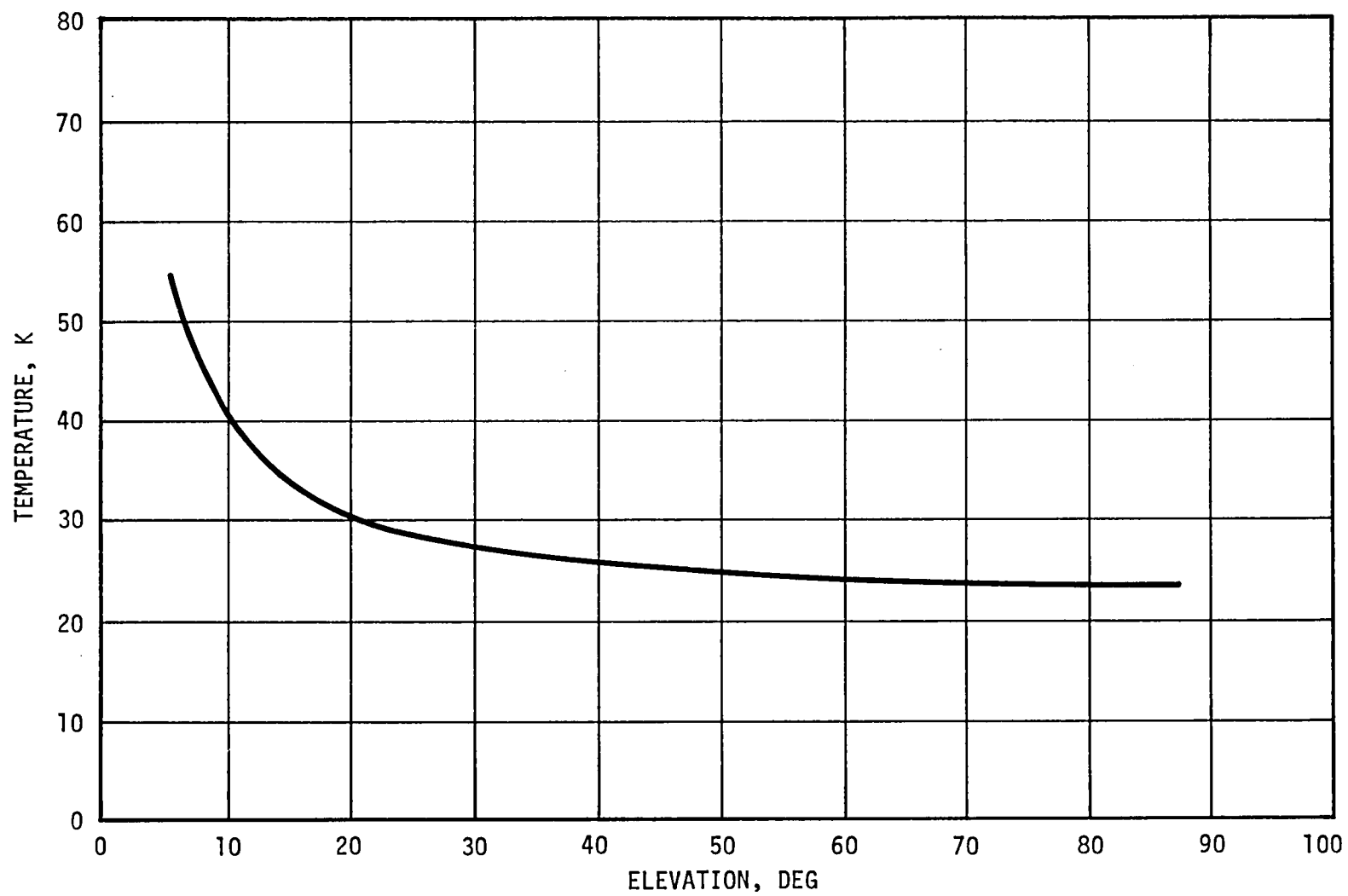


Figure 79. DSS 12 X-Band System Temp vs Antenna Elevation

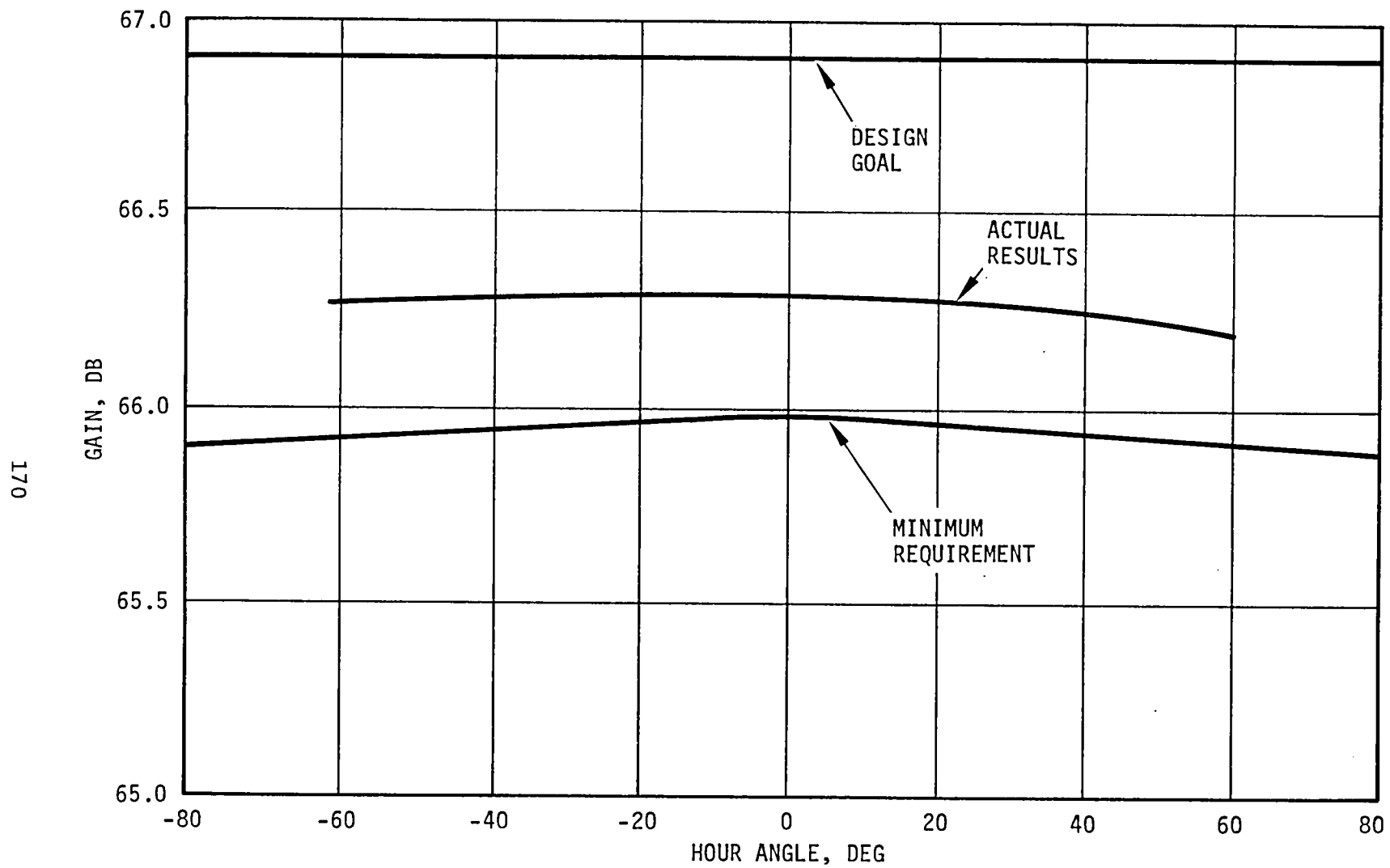


Figure 80. DSS 61 X-Band Antenna Gain vs Hour Angle

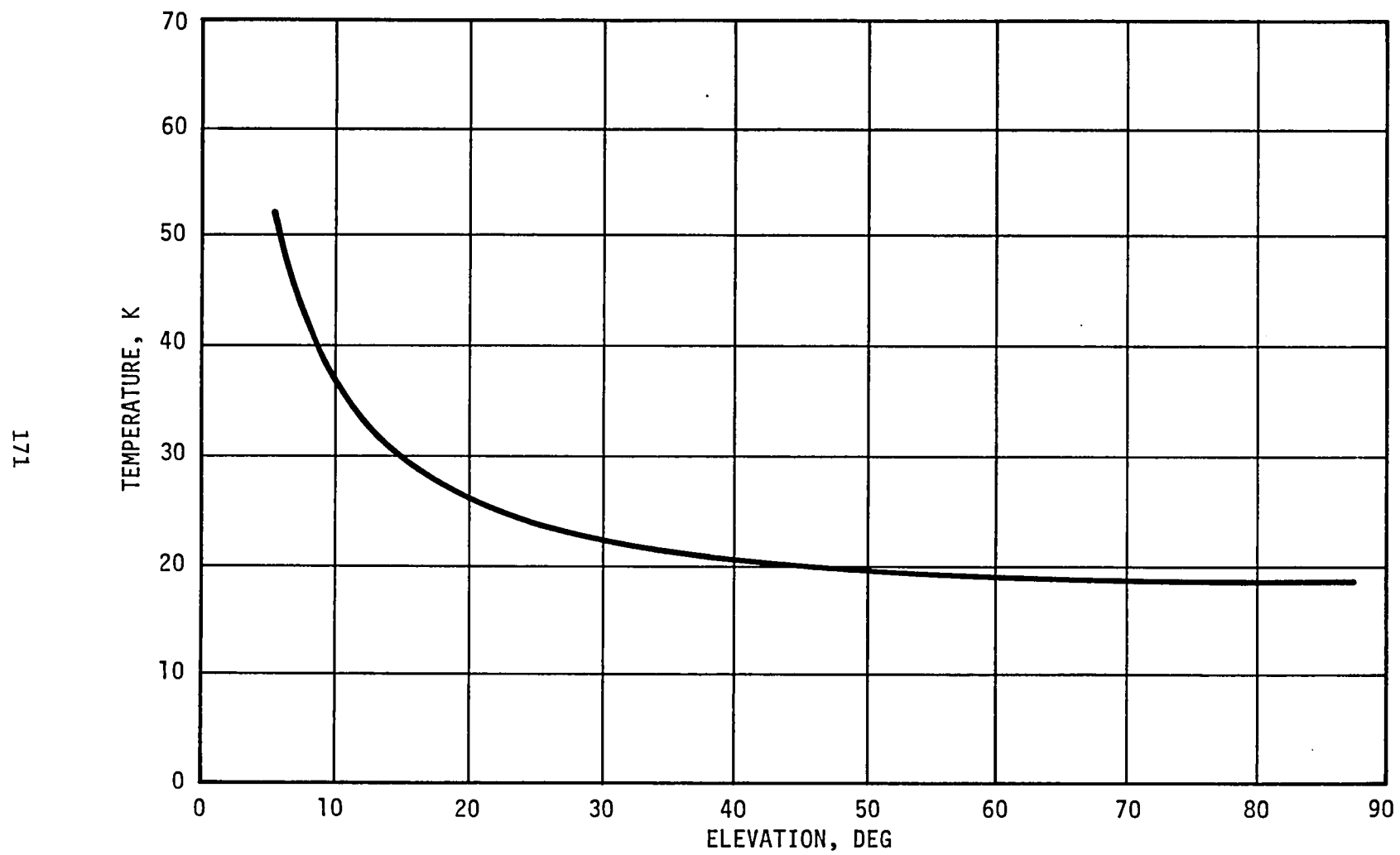


Figure 81. DSS 61 X-Band System Temp vs Antenna Elevation

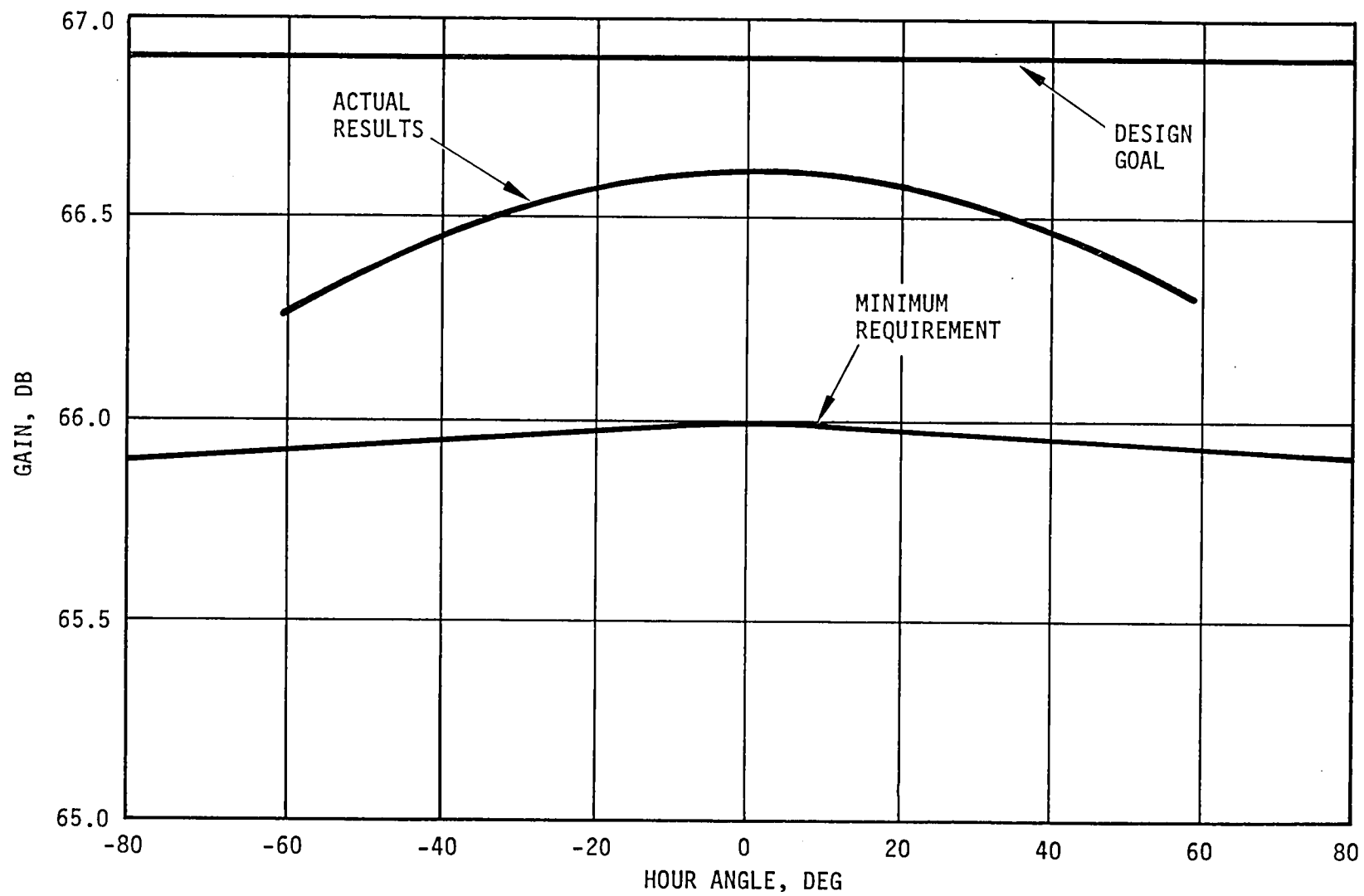


Figure 82. DSS 42 X-Band Antenna Gain vs Hour Angle

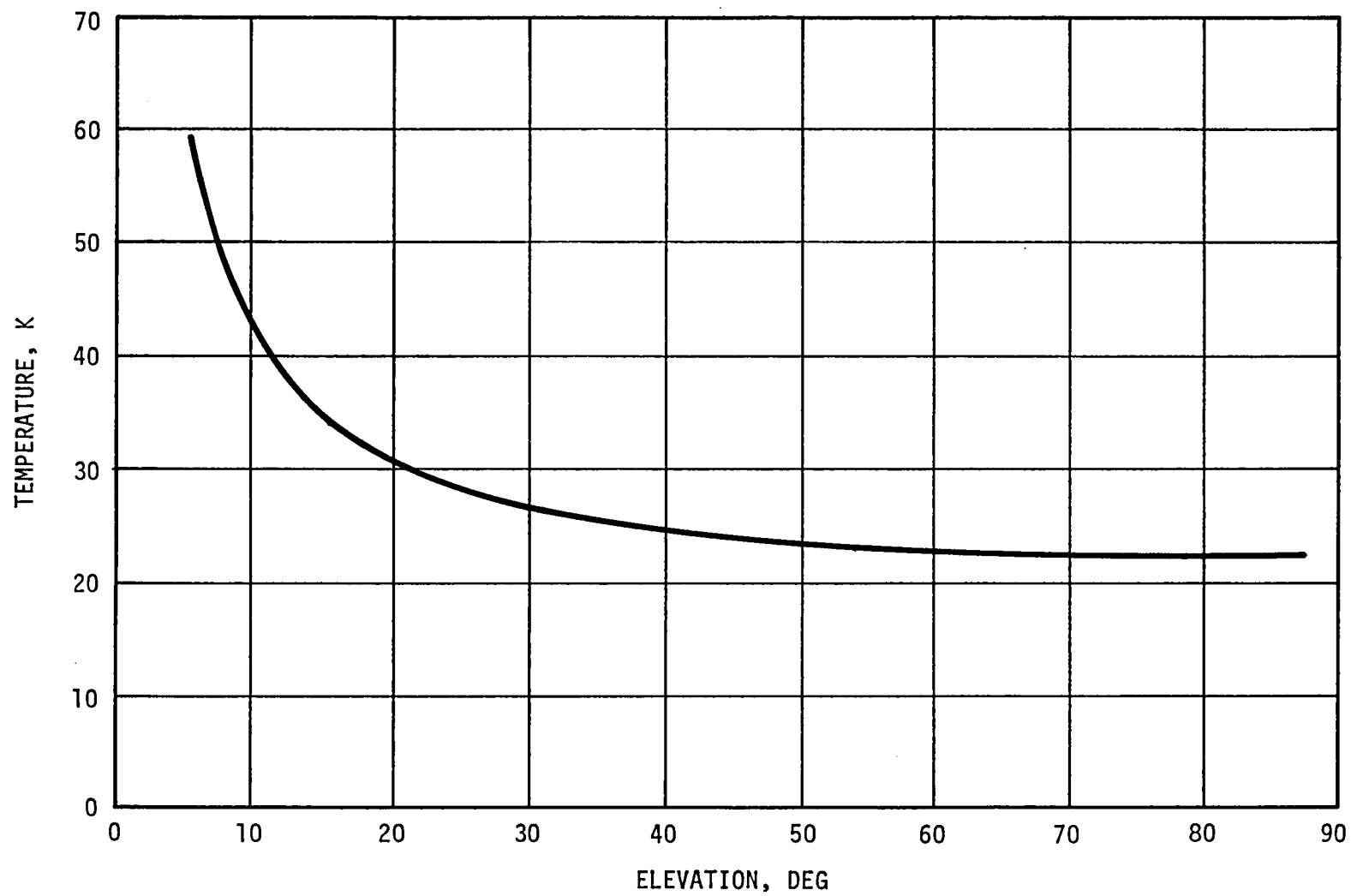


Figure 83. DSS 42 X-Band System Temp vs Antenna Elevation

0.040 inch to 0.100 inch with a composite value of 0.055 inch. Since the two outer rings, which were added to expand from 26 to 34 meters, comprise about one-half the area of the dish, this could account for about 0.75 dB of gain loss (using the classic formula by Ruse). New panels were procured, installed, and aligned between the Voyager 1 and 2 Saturn encounters. At that time a correction was made to the inner panels due to a misalignment that occurred when the panel adjustment jackscrews vibrated loose after the antenna upgrade was completed. The panels were reset with the theodolite on top of the cone instead of at the vertex, which required using sweep templates for the inner rows. The setting rms from this was estimated at 0.030 inch instead of the 0.010 inch that was achievable with the theodolite at the vertex. The 0.030-inch estimate was somewhat confirmed by data taken and reduced by M. Klein which showed a power pedestal at the base of the antenna patterns that was about 0.8 degree wide (see Figure 84). This indicated a correlation distance (from Ruse) of about 2.74 meters (9 feet), approximately the panel size. The amplitude of the pedestal was -30 dB or, from Ruse, a setting of 0.036 inch.* As would be expected, the gain of the antennas also varied with declination. Figure 85 shows this variation at DSS 12 for transit crossing. Figure 86 shows the gain variation for hour angle motion at three different declinations, as calculated by S. Katow.

Another significant finding that came from the series of star tracks at DSS 12 was that the side lobes on the beam were excessively high and uneven. The side lobes also appeared to vary in different portions of the sky. DSS 61 also reported uneven side lobes. This indicated that there was misalignment in the optics and that it varied as the antenna was moved. This was traced to an incorrect map of subreflector position in the X (east-west) axis (see Figure 87). The map was corrected for the Y and Z axes, however. Six new circuit cards (an operating card plus a spare for each station) were prepared with a modified map and tested at DSS 12. The recalculated map values tended to overcompensate from the

* Total rms consists of the parabola panel component, parabola setting component, hyperbola component, and structural component (applicable only away from rigging angle).

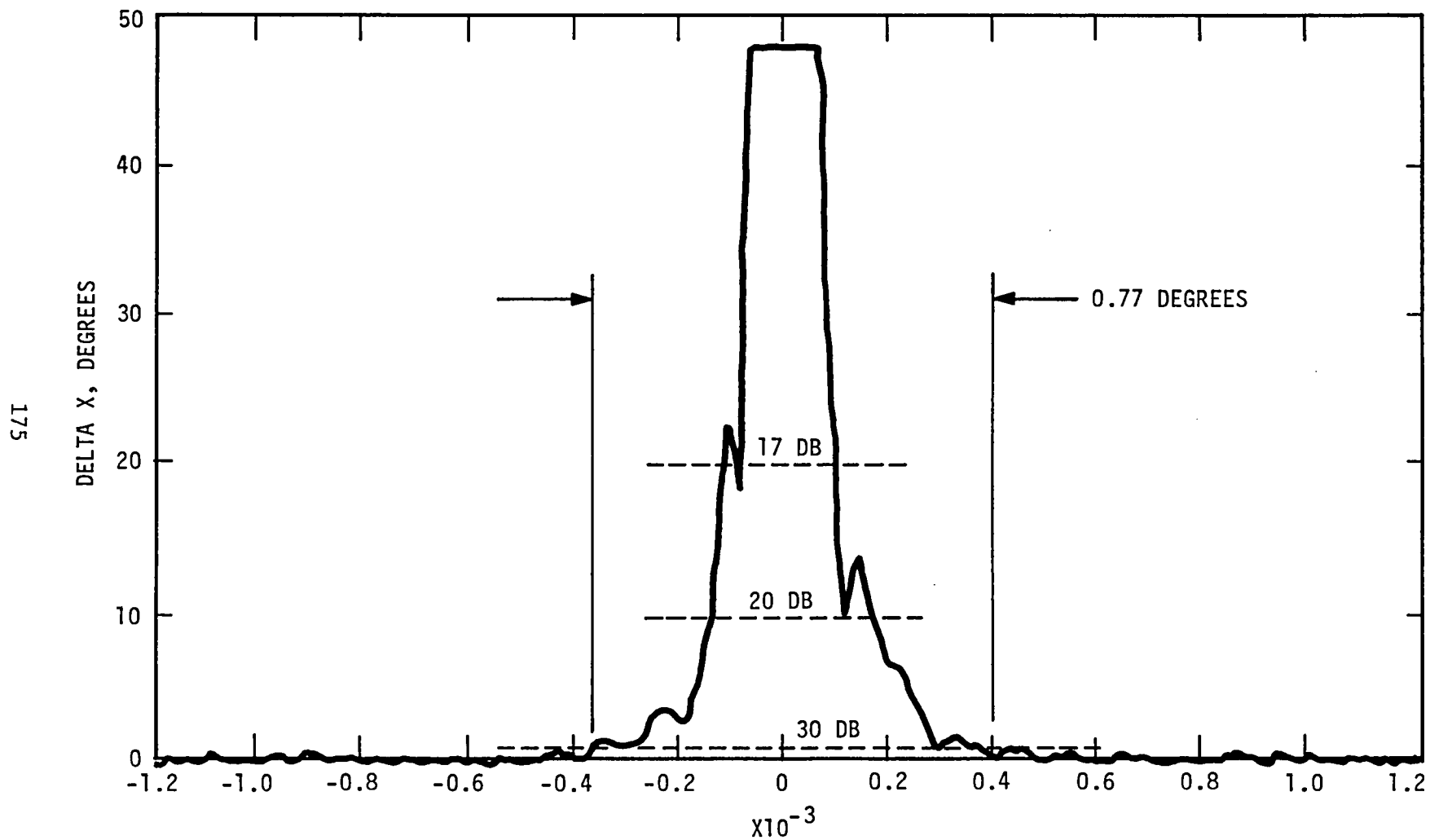


Figure 84. DSS 12 X-Band Beam Map

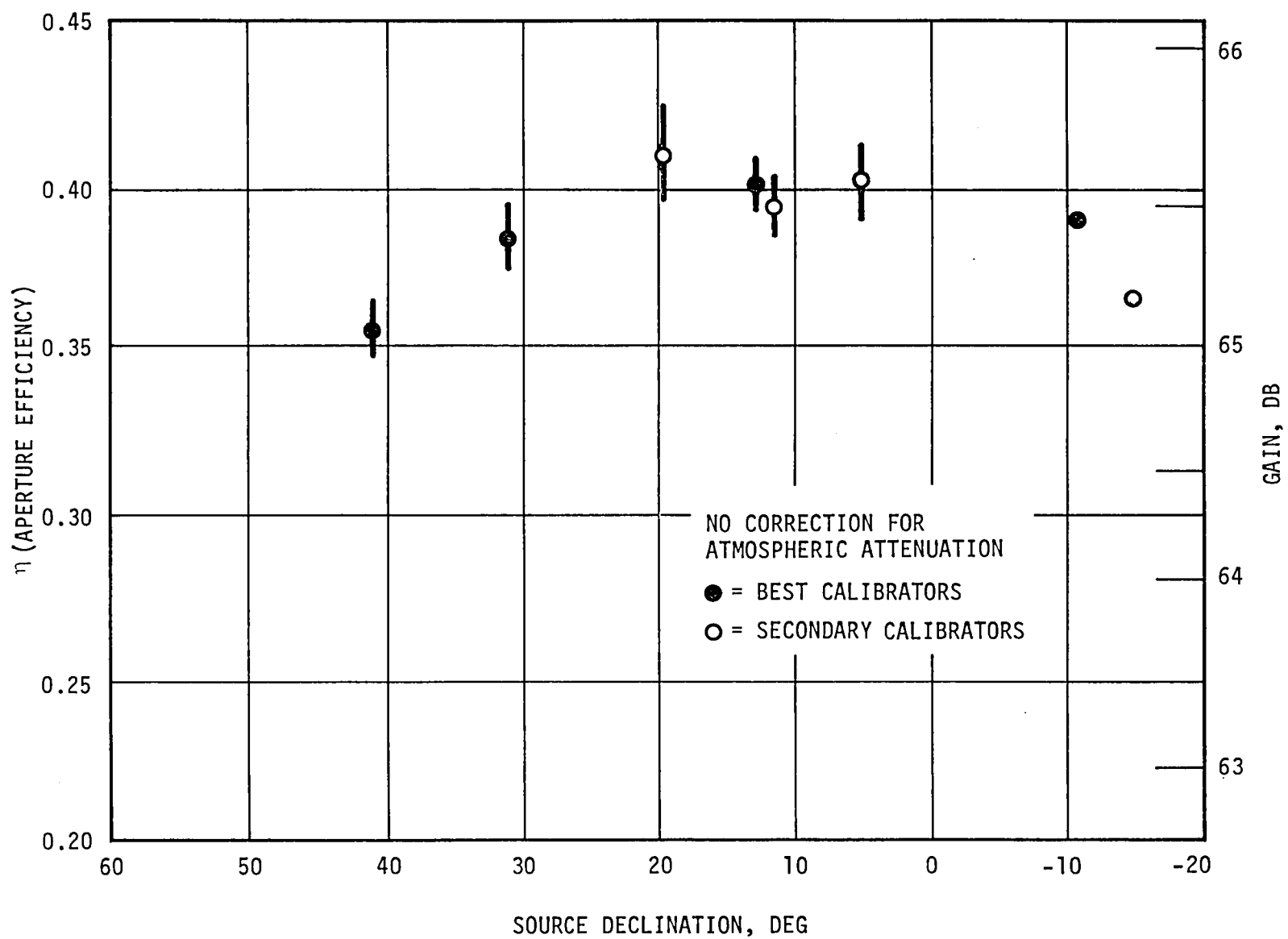


Figure 85. DSS 12 X-Band Aperture Efficiency from Radio Source Measurements (Mar-Aug 1980)

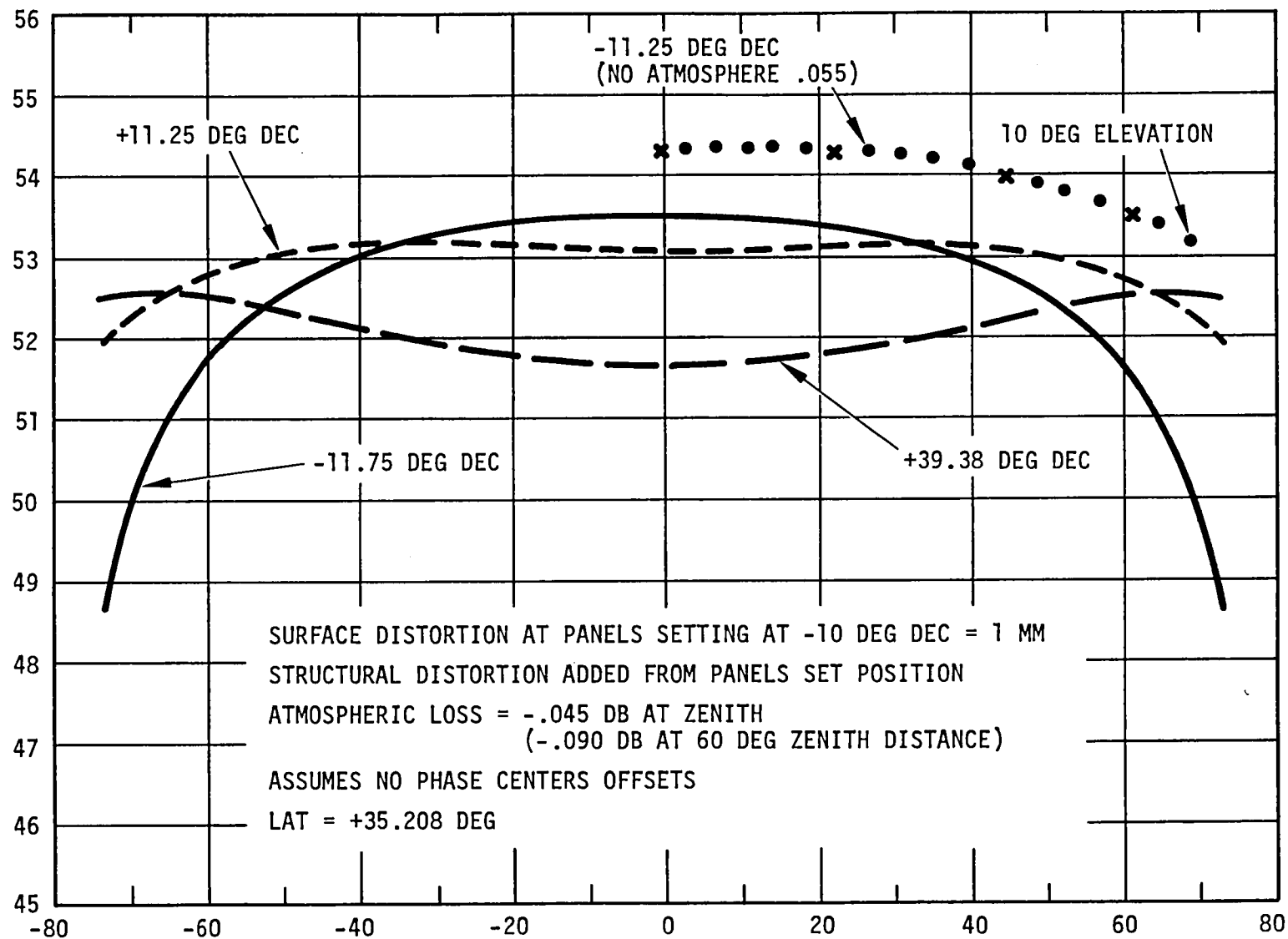


Figure 86. DSS 12 34M Computed Efficiency vs Hour Angle

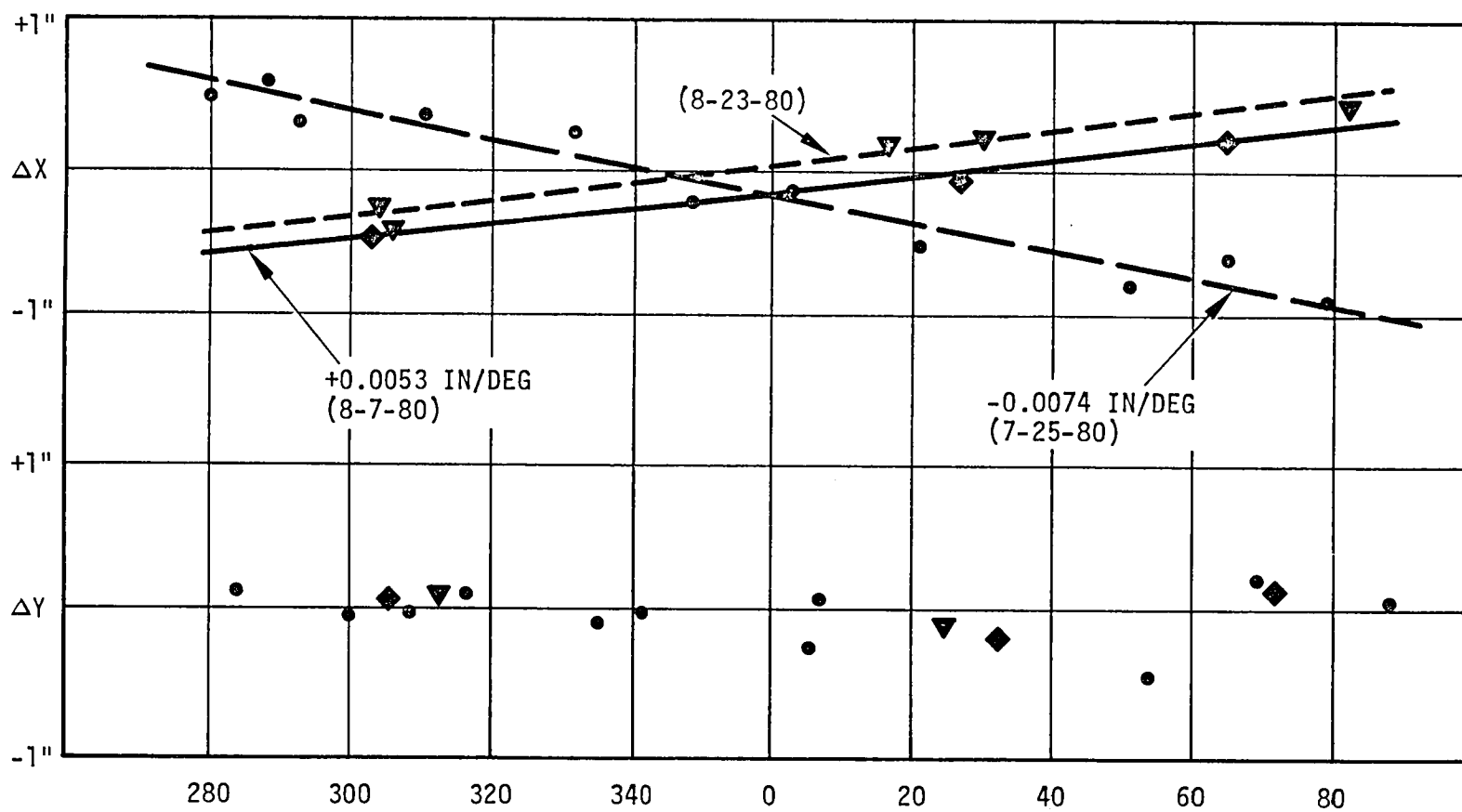


Figure 87. DSS 12 Antenna Performance, X-Y Offset Errors at 8420 MHz
Before vs After SRC Card Modification

prior values, but since the Voyager 1 Saturn encounter was imminent, it was decided to proceed with the temporary implementation at all three sites since the gain was improved somewhat even if not optimized (see Figure 88). After the first Saturn encounter, tests were scheduled and performed at each 34m station to optimize the maps individually and provide permanent circuit cards.

3. Recommended Modifications

As stated above, there were three modifications recommended by the study team:

- a. Between February 1 and March 23, 1981, replace the outer two rings of panels at DSS 12. Reset all panels with the theodolite at the vertex.
- b. Temporarily replace the subreflector position map with an improved map for use during the Voyager 1 Saturn encounter.
- c. Between January 15 and April 7, 1981, calibrate each antenna and provide permanent optimum subreflector position maps.

4. Conclusions

Table XVI shows the calculated gain and calculated or measured losses for each of the 34m antennas. After the measurements there was from 0.3 to 0.6 dB loss at the various antennas. D. Bathker issued a memo stating that the star sources and factors used appeared to cause a 0.3 dB error in resulting measurements, which accounted for most of the error.

After modification of DSS 12 the measured gain was 66.6 dB, the same as DSS 42, with the only unexplained loss being 0.3 dB at DSS 61. This loss may have been caused by small accumulations of errors in the measurements and certainly was well within the tolerance allowed of +0.3 dB to -0.9 dB. The final gain of the three antennas at the setting position were 66.6 dB for DSS 12 and DSS 42, and 66.3 dB for DSS 61 versus a requirement of $66.9^{+0.3}_{-0.9}$ dB.

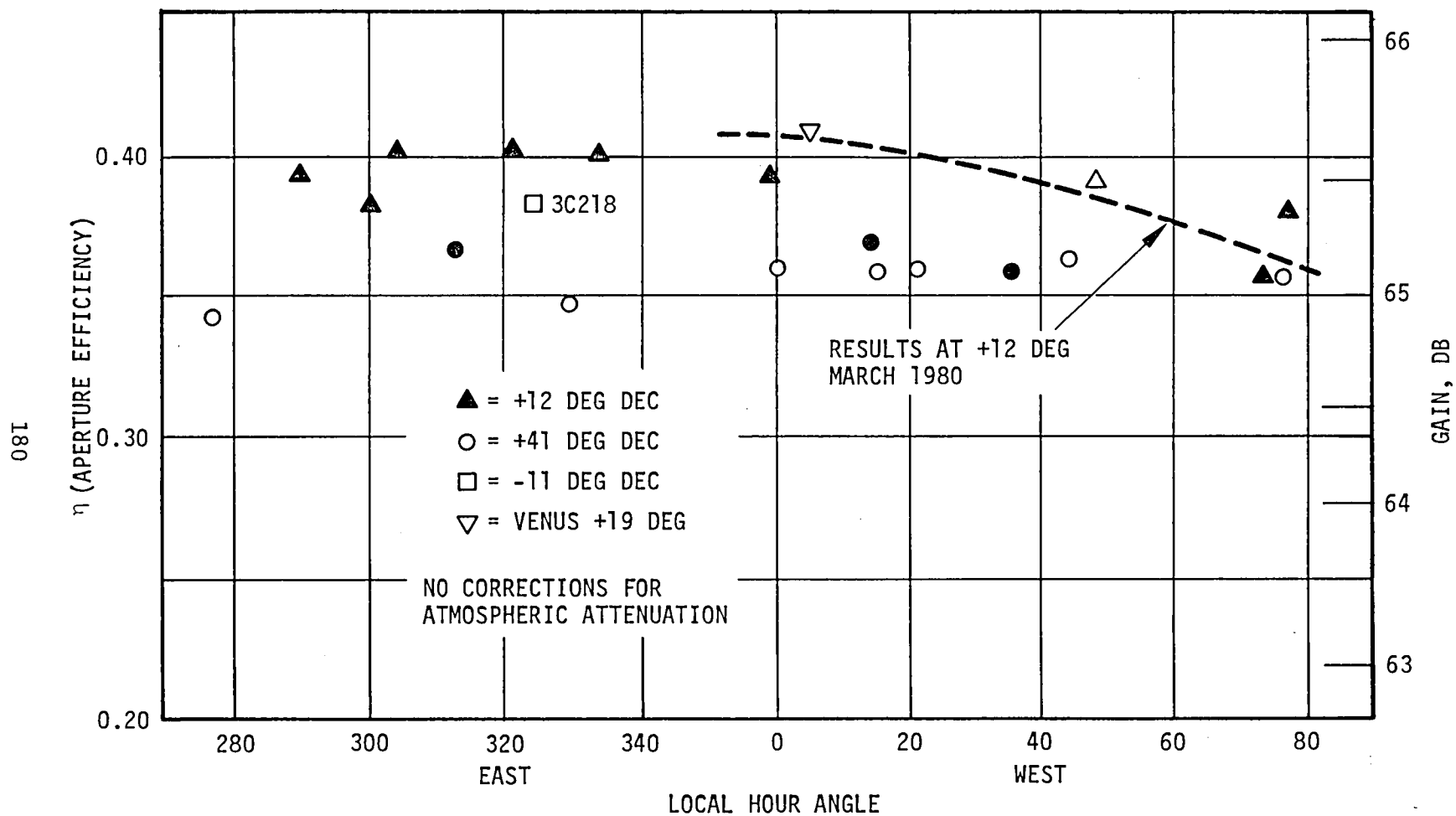


Figure 88. DSS 12 X-Band Aperture Efficiency from Radio Source Measurements

Table XVI. Performance Calculations (8420 MHz)

Calculated Losses	DSS 12 Loss (dB)	DSS 12 Gain (dB)	DSS 42 Loss (dB)	DSS 42 Gain (dB)	DSS 61 Loss (dB)	DSS 61 Gain (dB)
Perfect Antenna	0	69.537	0	69.537	0	69.537
Forward Spillover	0.1771	69.360	0.1771	69.360	0.1771	69.360
Rear Spillover	0.0188	69.341	0.0188	69.341	0.0188	69.341
Nonuniform Amp Illum	0.7423	68.599	0.7423	68.599	0.7423	68.599
Nonuniform 0 Illum	0.3954	68.203	0.3954	68.203	0.3954	68.203
Cross Polarization	0.0025	68.201	0.0025	68.201	0.0025	68.201
Mode Conversion	0.0420	68.159	0.0420	68.159	0.0420	68.159
Central Blockage	0.1748	67.984	0.1748	67.984	0.1748	67.984
Quad Blockage	0.5010	67.483	0.5010	67.483	0.5010	67.483
Dichroic Loss	0.0218	67.461	0.0218	67.461	0.0218	67.461
Waveguide Loss	0.1070	67.354	0.1070	67.354	0.1070	67.354
Atmospheric Loss (30-deg E1)	0.1	67.254	0.1	67.254	0.1	67.254
Surface RMS	0.9100	66.344	0.1300	67.124	0.1500	67.104
Hyperbola Position	0.2	66.144	0.2	66.924	0.2	66.904
Measured Gain at Rigging Position		65.7		66.63		66.30
Before DSS 12 Modifications		0.444		0.294		0.604
Star Source Factor		-0.3		-0.3		-0.3
Residual Error		0.14		0		-0.3
DSS 12 measured gain after new panels, reset, and cards		66.6				

5. Recommendations.

There were several recommendations made by the Study Team in regard to future projects; these are listed below:

- a. Investigate and develop techniques to accurately and quickly measure antenna gain (particularly at X-band where the shorter wavelength makes surface tolerances more critical), surface tolerance, gravity distortions, and other critical factors. Star tracks, which are presently used, are very time-consuming and laborious to perform and provide only moderately accurate results. One such technique was presented at a seminar on September 5, 1980 by two individuals from the University of Sheffield, England. This is particularly important in the impending Network Consolidation Project (NCP) and during arrayed operation with several antennas operating in the unattended mode.
- b. Provide adequate test time after a major upgrade to measure, calibrate, and fine tune the antennas and microwave to optimize the performance. DSS 12, in particular, should have had another month of dedicated test time after the 34m S-X conversion to investigate and correct the problems that caused the gain loss. This would have reduced the effort expended at DSS 42 and 61.
- c. Establish a recognized and funded "keeper of the decibels and kelvins" whose primary task is to establish the initial gain, efficiency, and system temperature for each antenna as it is modified; investigate differences between anticipated and actual performance values; frequently recheck those parameters to ensure that network performance is not degrading; and to participate in development of higher performance subsystems and assemblies.

- d. Support an active, aggressive research development program with adequate resources, including availability of a suitable antenna in a field environment, to investigate and demonstrate improvements to increase antenna and microwave efficiency. Two 34m antennas at 75 percent efficiency equal three 34m antennas at 50 percent efficiency. A significant cost saving or network improvement could be realized.

6. DSS 12 Antenna Modifications

The modification implementation started February 18, 1981 with the removal of the Cassegrain cone, the subreflector, and the 96 suspect surface panels (two outer rows).

The subreflector was transported to the antenna engineering yard at GDSCC and mounted to a test fixture for measurement and rework of the surface (see Figure 89). Additional bracing and push-pull adjusters were added to the backup structure to enable the subreflector surface to be reset from an rms of 0.029 inch to an overall rms of 0.016 inch (see Figure 90).

The surface panels were fabricated by Capital Westward Inc. to an rms of less than 0.012 inch, carefully packed, and transported to GDSCC. These panels were uncrated and immediately installed on the antenna, taking care not to deform the surface accuracy of the individual panels.

The vertex of the parabola was reestablished per JPL specifications, and with a modified drill tape, new target holes were drilled in the reflector surface. Targets were installed and the reflector surface measurements and reset began.

Since all measurements were obtained at the rigging angle (50 degrees dec, 0 degree HA), a two-shift operation was necessary. The night shift recorded the raw data and obtained a computer printout, and the day shift reset the panels with the antenna at the zenith position.

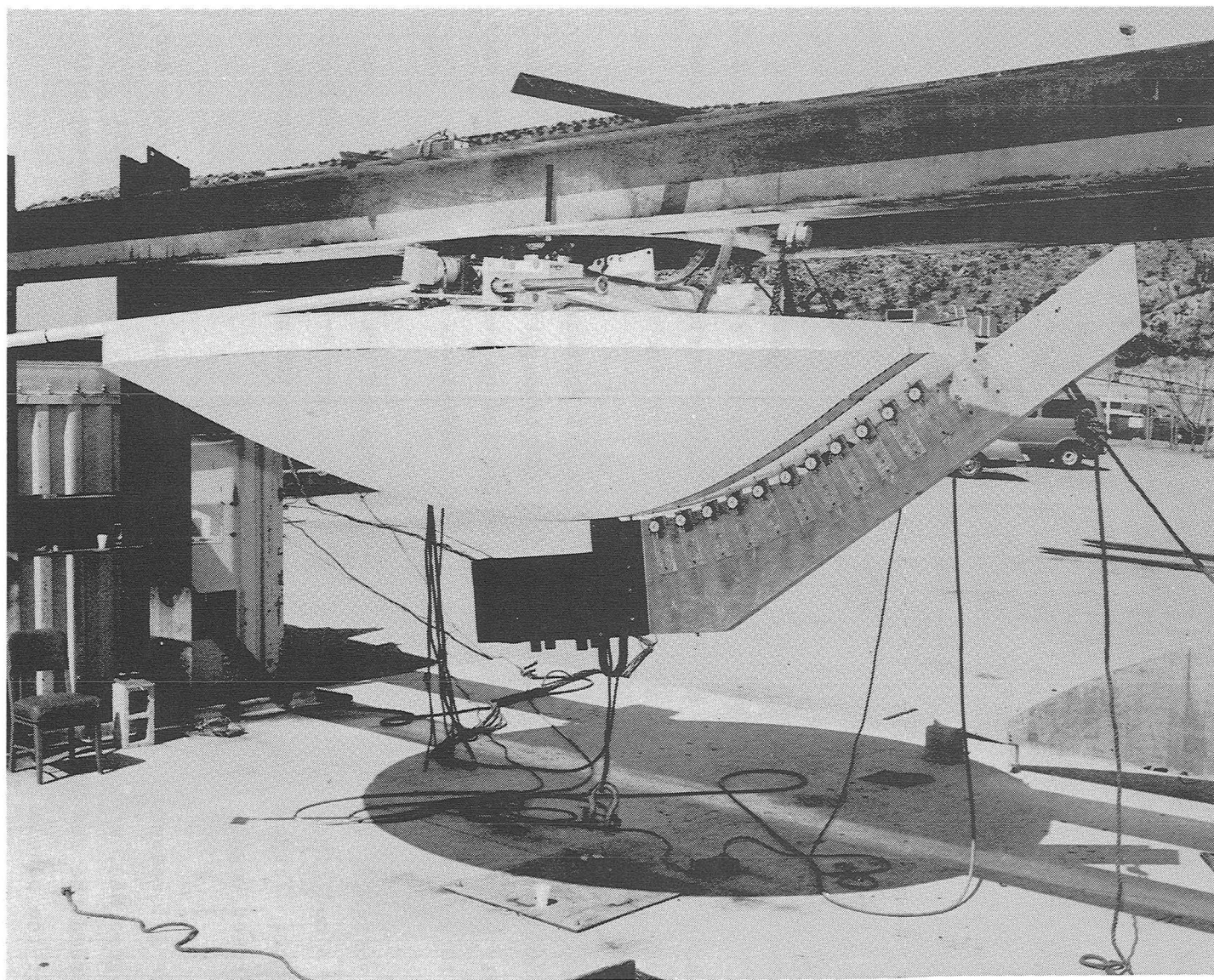


Figure 89. Subreflector Mounted to Test Fixture

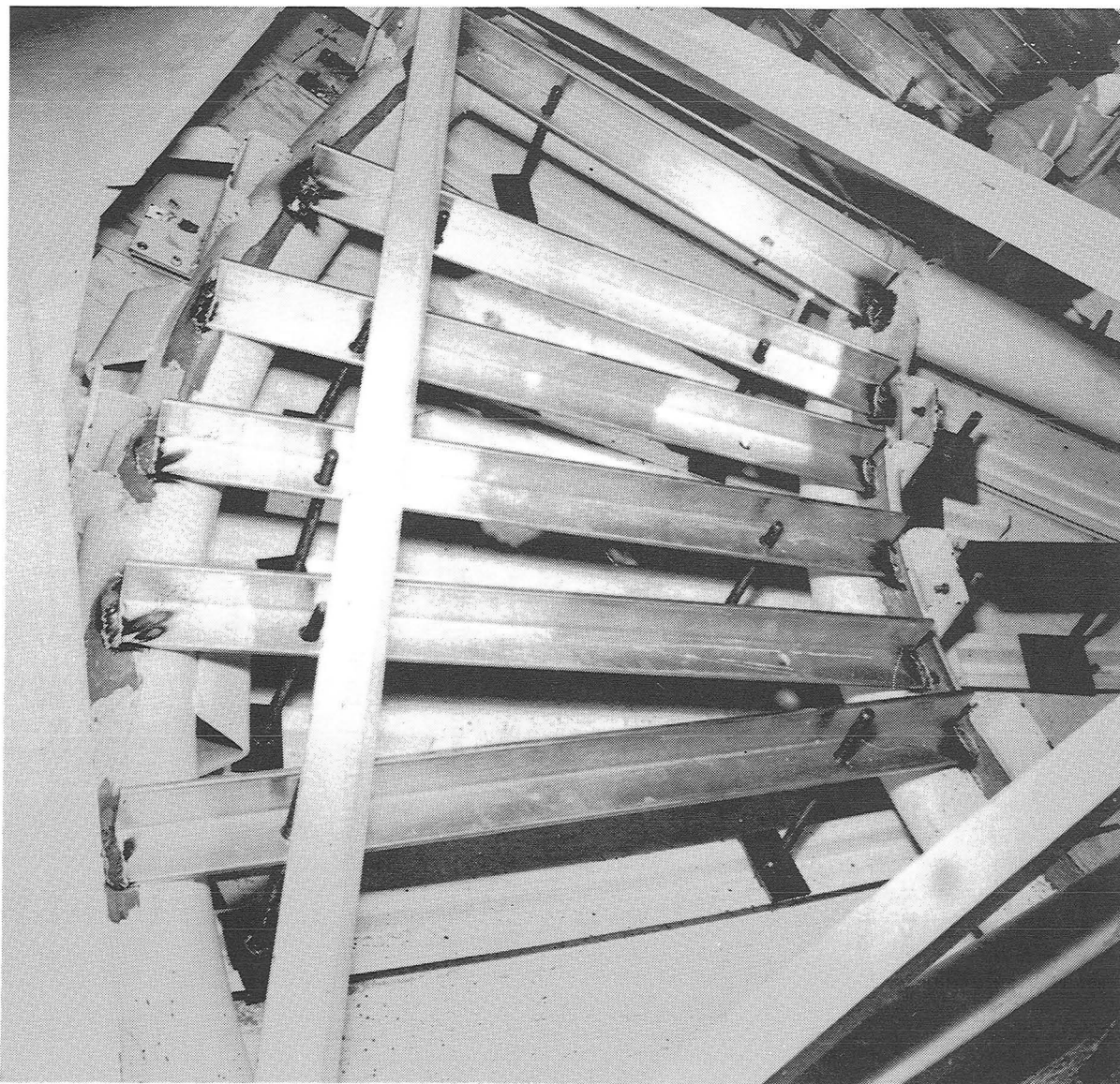


Figure 90. Subreflector Bracing and Push-Pull Adjusters

This team work produced the desired results of 0.008 inch rms of the surface panels and a best fit rms of 0.0067 inch (see Figure 91). The subreflector was installed and aligned for focal distance, line of sight, X and Y position, and north-south position from the vertex. All alignments were well within specifications.

Listed below are the final measurements of the reflector, subreflector, feedcone mounting ring, datum plane, and the RF performance gain improvement:

- a. Subreflector rms = 0.016 inch (0.015 inch specified; originally was 0.029 inch)
- b. Panel setting rms = 0.008 inch
- c. Best fit rms = 0.007 inch
- d. Subreflector position alignment:
 - (1) Focal distance ± 0.062 (± 0.125 specified)
 - (2) Normal to line of sight <20 seconds (<60 seconds specified)
 - (3) X and Y position within 0.010 inch (0.125 inch total indicator reading (TIR) specified)
 - (4) N and S <12 seconds (10 minutes specified)
- e. Feedcone ring parallel to datum plane $16.125^{+0.035}_{-0.015}$ (16.125 ± 0.020 specified)
- f. Secondary datum plane parallel to primary datum within 3 arc seconds
- g. RF performance gain improvement approximately 0.7 dB.

E. ANTENNA ACCIDENT AT DSS 61

1. General

An accident occurred on the evening of 31 January 1980 during an alignment of the polar shaft. At the time of the accident, the implementation was behind schedule 15 days. The implementation was being carried out by a combination of JPL, local contractor, and station efforts, with the

FOCAL LENGTH FIT RMS = 0.169-MM. (0.0067-IN.)

ORIGINAL FOCAL LENGTH = 10.97280 M. (432.000 IN.)

NEW FOCAL LENGTH = 10.97243 M. (431.986 IN.)

TRANSLATED VERTEX X = 0.016 CM. (0.006 IN.)

 Y = -0.066 CM. (-0.026 IN.)

 Z = 0.000 CM. (0.000 IN.)

ROTATION ABOUT AXES X = -0.000027

 Y = -0.000014 RAD.

CONTOUR DEFINITIONS

NORMAL ERROR

MM.

-0.50

-0.40

-0.30

-0.20

-0.10

-0.00

0.10

0.20

0.30

0.40

0.50

0.60

0.70

LABEL

A

B

C

D

E

F

G

H

I

J

K

L

M

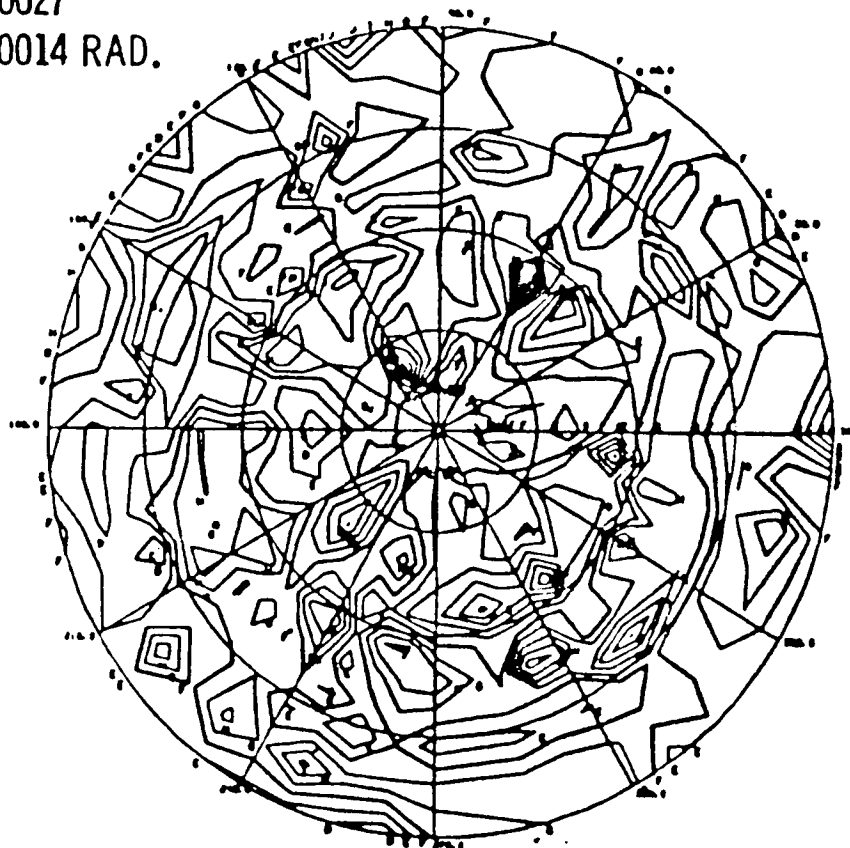


Figure 91. Final RMS of 34M HA-DEC Field Readings

contractor having prime access to the antenna structure. The contractor worked 5 days per week, 10 hours per day, and the station personnel had access for the remaining hours. The contractor was scheduled to complete his task by 1 February 1980. The only remaining item requiring his support was the alignment of the polar shaft, which required adjustment of the pedestal anchor bolts to move the polar shaft. The prelimit and final limit settings were scheduled to start on 1 February and be completed by 8 February 1980. The servo subsystem had been verified and was operational.

2. Description of the Accident

On the evening of 31 January, the antenna was placed in the stowed position with surveying theodolite and autocollimating mirror placed on the north end of the polar shaft. The alignment procedure for the polar shaft calls for a series of 180-degree rotations in HA that allow the mirror to be aligned orthogonal to the polar axis. These motions must be preceded by at least a full cycle movement to release the structural stresses.

The servo operator proceeded to drive the antenna to the east from the stow position. The antenna was stopped by releasing the spring-loaded, self-centering slew control knob. The slew control knob has markings indicating antenna motion to the east and west.

The next motion should have been to the west with an excursion of 180 degrees, commanded again by the slew control knob. As the servo console operator faces north and has no direct view of the antenna, this position makes the above-mentioned markings of the control opposed to the local directions of east and west. The servo operator commanded the antenna in the easterly direction, ignoring the markings on the servo console and the readings of the encoders, following his intuitive feeling of his local position of the west. The structure self-interference position is about 15 degrees from the 270-degree reading at local dec angle. At the time of the accident, the servo monitor readout was giving the output of the HA tachometer and was being monitored by the servo operator. He observed the

voltage corresponding to full speed, fall suddenly. This drop in voltage led him to suspect a failure and to release the slew knob, thus halting the antenna.

3. Personnel Involved

The personnel assigned to the alignment crew were considered to be highly experienced and qualified in the capacities to which they were assigned at the time of the accident. Their tenures of service were as follows:

Supervisor - 15 years

Servo Operator - 10 years

Alignment Man - 15 years

These years of experience were all applicable to the function performed at the time.

4. Damage Caused by the Accident

The antenna, when rotated approximately 105 degrees about the HA axis, caused the HA wheel weldment and the declination encoder knee weldment to strike the pedestal and the pedestal A-frame (see Figure 92). The resulting damage was the destruction of the declination encoder, knee weldment, and encoder cable end. The pedestal damage resulted in the shearing of a gusset plate and denting of a frame splice plate. The frame splice plate dent was minor, but it caused a displacement and slip of that joint (see Figure 93). In addition, a bearing retainer on the declination bearing was dented (minor), the HA encoder was misaligned by 1 degree, and the HA bullgear clearances were reduced by 0.040 inch with respect to previous readings taken 2 weeks earlier.

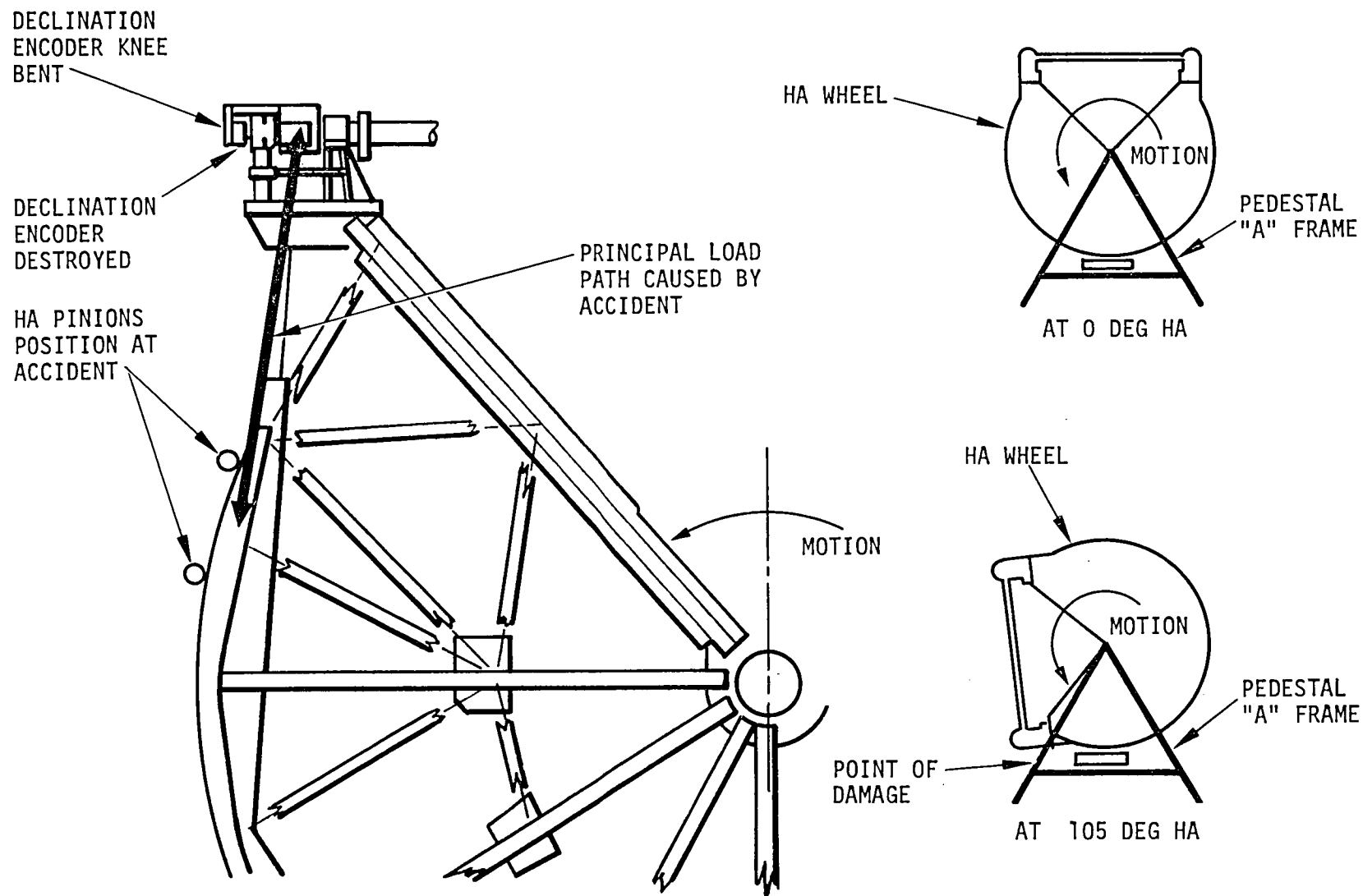


Figure 92. HA Structure Damage

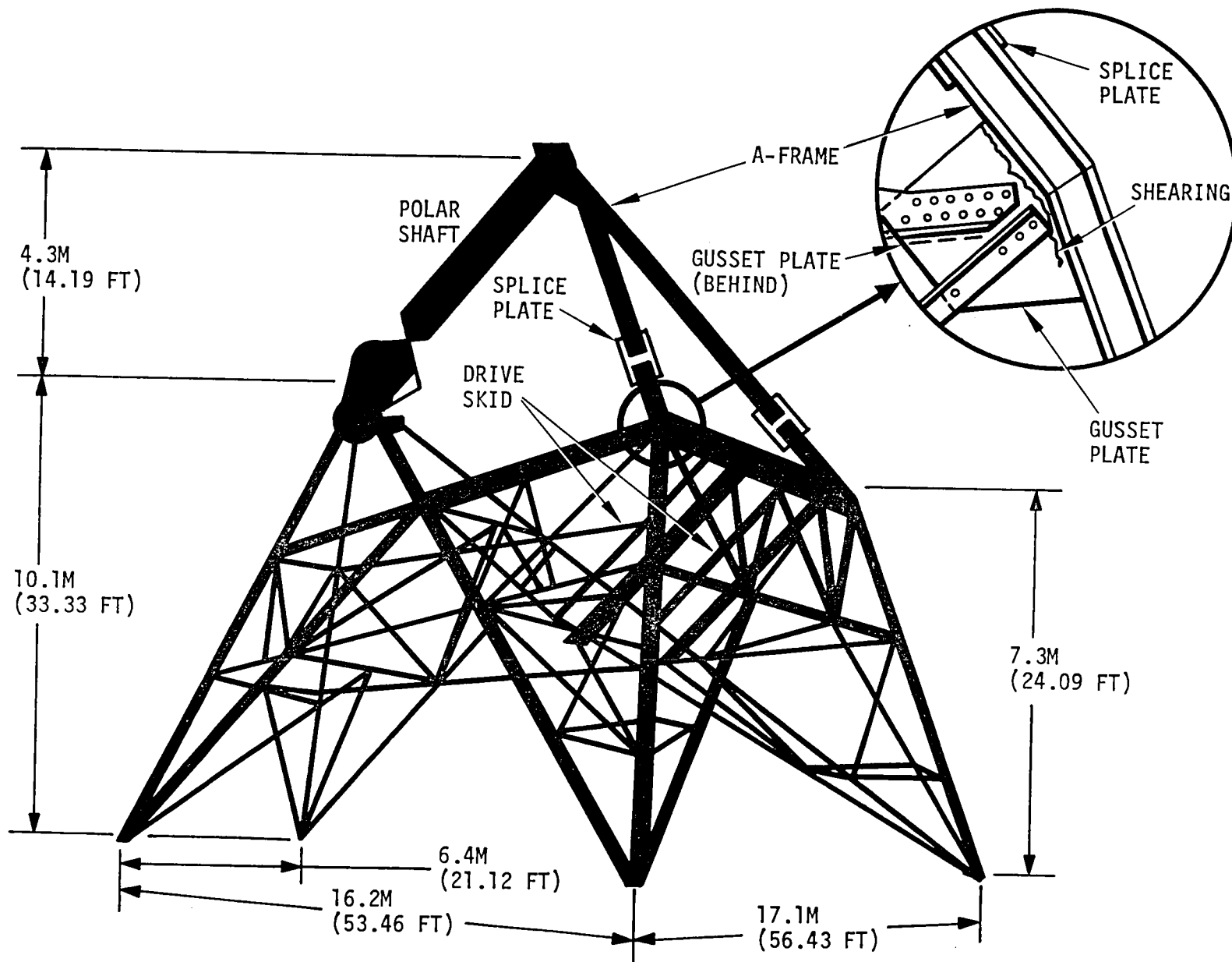


Figure 93. Pedestal Structure Damage

The following is a breakdown of the cost to repair the damaged parts:

<u>Item</u>	<u>Encoder</u>	<u>Cost</u>
1.	1 - Transducer	\$ 5,450
2.	2 - Couplings	1,350
	1 - knee	2,000
3.	1 - Cable	150
4.	1 - Seal	10
5.	1 - Bellows	550
6.	JPL Shop Fab Parts (Gusset Plates)	1,650
		<hr/>
		\$11,160
7.	Repair of pedestal damage and reset of HA drive skids	10,000
	Total	<hr/>
		\$ 21,160
	Burden at 10%	2,116
		<hr/>
	Grand Total	\$ 23,276

5. Investigations and Engineering Analysis

- a. Visual QA inspection of all weldings in the polar wheel. Nothing abnormal was observed.
- b. Visual inspection of all bullgear segments. No signs of deterioration in bullgear teeth. No cracks in the backup material. No signs of displacement of bullgear segments.
- c. Visual inspection of all members of the polar wheel. Nothing abnormal.
- d. Verification of precision holes in the polar wheel. All passed through the 1/4-inch caliper.

- e. Drive pinions. No drive pinion damage was observed.
- f. Drive pinion to bullgear clearances. A drop of 0.10 cm (0.040 in.) was observed in the overall length of the bullgear. This effect was corrected by lowering the HA skid. It is worth mentioning that a normal settling of the bullgear requires from 6 to 13 months.
- g. Verification of the secondary datum plane data in agreement with previous measurements. Level vials in agreement.
- h. HA axis alignment showed a polar shaft displacement of $0^{\circ}3'56''$ toward the east and $0^{\circ}2'23''$ below local latitude. However, this could have been a result of the antenna lifting operation and dead load weight.
- i. Dec wheel gear and drive pinions showed no change.
- j. Size and depth of indentations caused by impact of bearing weldment and A-frame:
 - (1) Bearing and weldment area equaled 22.6 cm^2 (3.5 in.^2) by 0.43-cm (0.170-in.) deep at center.
 - (2) A-frame area equaled 13.5 cm^2 (2.1 in.^2) by 1143-cm (450-in.) deep at center. The impact was on the corner edge of both members.
- k. Velocity of antenna upon impact was 0.5 degree/second.
- l. Travel distance in degrees between initial and final impact was 23 cm (9 in.), or 2.0 degrees.
- m. Time interval between initial and final impact was 3 seconds.

- n. When was antenna direction reversed? The control was released when decreasing tachometer voltage was observed. The direction was reversed after the accident.
- o. The hour angle gear-to-pinion backlash clearance was checked. The HA wheel concentricity was not changed, but the backlash clearance, after the accident, was 0.000-inch at segments 7, 8, 9, and 10.
- p. Was there unusual noise when driving in HA? No.
- q. Was there any change in motor currents when driving in HA? No.
- r. The secondary datum plane was rechecked. Hour angle equaled -2 second/arc. Dec angle equaled -4 second/arc. The bubble levels remained centered.
- s. Ten joint/holes were checked.
- t. In addition, the welds were checked on the cone ring, quadripod, and reflector backup structure. No apparent damage.

Actions taken were:

- a. The hour angle drive shed on the east side was lowered 0.127 cm (0.050 in.) and the west side was lowered by 0.076 cm (0.030 in.), which restored the pinion to wheel gear clearance to the preaccident status.
- b. The bolts from the splice plate in the A-frame that were hit by the hour angle wheel declination bearing were removed. The bolts were bowed and the joint evidenced a slipped condition. These plates were rebolted and then welded so the welds would carry all the load across that joint.

An engineering analysis was made of the forces generated by the accident. Figure 94 represents the polar wheel and bullgear pivoted at the top of an A-frame. If the wheel is rotated counterclockwise approximately 100 degrees, the declination bearing housing moves to the position at which the declination encoder knee impacted the A-frame structure. Inertia forces from the motors produced forces on the bullgear labeled R and these were essentially equilibrated by a reaction from the A-frame labeled $2R + H$, where H is the horizontal reaction at the apex of the A-frame.

In order to estimate the magnitude of the forces R and H, a two-inertia model was employed which is derived by referring to Figure 95. The upper part of Figure 95A represents the polar wheel, bullgear, and all the antenna structure attached above it. The inertia of these components is called I_2 . The lower parts of Figure 95B represent the gear reducers and drive motors. The inertia of each drive motor/gear reducer set, when referred to the antenna polar axis, is $I_1/2$. A model composed of three inertias is shown in Figure 95B. By lumping the two $I_1/2$ inertias, the two-inertia model shown in Figure 95B is obtained; it consists of the known inertias I_1 and I_2 , the known combined gear box equivalent torsional spring k, and a torsional spring K representing the structure at the point of impact. The spring constant K, obtained by a consideration of the pedestal stiffness, was found to be 1/4 of k. The combined inertia of the motors and gear reducers when referred to the antenna polar axis is approximately 13 times I_2 . The model consists of these two inertias, I_1 and I_2 , connected by the torsional spring k, rotating at the uniform angular velocity of 0.50 degree/second. Suddenly the end of torsional spring K is stopped and the response of the two inertias is analyzed. The initial conditions are $\theta_1 = \theta_2 = 0$ and $\dot{\theta}_1 - \dot{\theta}_2 = \omega_0 = 0.0087$ rad/s, or 0.50 deg/s. The values of I_1 , I_2 , k, and K are respectively $155 (10)^6$ pound feet second², $13 (10)^6$ pound feet second², $4777 (10)^6$ pound feet/radian, and $K = 1194 (10)^6$ pound feet/radian. For these values the appropriate equations of motion are solved. The resulting displacements, $\ddot{\theta}_1$ and $\ddot{\theta}_2$ are:

$$\ddot{\theta}_1 = [0.419 \sin 2.417 t - 0.000555 \sin 22.007 t] (0.0087) \quad (1)$$

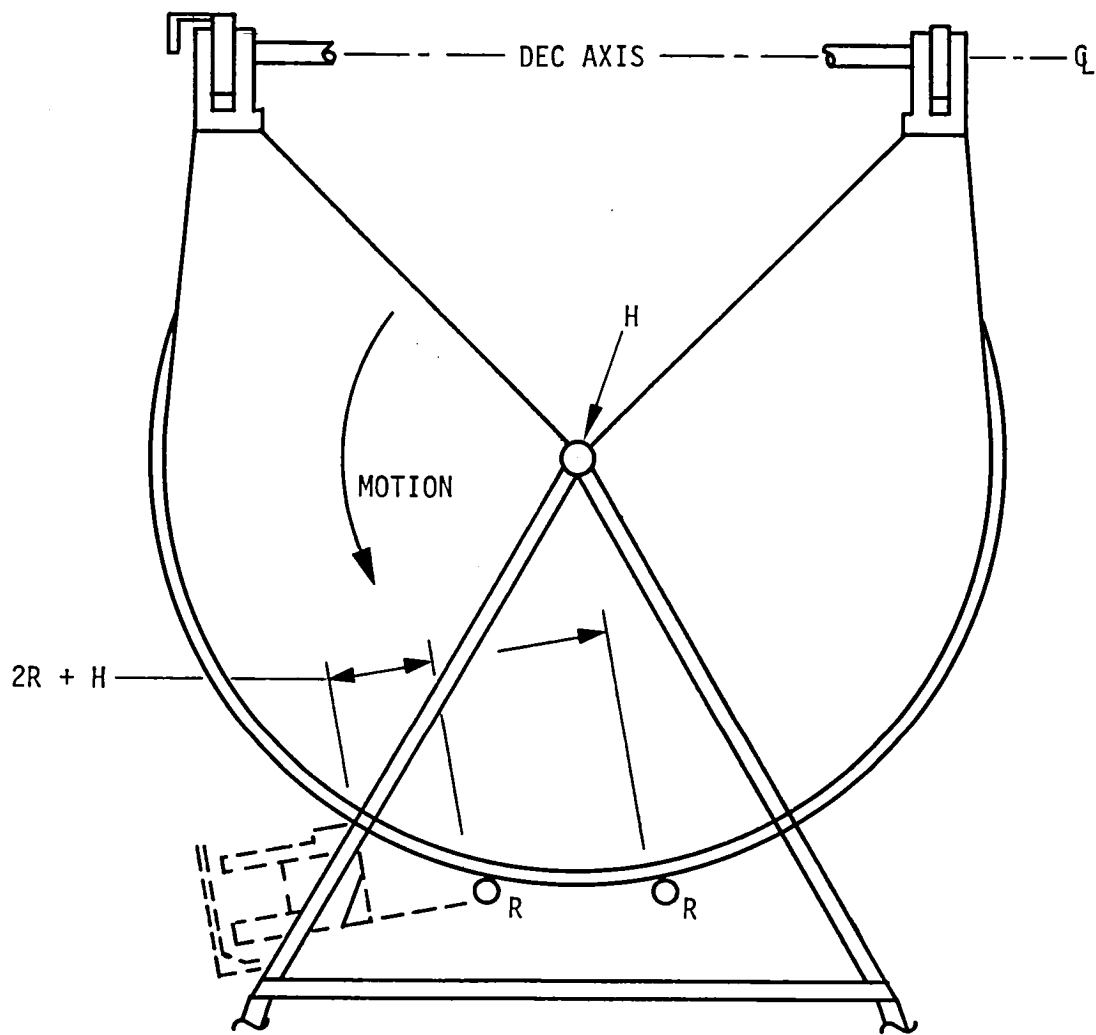


Figure 94. Impact Force Configuration

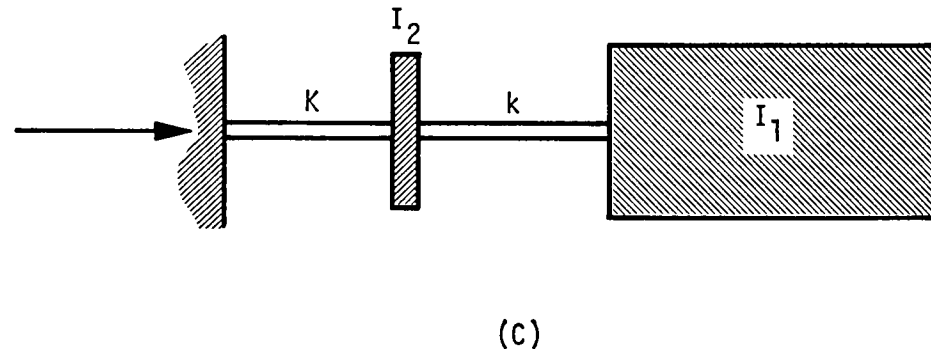
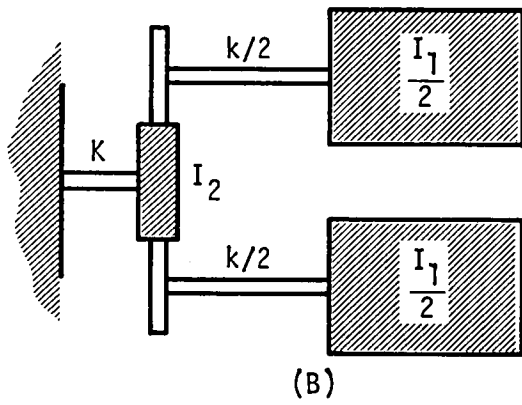
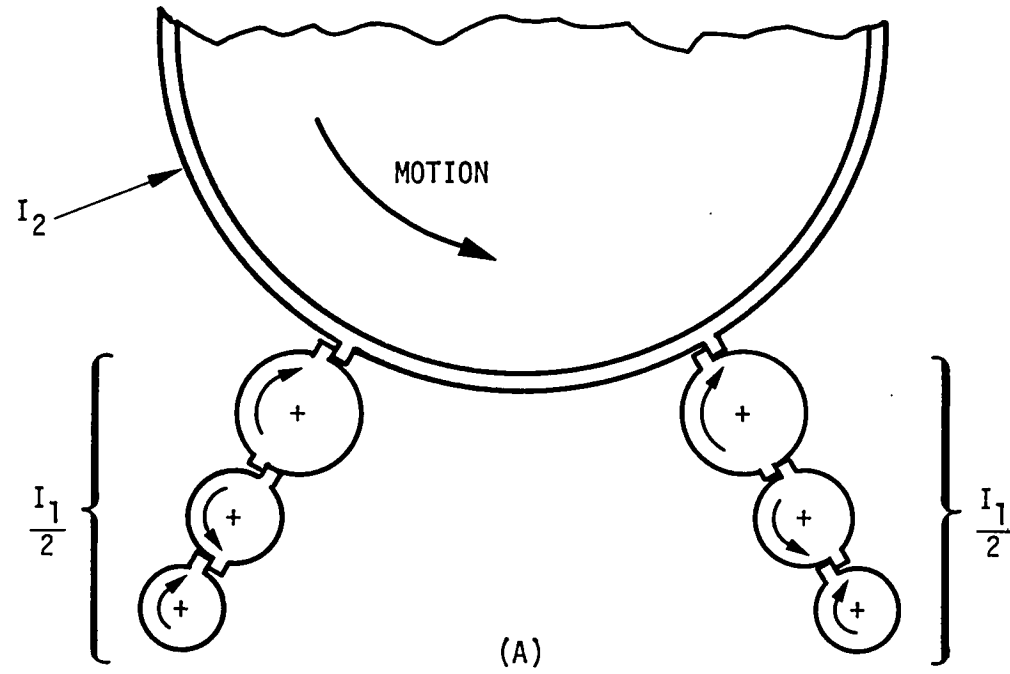


Figure 95. Two-Inertia Model

$$\ddot{\theta}_1 = [-2.45 \sin 2.417 t + 0.269 \sin 22.007 t] (0.0087) \quad (2)$$

$$\theta_2 = [0.339 \sin 2.417 t + 0.00817 \sin 22.007 t] (0.0087) \quad (3)$$

$$\ddot{\theta}_2 = [-1.98 \sin 2.417 t - 3.96 \sin 22.007 t] (0.0087) \quad (4)$$

where t is the time in seconds.

The relationship between the forces R and H and the angular accelerations are:

$$2PR = T_1 = I_1 \ddot{\theta}_1 \quad (5)$$

$$PH = T_2 = I_2 \ddot{\theta}_2 \quad (6)$$

where P is the radius of the bullgear and T_1 and T_2 are torques. The substitution of equations (2) and (4) into (5) and (6), respectively, yield expressions for the forces R and H . In Figure 96 these forces are plotted versus time. Also plotted in Figure 96 is the angular coordinate θ_2 . It can be seen that at approximately 0.60 second from beginning of impact, both the R and H forces are near their maximum values. At this point the value of $2R + H$ is approximately 66.182 kg (150,000 lb), thus this is the estimate of the maximum impact force. Also at $t = 0.60$ second, the value of θ_2 is 0.0029 radian. The corresponding linear displacement is the product of this angle and the radius to the impact point which is (0.0029) (288) or 2 cm (0.83 in.). Since 2 cm is less than the observed displacement at impact, the calculated maximum forces during impact are greater than those which actually occurred.

In order to determine the antenna angular accelerations produced when an emergency stop is made by applying brakes on both drive motors, a two-inertia model as shown in Figure 97 is analyzed. I_2 represents the inertia of the antenna structure, I_1 is the combined inertia of the two motors and two gear reducers, and k is the equivalent torsional spring

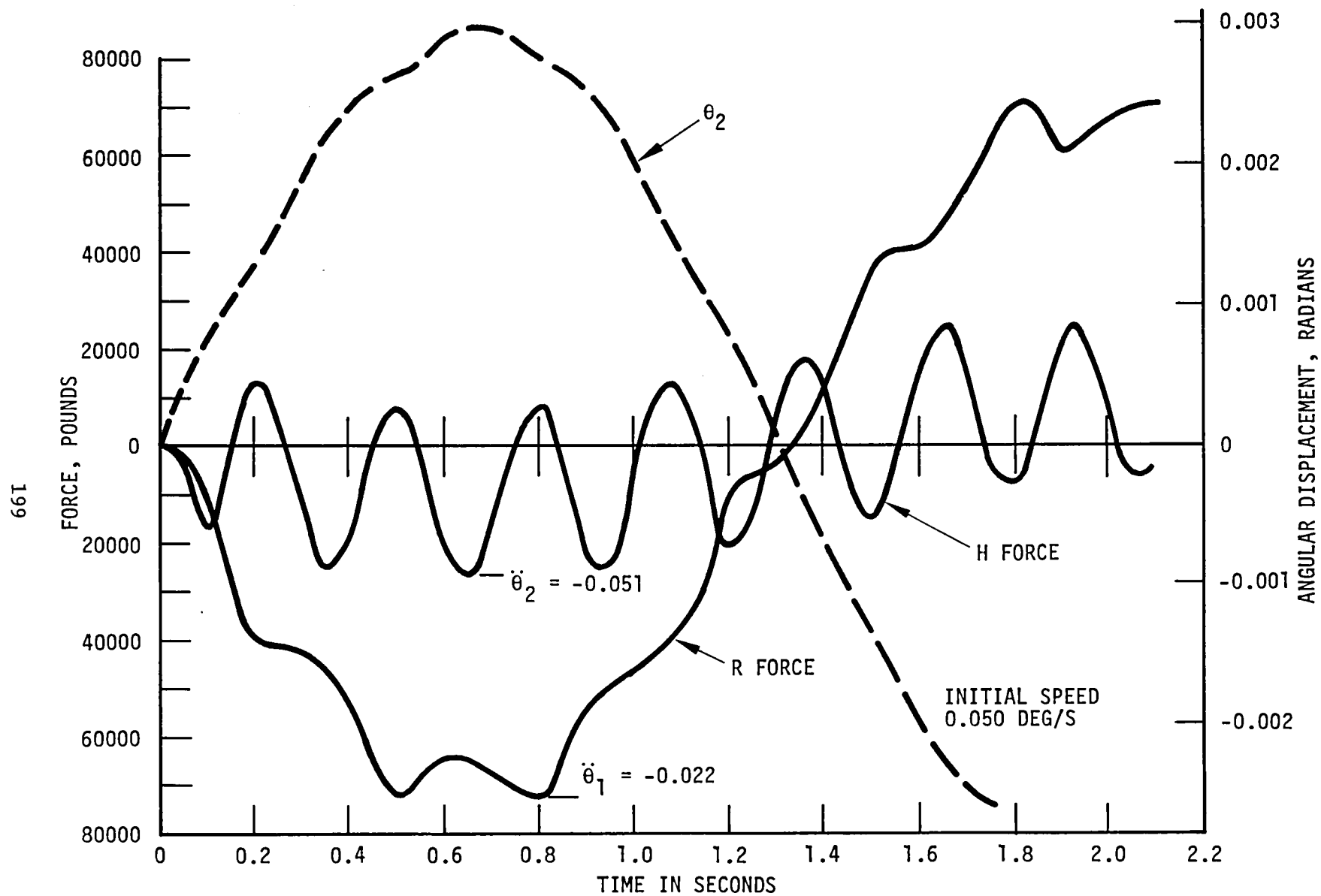


Figure 96. Impact Forces from Model

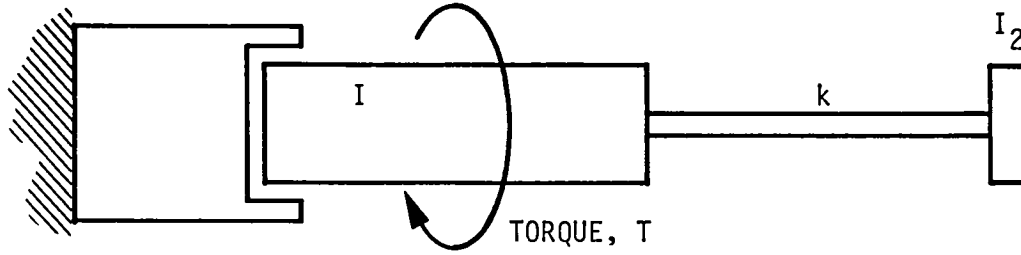


Figure 97. Model for Emergency Braking

constant of the combined gear reducers. The initial conditions are $\theta = \theta_0 = 0$ and $\dot{\theta}_1 = \dot{\theta}_2 = \omega_0 = 0.0087 \text{ rad/s}$, or 0.50 deg/s . When the appropriate equations of motion, subject to these initial conditions, are solved, the following is obtained:

$$\theta_1 = \omega_0 t - \frac{T}{I_1 + I_2} t^2 - \frac{T}{k} \frac{I_2^2}{(I_1 + I_2)^2} (1 - \cos \omega t) \quad (7)$$

$$\dot{\theta}_1 = \omega_0 - \frac{T}{I_1 + I_2} t - \frac{T}{\sqrt{k}} \frac{I_2^2}{(I_1 + I_2)^2 \sqrt{I_1 I_2}} \sin \omega t \quad (8)$$

$$\ddot{\theta}_1 = - \frac{T}{I_1 + I_2} \left[1 + \frac{I_2}{I_1} \cos \omega t \right] \quad (9)$$

$$\theta_2 = \omega_0 t - \frac{T}{I_1 + I_2} \left[\frac{t^2}{2} - \frac{1}{\omega^2} (1 - \cos \omega t) \right] \quad (10)$$

$$\dot{\theta}_2 = \omega_0 - \frac{T}{I_1 + I_2} \left[t - \frac{1}{\omega} \sin \omega t \right] \quad (11)$$

$$\ddot{\theta}_2 = - \frac{T}{I_1 + I_2} [1 - \cos \omega t] \quad (12)$$

where $\omega = \sqrt{\frac{k(I_1 + I_2)}{I_1 I_2}}$ and T is the combined torque from the two motor

brakes referred to the antenna polar axis.

$$T = 2 (100) 21232 = 4.246 (10)^6 \text{ lb ft} \quad (13)$$

where 100 foot pounds is the brake torque capacity of each drive motor and 21232 is the speed ratio between motor and antenna polar axis. Using this value of T, the time required to stop the motor from its slewing speed can be obtained by setting equation (8) to zero and solving for the time t. The value obtained is 0.343 second. The maximum angular acceleration of the antenna structure, $\ddot{\theta}_2$, can be obtained from equation (12) by setting ωt equal to π provided that t does not exceed 0.343 second, which is the range of validity of equation (12). Since ω is 19.956 radians/second, t is 0.157 when ωt is π , thus t is less than its limiting value of 0.343 and the maximum angular acceleration of the antenna structure may be obtained from equation (12) by setting $\omega t = \pi$. This gives:

$$\ddot{\theta}_{2 \text{ max}} = - \frac{4.246(10)^6}{168(10)^6} \left[1 - \cos \pi \right] = -0.0505 \text{ rad/s}^2 \quad (14)$$

The maximum acceleration of the motor, $\ddot{\theta}_1$ occurs at $t=0$ and from equation (9) is:

$$\ddot{\theta}_{1 \text{ max}} = - \frac{4.246(10)^6}{168(10)^6} \left[1 + \frac{13}{155} \cos 0 \right] = -0.027 \text{ rad/s}^2 \quad (15)$$

From equations (2) and (4), the maximum accelerations of the impact model can be calculated and are found to be $\ddot{\theta}_1 = -0.022$ and $\ddot{\theta}_2 = 0.051$. Therefore it is seen that the accelerations produced by an emergency braking are as much as the accelerations given by the impact model. The antenna was designed to safely withstand the loads induced by emergency braking; therefore it would follow that the accidental impact did not harm the antenna other than the damage in the immediate vicinity of the impact.

At the slewing speed of 0.50 degree per second, the kinetic energy of the system is 6358 pound feet. If this is equated to the potential energy of a linear spring, formed by the structure at the point of impact, the following expression is obtained:

$$\frac{1}{2} F_i X = \frac{1}{2} (I_1 + I_2)(0.0087)^2 = 6358 \quad (16)$$

where F_i is the maximum force of impact and X is the displacement of the linear spring. Solving for $F_i X$ there is obtained:

$$F_i X = 12,716 \text{ lb ft} \quad (17)$$

If F_i is set at 68,182 kg (150,000 lb), which is the estimate of impact force, $2R + H$, from the analysis of the two-inertia model, the value of X is 0.025m (0.085 ft) or 2.6 cm (1.02 in.). Since this is much less than the observed total displacement of 22.9 cm (9 in.), it is most likely that the maximum force of impact did not reach the value of 68,182 kg (150,000 lb). It is probable that both drive motors reached their stalled torque condition and produced a force at the contact point which existed for several seconds after the impact force ceased to exist.

The stalled torque of one motor can be 2.5 times its rated value of 45 pound feet. The force produced at the impact point, F_m , would be:

$$F_m = \frac{2.5(45)21232(2)}{24} = 199,000 \text{ lb} \quad (18)$$

where 21232 is the speed ratio and 24 is the radius to the impact point. At the contact area, it was observed that the indentation in the frame splice joint was 1.14 cm (0.45 in.) deep and the area of contact was 12.9 cm^2 (2.00 in.^2). From the force of two stalled motors, the average compressive stress, σ_c , would have been:

$$\sigma_c = \frac{199000}{2} = 99,500 \text{ psi} \quad (19)$$

Since the compressive yield of this material is 36,000 psi, it is expected that the force of either of the stalled motors would have produced a considerable amount of local damage.

The foregoing discussion indicates that the horizontal force at the impact point was initially less than $2R + H = 68,182 \text{ kg}$ (150,000 lb), and subsequently was $F_m = 90,455 \text{ kg}$ (199,000 lb). The latter value will be used to assess possible damage to the drive gears, speed reducers, polar axis bearings, and declination axis bearings.

a. Gear Tooth Bending Stress.

When a motor is stalled at 2.5 times its rated torque of 45 pound feet, the tangential force at the gear pitch circle, F_T , is

$$F_T = 2.5(45) \frac{21232}{24} = 99,525 \text{ lb}$$

where 21232 is the speed ratio between motor and antenna axis and 7.32m (24 ft) is the pitch radius of the bullgear.

The tooth bending stress, σ_B , is estimated by multiplying this tangential force by the distance from the pitch circle to the tooth root, 2.4 cm (0.95 in.), and dividing by the section modulus of the tooth, 26.38 cm^3 (1.61 in.³), obtaining:

$$\sigma_B = \frac{99525(0.95)}{1.6} = 59,000 \text{ psi}$$

Since the bullgear material is 4140 steel having a minimum specified Brinell hardness of 220, which corresponds to a tensile yield strength of 95,000 psi, it is considered that no damage was done to the bullgear by the accident. The pinion teeth are both wider and harder, having a minimum tensile yield of 130,000 psi.

b. Speed Reducer Forces.

The speed reducers have a continuous power rating of 40 horsepower at 3450 r/min. This corresponds to an input torque of 60 pound feet. When the motor stall torque of $2.5 (45) = 112$ pound feet is applied to the input end of the reducer, an overload factor of $112/60 = 1.87$ exists based upon the manufacturer's rating of 60 pound feet as a continuous torque at 3450 r/min. The manufacturer also gives the factor 5 as a permissible transient overload. Therefore, the forces developed within the reducer during the accident are well within its capacity to sustain without damage.

c. Upper Polar Bearing.

From Figure 94 it may be seen that the stalled motor condition would not substantially affect the load on the polar axis bearing because the two R forces acting tangentially to the bullgear are essentially in line with the impact point; thus the two R forces are equilibrated by an opposite force of $2R$. The force H exists from the impact condition and Figure 96 shows the maximum value of H to be 11,364 kg (25,000 lb) approximately.

During an emergency stop by the application of both motor brakes, an acceleration of $-0.0505 \text{ radian/second}^2$ is produced according to equation (14). The polar axis torque would be the product of this acceleration and the mass moment of inertia, I_2 , which is $13(10)^6 \text{ pound feet second}^2$. The product of 656,500 divided by the bullgear radius of 7.32m (24 ft) yields the force of 12,432 kg (27,350 lb) acting horizontally on the upper polar bearing.

Gravity produces a radial load of 291,818 kg (642,000 lb) on the upper polar bearing, which has a static radial rating of 393,182 kg (865,000 lb). It is clear that the effect of the accident could not have damaged the upper polar bearing, since the extra force produced is approximately the same as that caused by dynamic braking, and each is small in comparison to the gravity load.

d. Polar Thrust Bearing.

It is highly unlikely that the accident caused any appreciable change in the static load of 218,182 kg (480,000 lb) acting on the thrust bearing. But if it is assumed that by some wedging action the full value of the stalled motor force of 90,455 kilograms (199,000 pounds) were added to the 218,182 (480,000) steady force, producing a total force of 308,636 (679,000), then this total may be compared to the bearing static rating of 568,182 kg (1,250,000 lb). It must be concluded that the thrust bearing was not damaged.

e. Declination Bearing.

Referring to Figure 94 it may be seen that the impact loading on the declination bearing has a bearing axial component opposite to that caused by gravity loading. The radial load from stalled motors could not possibly add more than 90,455 kg (199,000 lb) to the radial load. Since the radial load from gravity is 33,182 kg (73,000 lb), the total radial load could not have exceeded 123,636 kg (272,000 lb). The total axial load could not have exceeded 51,818 kg (114,000 lb). The total equivalent load, calculated in the way dictated by the bearing manufacturer, would have been 232,727 kg (512,000 lb). The rated static capacity of this bearing is 454,545 kg (1,000,000 lb), therefore, the conclusion is that it was in no way harmed by the accident.

f. Drive Pinion Tightness.

After the accident it was observed that both polar drive pinions were tight against the bullgear. To restore the original amount of pinion backlash, the east pinion was lowered by 0.127 cm (0.050 in.) and the west pinion lowered by 0.076 cm (0.030 in.). A rotation about the lower west corner of the A-frame of Figure 94 is consistent with these dimensions. Apparently, the east leg of the A-frame was shortened by approximately 0.203 cm (0.080 in.). An examination of the lower splice joint indicated an

indeterminate amount of shortening, which would cause the upper end of the polar axis to move eastward and downward. Observations did indeed indicate that the movement of the upper end of the polar axis was eastward and downward by amounts consistent with a 0.203 cm (0.080 in.) shortening of the east leg.

The conclusion is that since the lowering of both pinions restored the original pinion backlashes over their entire hour angle range, the east leg was in fact shortened by approximately 0.203 cm (0.080 in.), because it is highly unlikely that the polar wheel structure would have deformed uniformly in all radial directions.

g. Maximum Member Stresses

Table XVII lists the stresses, in KSI, in various members of the structure due to an assumed impact force of 200,000 pounds, gravity loading, and gravity combined with wind loading. These may be compared with stresses allowed by AISC codes. It may be seen that the only expected damage is in the immediate vicinity of the impact.

h. Summary of the Engineering Review

- (1) The pedestal structure, polar wheel, polar axis drive elements, and the declination bearing housing were subjected to a force at impact not greater than 200,000 pounds.
- (2) Other than in the immediate vicinity of the impact point, no damage can be determined by calculations.
- (3) The east pedestal post joint at the bend was subjected to stresses beyond the yield.
- (4) Movement of the splice joint on the east pedestal leg to the A-frame connection is believed to have occurred, thereby lowering the polar wheel and moving it eastward.

Table XVII. Maximum Member Stresses, KSI

Member	Accident (Impact)+(Gravity) = (Sum)			Design (Sum of Gravity and Wind)	AISC Specs
<u>Pedestal</u>					
(164) A-Frame splice 200,000 pound impact	-55.0	-5.0	-60.0	-15.0	20.0
(170) Horizontal beam with above located impact point	0.2	9.5	9.7	18.8	20.0
(194) Horizontal beam - gusset on H-beam 113,000 pound impact or beam flange	105.0	9.5	114.5	18.8	20.0
<u>Polar Wheel</u>					
(36) Horizontal 200,000 pound impact	7.3	-2.2	5.1	6.1	20.0
(54) Horizontal	7.2	-2.6	4.6	5.6	20.0
(55) Horizontal	12.5	-4.5	8.0	9.7	20.0

i. Summary of Accident Prevention Recommendations

- (1) Prevent antenna driving from control room servo rack without antenna limits set.
- (2) Perform all necessary antenna movement prior to limits setting via the remote control box that may be operated from the antenna skids, or hydromechanical building.
- (3) Perform all precision antenna movements via the remote control box, obtaining the required accuracy through verbal communication with an observer of the encoder readings in the control room.

